Dissertation

submitted to the
Combined Faculties for the Natural Sciences and for Mathematics
of the Ruperto-Carola University of Heidelberg, Germany
for the degree of
Doctor of Natural Sciences

presented by
Diplom-Biologist
Haniyeh Yazdanparast
born in: Teheran, Iran
Oral-examination: 6th March 2018

Myeloid cells and therapy resistance in Chronic Lymphocytic Leukemia

Referees: **Prof. Dr. Viktor Umansky**
Prof. Dr. Peter Lichter

CONTENT

ABBREVIATIONS

AT	adoptive transfer
BCR	B cell receptor
BM	bone marrow
BTK	Bruton's tyrosine kinase
CLL	Chronic lymphocytic leukemia
cDC	conventional dendritic cell
CSF-1	Colony stimulating factor 1
CSF-1R	Colony stimulating factor 1 receptor
DNA	Deoxyribonucleic acid
DEG	differentially expressed genes
DAPI	4',6-Diamidin-2-phenylindol
DAMPs	damage-associated molecular patterns
FCS	Fetal calf serum
HSC	Hematopoietic stem cells
IFN	Interferon
IPA	Ingenuity Pathway analysis
iwCLL	International Workshop on Chronic Lymphocytic Leukemia
IGHV	Immunoglobulin heavy variable group
i.p.	intraperitoneal
i.v.	intravenious
ITK	Interleukin-2-inducable T cell kinase
LN	lymph node
LPS	lipopolysaccharide
MHC I/II	Major histocompatibility complex I/II
MACS	magnetic activated cell sorting
MDSC	myeloid-derived suppressor cell
NLC	nurse like cell
PAMP	pathogen-associated molecular patterns
PRR	Pattern recognition receptor
PB	peripheral blood
PBMC	peripheral blood mononuclear cell
PD-L1	Programmed cell death ligand 1
PMA	phorbol myristate acetate

PLCγ2	1-Phosphatidylinositol-4,5-bisphosphate phosphodiesterase gamma-2
RNA	Ribonucleic acid
RT	room temperature
SNP	single nucleotide polymorphism
SPL	spleen
TCL-1	T cell leukemia 1
TGI	tumor growth inhibition
TLR	Toll-like receptor
TME	tumor microenvironment
Treg	regulatory T cells
TREM-1	Triggering receptor expressed on myeloid cells 1
UTR	untranslated region
WT	wild type

SUMMARY

Chronic lymphocytic leukemia (CLL) is characterized by an accumulation of mature malignant $CD5^+CD19^+$ B cells. Survival and proliferation of these B cells are highly dependent on the tumor microenvironment, which comprises monocyte-derived nurse-like cells (NLCs) as key players that possess tumor-supportive properties and resemble tumor-associated macrophages (TAMs). One of the main goals of this thesis was to understand and target the tumor supportive properties of myeloid cells in CLL.

Colony Stimulating Factor 1 Receptor (CSF-1R) is expressed on cells of the myeloid lineage and known to be important for TAM differentiation in solid tumors. Targeting CSF-1R using the monoclonal antibody TG3003, reduced NLC numbers in CLL cocultures, a well-accepted *in vitro* model mimicking the lymph node microenvironment in CLL, slightly reduced the expression of factors with functional relevance in the CLL tumor microenvironment (e.g. CCL2, sCD14), and significantly reduced NLC-mediated survival support for primary CLL cells *in vitro*. Further, a potential therapeutic effect of TG3003 was investigated in a preclinical model of CLL by adoptively transferring splenocytes from leukemic Eμ-TCL-1 mice into C57BL/6 mice (TCL-1 AT) with a humanized CSF-1R gene. TG3003 treatment resulted in reduced monocyte numbers with a stronger effect on $Ly6C^{low}$ monocytes, a subset that is highly enriched in CLL patients. The observed reduction did, however, not lead to a complete normalization of monocytic cell subsets. In conventional dendritic cells (cDCs), the expression levels of surface molecules required for adhesion, co-stimulation of T cells, and antigen presentation remained at low levels in leukemic mice after treatment with TG3003. In line with this, adaptive immunity with respect to T cells was also not altered. Finally, TG3003 treatment did not lead to an improvement of disease outcome in the TCL-1 AT model, possibly due to insufficient changes in the immune status of treated mice.

The second focus of this thesis was a comprehensive investigation of the myeloid tumor microenvironment in the TCL-1 AT model and under the influence of Ibrutinib, a Bruton's tyrosine kinase (BTK) inhibitor that blocks B-cell receptor (BCR) signaling, and thereby efficiently controls and inhibits CLL development in patients. As BTK is also expressed in myeloid cells, an indirect activity of Ibrutinib on the CLL tumor microenvironment was hypothesized. Among other findings, this study revealed that Ibrutinib is capable of inhibiting the enrichment of the CLL-associated $Ly6C^{low}$ monocyte subset and normalizing several CLL-induced molecules associated with activation of cellular growth and proliferation, inflammation and immune suppression (e.g. PECAM-1, TREM-1, PD-L1). Ibrutinib further enhanced the CLL-associated tolerogenic/immature immunophenotype

of cDCs (e.g. expression of PD-L1). Thus, Ibrutinib's effect on the myeloid tumor microenvironment in CLL is of opposing nature, thereby inaugurating room for improvement with respect to therapy.

Exploring mechanisms of Ibrutinib resistance in the TCL-1 AT model was the third aim of the current work. Even though Ibrutinib represents a paradigm shift in the treatment of CLL, a growing number of resistant patients with highly aggressive disease are identified, whereby the underlying mechanism of resistance is so far only partly understood. Despite an initial response to Ibrutinib, continuous treatment of TCL-1 AT mice revealed a loss of therapeutic efficacy after several weeks. This observation was accompanied by an increase of proliferating leukemic cells in the blood and lymphoid organs and phenotypic alterations of Ibrutinib-resistant leukemia cells including deregulation of proteins that are involved in the BCR signaling. Re-transplantation of therapy-resistant tumor cells led to uncontrolled leukemia development under re-applied Ibrutinib treatment, demonstrating acquired tumor microenvironment-independent and cell-intrinsic resistance of these tumors. Whole exome and RNA sequencing of tumor cells revealed the absence of genetic mutations in Btk and its target molecule Plcγ2. Analysis of transcriptional changes identified several gene sets and biological complexes (e.g. Bcl-2 family and NF-αB complex) that are significantly different in Ibrutinib-resistant and –sensitive cells and which will be the focus of future investigations.

In summary, the current thesis illuminates several tumor-promoting as well as dysfunctional features of myeloid cells in CLL and under Ibrutinib treatment. These findings may serve as a basis for the design of specific therapeutic strategies targeting myeloid cells, and their rational combination, for example with existing tumor-targeting drugs, which such as Ibrutinib might harbor also non-beneficial effects on the tumor microenvironment. The identification of target molecules in leukemic cells that have become resistant to Ibrutinib and are highly independent of their tumor microenvironment launches novel therapeutic modalities for patients that relapse under Ibrutinib treatment.

ZUSAMMENFASSUNG

Chronische lymphatische Leukämie (CLL) ist durch eine Akkumulation von reifen malignen $CD5^+$ $CD19^+$ B-Zellen gekennzeichnet. Das Überleben und die Proliferation dieser B-Zellen sind in hohem Maße von der Tumor-Mikroumgebung abhängig, welches von Monozyten abgeleitete nurse-like cells (NLCs) als Schlüsselspieler umfasst, die tumorunterstützende Eigenschaften besitzen und tumor-associated macrophages (TAMs) ähneln. Eines der Hauptziele dieser Doktorarbeit war es, die tumorunterstützenden Eigenschaften von myeloischen Zellen in der CLL zu verstehen und zu untersuchen.

Colony Stimulating Factor 1 Receptor (CSF-1R) wird auf Zellen der myeloiden Linie exprimiert und ist bekanntlich für die TAM-Differenzierung in soliden Tumoren wichtig. Die Verwendung des monoklonalen Antikörpers TG3003 gegen CSF-1R, reduzierte NLC-Zahlen in CLL-Kokulturen, einem gängigen *in vitro* Modell, welches die Lymphknoten-Mikroumgebung in CLL nachahmt. Hierbei führte TG3003 zu einer geringfügig verringerten Expression von Faktoren mit funktioneller Relevanz in der CLL-Tumor-Mikroumgebung (z.B. CCL2, sCD14) und reduzierte die NLC-vermittelte Überlebensunterstützung für primäre CLL-Zellen *in vitro* signifikant. Darüber hinaus wurde ein potentieller therapeutischer Effekt von TG3003 in einem präklinischen Modell von CLL untersucht, indem Splenozyten aus leukämischen Eμ-TCL-1 Mäusen adaptiv in C57BL/6 Mäuse (TCL-1 AT) mit einem humanisierten CSF-1R Gen transferiert wurden. Die Behandlung mit TG3003 führte zu verringerten Monozytenzahlen mit einer stärkeren Wirkung auf $Ly6C^{low}$-Monozyten, einer Subpopulation, die bei CLL-Patienten stark angereichert ist. Die beobachtete Reduktion führte jedoch nicht zu einer vollständigen Normalisierung von monozytischen Subpopulation. In conventional dendritic cells (cDCs) blieben die Expressionslevel von Oberflächenmolekülen, die für Adhäsion, Kostimulation von T-Zellen und Antigenpräsentation benötigt werden, bei leukämischen Mäusen nach Behandlung mit TG3003 auf einem niedrigen Niveau. In Übereinstimmung damit wurde auch die adaptive Immunität in Bezug auf T-Zellen nicht verändert. Schließlich führte die Behandlung mit TG3003 nicht zu einer Verbesserung des Krankheitsergebnisses im TCL-1-AT Modell, welches möglicherweise auf die unzureichenden Veränderungen des Immunstatus in den behandelten Mäusen zurückgeführt werden kann.

Der zweite Schwerpunkt dieser Arbeit lag auf einer umfassenden Untersuchung der myeloischen Tumor-Mikroumgebung im TCL-1 AT Modell und unter dem Einfluss von Ibrutinib, einem Bruton's tyrosine kinase (BTK)-Inhibitor, der die B-Zell-Rezeptor (BCR)-Signalgebung blockiert und dadurch die CLL Entwicklung bei Patienten effizient kontrolliert und inhibiert. Da BTK auch in myeloischen

Zellen exprimiert wird, wurde eine indirekte Aktivität von Ibrutinib auf die CLL-Tumor-Mikroumgebung vermutet. Unter anderem zeigt diese Studie, dass Ibrutinib in der Lage ist, die Anreicherung der CLL-assoziierten Ly6C^{low}-Monozyten-Subpopulation zu inhibieren und mehrere CLL-induzierte Moleküle, die in Verbindung mit der Aktivierung von Zellwachstum und Proliferation, Entzündung und Immunsuppression stehen (z. B. PECAM-1, TREM-1, PD-L1), zu normalisieren. Ibrutinib erhöhte weiterhin den CLL-assoziierten tolerogenen/unreifen Immunphänotyp von cDCs (z. B. die Expression von PD-L1). Demzufolge ist die Wirkung von Ibrutinib auf die Mikroumgebung des myeloiden Tumors bei CLL von gegensätzlicher Natur und eröffnet somit Raum für Verbesserungen in Bezug auf die Therapie.

Die Erforschung der Entwicklung einer Resistenz gegen Ibrutinib im TCL-1 AT-Modell war das dritte Ziel der vorliegenden Arbeit. Obwohl Ibrutinib einen Paradigmenwechsel bei der Behandlung von CLL darstellt, wird eine wachsende Anzahl resistenter Patienten mit hochgradig aggressiven Erkrankungen identifiziert, wobei der zugrunde liegende Resistenzmechanismus bisher nur teilweise verstanden wird. Trotz eines anfänglichen Ansprechens auf Ibrutinib, zeigte die fortlaufende Behandlung in TCL-1 AT Mäusen nach einigen Wochen einen Verlust an therapeutischer Wirksamkeit. Diese Beobachtung wurde begleitet von einem Anstieg an proliferierenden leukämischen Zellen im Blut und den lymphoiden Organen und phänotypischen Veränderungen von Ibrutinib-resistenten Leukämiezellen, welche die Deregulierung von Proteinen, die an der BCR-Signalgebung beteiligt sind einschließt. Die Retransplantation von therapieresistenten Tumorzellen und erneute Behandlung mit Ibrutinib, führte zu einer unkontrollierten Leukämieentwicklung, welches die erworbene, von der Tumormikroumgebung unabhängige und zelleigene Resistenz dieser Tumoren verdeutlich. Vollständige Exom- und RNA-Sequenzierung von Tumorzellen zeigte das Fehlen von genetischen Mutationen in Btk und dessen Zielmolekül Plcγ2. Die Analyse von Veränderungen im Transkriptom identifizierte mehrere Gen-Sätze und biologische Komplexe (z. B. Bcl-2-Familie und NF-κB-Komplex), die sich in Ibrutinib-resistenten und -sensitiven Zellen signifikant unterscheiden und die im Fokus nachfolgender Untersuchgen stehen werden.

Zusammengefasst beleuchtet die vorliegende Arbeit mehrere tumorfördernde sowie dysfunktionale Merkmale von myeloischen Zellen in der CLL und unter Ibrutinib-Behandlung. Diese Ergebnisse werden als Grundlage für die Entwicklung spezifischer therapeutischer Strategien für myeloide Zellen und deren sinnvolle Kombination beispielsweise mit vorhandenen Tumortherapien, die wie im Falle von Ibrutinib möglicherweise auch partiell unvorteilhafte Auswirkungen auf die Tumor-Mikroumgebung haben können, dienen. Die Identifizierung von

Zielmolekülen in Leukämiezellen, die resistent gegenüber Ibrutinib und unabhängiger von ihrer Tumor-Mikroumgebung geworden sind, eröffnet neue therapeutische Möglichkeiten für Patienten, die unter Behandlung mit Ibrutinib einen Rückfall erleiden.

1 INTRODUCTION

1.1 Cancer and the role of chronic inflammation

The term “cancer” describes a group of diseases that shows abnormal cell growth in conjunction with the potential of uncontrolled, tissue-independent spreading of cells throughout the body, which usually is fatal to the affected individual without adequate treatment[1]. Cancer is thought to be the result of the acquisition of multiple hallmarks (such as sustained proliferation and replicative immortality, evasion of growth suppressors, activation of invasion and metastasis, induced angiogenesis, and resistance to cell death) and is further supported by enabling characteristics including tumor-promoting inflammation[1].

Inflammation can be sub-classified in acute and chronic inflammation. Acute inflammation mediated by immune cells is a response to an alteration induced by a pathogen or a physical or chemical insult that is usually followed by the elimination of the damage, tissue repair, wound healing and restoration of homeostatic state[2, 3]. Acute inflammation plays a central role in controlling tumor growth and is concurrently characterized to be of short-term and self-limiting[2, 3]. Chronic inflammation on the other hand, is a deregulated process that can instead promote malignant transformation of cells and carcinogenesis by supplying various molecules to the tumor microenvironment, including growth factors, survival factors, proangiogenic factors, and extracellular matrix-modifying enzymes[2, 4]. Eventually, these signals result in the activation of cancer-enhancing processes, such as epithelial-mesenchymal transition, invasion, metastasis, and angiogenesis which are especially relevant in the context of solid tumors[1, 2, 4].

It is well-known, that exogenous inflammation due to infections, exposure to irritants or autoimmune diseases can foster tumor formation and about 20% of human cancers are linked to infections[5]. *Helicobacter pylori* is a well-characterized example where gastritis caused by bacterial infection has been shown to markedly increase the risk for outgrowth of stomach cancer and also associated with gastrointestinal lymphoma[6, 7].

Beside the impact of extrinsically-induced inflammation processes for the induction of cancer, tumor cells also tend to modulate immune cells to establish a beneficial niche for their survival. For example, genetic mutations in cancer cells can trigger aberrant production of inflammatory mediators, which create an inflammatory microenvironment that further exacerbates tumor formation. For example, aberrant Ras-Raf signaling, a pathway that is frequently mutated and aberrantly activated in many cancers, can drive tumor-promoting inflammation to a certain extent[8].

Hence, chronic inflammation shares various signaling pathways and molecular targets with the carcinogenic process[2].

The concept of 'cancer immunoediting' describes the many facets of an interaction between the immune system and the tumor and is composed of three phases - elimination, equilibrium, and escape[9]. In the elimination phase of cancer immunoediting, the innate and adaptive arms of the immune system become alerted to danger signals deriving from stromal remodeling processes as a result of tissue disruption or from oncogene-induced transformed cancer cells themselves[10]. This phase represents the phase of an intact immunosurveillance, as immune cells detect and eradicate malignant cells before they become clinically established tumors [2, 9, 10]. During elimination phase, the balance favors an anti-tumor immune response due to an increase in expression of tumor antigens, MHC class I, Fas and TRAIL receptors on tumor cells and perforin, granzymes, IFN-γ, IL-12, and TNF-α in cells of the tumor microenvironment[2].

Equilibrium is the second phase of cancer immunoediting where the immune system is able to sustain the tumor in a state of functional dormancy[2, 9, 10]. However, some cancer cells evolve under the immune pressure and manage to resist immune recognition, for example through defects in antigen presentation and induce immunosuppression through upregulation of immune checkpoint molecules, such as PD-L1[2, 9]. In this phase, a balance exists between anti-tumor and tumor-promoting cytokines (IL-10, IL-23)[9, 10]. During the escape phase of cancer immunoediting, the immune system is no longer able to restrict tumor outgrowth and tumor cells manage to evade immune recognition[2, 9, 10]. The ability of the malignant cells to escape from the immune system's surveillance is assigned to acquired traits, such as the loss of tumor antigens, MHC I or co-stimulatory molecules, an increased expression of molecules, associated with survival (anti-apoptotic molecule Bcl-2), immunosuppression (IDO, PD-L1), resistance (STAT-3), and secretion of cytokines that can enhance angiogenesis (VEGF, TGF-β, IL-6, M-CSF)[2, 9, 10]. In addition, the immune cells within the microenvironment can promote the shifted balance towards tumor progression through the production of immunosuppressive cytokines and molecules such as IL-10, TGF-β, VEGF, IDO, PD-L1[2, 9, 10].

One disease that merits considerable attention in connection with chronic inflammation is chronic lymphocytic leukemia[11]. Initiation and progression of chronic lymphocytic leukemia are believed to result from the paradox situation of excessive inflammatory response on the one side and a poor response to infectious stimuli on the other side, suggesting that chronic inflammation is of prime importance for the pathophysiological role in this disease[11].

1.2 Chronic Lymphocytic Leukemia

Chronic lymphocytic leukemia (CLL) is the highest-incidence leukemia in Northern America and Europe, with an age-adjusted incidence rate of 4.7 newly diagnosed cases per 100,000 people and 1.3 number of deaths per 100,000 in the US[12]. CLL is a B cell malignancy affecting mostly elderly patients with a median age at diagnosis of 70 years and higher prevalence in males compared to females (1.7:1)[12, 13]. The increased risk of the disease with age and the general increasing life expectancy suggests that the CLL burden will continue to rise in the upcoming years[14].

1.2.1 CLL diagnosis and clinical staging

1.2.1.1 CLL diagnosis

Diagnosis of CLL is performed according to the latest recommendations of the International Workshop on Chronic Lymphocytic Leukemia (iwCLL) guidelines based on blood counts, blood smears, and immunophenotyping of circulating B cells[15]. The following criteria are included in the iwCLL guidelines from 2008 and were confirmed to be up-to-date recently[14]:

One criterion for CLL diagnosis is the presence of lymphocytosis (the abnormal increase in absolute number of blood lymphocytes) with at least 5,000 B cells per µL in the peripheral blood for a duration of at least three months[14, 15]. Furthermore, these highly enriched B cells should display the typical immunophenotype characteristic for CLL which comprehends the co-expression of the B cell surface antigens CD19, CD20, CD23 (whereby surface levels of immunoglobulin, CD20 and CD79b are typically low compared with the levels on normal healthy B cells), and the T cell antigen CD5[14, 15].

Typically, CLL is composed of one single B cell clone[14, 15]. Two types of light chains are found in immunoglobulin molecules, either the lambda chain or the kappa chain[16]. Since all progeny of a particular B cell will carry an identical light chain, testing for the expression of either kappa or lambda light chains is used in diagnosis to confirm the clonality of the CLL cells[14, 15, 16]. Morphologically, CLL cells appear as small mature B cells, with a compact nucleus filling the cell, surrounded by a narrow cytoplasm[14, 17]. Nucleoli are not or only rarely found and the chromatin appears to some extent aggregated[14, 17]. Besides the typical CLL cells, a larger fraction of smudge cells is found in blood smears of patients as a result of crushed cells during slide preparation[14, 17]. Moreover, prolymphocytes characterized by a single clear nucleolus and larger size as compared to CLL cells can also be identified in patients' blood smears[14, 17].

Other tests that are performed at diagnosis of CLL are molecular cytogenetics to determine aberrations in karyotype or frequently mutated genes like TP53, mutational status of

immunoglobulin genes (IGVH, VH3.21 usage) expression of ZAP-70 or CD38, quantification of serum markers (CD23, thymidine kinase, and β2-microglobulin), and bone marrow examination[14]. However, these tests are not required to establish the diagnosis but may help to predict prognosis in CLL[14].

Notably, CLL shares commonalities with other malignancies and thus needs to be distinguished from these: Small lymphocytic lymphoma (SLL) represents a malignancy of the hematopoietic and lymphoid tissue being mainly characterized by lymphadenopathy and distinguished from CLL by less lymphocytosis and absence of cytopenia[14]. Monoclonal B-lymphocytosis (MBL) is characterized by the presence of less than 5,000 B cells/µL in peripheral blood and concurrent absence of lymphadenopathy or organomegaly, cytopenia, or disease-related symptoms[14, 18]. MBL may progress to CLL at an annual rate of 1% to 2% and is considered as an asymptomatic CLL precursor state[14, 18].

The majority of patients are asymptomatic at the time of diagnosis and treatment is not considered for this group[14]. Patients entering a more advanced disease stage display increased involvement of bone marrow, lymphadenopathy, splenomegaly and hepatomegaly as compared to an early and/or asymptomatic disease stage[14, 15]. Once identified with a symptomatic stage, patients are enrolled into appropriate treatment regiments[14, 17]. Despite initial treatment response some patients eventually display MRD (Minimal residual disease), which might lead to resistance to treatment and relapsed/refractory CLL[14]. Disease progression includes progressive CLL and Richter's Transformation[14]. Richter's Transformation is the emergence of an aggressive transformation of CLL into high-grade lymphoma that is either DLBCL (Diffuse large B-cell lymphoma) or HL (Hodgkin lymphoma) and associated with dismal clinical outcome[19].

1.2.1.2 Clinical staging

Once CLL is clearly diagnosed, one of the two co-existing clinical staging systems, the Rai and Binet staging, named after the first authors of the original publications, are applied [20, 21]. The Rai staging system is practiced more in the U.S. while the Binet staging system is more common in Europe[14, 15]. The Rai staging system defines three risk groups and is based on clinical symptoms of lymphocytosis in the blood and/or marrow, presence or absence of lymphadenopathy, organomegaly (splenomegaly and/or hepatomegaly), anemia and thrombocytopenia[20, 21]. The very similar Binet staging system considers the actual number of the involved areas affected by lymphadenopathy and/or organomegaly. Both systems are widely accepted and serve as a prediction of clinical outcome. However, it was reported that the Rai staging system may have an advantage in the prediction of clinical outcome by a better definition of a subgroup with good prognosis[22].

1.2.2 B cell development and proposed cellular origin of CLL

1.2.2.1 Normal B cell development

B cells undergo several developmental stages during lymphopoiesis, initiated by the differentiation of hematopoietic stem cells (HSCs) that first give rise to multipotent progenitor cells and subsequently either to common lymphoid progenitors or common myeloid progenitor cells[16]. Common lymphoid progenitors subsequently commit themselves either to the B cell lineage or the T cell lineage[16]. In the early stages of B cell development, precursor B cells are generated in the bone marrow where they receive signals from the specialized microenvironment, in particular from stromal cells providing ligands, cytokines, and chemokine[16]. These signals stimulate the rearrangement of the B cells' immunoglobulin genes in order to generate the B cell receptor (BCR) in form of cell surface immunoglobulin M (IgM)[16]. These immature B cells then undergo a process of 'negative selection', eliminating B cells that bind to self- antigens, thereby reducing the BCR repertoire[16]. At this point, immature B cells are ready to migrate out of the bone marrow through the circulatory system to the spleen to proceed through the final transitional stages in B-cell follicles to become fully mature[16]. There, B cells bind to foreign antigens leading to their activation and affinity maturation of the BCR, followed by production of long-lived memory cells and antibody-secreting plasma cells which reside in the bone marrow and lymphoid tissues[16]. The majority of B cells in the secondary lymphoid organs consists of follicular B cells (or B2 B cells) and a minor population of marginal zone B cells, named after their location in the marginal zone of the spleen. Both, follicular B cells and marginal zone B cells, derive from a common lineage and diverge at the transitional stages and are components of the adaptive immune system[16]. In addition, there is a third subset of B cells that are considered as part of the innate immune system, which are B1 B cells[16]. B1 B cells display a high spontaneous production of immunoglobulins and do not depend on T cell help or stromal cell-derived stimuli for their activity[16]. Their BCR shows no signs of affinity maturation and they are not able to develop substantial memory [16]. Different than follicular B cells and marginal zone B cells, B1 B cells are generated from a separate lineage of progenitor cells in the fetal liver during fetal and neonatal stages and are mainly found in the body cavities and only in low numbers in lymphoid organs[16]. In addition, these cells possess self-renewing capacity[16]. However, the knowledge on B1 B cells is mainly gained through mouse experiments and their role in humans is not fully understood[16].

1.2.2.2 Cellular origin of CLL

During the recent years, the concept of CLL as a disease arising from mature B cells was challenged by indications of the involvement of hematopoietic stem cells HSCs as cell of origin of CLL. HSCs from CLL patients transplanted into immunocompromised mice were capable of self-renewal followed by clonal selection of their B cell progeny leading to a CLL-like disease[23]. This indicated the presence of early genetic and/or epigenetic changes in HSCs as a primary event followed by further oncogenic events in the B cell lineage promoting the disease. Some early mutational events identified in multipotent progenitor cells are located in well-known CLL oncogenes (such as *NOTCH1*, *TP53*, and *SF3B1*) and may therefore, serve as driver mutations[24].

Apart from a suggested HSC or early progenitor cell as origin of CLL, B1 B cells had been proposed as the direct precursor cell for the CLL clone[25, 26]. In contrast to B cells from the conventional B2 lineage, B1 B cells (in particular B1a B cells) express CD5 on their surface[27]. The self-renewal capacity of B1 cells prompted the question whether $CD5^+$ B1 B cells might be the cellular origin of CLL with increasing age.

The discovery of the two main CLL subsets, cases with mutated (M-CLL) or unmutated (UM-CLL) immunoglobulin genes led to the assumption that M-CLL must derive from a cell that has undergone somatic hypermutation of the BCR genes in the germinal center[28].

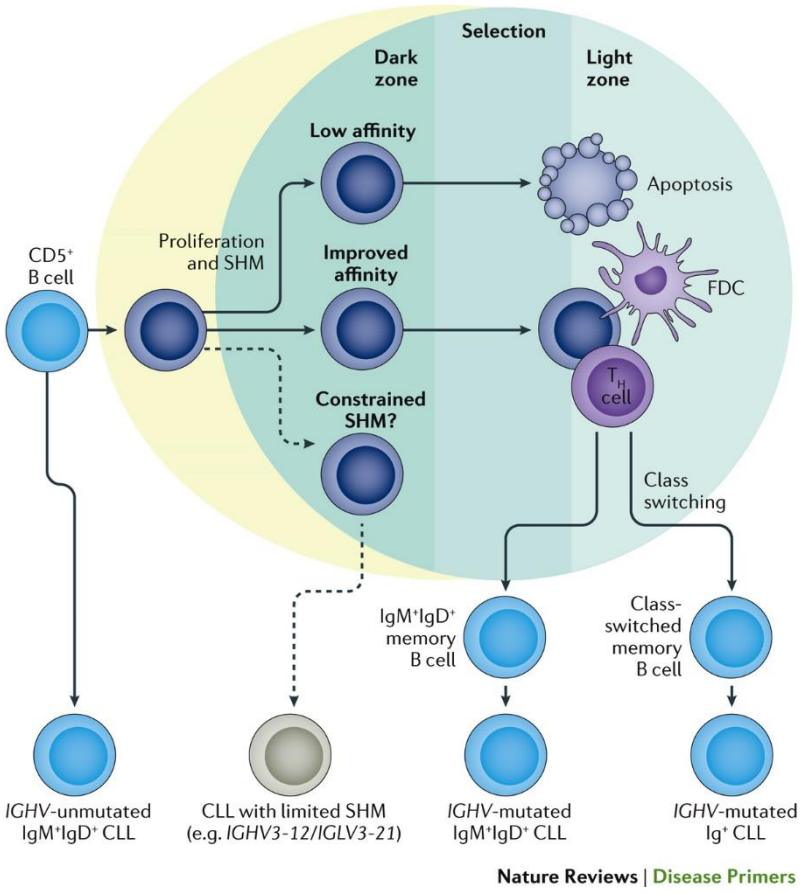

Figure 1: Cellular origins of CLL.
This figure is derived from Kipps, T. J. *et al. Nature Reviews Disease Primers*, 2017[17].

Therefore, the proposal of B1 B cells as the cell of origin for all CLL subtypes became incompatible leaving still the possibility that UM-CLL could be derived from naïve B cells that have not gone through germinal center maturation. A detailed gene expression profiling study from 2012 included different healthy B cell subsets isolated from human blood and the two main CLL subsets, M-CLL and UM-CLL, and showed high similarities of both CLL subtypes in their gene signature, suggesting that both subsets most likely derive from an antigen-experienced cell[29]. Indeed, in the same study, the existence of a small $CD5^+CD27^+$ post-germinal center B cell population (with CD27 marking somatically mutated cells) was reported and shown to have the highest similarity to CLL cells[29]. Hence, it was postulated that UM-CLL derives from $CD5^+CD27^-$ B cells, while M-CLL derives from $CD5^+IgM^+CD27^+$ B cells. Notably, $CD5^+$ B cells possess similar traits as CLL cells since they were described to possess a tendency for 'stereotyped' BCRs, a hallmark of CLL that will be explained in chapter 1.2.4.2 in more detail[30, 31, 32]. A recent publication further pointed out that early generated B1 B cells can be the origin of a CLL-like disease in aged mice[33]. These B1 B cells were equipped with restricted BCRs and displayed continuous expression of moderately up-regulated c-Myc and down-regulated Bmf[33]. The transcription factor c-Myc regulates cell cycle, as well as apoptosis by targeting

Bcl-2, while reduction of Bmf expression promotes B cell survival with disease development independent of T cells and BCR mutations[33, 34, 35]. A more recent publication with focus on DNA methylation data, not only classified CLL into three subtypes but also demonstrated that CLL tumors originate largely from a continuum of different maturation states, which reflect normal B cell developmental stages[36]. Even though the authors did not include $CD5^+$ and $CD5^-$ B cells into their analyses, they could demonstrate that CLL cells resemble memory B cells with respect to their global methylation landscape, as they exhibit ~70-100% of the pattern for high-maturity memory B cells[36]. However, despite several proposed hypotheses, the precise cell of origin of CLL is still under debate and active investigation.

1.2.3 Genetic alterations in CLL

There exists a high degree of genetic variability in CLL, involving several cellular pathways and functions, such as cell cycle, apoptosis, NOTCH signaling, WNT signaling, inflammatory pathways, RNA processing, DNA damage, chromatin remodeling and transcription regulation, and B cell receptor-related pathway[17, 37].

Despite the highly diverse mutational landscape in CLL patients, there is a small number of consistently recurrent genetic alterations including chromosomal alterations, somatic mutations, and epigenetic alterations[17, 37]. The mechanisms of pathogenesis of CLL remain elusive because no genetic alteration has been ultimately proven to initiate CLL development.

1.2.3.1 Recurrent chromosomal alterations and somatic mutations

By using fluorescence in situ hybridization (FISH) to detect chromosomal aberrations in 325 CLL cases, over 80% of patients were shown to carry chromosomal abnormalities at diagnosis[38]. The five most common chromosomal abnormalities are deletion in 13q (55%), deletion in 11q (18%), trisomy of 12q (16%), deletion in 17p (7%), and deletion in 6q (6%)[38]. These aberrations helped to define several risk groups and serve as useful predictors for survival[38]. Deletion of 17p or 11q predicts poor survival, whereby 17p deletion forecasts the worst prognosis[38]. They are followed by 12q trisomy and normal karyotype cases[38]. Interestingly, patients with 13q deletion as a single aberration had the longest estimated survival time[38]. The prognostic value of these chromosomal alterations helped in improving treatment decisions.

For some of these aberrations, disease-associated genes have been identified. The most common chromosomal alteration, del13q contains the *DLEU2/miR-15a/16-1* cluster within the deleted region[39]. This cluster was suggested to exhibit a tumor suppressor role in CLL through

downregulation of genes controlling cell cycle entry and by this controlling the expansion of the mature B cell pool[39]. MiR-15a and miR-16-1 expression were also shown to be inversely correlated with Bcl-2 expression in CLL[40]. Both microRNAs were able to negatively regulate Bcl-2 at a posttranscriptional level and their absence was shown to trigger apoptosis resistance in cell lines[40]. The 17p deletion leads to the loss of the tumor suppressor gene TP53[41]. And deletion of the 11q region is mainly linked to alterations in the ATM gene coding for a protein that is important for DNA repair[42, 43, 44]. The impact of trisomy 12q and chromosome 6q deletions on disease relevant genes and pathways remain yet unclear and are under current investigation.

The most recent insights into the genomic landscape of CLL are attributed to next generation sequencing techniques that tremendously helped to identify biologically relevant mutations in CLL and their frequencies. The spectrum of somatic mutations found in CLL comprises a long list of affected genes involving several cellular pathways. Some of the most recurrent somatic mutations found in patients involve *NOTCH1*, *TP53*, *SF3B1*, *ATM*, *POT1*, *PAX5*, *MYD88*, and *CHD2*[37, 45]. The most recurrent genetic alterations including chromosomal aberrations and somatic mutations and their contribution to biological pathways are illustrated in Figure 1.

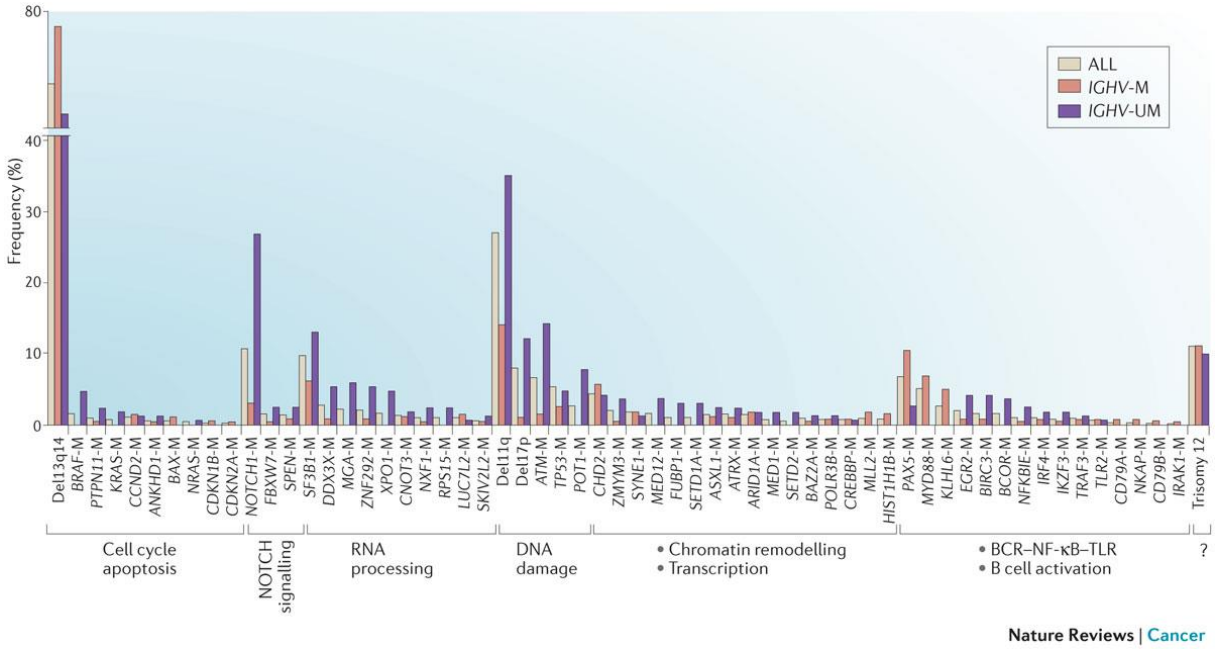

Figure 2: The genetic landscape of CLL.
The percentage of patients with CLL who harbor recurrent CLL-associated genetic lesions grouped according to biological pathways in which they are involved. The frequency of genetic alterations in unselected cases (ALL) (grey) and in the IGHV-M (red) and IGHV-UM CLL (purple) subgroups. This figure is derived from Fabbri and Dalla-Favera, *Nature Reviews Cancer*, 2016[37]. IGHV-M and IGHV-UM further referred to as M-CLL and UM-CLL in this work.

Recent attempts were aiming at studying clonal evolution in CLL and the identification of tumorigenic driver mutations on one side and passive, passenger mutations on the other side[46]. For this purpose, the frequency of mutations in a few pre-treatment, post-treatment, and relapsed patients was monitored and indeed was reported to change over time, reflecting a dynamic composition of subclones[46]. Moreover, the patterns of clonal evolution appear rather heterogeneous between patients, whereby a relatively stable molecular phenotype is correlated with milder disease progression and better drug response, whereas an increased subclone development rather correlates with resistance to treatments and bad disease outcome[46]. Larger cohort studies confirmed indications for clonal evolution when comparing matched pre-treatment samples with samples from relapsed patients[46, 47]. Notably, subclone development was already identified in the pre-treatment samples[46, 47]. Moreover, the dynamic intra-tumoral genetic heterogeneity may provide insight into the order of mutation acquisition in CLL and therefore may be indicative of events present in the founder subclone in contrast to later occurring events[47].
Hence, the overall goal of such large-scale longitudinal studies will be the implementation of the gained information into the improvement of response prediction for individual patients for instance through earlier targeted and sequential treatment directed against CLL subclones.

1.2.3.2 Epigenetic changes

Comparing CLL methylomes to several normal mature B cell subsets using whole-genome bisulfate sequencing and microarrays disclosed a widespread hypomethylation of DNA, affecting mostly enhancer loci, combined with local hypermethylation[48]. Interestingly, the two CLL subtypes, UM-CLL and M-CLL, display differential DNA methylation profiles and further seem to reflect the methylation imprint of naïve and memory B cells, that have been proposed as their putative cells of origin[48, 49]. Intra-tumoral DNA methylation studies revealed that the CLL methylome is remarkably stable over time when comparing samples at diagnosis with follow-up samples[49]. Similarly, also resting CLL cells derived from peripheral blood (G0 or early G1 phase of the cell cycle) and CLL cells from lymph nodes of the same patients showed a relatively similar methylation profile[49]. In contrast to the overall maintenance of DNA methylation profiles within individuals, a high degree of methylation heterogeneity between different patients was observed[50, 51]. Moreover, the genetic evolution of CLL mentioned before is similarly reflected in the 'methylation evolution': High levels of stochastically disordered intra-sample methylation heterogeneity correlate with high-risk genetic lesions, CLL clonal evolution, and an adverse clinical outcome[50, 51]. Hence, the methylation profile in CLL may be used to further support clinical subgroup classification for optimal risk management.

1.2.4 B cell receptor signaling

Two forms of B cell receptor signaling are distinguished, which are termed 'active' and 'tonic' BCR signaling[52]. Active BCR signaling is initiated in an antigen-dependent fashion and leads to the initiation of germinal center reactions, while tonic BCR signaling most likely appears in an antigen-independent fashion leading being required for B cell survival[52].

1.2.4.1 BCR signaling in normal B cells

The BCR is composed of membrane-bound immunoglobulin molecules that are able to bind antigen, which results in receptor aggregation and thus initiation of active BCR signaling[52]. Two heavy and two light chains form the mIg, which is non-covalently bound at the cytoplasmic part of the receptor to a heterodimer consisting of the subunits CD79a and CD79b. These proteins pass on signals through their immune-receptor tyrosine-based activation motifs (ITAMs) to the cell interior as illustrated in Figure 3[52, 53]. The aggregation of the BCR leads to phosphorylation of ITAM tyrosines by SRC-family kinases, including LYN, BLK5, and FYN[54]. Next, the tyrosine kinase SYK is recruited to the phosphorylated ITAMs leading to its phosphorylation and activation by SRC-family kinases and by autophosphorylation[55]. The SRC-family kinases together with SYK form a 'signalosome' assembling various other kinases and adaptor proteins[52]. SYK recruits a complex of CIN85 and BLNK, which in turn coordinates the phosphorylation and activation of BTK followed by PLCγ2 activation[56]. The signaling enzyme PLCγ2 then catalyzes the hydrolysis of PIP2 into DAG and IP3 triggering calcium release[52]. DAG and the increased intracellular calcium level are required for activation of PKCβ, which in turn phosphorylates different molecules, among others CARD11, a signaling adaptor that orchestrates a signaling complex for the activation of the nuclear factor-κB (NF-κB) pathway[57].

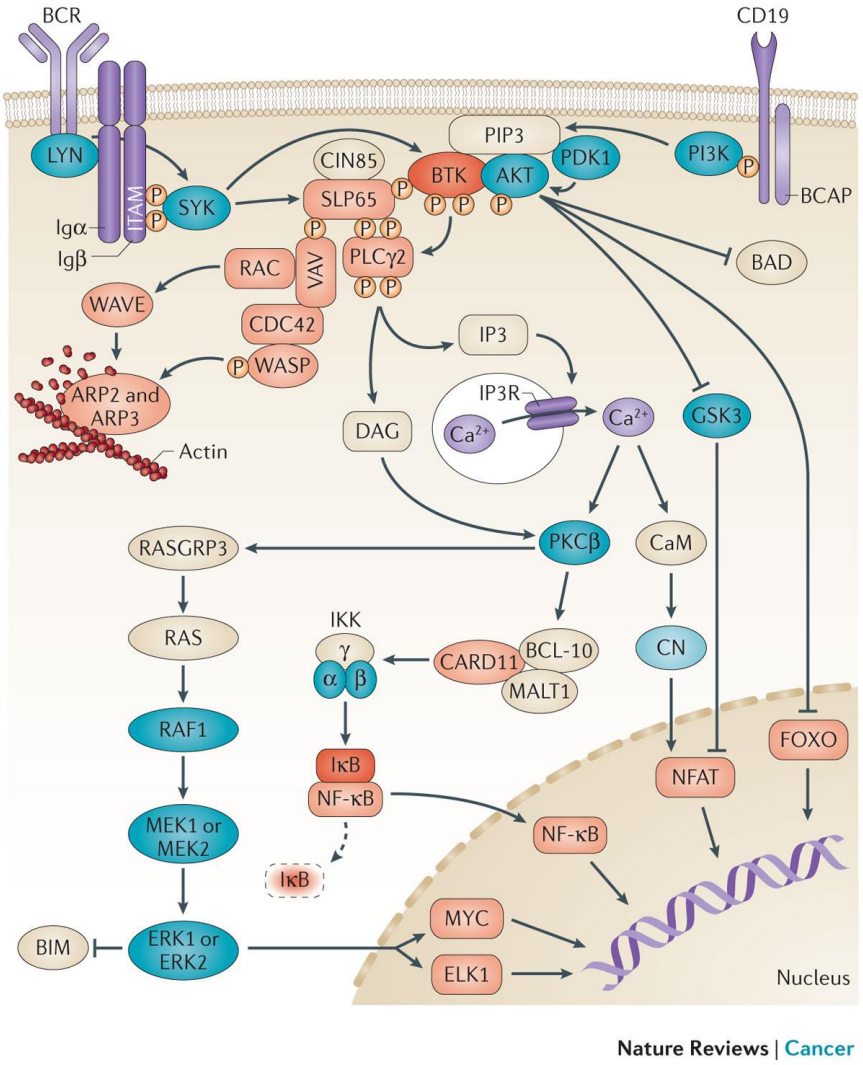

Figure 3: B cell receptor signaling.
This figure is derived from Hendriks, Yuvaraj & Laurens; Nature Reviews Cancer, 2014[58].

In parallel, the transmembrane receptor CD19 is phosphorylated by the SRC family kinase LYN, recruiting PI3K to the BCR. PI3K phosphorylates PIP2 resulting in generation of PIP3, which is responsible for recruitment of BTK and AKT to the plasma membrane[59]. The result of proximal BCR signaling is the activation of NF-κB, PI3K, MAPK, NFAT and RAS pathways, which promote proliferation and survival of normal as well as malignant B cells[60].

1.2.4.2 BCR signaling in CLL and the central role of BTK

BCR expression is a hallmark of CLL, but it has been unclear whether the leukemia is actually driven by BCR signaling and specific antigens. One-third of CLL patients, including both M-CLL and UM-CLL cases, carry highly similar BCR immunoglobulins, referred to as 'stereotyped' BCRs[32]. Out of the repertoire of 65 existing functional human IGHV gene segments, only a few are found to be

expressed in CLL[32, 61]. This limited use of variable regions of Ig genes and the selection of stereotyped BCRs indeed highly suggest a role for involvement of specific antigens. Candidate antigens proposed include proteins associated with apoptotic cells and known self-antigens[31, 62, 63, 64].

Indeed, for a subset of CLL cases, it has been demonstrated, that BCR signaling does not dependent on exogenous antigens[64]. Instead, BCR activation involves the binding of one region of the BCR (the heavy-chain complementarity-determining region) to self-epitopes on variable regions of the receptor itself[64].

The two main outcomes of BCR signaling in CLL are either enhanced B cell activation or B cell anergy, a state defined by unresponsiveness to antigen stimulation[65]. While the latter outcome is less well understood in the context of CLL, it seems to involve activation of inhibitory molecules accompanied with only restricted activation of pathways typically associated with B cell activation[65]. One important molecule suggested to be involved in the limitation of B cell activation is SHIP1 which is counteracting the activity of PI3K[66, 67]. Interestingly, B cell anergy predominates in M-CLL cases while elevated B cell activation is more commonly observed in UM-CLL cases[68]. As anergic B cells are less expected to proliferate, this is in line with the observation of a rather indolent disease course for M-CLL[69].

In support of that, ZAP70, a paralogue of SYK, is expressed in UM-CLL but not the M-CLL subtype and capable of enhancing BCR signaling[70, 71]. Another molecule that has a central role in BCR signaling is Bruton's tyrosine kinase (BTK)[68]. In some patients, BTK is overexpressed and constitutively phosphorylated[72]. Activation of BTK is initiated by its association with the cell membrane and its phosphorylation by a SRC kinase or SYK, at position Y551 in the kinase domain[73, 74]. This results in the autophosphorylation of BTK at position Y223 promoting its catalytic activity[73, 74]. BTK is mostly responsible for the phosphorylation of PLCγ2 which induces its lipase activity [75]. Moreover, BTK is important for BCR-mediated NF-κB signaling, exemplified by the lack of NF-κB activation upon BCR stimulation in BTK-deficient B cells[76, 77]. However, T cell-dependent NF-κB activation that is mediated by CD40 ligand (CD40L)–CD40 interaction between T cells and B cells, respectively, remains unchanged[76, 77].

1.2.5 Tumor microenvironment in CLL

During the recent years, researchers have solidified the pivotal role of the tumor microenvironment (TME) in cancer development[1]. The TME comprises a diverse composition of cells that in addition to cancer cell-intrinsic traits, contribute to tumorigenesis[1]. The dependency of CLL cells on the crosstalk with non-malignant accessory cells in the tissue TME is exemplified by their characteristic to rapidly undergo apoptosis *in vitro*, when cultured in monocultures[78]. This illustrates that apoptosis resistance, one of the hallmarks of cancer, is not a cell-intrinsic feature of CLL cells[1]. In contrast, survival of CLL cells depends on the presence of non-malignant bystander cells or on soluble factors released by them [79, 80, 81, 82]. While CLL cells in peripheral blood attain a gene expression profile similar to that of resting, non-proliferative cells, active division of CLL cells (0.1-1% proliferation of the entire CLL clone per day) is locally restricted to proliferation centers or so-called pseudofollicles in the lymph nodes, the bone marrow, and the spleen where the cells are in close proximity to bystander cells[62, 70, 83, 84, 85]. The importance of microenvironmental signals is further underscored by the observation that the expression of genes involved in CLL cell migration and motility are associated with poor prognosis in patients [86, 87]. Hence, gene expression of CLL cells is induced by intrinsic oncogenic hits as well as by extrinsic microenvironmental cues. Indeed, CLL cells also shape their microenvironment by contributing to the recruitment of supportive cell populations[86, 88]. Key players of bi-directional crosstalk between leukemia cells and their niche are stromal cells, endothelial cells, T cells, NK cells, follicular dendritic cells, as well as different myeloid cells (monocytes and macrophages) and communicate via cell-cell contact, soluble factors and, as more recently demonstrated, through extracellular vesicles[89, 90, 91].

Similar to the steady state, **stromal cells** provide CLL cells with different factors and by this mediate tissue homing[16, 92, 93]. Stromal cells secrete the chemokine CXCL12 (also known as SDF-1) that binds to its receptor CXCR4 on CLL cells, leading to their attraction to the lymphoid organs, e.g. into the bone marrow[92, 93]. They mediate cell-cell adhesion through the interaction of VCAM-1 or fibronectin with VLA-4 integrins on CLL cells[94]. Moreover, CLL cells (but not normal B cells) can be rescued from apoptosis and conferred with drug resistance by stromal cells as lately exemplified in a study showing that uptake of cysteine (converted from cystine) released from stromal cells compensates for the limited ability of CLL cells to transport cystine for glutathione synthesis[95]. But also stromal cells themselves are a target of different CLL-derived stimuli, for example by CLL cell-derived vesicles that can enhance stromal cells to differentiate into αSMA+ cancer-associated fibroblasts[96].

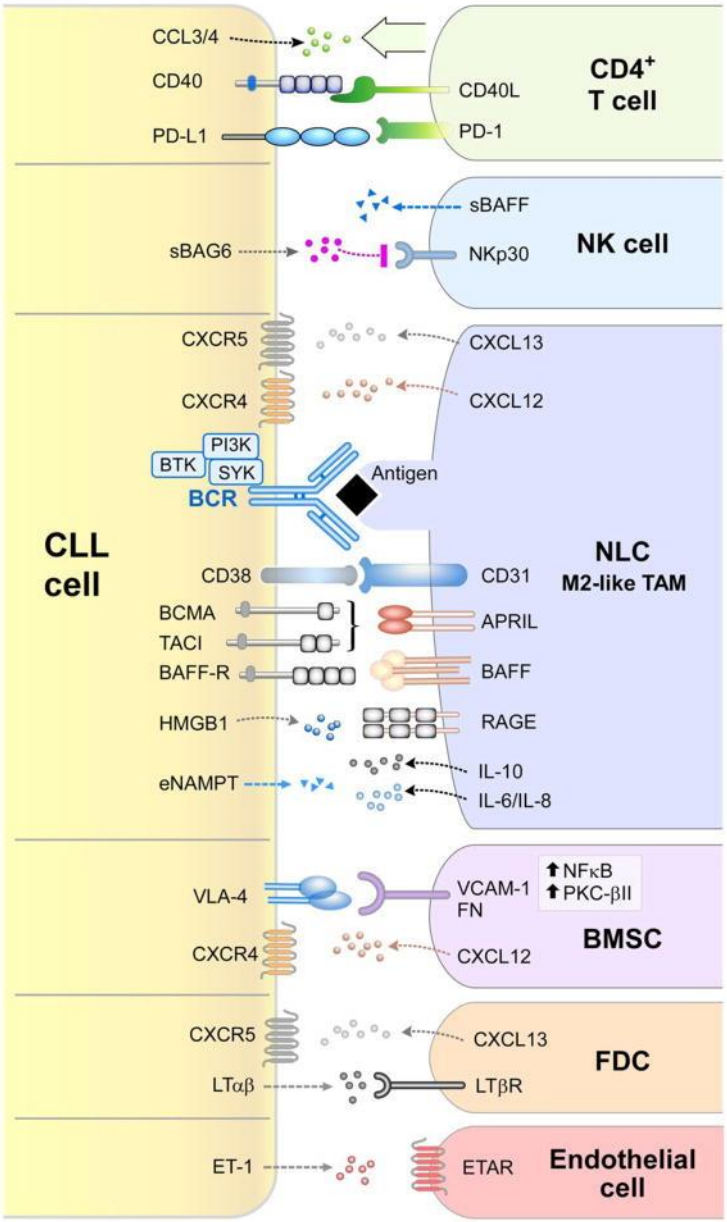

Figure 4: Cellular and molecular components of the CLL microenvironment.
This figure is derived from Hacken and Burger, *Biochim Biophys Acta.*, 2016[89].

Endothelial cells are an additional cellular component of the CLL TME, which induce an increased expression of the survival factor ET-1 in CLL cells in a contact-dependent manner[97]. Endothelial cells (as well as CLL cells) express the ETA receptor on their surface suggesting that CLL-released ET-1 may contribute to establishing a nursing and protective niche by setting up an autocrine loop and/or by acting on the microenvironment[98]. In addition, endothelial cells protect leukemic cells from apoptosis mainly mediated through β1- and β2- integrins[97].

Also, **follicular dendritic cells** attract CLL cells via the CXCL13/CXCR5 axis into the growth-promoting TME of secondary lymphoid organs where they tightly co-localize resulting in a strong ZAP-70/Syk

and BTK activity and enhanced proliferation of the leukemic cells[99, 100]. The expression of LTαβ (lymphotoxin αβ) on leukemic cells activates follicular dendritic cells through LTαβ/LTβR axis leading to upregulation of CXCL13 resulting in a regulatory feedback loop[99]. Follicular dendritic cells have been demonstrated to protect CLL B cells from undergoing apoptosis, at least in part through a CD44-dependent mechanism involving up-regulation of the anti-apoptotic protein Mcl-1[101]. Furthermore, TNF superfamily members BAFF and APRIL are follicular dendritic cell-derived key molecules in normal B cell survival and differentiation and likewise also serve as pro-survival factors for CLL B cells[16, 102]. They can among others be produced by follicular dendritic cells and stromal cells and were suggested to mediate survival in CLL through the NF-κB pathway[103, 104, 105]. Of note, also the normal B cell homeostasis and response to antigen requires the interaction of B cells with the respective cellular counterparts in the healthy microenvironment. Hence, the dependency of CLL cells on their TME partly reflects the natural demand of B cells to receive and send signals from and to their neighboring compartments[89, 90].

In addition, **T cells and Natural killer (NK) cells** contribute to CLL pathogenesis. Both provide pro-survival signals to CLL cells and their functional impairment is of pathological relevance. **T cells** and CLL cells co-localize in the pseudofollicles where T cells facilitate the engagement of CD40 on the leukemic cells promoting survival and proliferation[106, 107, 108, 109]. The T cell compartment in CLL is altered in different ways: Absolute numbers of T cells are elevated while T cell subsets are shifted towards a relative increase in cytotoxic $CD8^+$ T cells[110, 111]. These elevated T cell counts are associated with poor patients' outcome suggesting a tumor-supportive T cell phenotype[112]. Interestingly, T cells from CLL patients are characterized by their inability to form intact immune synapses pointing to a failure of adequate immune response[110, 112, 113, 114, 115]. T cells from CLL patients also highly upregulate the immune checkpoint molecule PD-1, an immune inhibitory T cell exhaustion marker, and its ligand PD-L1 is upregulated on CLL cells, together favoring immune evasion of CLL cells from T-cell cytotoxicity[112, 113].

NK cells in CLL are expanded too and exhibit a reduced cytotoxic capacity linked with low expression of NK cell activating receptors NKp30 and NKGD2[116, 117, 118]. Also CLL and NK cells cross-talk, as for example through soluble BAG6, released by CLL cells, was identified to contribute to the inhibition of NKp30 on NK cells[119].

Another group of immune cells, which play a major role in the CLL microenvironment, are monocytes and macrophages. As they are of special relevance for the current thesis, they will be introduced in more detail in a separate chapter.

In brief, over the last decades many studies have demonstrated that CLL pathobiology is not solely tumor cell-autonomous but rather involves systemic defects in the immune system, chronic

inflammation, and dependency on the TME. Hence, CLL has become a model for research on TME in cancers.

1.3 The myeloid cell lineage

1.3.1 Development of the myeloid cell lineage

Cells of the myeloid cell lineage originate in the bone marrow, initiated by the differentiation of HSCs that first give rise to multipotent progenitor cells and subsequently develop via various myeloid progenitor stages into the different myeloid cell types[16]. Several models for the differentiation of the myeloid cell lineage have been proposed, which predominantly suggest a common myeloid progenitor cell (CMP) expressing the surface glycoprotein CD34, but not the stem cell antigen-1 (SCA-1) as earliest precursor cell [120, 121, 122]. CMPs give rise to granulocyte and macrophage progenitor cells (GMPs), characterized by expression of the Fcγ receptors CD16 and CD32[120]. Subsequently, GMPs diverge into (1) granulocyte progenitor cells (GP), serving as a source for basophils, eosinophils, and neutrophils, or (2) myeloid-dendritic progenitor cells (MDP)[123]. The latter cell population is characterized by the expression of the CSF-1 receptor (CSF-1R), CX3CR1 and Flt-3 (CD135)[124, 125]. MDPs serve as progenitors for osteoclast (bone marrow macrophages) precursors and common monocyte precursors (cMoP) [126, 127, 128]. cMoPs subsequently differentiate into monocytes in response to CSF-1 and are then released into the circulation[128]. Monocytes then further differentiate into dendritic cell (DC) subsets[125, 129, 130]. In addition, conventional and plasmacytoid DCs can also arise directly from MDPs[125, 129, 130]. There are reports on a common DC precursor cell (CDP), proposed to be DC-restricted, but this is still under debate[125, 131, 132].

1.3.1.1 The central role of the CSF-1/CSF-1R axis

The CSF-1/CSF1-R axis plays a crucial role in pushing the different progenitor cells towards their fate and is also of special interest regarding the current work. CSF-1 is a glycoprotein that was initially shown to stimulate the formation of macrophage colonies[133]. Subsequently, the CSF-1 receptor (CSF-1R or cFms) was identified and described to possess intrinsic tyrosine kinase activity[134, 135]. The receptor is expressed at low levels on HSCs and at higher levels on monocytes and tissue macrophages, osteoclasts, myeloid dendritic cells, and microglia and is responsible for the development of these cell types[134, 136, 137, 138, 139, 140]. CSF-1R downstream signaling promotes a number of pathways leading to (1) myeloid differentiation, (2) monocytic commitment, and the (3) survival, proliferation as well as chemotaxis of macrophages[141].

For example, during differentiation of GMPs (1) that is initiated by the CSF-1R, Erk1/2 plays a central role[142, 143]. Moreover, further commitment to the monocytic cell fate (2) is instructed through the CSF-1R-mediated up-regulation of the myeloid transcription factor PU.1[137]. Additionally, CSF-1/CSF-1R-mediated macrophage survival and proliferation (3) involves several pathways including PI3K, Akt, and Mek[144, 145, 146, 147, 148, 149]. Despite the important role of the CSF-1R signaling, additional factors, such as CSF-2, IL-3, and IL-4 are involved in driving the different progenitor cells towards their fate, which is also dependent on the context[150, 151]. For example, CSF-1 receptor downstream signaling together with IL-4 is required for Langerhans cell development and leads to inhibition of dendritic cell differentiation – illustrating the complexity of myeloid cell development[152].

1.3.2 Monocytes, macrophages and dendritic cells in steady state

1.3.2.1 Monocytes

After being generated in the bone marrow from cMoP cells, monocytes enter the bloodstream, from where they can again be recruited into different tissues of the body[153]. Monocytes have been regarded for a long time to mainly serve as precursors for macrophages in tissues. This is a well-accepted concept as for example blood-derived and bone marrow-derived monocytes can be differentiated into macrophages with serum or adequate growth factors such as CSF-1 *in vitro*. However, this view is currently being revised based on reports about the existence of tissue-resident macrophages[154].

Two subsets of circulating monocytes exist: The first is thought to remain in the vasculature and 'patrol' the blood vessels with endothelial cell-supporting function while the second type acquires the ability to migrate through the endothelium into tissues and lymphoid organs once receiving respective signals. Accordingly, the first subset is usually referred to as 'patrolling monocytes' and the latter as 'migratory monocytes' or even more commonly as 'inflammatory monocytes' since they can be recruited to the site of inflammation.

However, this terminology might be misleading as migratory/inflammatory monocytes also perform constitutive extravasation independent of incoming inflammatory signals[155]. In this context, expression of the chemokine receptor CCR2 on migratory monocytes has been reported to facilitate egress from the bone marrow[156]. Moreover, these cells gain many properties in response to inflammation and substantially help to dissolve inflammation and restore normal tissue structure and function[157]. An alternative terminology for the two distinct subsets of monocytes (used throughout this thesis from here on) is based on their typical surface expression of marker proteins. Marker proteins that distinguish the two monocyte subsets in humans are CD14 and CD16, whereby inflammatory monocytes show high expression of CD14, whereas patrolling monocytes

are recognized by high CD16 expression[158, 159]. In mice, high Ly6C expression (Ly6C^{high}) is typical for inflammatory monocytes and low Ly6C expression (Ly6C^{low}) for patrolling monocytes.

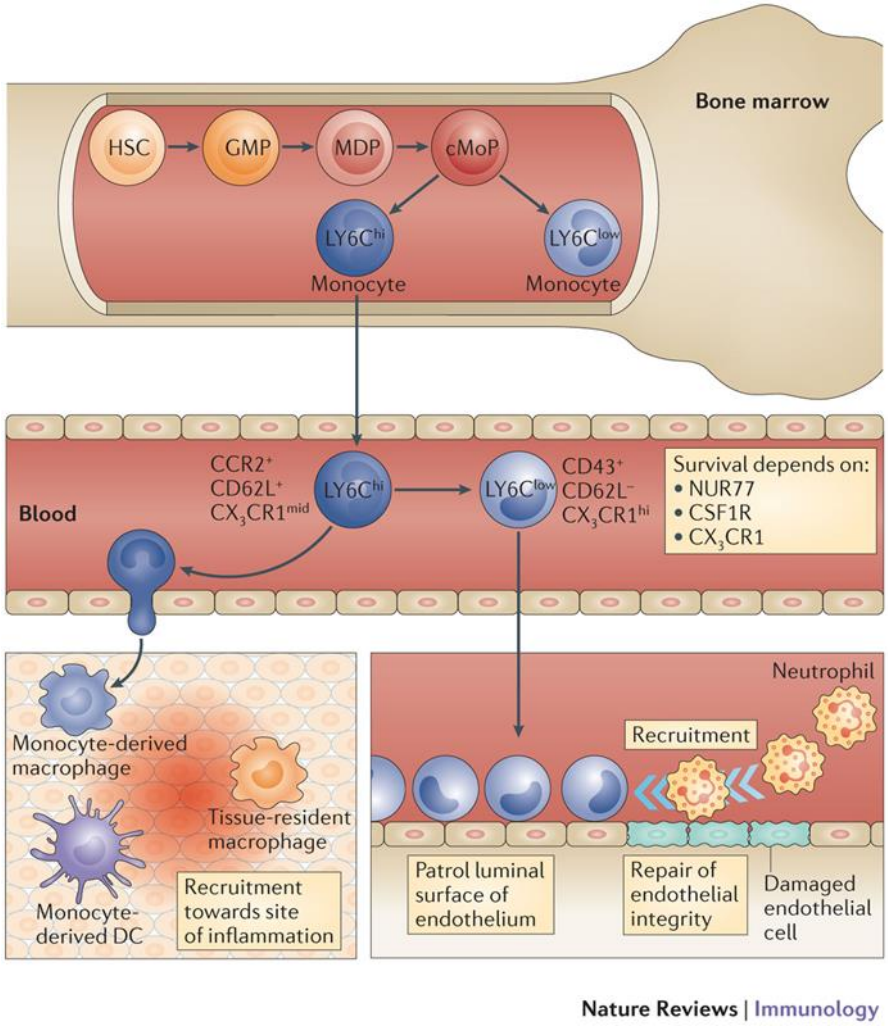

Figure 5: The mouse monocyte compartment.
This figure is derived from Ginhoux and Jung *Nature Reviews Disease Primers,* 2014[128].

Notably, a direct lineage dependency between the two subsets is widely accepted by now, with Ly6C^{low} monocytes arising from their Ly6C^{high} counterparts[160]. However, not much is known about the details which mediate monocyte cell fate. The transition from Ly6C^{high} to Ly6C^{low} monocytes is believed to occur in a NR4A1-dependent manner[161, 162]. Also, CX3CR1 has been reported to be highly expressed on Ly6C^{low} monocytes and is important for their survival[163]. More recently, a study revealed that DLL1 expression on endothelial cells mediates the transition of Ly6C^{high} to Ly6C^{low} monocytes via NOTCH signaling[164]. In steady state, Ly6C^{high} monocytes have a short half-life in the circulation of approximately 1 day and rapidly convert into Ly6C^{low} or migrate from the circulation into the tissue as exemplified in experiments with parabiotic mice, showing that donor Ly6C^{high} monocytes do not reach equilibrium with host Ly6C^{high} monocytes[155, 160, 165].

Besides their role to serve as a source for macrophages and dendritic cells, monocytes play a crucial role in host defense as players of the innate immune system[166, 167]. Notably, work by several groups has now demonstrated a role for Ly6C^{high} monocytes in adaptive immunity mediated by their ability to present antigens to cognate T cells, supporting their differentiation in T helper cell subsets, follicular T cells, and cytotoxic CD8$^+$ T cells [157]. Yet, it is unclear whether monocytes are poor antigen presenting cells (APCs) or perform antigen presentation in a similar fashion as dendritic cells, the so-called 'professional' APCs of the immune system[157]. Last but not least, monocytes are also involved in the suppression of T cell immunity by three different mechanisms: (1) direct killing of effector T cells or antigen-bearing DCs via nitrogen or oxygen, (2) indirect killing of T cells as a result of amino acid deprivation, and (3) suppressive effect on T cell function through enhanced Treg production, induced by recruitment of IL-10 producing monocytes[168, 169, 170].

1.3.2.2 Macrophages

During inflammation and injury, monocytes are attracted by a number of pro-inflammatory mediators and terminally mature in the tissues into long-lived macrophages[157]. In addition, most tissues contain also tissue-resident macrophages that develop from embryonic monocyte precursor cells in the yolk sac and fetal liver and possess self-renewing capacity[128, 154]. Historically, these tissue macrophages were given specific names, such as red pulp macrophages (in the spleen), microglia (in the brain), alveolar macrophages (in the lung), Langerhans cells (in the skin), Kupffer cells (in the liver), and osteoclasts (in the bones)[152, 157]. Depending on the tissue site, macrophages fulfill a number of trophic functions and are involved in bone morphogenesis, ductal branching, and neural networking[152]. Besides granulocytes and dendritic cells, macrophages together with monocytes are the main phagocyting cells of the immune system[16, 157]. Macrophages constitutively express pattern recognition receptors (PRRs) such as toll-like receptors (TLRs) that enable them to recognize extracellular and intracellular PAMPs (pathogen-associated molecular patterns) and DAMPs (damage-associated molecular patterns)[16].

In addition to first-line pathogen defense, macrophages orchestrate immune functions, help induce inflammation, and produce a number of cytokines and chemokines that recruit and activate other cells of the immune system, which results in the release of ROS, high expression of inflammatory cytokines (e.g. IL-12), and upregulation of MHC class II (MHC-II) molecules[171, 172]. Much effort was spent to classify macrophage subsets that are simplified referred to as pro-inflammatory versus pro-resolving, or M1-type versus M2-type macrophages, respectively, mirroring T helper type 1 (Th1) and T helper type 2 (Th2) polarization[172, 173]. However, these terms have become mostly obsolete and many more subsets have been discriminated reflecting the 'macrophage plasticity'

that depends on the signals in their local microenvironment[172]. The main two phenotypes of macrophages can be recapitulated *in vitro* by their stimulation with lipopolysaccharides and IFN-γ (M1-like) or IL-4 (M2-like), respectively[174, 175]. However, cross-differentiation of macrophages in yet undefined numbers of phenotypes during the course of an immune response is very likely[152].

1.3.2.3 Dendritic cells

Similar to monocytes and macrophages, also dendritic cells develop from progressively restricted bone marrow progenitors[165]. There are two major types of dendritic cells: conventional (or classic) dendritic cells (cDCs) and plasmacytoid dendritic cells (pDCs)[16]. pDCs are thought to be involved in early defense against viral infection, exemplified by their expression of TLRs and high IFN-γ production[176, 177]. They are not considered to perform efficient antigen-specific activation of naïve T cells, exemplified by their low surface expression of MHC-II, co-stimulatory molecules, and also a rapid recycle of their MHC-II molecules. This suggests that they are not capable to present antigen to T cells for longer periods compared to cDCs[178, 179]. However, pDCs have been reported to act as helper cells for cDCs to sustain their secretion of the pro-inflammatory molecule IL-12[180].

In contrast, cDCs make up the majority of dendritic cells and their main role is the uptake of extracellular antigens or viruses and their processing in an increasingly harsh environment[181, 182]. As phagocytes, they alert the immune system that an invader is present via pathways initiated by PRRs, such as TLRs and optimize cytokine secretion to stimulate and direct T cell responses[183]. Eventually, cDCs perform antigen presentation to $CD4^+$ or $CD8^+$ T cells via MHC-I or MHC-II molecules, respectively[184, 185].

In mice, splenic cDCs can be categorized into $CD8^+CD11b^-$ and $CD8^-$CD11b+ dendritic cells[186]. Gene expression (meta) analysis of the transcriptome of several murine and human DC subsets has revealed that mouse $CD8^+$ DCs are related to human $CD141^+$ DCs, whereas mouse $CD11b^+$ DCs are related to human $CD1c^+$ DCs[187]. These two cDC subpopulations possess distinct functions. $CD8^+$ DCs have the potential to induce Th1 responses, cross-prime $CD8^+$ T cells and produce large amounts of IL-12[188, 189]. $CD8^-$ DCs in contrast, do not have the ability to cross-prime $CD8^+$ T cells, but preferentially induce Th2 responses[188, 189]. The $CD8^+$ cDC subset can be further subdivided into $CD4^+$ and $CD4^-$ subsets, whereby the functional differences of these are yet unclear[190]. Moreover, they are also considered as products of separate lineages[191].

1.3.3 Monocytes and macrophages in CLL

In cancer, including CLL, myeloid cells show tumor-induced alterations, even though many of their principal biological pathways are maintained. In addition to stromal cells, follicular dendritic cells, T cells and NK cells, the tumor-supportive microenvironment consists also of monocytes, macrophages and possibly dendritic cells and plays a major role in CLL pathogenesis[89]. Burger *et al.* provided the first evidence for the existence of so-called nurse-like cells (NLCs), which are located in the lymph nodes of CLL patients and were demonstrated to be monocyte-derived[78, 192]. NLCs spontaneously differentiate in high-cell-density co-cultures of CLL cells and monocytes and are able to promote CLL cell survival and drug resistance[78, 192]. A gene expression profiling analysis revealed that NLCs resemble tumor-associated macrophages (TAMs) that were initially described for solid tumors and have features similar to tumor-supportive M2-type macrophages, such as for example expression of CD163[193, 194, 195]. Soluble factors, such as the chemokines CXCL12 and CXCL13 are secreted by NLCs and attract CLL cells through binding to their cognate receptors CXCR4 and CXCR5[196, 197]. Cell-cell contact of NLCs and CLL cells induces pro-survival pathways via the CD38/CD31 axis, and the TNF family members BAFF and APRIL, which interact with their receptors BCMA, TACI, and BAFF-R[86, 104, 198]. Interestingly, the gene expression pattern of CLL cells co-cultured with NLCs is similar to that of CLL cells that were freshly isolated from lymph nodes[62]. Moreover, BCR signaling is activated in CLL cells after co-culture with NLCs[196]. This pointed to the possibility that CLL cells might recognize BCR ligands that are expressed by NLC[199]. The impact of CLL cells on the differentiation of NLCs is based on the observation that $CD14^+$ monocytes from healthy donors differentiated to NLCs in co-culture with CLL cells. In fact, the release of extracellular NAMPT, an enzyme with cytokine-like properties, by CLL cells, with an associated release of tumor promoting and immunosuppressive cytokines such as IL-6, IL-8, and IL-10, respectively, promoted M2-skewing of macrophages[200]. Further, NLC differentiation was shown to be induced by HMGB1/RAGE interaction in which CLL-secreted HMGB1, a chromatin protein secreted by injured or dying cells, leads to stimulation of TLR9-signaling in macrophages[201].

Analysis of monocytes in human CLL blood samples showed an abnormal distribution of the two main subsets of $CD14^+$ and $CD16^+$ monocytes favoring a shift towards the $CD16^{hi}$ (patrolling) subset[202]. This shift was recently confirmed in blood, spleen and bone marrow of leukemic Eμ-TCL1 mice, the most commonly used mouse model for CLL[203]. Moreover, monocytes showed an increased expression and secretion of chemoattractive cytokines, such as CCL2, CCL3, CCL4, CXCL9, and CXCL10, as well as of immunosuppressive IL-10, which are elevated in plasma of diseased mice[203]. These data confirmed previous findings that many of these cytokines are upregulated in

blood serum of CLL patients[79]. CCL2 is one of the factors extensively studied as it was shown to be upregulated in monocytes upon coculture with CLL cells and, similar as in other cancer entities, might be responsible for monocyte recruitment to secondary lymphoid tissues[79]. Additional co-culture approaches also revealed that CLL cells stimulate monocytes to release soluble CD14, which mediates CLL cell survival *via* induction of NF-κB signaling[80]. More recently, the pivotal role of monocytes and macrophages as main drivers of CLL progression was shown in a mouse study using Clodronate liposomes to deplete all phagocytic cells. This resulted in reduction of immune dysfunction and reduced systemic inflammation and impaired disease development[203].

Lately, several studies have proposed the existence of myeloid-derived suppressor cells (MDSC) in CLL[204]. MDSCs are defined as cells of myeloid origin that, due to an imbalance in myelopoiesis, expand in the context of cancer and possess immune-suppressive properties[205]. Accordingly, $CD14^{+}HLA\text{-}DR^{low}$-expressing MDSCs in CLL were described to be increased and to significantly contribute to immune dysfunction in CLL patients[204]. These MDSCs expressed a number of markers associated with an anti-inflammatory, tolerogenic monocyte phenotype as well as with inhibition of T cell response, including PD-L1, CD124, CD163, and HLA-G[204]. Their functional ability to significantly decrease T-cell proliferation and promote T cell differentiation towards immunosuppressive regulatory T cells confirmed their identity as MDSCs[204]. Moreover, this study confirmed that CLL cells actively shape the phenotype of monocytes, as CLL cells, but not healthy B cells, induced the expression of IDO1 on monocytes, which is an important mediator of T cell suppression[204].

A recent study by Haderk *et al*. illustrated that CLL-derived exosomes can be taken up by monocytes, leading to cytokine release and PD-L1 expression in monocytes[91]. The mechanism was proposed to act via binding of hY4 (a noncoding Y RNA enriched in CLL exosomes) to TLR7, initiating the observed downstream effects[91].

The role of dendritic cells in CLL is not as clear as in solid tumors, where a functional impairment of DCs appears as one of the mechanisms of tumor escape from the control of the immune system[206]. However, there are a number of indications that suggest a similar mechanism in CLL, as for example MHC-II was recently reported to be downregulated on dendritic cells of TCL-1 mice[203].

In summary, by a bi-directional crosstalk CLL cells induce major changes in the myeloid microenvironment, in particular mediating an immunosuppressive and tolerogenic phenotype in monocytes and macrophages that might in part explain T cell dysfunction and impaired anti-tumor response in CLL. Consequently, the interaction between CLL cells and their microenvironment is

often accused to be involved in therapy failure and therefore itself is becoming an attractive target for therapy[207].

1.3.4 Targeting myeloid cells in cancer

A number of different monocyte/myeloid cell-targeting strategies have been applied to various cancer models over the recent years that will be briefly introduced in the following section.

(1) Preventing macrophage mobilization and recruitment to the tumor site via blockade of chemokine gradients:

Two examples of well-investigated chemokine axes for monocyte recruitment are CXCL12/CXCR4 and CCL2/CCR2. In a study with a mammary tumor mouse model, which is linked to enhanced CXCL12 production and increased metastasis, the inhibition of CXCR4 reduced invasion, intravasation, and metastasis[208]. Inhibition of CCL2 in a mammary tumor model with pulmonary metastasis blocked the recruitment of inflammatory monocytes that promote metastatic seeding of tumor cells and by this favored the inhibition of metastasis and extended the survival of tumor-bearing mice[209].

(2) Reprogramming/Re-education of M2-like macrophages to receive an anti-tumor M1-like phenotype or improved antigen-presenting capacity:

For example, NF-κB targeting reeducated TAMs as demonstrated by changes towards an M1-like phenotype with higher IL-12 and MHC-II expression levels, but low IL-10 and arginase-1 levels[210]. Tumor regression was promoted and proposed to be a consequence of regained antitumor cytotoxicity and IL-12-dependent recruitment of NK cells[210]. In another study, a small molecule antagonist against the macrophage migration inhibitory factor MIF attenuated its contribution to TAM alternative activation, immunosuppression, neoangiogenesis, and tumor outgrowth in a melanoma mouse model[211].

(3) Enhancing immune responses of antitumor T cells through reprogramming of the immunosuppressive tumor microenvironment via macrophage targeting:

For example, the use of a CD40 agonist showed efficacy in a model of pancreatic ductal adenocarcinoma[212]. CD40 is expressed on APCs and known for its ability to regulate antitumor immune responses, in part by improved immune activation[213]. The application of the CD40 agonist caused macrophages to infiltrate tumors, increase their antigen presentation, upregulate MHC-II and CD86 expression, and disrupted the dense tumor stroma, all together leading to an improved antitumor outcome[212].

(4) Addressing myeloid cell subpopulations in cancer by specific pro-tumorigenic traits, such as angiogenesis:

TIE-2-expressing macrophages have been suggested to limit the success of therapeutic agents that aim at disrupting the vasculature in tumors[214]. Hence, TIE-2-expressing monocytes/macrophages could be targeted using neutralizing TIE-2 antibodies or angiopoietins[215].

(5) Macrophage-depleting strategies involving inhibitors and antibodies against the CSF-1R:

In a mouse model of orthotopically transplanted cancer cell lines, derived from the mammary MMTV-PyMT mouse model, CSF-1R inhibition depleted macrophages within the tumor, accompanied with high numbers of infiltrating cytotoxic T cells and delayed tumor growth[216].

In reality, these different monocyte/myeloid cell-targeting strategies are likely to act through different mechanisms simultaneously such as for example reprogramming (2) and enhancing an immune response of antitumor T cells (3).

In fact, in some studies the applied 'strategy' was not clearly defined in the beginning and such classification rather took place afterwards. The gained results and herein raised questions have been motivating for researchers to unravel the different mechanisms accounting for the various outcomes – particularly understanding the different myeloid subpopulations, such as tissue-resident macrophages, and repopulating macrophages that are derived from blood monocytes and their interplay with cytotoxic T cells in different cancers.

1.4 Genetically engineered mouse models of CLL

Genetically engineered mouse models together with xenograft models represent a valuable tool for studying disease pathogenesis and its underlying asymptomatic disease states. Several genetically engineered mouse models have been generated that mirror human CLL disease. This is exemplified by their common feature of long latency, which mimics human CLL as a disease of the elderly[217]. These mouse models can be divided into two categories: (1) Mouse models mimicking the spectrum of deletions of chromosomal region 13q14, and (2) mouse models mimicking the deregulated expression of genes in human CLL.

The 13q14 deletion models, carrying deletions of varying lengths in the murine chromosome 14qC3 provided the first *in vivo* evidence for a tumor-suppressor function of the most frequent genetic deletion in human CLL patients[38, 39, 218]. Albeit a considerable number of these mice develop CLL-like symptoms, these models possess a relatively low penetrance (20-50%) which makes them rather unsuitable for testing of new therapies or to study the CLL microenvironment[39, 218].

In addition, several mouse models have been generated based on the deregulated expression of genes in human CLL, such as double transgenic mice with overexpression of the anti-apoptotic protein BCL-2 and the tumor necrosis factor receptor-associated factor TRAF, or the Eμ-TCL1 mouse

line [219, 220]. While all the above-mentioned models offer valuable insights into the pathogenic mechanisms of CLL, the Eμ-TCL1 mouse line represents the most comprehensively studied mouse model of CLL, at the same time being a convenient preclinical model.

1.4.1 Eμ-TCL-1 mouse model of CLL

The principle of the Eμ-TCL1 transgenic mouse model is an aberrantly high expression of the T-cell leukemia-1 (TCL-1) gene, a protooncogene originally associated with T cell leukemia and expressed in malignant cells of almost all CLL patients[220, 221, 222]. Although the TCL-1 gene shows variable expression in CLL patients, its expression positively correlates with the aggressive UM-CLL phenotype, 11q deletion and a shorter lymphocyte doubling time[221, 223, 224]. As its name indicates, TCL-1 was identified in T cell lymphomas and leukemias[222]. By introducing the human TCL-1 gene into the murine genome under the control of the IGHV promoter and IGH enhancer (Eμ), the expression of TCL-1 is confined to mature and immature B-cells[220]. These Eμ-TCL-1 transgenic mice develop a CLL-like disease characterized by an expanded $CD5^+IgM^+$ B cell population that is arrested in the G0/G1 phase of the cell cycle[220]. Based on the occurrence of IGHV unmutated BCRs with stereotyped HCDR3 regions, the Eμ-TCL-1 mouse model corresponds to the aggressive, treatment-resistant UM-CLL subtype in humans[221, 225]. Moreover, similarly as in patients, it was reported that autoantigens might play a key role in driving leukemia development in this model[226, 227].

Starting from 4 months of age, CLL-like cells appear first in the peritoneum, then in the peripheral blood and spleen. Finally, at 10 - 15 months of age, the mice develop CLL-like disease affecting almost 100% of the animals[220]. The mode of action through which TCL-1 promotes oncogenic progression was proposed to be through binding and regulation of molecular factors implicated in proliferation, survival, inhibition of apoptosis and epigenetic regulation. In particular, TCL-1 was identified as a co-activator of AKT, a key member of the BCR pathway leading to enhanced AKT kinase activity and its translocation to the nucelus[228, 229]. TCL-1 also interacts with the p300 transcription factor resulting in NF-κB activation in human B cells[230]. Hence, TCL-1 leads to an enhanced BCR responsiveness upon stimulation[224]. However, the long disease latency of CLL in this model may suggest that the ectopic TCL-1 overexpression acts as an initial hit or a predisposing factor for a further oncogenic transformation of B cells. Hence, it is assumed that various other genetic or microenvironmental aberrations may be required for full CLL development[231]. At the same time, this points to the possibility that CLL-associated inflammation may contribute and to some extent drive disease development in these mice. Various genetic players of CLL disease have been extensively investigated in the Eμ-TCL-1 mouse model or after it was crossed with mice of different genetic backgrounds as illustrated in Figure 6[232, 233].

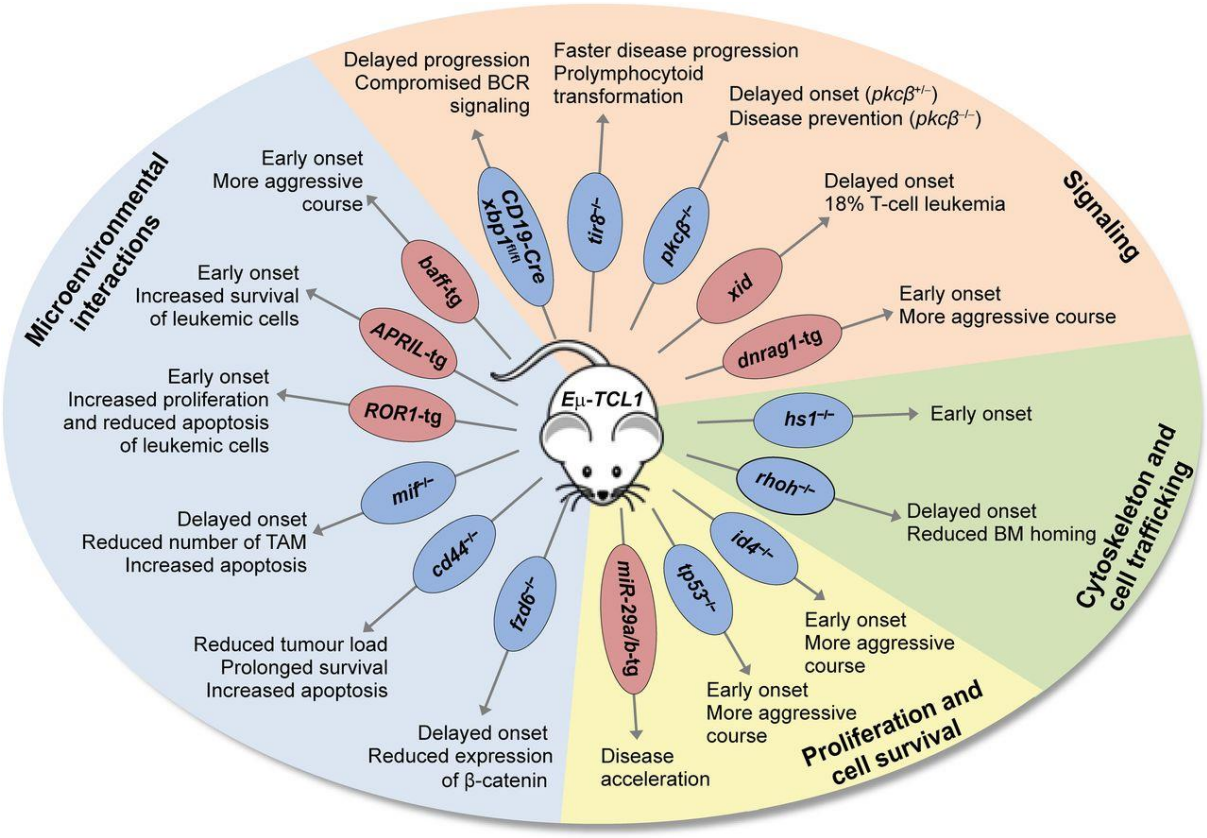

Figure 6: Study of pathogenic mechanisms of CLL in the TCL-1-driven leukemia model.
Various mouse models have been crossed with Eμ-TCL-1 mice to generate overexpression (transgenic [tg]) or deficiency of different molecules in the Eμ-TCL-1 transgenic mouse model resulting in variable effects on the disease phenotype (BM, bone marrow; TAM, tumor-associated macrophages). This figure is derived from Simonetti *et al*., *Blood*, 2014[231].

Microenvironmental interactions have been the focus of several of these studies and play also a major role in this thesis. Ectopic expression of BAFF and APRIL, which mediates the interaction between CLL cells and CLL-associated macrophages in TCL-1 mice led to an accelerated and more aggressive disease development[234, 235]. In a study were Eμ-TCL-1 mice were crossed with (macrophage migration inhibitory factor) MIF-/- mice, animals showed delayed leukemia onset highlighting the role of MIF for disease development[236].

Other players of the TME, such as T cells, have been demonstrated to exhibit dysfunctions in this model, and skewing of subpopulations, similarly as in CLL patients, could be addressed with immunotherapy approaches, again confirming the suitability of this model for studying the CLL microenvironment [237, 238].

However, one downside of the transgenic CLL models including the Eμ-TCL-1 model for their use as preclinical models is the long latency and heterogeneous disease development. This issue can be

solved by adoptively transferring splenic leukocytes or B cells from diseased donor Eμ-TCL-1 mice into syngeneic wildtype or immunodeficient recipient mice, which results in leukemia development within 2 to 3 months[237, 239, 240]. This transplantation method benefits from an accelerated and more homogeneous disease course and a genetically homogeneous population of leukemic mice, thereby allowing for a more systematic study of novel therapies.

1.5 Current and emerging therapies in CLL

A large number of agents are available for treatment of CLL patients covering different categories of therapeutics including cytostatic agents, monoclonal antibodies, small molecule inhibitors, and immunomodulatory agents. For several decades, treatment of CLL included only monotherapy with cytostatic agents: alkylating agents such as Chlorambucil or Bendamustine and purine analogs, with Fludarabine being the most commonly used[14, 241]. The development of Rituximab, a monoclonal antibody against CD20, enabled the introduction of immunochemotherapy as a standard frontline therapy with Rituximab, Fludarabine and Cyclophosphamide (FCR) proven to improve outcome for patients in the CLL8 study of the German CLL study group[242, 243]. A recent, randomized study (CLL10) comparing FCR to Bendamustine and Rituximab (BR) confirmed FCR as standard first-line therapy for fit patients. However, even though the combination with BR was found to be less active than FCR it has been also accepted as an alternative treatment approach for patients with higher comorbidities due to less toxic effects and similar overall survival[244]. Furthermore, the newer FDA approved anti-CD20 antibodies Ofatumumab and Obinutuzumab enriched the options for immunochemotherapy leading to improvement for Fludarabine-refractory patients[245, 246].

Lenalidomide is an immunomodulatory drug, mostly used for CLL second-line treatment with a unique and multifactorial mode of action in CLL, comprising a wide range of immunomodulatory actions, the disruption of interactions in CLL microenvironment and direct effects on the leukemic cells[14, 247]. Its main target is the protein cereblon and Lenalidomide was shown to inhibit the proliferation of CLL cells via a cereblon/p21 (WAF1/Cip1)-dependent mechanism[248, 249]. Lenalidomide shows promising results in the treatment of high-risk CLL patients including patients with 17p deletion, and achieves even better response rates in combination with Rituximab[250, 251, 252].

Especially, the deeper molecular understanding of the BCR signaling gained in the recent years has enhanced the rapid development of novel small molecular inhibitors, including Ibrutinib (a BTK inhibitor which is covered in more detail in the following chapter) and Idelalisib (a PI3Kδ inhibitor) that were included into the therapeutic repertoire for CLL[253, 254].

More recently, Venetoclax was approved for treatment of CLL patients[255]. In CLL, the expression of the anti-apoptotic protein BCL-2 is constitutively elevated facilitating resistance to apoptosis[256]. Venetoclax belongs to the class of BH3-mimetic anticancer agents and mimics the activity of the physiologic antagonists of BCL-2 and related proteins and by this initiates apoptosis of CLL cells[257, 258, 259].

These novel agents more and more shift treatment of CLL from toxic chemotherapy toward specific, low toxic, targeted therapy. The choice for optimal treatment depends on different parameters that need to be considered: the clinical stage of disease, the patient's physical condition and symptoms, genetic alterations (presence or absence of 17p deletion and *TP53* mutations), and response to previous treatment (first or second line treatment)[14, 241].

In addition to approved drugs for CLL, several promising novel agents in phase I-III trials may challenge existing therapeutics and add combination possibilities, such as Ublituximab (anti-CD20), the next-generation BTK inhibitors, Acalabrutinib and ONO-4059, proposed to possess higher specificity for BTK, and additional PI3Kγ and PI3Kδ inhibitors, Duvelisib (PI3Kγ and PI3Kδ inhibitor), and TGR-1202 (PI3Kδ inhibitor)[260, 261, 262, 263, 264].

CAR (chimeric antigen receptor) T cell therapy is another promising approach where autologous T cells are engineered to express artificial receptors that recognize and eliminate tumor cells. In 2011, Porter *et al.* reported the first successful use of CAR T cells generated with a lentiviral vector in 3 refractory CLL patients[265]. The used CAR consisted of an antigen recognition domain for CD19 and an intracellular T cell receptor-ζ (TCR-ζ) (a signal-transduction component of the TCR) domain that was coupled with CD137 (a costimulatory receptor in T cells) causing augmented T cell response and anti-tumor efficacy[266, 267]. Lately, CD19-specific CAR-T cells were shown to be highly effective in relapsed/refractory CLL high-risk patients or patients who have experienced treatment failure with Ibrutinib therapy[266, 268]. However, clinical outcome of CLL patients is inversely correlated with tumor burden which lead to the speculation that excessive tumor mass results in non-functional infused T cells that suffer from exhaustion[269]. Thus, the area of CAR-T cell therapy in CLL remains a challenging field of research.

1.5.1 Targeting Bruton's tyrosine kinase in CLL with Ibrutinib

1.5.1.1 The effect of Ibrutinib on CLL cells

Ibrutinib (also known as PCI-32765) is a small molecule BTK inhibitor that has shown clinical activity in patients with various B cell malignancies, including CLL and mantle cell lymphoma (MCL) [270, 271]. Ibrutinib irreversibly and selectively binds to the C481 site of BTK and by this inhibits its kinase activity with an IC_{50} value of 0.5 nM[272]. BTK was initially discovered in XLA (inherited

immunodeficiency disease X-linked agammaglobulinaemia) patients[273]. XLA patients carry a mutated version of the gene causing defective B cell development and leading to an almost complete absence of B cells and immunoglobulins while other cells remain unaffected[274, 275]. Subsequently, BTK was shown to be involved in BCR pathway as stimulation of B cells induces phosphorylation and kinase activity of BTK[276, 277]. Several findings demonstrated that BTK contributes to the pathogenesis of CLL. BTK was shown to be overexpressed and constitutively phosphorylated in some CLL patients[72]. Overexpression of human BTK in a mouse model dampened sensitivity to apoptosis whereas in a CLL mouse model, BTK deficiency prevented tumor formation[278, 279]. Besides its well-studied role in BCR signaling, BTK is also involved in signaling pathways downstream of other receptors, including G protein-coupled chemokine receptors and Toll-like receptors (TLRs)[280]. Treatment of CLL cells with Ibrutinib inhibits the tonic BCR pathway and reduces survival and proliferation of CLL cells *in vitro*[281, 282]. Ibrutinib treatment also efficiently blocks CXCL12-induced and CXCL13-induced migration of CLL cells *in vitro* suggesting that BTK might be required for migration of leukemic cells to proliferation centres in lymph nodes of patients[281, 282]. Ibrutinib's effect on migration of CLL cells may also explain the induced transient lymphocytosis observed in CLL patients as well as in a mouse model following the initiation of therapy[270, 282]. This mobilization out of the lymph nodes detracts CLL cells from their nursing microenvironment as well as antigenic BCR stimulation[62].

1.5.1.2 The effect of Ibrutinib on the microenvironment

Despite the obviously B cell-restricted phenotype in XLA patients, BTK is not only expressed in B cells but in all hematopoietic cells, except T cells[283, 284]. Indeed, several pieces of evidence suggest that the response to Ibrutinib cannot be solely explained by direct effects on BCR signaling in CLL cells. CLL patients show variation in response which is not correlated to BTK protein expression suggesting that in addition to intrinsic dependencies also microenvironmental signals might play an important role in this context. Hermann *et al.* have shown that Ibrutinib was able to overcome protection of CLL cell apoptosis by stromal cells by reducing different microenvironmental stimuli such as CD40L, BAFF, TNF-α, IL-4, and IL-6[72].

Of interest, BTK is a key regulator of multiple functions in monocytes and macrophages. In bone marrow-derived macrophages, BTK has been described to be required for phagocytosis of apoptotic cells as a downstream function of TLR signaling[285]. Multiple TLRs in myeloid cells are known to signal via BTK. As BTK is involved in the response of macrophages to LPS, a ligand of TLR4, Ibrutinib might impact on their polarization[286]. Because BTK was proposed to be a positive regulator of the TREM-1 signaling pathway, Ibrutinib might also inhibit the inflammatory potential of monocytes and

macrophages[287, 288]. In addition, BTK inhibition can inhibit downstream signaling of Fc receptors in monocytes and macrophages *in vitro*[289] . Moreover, BTK has been identified to be constitutively phosphorylated in acute myeloid leukemia (AML) where Ibrutinib was able to inhibit cell proliferation of AML cells, NF-κB activity, adhesion to bone marrow stromal cells, and CXCL12/CXCR4 mediated migration[290, 291]. These observations highlight the importance of investigating effects of BTK inhibition by Ibrutinib in myeloid cells within the CLL microenvironment. In addition, it has been shown that Ibrutinib inhibits kinases that are similar to BTK, like BLK (IC_{50}=0.5 nM), ITK (IC_{50}=10.7 nM), and TEC (IC_{50}=78 nM)[272]. Blockade of ITK (IL-2 T cell inducible kinase) appears to mediate an off-target effect of Ibrutinib with clinical importance since it transmits a selective advantage for T helper 1 (Th1)-based immune response[292]. T cells from patients with CLL show only minor proliferation in response to TCR stimulation using anti-CD3/CD28 beads[293]. However, 5–11 cycles of Ibrutinib treatment reversed this proliferation defect in T cells to levels comparable to those of healthy donors[293]. Most recently, Ibrutinib has been shown to decrease the number of regulatory T cells in patients and impact on the cytokine network[294, 295]. In addition, Ibrutinib impacts on CLL-associated clonal T cell expansion through an increase of the T cell repertoire diversity[296].

1.5.1.3 Ibrutinib resistance in CLL patients

Despite the remarkable success of Ibrutinib during the recent years, there have been reports on the occurrence of acquired resistance to Ibrutinib in a subset of patients[297]. Two types of Ibrutinib resistance have been proposed. In the first group of patients, Richter's transformation occurs rather early after treatment initiation within 12 to 15 months[298]. In the second group of patients, CLL progresses at a later time point (15+ months) and the resistance development is associated with somatic mutations in genes of the BTK pathway, in particular mutations of the Ibrutinib-binding site of BTK and/or different mutations of the direct downstream molecule PLCG2[298]. Accordingly, high-sensitivity sequencing approaches have been developed for early detection of mutations in *BTK* or *PLCG2* in patients treated with the BTK inhibitor[299].

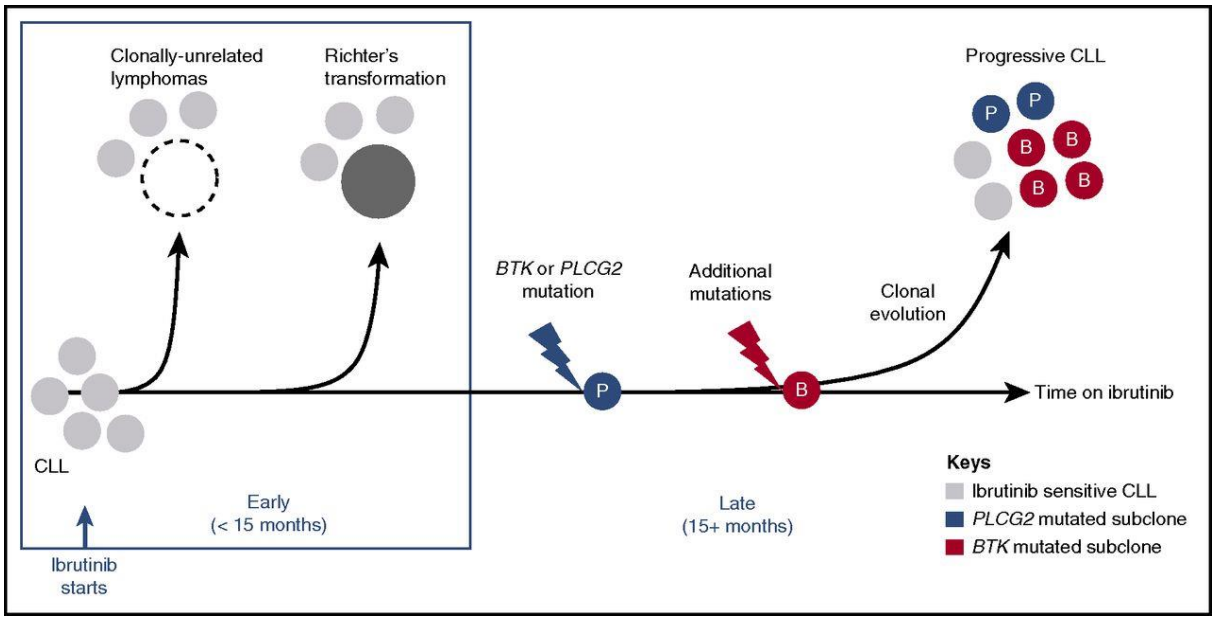

Figure 7: Molecular patterns of Ibrutinib-resistant disease.
This figure is derived from Ahn, I.E. *et al. Blood*, 2017[298].

The identification of a resistant case as part of the response assessment is a challenge for clinicians. Since most patients will not achieve a complete response and many will have circulating CLL cells in the blood for long periods of time, determining which patients are indeed relapsing and discriminating them from patients that are still sensitive for Ibrutinib treatment can be a difficult task[300]. One hallmark of patients under Ibrutinib treatment is clonal evolution of CLL, favoring selection and expansion of rare subclones that are already present before start of treatment[298, 301].

Targeting of BTK with other promising small molecule inhibitors that do not depend on binding to the mutated site of the enzyme, such as GDC-0853 may be a feasible therapy option for Ibrutinib-resistant patients[302]. In addition, targeting of the BCR pathway downstream of BTK and PCLG2 such as via PKCβ may be an alternative and effective treatment strategy. However, clinical studies need to be conducted in this respect. One promising treatment approach lately applied for Ibrutinib-treated relapsed/refractory CLL patients is by therapy with the BCL-2 inhibitor Venetoclax. In an ongoing clinical phase II study, Venetoclax treatment of CLL patients who have relapsed or are refractory to Ibrutinib and/or Idelalisib showed an overall response rate of 61% among patients that are refractory to Ibrutinib[303]. This may be related to the finding that BTK inhibition enhances mitochondrial BCL-2 dependence, which is accompanied by an increase in the pro-apoptotic protein BIM[304].

However, even though CLL relapse on Ibrutinib is primarily mediated through the acquisition of mutations, there are rare cases where neither mutations in the targeted or downstream genes were

found, nor Richter transformation was observed. Therefore, there will be increasing attempts not only to find rational treatment regimens for patients with identified mutations, but also to understand the so far elusive events causing progression of disease under Ibrutinib treatment.

1.6 Objectives

The first aim of this thesis was to test the potential of therapeutically targeting myeloid cells in CLL, which were previously suggested to possess tumor-promoting abilities in this disease. As CSF-1R is expressed on all cells of the myeloid lineage and known to be important for TAM differentiation in solid tumors, it was hypothesized that therapeutic intervention with the CSF-1/CSF-1R axis would lead to an improvement of disease outcome. An antibody-mediated strategy was chosen using TG3003, a monoclonal antibody that specifically targets human CSF-1R. Initial in vitro tests aimed at characterizing the effect of TG3003 on NLC generation and activity, which represent a well-accepted culture model, mimicking the lymph node microenvironment in CLL. A special focus was given here to changes in NLC-mediated survival support of CLL cells and to potential changes in the profile of secreted factors with functional relevance for CLL. In addition, the effect of TG3003 was addressed in a preclinical model of CLL by adoptively transferring splenocytes from leukemic Eμ-TCL-1 into C57BL/6 mice (TCL-1 AT) with a humanized CSF-1R locus. The question was whether treatment with TG3003 would induce changes in the TME, and specifically in myeloid cells, including Ly6Clow monocytes, the subset that is highly enriched in CLL. The final question of this part was, whether this treatment would lead to an improved disease outcome and therefore represent a promising therapy approach for CLL.

The second goal of this work was an extensive comparison of myeloid cells in mice in steady state and in the leukemia model to obtain insights into their pathological role in CLL. In addition to the proposed tumor-promoting abilities of myeloid cell in CLL, there have been also reports, that cells of the myeloid lineage may exhibit immunosuppressive properties. Multicolor-flow cytometry and flow sorting of specific myeloid cell subset (Ly6Clow and Ly6Clow monocytes, and conventional dendritic cells) followed by gene expression profiling were used to gain a comprehensive overview about specific characteristics and potential functionalities of these cells. One further research interest was the influence of the BTK inhibitor Ibrutinib on myeloid cell subsets that also express BTK, suggesting an indirect activity of Ibrutinib on the CLL tumor microenvironment. The intention was to unravel, if Ibrutinib induces a normalization of the CLL-associated phenotype of myeloid cells

and thereby contributes to the clinical success of this drug, or if Ibrutinib negatively impacts on these cells, which would require therapeutic intervention.

The third objective of the current work was the investigation of resistance development to Ibrutinib treatment in the TCL-1 AT model. This is of importance given the fact that a raising number of patients relapse with severe disease progression under Ibrutinib treatment, while the underlying mechanism is not fully understood, except for those cases that present with mutations in BTK or PLCγ2. A major focus of this part was to analyze tumor kinetics and tumor phenotypical features during resistance development in the TCL-1 AT model. Moreover, whole exome and RNA sequencing served as selected methods for identification of resistance-underlying mechanisms. Finally, these analyses aimed at identifying and understanding molecular mechanisms of Ibrutinib resistance in CLL patients which can be used to design and optimize future therapy options.

2 MATERIAL AND METHODS

2.1 MATERIAL

2.1.1 Mouse lines

Lines	Distributor/source
C57BL/6 (J and N substrain)	Charles River Laboratories, Sulzfeld, Germany
Eμ-TCL1 on C57BL/6 (J and N substrain)	Dr. Carlo M. Croce, The Ohio State University, College of Medicine, USA
CSF-1 KI on C57BL/6 background, N substrain	Taconic Biosciences, Hudson, New York

2.1.2 Human and murine flow cytometry antibodies

Antibody	Fluorochrome	Clone	Distributor
anti-human CD5	FITC	L17F12	BD Biosciences
anti-human CD19	APC	HIB19	BD Biosciences
anti-mouse CD3e	FITC	145-2C11	eBioscience
anti-mouse CD3e	V450	500A2	BD Biosciences
anti-mouse CD4	APC	RM4-5	eBioscience
anti-mouse CD4	APC/Cy7	GK1.5	Biolegend
anti-mouse CD5	APC	53-7.3	BD Biosciences
anti-mouse CD8a	Alexa Fluor® 700	53-6.7	Biolegend
anti-mouse CD8a	APC/Cy7	53-6.7	Biolegend
anti-mouse CD11b	APC	M1/70	eBioscience
anti-mouse CD11b	PE/Cy7	M1/70	eBioscience
anti-mouse CD11b	PerCP	M1/70	Biolegend
anti-mouse CD11c	Brilliant Violet 605	N418	Biolegend
anti-mouse CD11c	PerCP	N418	Biolegend
anti-mouse CD11c	PerCP/Cy5.5	N418	Biolegend
anti-mouse CD19	FITC	1D3	eBioscience
anti-mouse CD19	PE	1D3	eBioscience
anti-mouse CD19	PE/Dazzle™ 594	6D5	Biolegend
anti-mouse CD31	PE	390	eBioscience
anti-mouse CD38	PE	90	eBioscience

anti-mouse CD43	PE	S7	BD Biosciences
anti-mouse CD43	PerCP/Cy5.5	S7	BD Biosciences
anti-mouse CD44	Alexa Fluor® 700	IM7	eBioscience
anti-mouse CD45	APC/Cy7	30F-11	Biolegend
anti-mouse CD45	PerCP/Cy5.5	30F-11	Biolegend
anti-mouse CD54	PE	YN1/1.7.4	eBioscience
anti-mouse CD83	APC	Michel-19	Biolegend
anti-mouse CD86	PerCP/Cy5.5	GL-1	Biolegend
anti-mouse CD115	PE	AFS98	eBioscience
anti-mouse CD117	Brilliant Violet 605	2B8	BD Biosciences
anti-mouse CD86	PE	GL-1	eBioscience
anti-mouse F4/80	APC	BM8	eBioscience
anti-mouse F4/80	PE	BM8	eBioscience
anti-mouse Ki67	FITC	SolA15	eBioscience
anti-mouse KLRG1	PE/Cy7	2F1	eBioscience
anti-mouse LAG3	PE	eBioC9B7W	eBioscience
anti-mouse Ly6C	APC/Cy7	HK1.4	Biolegend
anti-mouse Ly6G	FITC	1A8	Biolegend
anti-mouse Ly6G	PE	1A8	BD Biosciences
anti-mouse Ly6G	V450	1A8	BD Biosciences
anti-mouse MHC-II I-A/I-E	Alexa Fluor® 700	M5/114.15.2	eBioscience
anti-mouse MHC-II I-A/I-E	PE	M5/114.15.2	eBioscience
anti-mouse NK1.1	FITC	PK136	Biolegend
anti-mouse NK1.1	V450	PK136	BD Biosciences
anti-mouse PD-L1	PE	MIH5	eBioscience
anti-mouse PD-L1	APC	B7-H1	Biolegend
anti-mouse TER-119	FITC	TER-119	Biolegend
anti-mouse TREM-1	PE	174031	R&D
anti-mouse IL-12/IL-23	PE	C17.8	eBioscience
anti-mouse Il-1b	APC	NJTEN3	eBioscience

anti-mouse TNF-a	PerCP/Cy5.5	MP6-XT22	Biolegend
pBTK (pY223)/Itk (pY180)	PE	N35-86	BD Biosciences
Rat IgG1 κ Isotype Control	PerCP/Cy5.5	eBRG1	eBioscience
Rat IgG1 κ Isotype Control	FITC	eBRG1	eBioscience

2.1.3 Other antibodies

Antibody	**Fluorochrome**	**Clone**	**Distributor**
F(ab')2-Goat anti-Mouse IgM (mu) Secondary Antibody	unconjugated	polyclonal	eBioscience
TG3003 (/H27K15)	unconjugated	monoclonal	Transgene SA, Illkirch Graffenstaden Cedex, France
human IgG1 kappa control antibody	unconjugated	monoclonal	GeneTex , Inc., Irvine, California
anti-IL-10R	unconjugated	clone 1B1.3A	BioXcell, West Lebanon, NH
rat IgG1 isotype contol	unconjugated	clone: HRPN	BioXcell, West Lebanon, NH
anti-IFNγ	unconjugated	clone: XMG1.2	BioXcell, West Lebanon, NH

2.1.4 Buffers

Buffer	**Composition/Distributor**
ACK buffer	150 mM NH4Cl, 10 mM KHCO3, 0.1 mM EDTA, pH 7.2-7.4
Annexin V Binding Buffer (10X)	BD Biosciences, Heidelberg, Germany
FACS (Fluorescence-activated cell sorting) buffer	1x PBS, 2% FCS, 0.02% (v/v) NaN3

Freezing medium for human cells	Respective complete medium + 10% FCS + 10% DMSO
Freezing medium for mouse cells	90% FCS + 10% DMSO
MACS buffer (autoMACS Running Buffer)	Miltenyi Biotec, Bergisch Gladbach, Germany
Phosphate Buffered Saline (PBS, pH7.4)	NaCl (137mM), Na2HPO4 (9.2mM), KCL (2.7mM), KH2PO4 (1mM)
eBioscience™ IC Fixation Buffer	eBiosciences, Frankfurt am Main, Germany
eBioscience™ 1-step Fix/Lyse Solution (10X)	eBiosciences, Frankfurt am Main, Germany
RBC Lysis Buffer (10X)	Biolegend, San Diego, California, USA
eBioscience™ Permeabilization Buffer (10X)	eBiosciences, Frankfurt am Main, Germany
Foxp3 / Transcription Factor Staining Buffer Set	eBiosciences, Frankfurt am Main, Germany
Complete medium for human cells ('complete human medium')	DMEM High Glucose + 10% FCS + 1% penicillin/streptomycin
Complete medium for mouse cells ('complete mouse medium')	RPMI 1640 (2mM Glu) + 10% FCS + 4 mM L-glutamine + 1% penicillin/streptomycin + 0.1% 2-mercaptoethanol
T cell stimulation medium	DMEM High Glucose + 10% FCS + 1% penicillin/streptomycin + 10 mM HEPES + 1 mM sodium pyruvate

2.1.5 Cell culture reagent and material

Material	**Distributor**
Biocoll separating solution	Biochrom, Berlin, Germany
DMEM High Glucose (4.5g/L Glucose, 4mMGlu)	Gibco / Life Technologies, Karlsruhe, Germany
Fetal Calf Serum (FCS)	Biochrom / Merck, Darmstadt, Germany
Normal Rat Serum	Jackson ImmunoResearch Laboratories, West Grove, PA, USA
PBS Dulbecco's Gibco	Gibco / Life Technologies, Karlsruhe, Germany
Penicillin / Streptomycin (10.000 U/ml)	Gibco / Life Technologies, Karlsruhe, Germany
RPMI 1640 (2mM Glu)	Gibco / Life Technologies, Karlsruhe, Germany

Histopaque®-1083	Sigma-Aldrich, Munich, Germany

2.1.6 Cell isolation

Material	**Distributor**
CD14 MicroBeads, human	Miltenyi Biotec, Bergisch Gladbach, Germany
CD19 MicroBeads, mouse	Miltenyi Biotec, Bergisch Gladbach, Germany
Leucosep™ tubes, 50 mL	Greiner Bio-One International GmbH, Kremsmünster, Austria
Lipopolysaccharide (LPS)	Sigma-Aldrich Gmbh, Munich, Germany
MACS LS separation columns	Miltenyi Biotec, Bergisch Gladbach, Germany
MACS Magnet and stand	Miltenyi Biotec, Bergisch Gladbach, Germany
M-CSF, human recombinant	R&D Systems, Minneapolis, MN, USA
Monocyte Isolation Kit II, human	Miltenyi Biotec, Bergisch Gladbach, Germany
Monocyte Isolation Kit (BM), mouse	Miltenyi Biotec, Bergisch Gladbach, Germany
Multiwell plates, 12-well, 24-well, 48-well	TPP Techno Plastic Products AG, Trasadingen, Switzerland Pasteur pipettes / VWR®
Disposable Transfer Pipets	VWR International, Radnor, PA, United States
Red Blood Cell Lysis Solution (10X)	Miltenyi Biotec, Bergisch Gladbach, Germany
Easysep™ Mouse Pan-B Cell Isolation Kit	Stemcell Technologies, Vancouver, Canada
C-tubes	Miltenyi Biotec, Bergisch Gladbach, Germany

2.1.7 Chemicals and other reagents

Material	**Distributor**
2-mercaptoethanol	Sigma-Aldrich, Munich, Germany
β-Cyclodextrin	Sigma-Aldrich, Munich, Germany
Bovine serum albumin (BSA)	Sigma-Aldrich, Munich, Germany
Ethanol	Merck, Darmstadt, Germany
Methanol	Roth, Karlsruhe, Germany
7-aminoactinomycin (7-AAD)	BD Biosciences, Heidelberg, Germany
Dimethylsulfoxid (DMSO)	Sigma-Aldrich, Munich, Germany
Fixable Viability Dye eFluor 506™	eBiosciences, Frankfurt am Main, Germany

Fixable Viability Dye eFluor 780™	eBiosciences, Frankfurt am Main, Germany
Fludarabine	Enzo Life Sciences, Lörrach, Germany
Ibrutinib/ PCI-32765 (for *in vitro* purposes)	Selleckchem, Munich, Germany
Ibrutinib/ PCI-32765 (for *in vivo* purposes)	Provided by collaboration partner Prof. Stephan Stilgenbauer
Idelalisib	Selleckchem, Munich, Germany
Ionomycin	Sigma-Aldrich, Munich, Germany
L-Glutamine	Gibco / Life Technologies, Carlsbad, USA
PE Annexin V	BD Biosciences, Heidelberg, Germany
RNaseZap®	Life Technologies, Carlsbad, USA
123count™ eBeads Counting Beads	eBiosciences, Frankfurt am Main, Germany
DAPI (4',6Diamidin-2-phenylindol)	Life Technologies, Carlsbad, USA
eBioscience™ Protein Transport Inhibitor Cocktail	eBiosciences, Frankfurt am Main, Germany
eBioscience™ Cell Stimulation Cocktail (500X)	eBiosciences, Frankfurt am Main, Germany
Thiazolyl blue (MTT) 3-(4,5-Dimethyl-2-thiazolyl)-2 ,5-diphenyl-2H-tetrazolium bromide	Biomol GmbH, Hamburg

2.1.8 Instruments

Instrument	**Distributor**
ABI Prism 7900HT	Life Technologies, Carlsbad, USA
Agilent 2100 Bioanalyzer	Agilent Technologies GmbH, Berlin, Germany
BD FACSAria™ II	BD Biosciences, Heidelberg, Germany
BD FACSCanto II	BD Biosciences, Heidelberg, Germany
BD LSRFortessa™	BD Biosciences, Heidelberg, Germany
gentleMACS™ Dissociator	Miltenyi Biotec, Bergisch Gladbach, Germany
Incubator Hera Cell 150i	ThermoFischer Scientific, Scoresby Vic, Australia
Mithras LB940 Plate Reader	Berthold Technologies, Bad Wildbad, Germany
NanoDrop® ND-1000 Spectrometer	NanoDrop, Wilmington, US
OctoMACS Separator	Miltenyi Biotec, Bergisch Gladbach, Germany
Pipet-Lite XLS+ Multichannel	Mettler Toledo, Giessen, Germany

Pipettes (20µl, 100µl, 200µl, 1000µl)	Gilson, Middleton, Germany
QuadroMACS Separator	Miltenyi Biotec, Bergisch Gladbach, Germany
Vi-CELL XR 2.03	Beckman Coulter Inc.,Brea, USA
Water Bath GFL 1086	GFL Gesellschaft für Labortechnik GmbH, Hannover
Easysep™ Magnet	Stemcell Technologies, Vancouver, Canada
UV-Gel Documentation System	BioRad, Hercules, USA

2.1.9 Kits

Kit	**Distributor**
DNeasy Blood & Tissue Kit	Qiagen, Hilden, Germany
RNeasy Micro Kit	Qiagen, Hilden, Germany
AllPrep DNA/RNA/Protein Mini Kit	Qiagen, Hilden, Germany
BD Cytometric Bead Array (CBA) Human Enhanced Sensitivity Master Buffer Kit	BD Biosciences, Heidelberg, Germany
BD Cytometric Bead Array (CBA) Human IL-6 Flex Set	BD Biosciences, Heidelberg, Germany
BD Cytometric Bead Array (CBA) Human Soluble CD14 Flex Set	BD Biosciences, Heidelberg, Germany
BD Cytometric Bead Array (CBA) Human MCP-1 (CCL2) Flex Set	BD Biosciences, Heidelberg, Germany
MILLIPLEX MAP Mouse Cytokine/Chemokine Magnetic Bead Panel	Merck Millipore, Germany
Quantikine® ELISA Human M-CSF	R&D Systems, Minneapolis, MN, USA
Quantikine® ELISA Human TNF-α	R&D Systems, Minneapolis, MN, USA

2.1.10 Database and online tools

Databases and online tools	**Source**
Immgen	https://www.immgen.org/
Pubmed	www.ncbi.nlm.nih.gov/pubmed/
Venny	http://bioinfogp.cnb.csic.es/tools/venny/

2.1.11 Software

Software	Distributor
BD FACS Diva	BD Biosciences, San Jose, USA
Bioanalyzer 2100 Expert	Agilent Technologies, Santa Clara, USA
Chipster v3.11	http://chipster.csc.fi/ (open source)
EndNote X8	Thomson Reuters, Carlsbad, USA
FlowJo V10	FlowJo, Ashland, OR, USA
ImageJ 1.47v	Wayne Rasband, National Institutes of Health, USA
Ingenuity® Systems IPA	http://www.ingenuity.com/
Inkscape	https://inkscape.org/de/ (open source)
Microsoft Excel 2013	Microsoft, Redmond, USA
Microsoft PowerPoint 2013	Microsoft, Redmond, USA
Microsoft Word 2013	Microsoft, Redmond, USA
Prism 7 GraphPad	GraphPad Software, La Jolla, USA
R	https://www.r-project.org/ (open source)

2.2 METHODS

2.2.1 Cell culture of primary CLL cells and monocytes

2.2.1.1 Isolation of human PBMC and monocytes

For experiments with human CLL cells, peripheral blood mononuclear cells (PBMCs) were retrieved from CLL blood samples provided by collaboration partners at University Clinic, Ulm and National Center for Tumor diseases (NCT), Heidelberg. For experiments with monocytes, PBMCs were isolated from peripheral blood buffy coat samples, purchased from the Institute for Clinical Transfusion Medicine and Cell Therapy (IKTZ, Heidelberg, Germany). Primary human monocytes were subsequently isolated from PBMCs samples.

In brief, 15mL Biocoll solution, adjusted to RT, was added into Leucosep™ tubes and then centrifuged at 1,000 x g for 1 min. Blood samples were diluted (buffy coat samples 1:4, CLL patient's blood 1:2) in room-tempered PBS and transferred to Leucosep™ tubes, adding 35mL per tube to obtain a total volume of 50mL. Samples were then centrifuged at 1,000 x g for 20 min, at RT, without brake. The PBMC interphase was carefully transferred to a new 50mL Falcon tube using a 5mL pipet while avoiding excess transfer of the upper plasma layer and lower Biocoll layer. PBMCs were washed twice in cold PBS, centrifuged at 300 x g for 10 min and then resuspended in ice-cold MACS buffer, prior to cell counting.

As approximately 10% of PBMCs are monocytes, respective cell numbers were used for further positive selection of $CD14^+$ monocytes to retrieve the needed cell numbers for downstream experiments. Isolation of monocytes was conducted by magnetic activated cell sorting (MACS), by labeling monocytes directly with magnetic bead-coupled anti-human CD14 antibodies (positive selection) according to manufacturer's instructions. In brief, cells were centrifuged at 300 x g for 10 min and resuspended in ice-cold MACS buffer (80µL per $1x10^7$ cells) and anti-human CD14 microbeads (20µL per $1x10^7$ cells). Samples were incubated for 15 min at 4°C followed by washing in MACS buffer and centrifugation at 300 x g for 5 min. Cells were resuspended (500µL per $1x10^8$ cells) in ice-cold MACS buffer and applied onto columns, which were previously equilibrated with ice-cold MACS buffer and placed at the magnetic stand. Flow through was discarded and magnetic columns were washed three times with 2mL ice-cold MACS buffer. Magnetically labelled monocytes were eluted in 5mL ice-cold MACS buffer. Monocytes were centrifuged at 300 x g for 10 min, resuspended (500µL per $1x10^8$ cells) in ice-cold MACS buffer and column-based purification was repeated one additional time to achieve better purity. $CD14^+$ monocytes were counted and resuspended in complete human medium (DMEM High Glucose + 10% FCS + 1% penicillin/streptomycin).

2.2.1.2 Co-culture of primary CLL cells with monocytes and NLC co-cultures

For NLC cocultures, PBMCs from CLL patients with high tumor load were seeded in a high cell density ($1.5x10^7$/mL), in 500µL volume of complete human medium per well of a 48-well plate, as described previously and cultured for 12 to 14 days to induce NLC differentiation[305].
For CLL-monocyte cocultures, CLL-PBMCs and $CD14^+$ monocytes were retrieved as described above. Cells were co-seeded, whereby CLL cell were added in excess. The detailed conditions are indicated in the respective result part.

2.2.2 Animals and tumor models

All animal experiments were carried out according to governmental and institutional guidelines and authorized by the local authorities (Regierungspräsidium Karlsruhe, permit numbers: G42/15, G-16/15. Mice were monitored for signs of illness and were sacrificed at indicated time points.

2.2.2.1 Transgenic Eµ-TCL-1 mice

Eµ-TCL-1 transgenic mice were used as a source for primary tumors in the TCL-1 adoptive transfer model described in the following section. Eµ-TCL-1 (TCL-1) transgenic mice (C. Croce, OH, USA) were bred on a C57BL/6 background in pathogen-free conditions at the central animal facility of the German Cancer Research Center (DKFZ). In brief, heterozygous TCL-1 mice were bred with wild-type (WT) C57BL/6 mice generating progeny of heterozygous TCL-1 mice and WT littermates. Leukemia typically developed in TCL-1 transgenic mice at an age of 10-15 months, indicated by palpable spleens and followed by confirmed presence of $CD5^+CD19^+$ cells in the peripheral blood.

TCL-1 mice were bred separately for the two major C57BL/6 substrain backgrounds: C57BL/6 N and C57BL/6 J, which were confirmed by single nucleotide polymorphism analysis of tail DNA using the Genome Scanning Service at The Jackson Laboratory (Bar Harbor, Maine, USA).
Genotyping of TCL-1 mice was performed with DNA isolated from tail tissue using DNeasy Blood & Tissue Kit, Qiagen. The PCR reaction was conducted using Phire®Hot Start II PCR Master Mix and the following forward and reverse primers: forward_TCL-1-5'GCCGAGTGCCCGACACTC'3 and reverse_ TCL-1-5'CATCTGGCAGCAGCTCGA'3. The PCR program comprised the following steps: initial denaturation at 98°C for 30 seconds, denaturation at 98°C for five seconds, annealing at 59°C for five seconds, extension: 72°C for one min (30 cycles), and final extension at 72°C for one min. The PCR products were separated on 1% agarose gel, stained with ethidium bromide, and visualized using UV-Gel Documentation System.

2.2.2.2 Eμ-TCL-1 adoptive transfer model

Two different strategies for Eμ-TCL-1 adoptive transfer (TCL-1 AT) model were applied: For the first approach, splenocytes from different leukemic Eμ-TCL-1 donor mice with primary disease were pooled and $2x10^7$ cells were transplanted into 6-12 weeks old WT C57BL/6 females via i.v. (intravenous) or i.p. (intraperitoneal) route. This strategies circumvented the limited availability of primary tumor cells and abated heterogeneity of single donor tumors as all animals within one study received an identical pool of tumor cells. For the second approach primary tumors isolated from primary TCL-1 mice were first expanded by i.p. injection of $2x10^7$splenocytes into 6-12 weeks old WT C57BL/6 females. Tumors arising from these expansions were used for further i.v. or i.p. AT of 1-$2x10^7$splenocytes into 6-12 weeks old WT C57BL/6 females. In line with previous observations, this strategy generated faster engraftment of tumors[226]. The applied approach was described in detail in the respective results sections.

Adoptive transfer of splenocytes was performed solely within the same C57BL/6 substrain. Accordingly, only tumors from TCL-1 mice with C57BL/6 N background were injected into WT C57BL/6 N mice and only tumors from TCL-1 mice with C57BL/6 J background were injected into WT C57BL/6 J mice.

2.2.2.3 Negative selection of B cells

Prior transplantation of splenocytes for TCL-1 AT experiments, splenocytes from TCL-1 mice were negatively depleted from unwanted cells to enrich for malignant B cells using the Easysep™ Mouse Pan-B Cell Isolation Kit. In brief, this kit makes use of an isolation cocktail, containing biotinylated antibodies recognizing the surface markers against CD4-, CD8-, CD11c-, CD49b-, CD90.2-, Ly-6C/G (Gr-1)-, and TER119-positive cell. Streptavidin-coated magnetic particles are then used to remove the labeled cells.

2.2.2.4 Randomization

For some experiments, treatment was started once a considerable tumor load in peripheral blood had been established. Animals were then randomized to the different treatment arms prior treatment start, in a fashion, resulting in comparable mean percentages or absolute numbers of $CD5^+CD19^+$ cells. The tumor load in peripheral blood at time of randomization is depicted in the respective results section.

2.2.2.5 Antibody treatment

Animals were injected i.p. every second day with TG3003 (anti-CSF-1R) or the control antibody Synagis in a concentration of 3mg/kg, as tested by the founder company before. Frozen aliquots of TG3003 (stock concentration: 5.8mg/mL) and Synagis (stock concentration: 7.6mg/mL) were thawed and diluted prior each injection in a total volume of 200µL PBS per mouse. Animals were weight weekly and amount of antibody was adjusted accordingly.

Antibody treatment with anti-IL-10RA and anti-IFNγ was performed as part of a study from Dr. Bola Hanna. Animals were i.p. injected with 1mg of anti-IL-10RA (clone 1B1.3A) or anti-IFNγ (clone: XMG1.2), or rat IgG1 isotype antibody (clone: HRPN) and subsequent doses of 0.5mg every three days for another two weeks.

2.2.2.6 Ibrutinib treatment

Ibrutinib was given to mice through the drinking water in a concentration of 0.16 mg/mL resulting in optimal doses (25mg/kg/day) as reported previously in the literature[282]. In brief, control vehicle drinking water was produced by dissolving 10g β-Cyclodextrin in 1L autoclaved tab water (1% β-Cyclodextrin) and pH was adjusted to 7-8. For preparation of Ibrutinib drinking water, control vehicle was prepared as described above and adjusted to <pH3. Then, 1.6mg Ibrutinib was dissolved in 1L vehicle water. After complete dissolution pH was adjusted to 7-8. Ibrutinib and vehicle drinking water were sterile filtered and kept for maximum one week at 4°C. Treatment water was replaced every two to three days freshly from the prepared stock. Animals were treated from the time point of randomization continuously with the drug until the end of the study.

2.2.2.7 Calculation of tumor growth inhibition (TGI)

Tumor growth inhibition (%TGI) at week 2 post treatment start was calculated by the formula: %TGI = (Ct-Tt)/(Ct-C0)*100 where Ct = median tumor volume of control group at time point t, Tt = median tumor volume of treated group at time point t, and C0 = median tumor volume at time 0. Tumor volume is absolute number of leukemic cells measured per µL blood, time 0 presented time point of randomization, time t is week 2 post treatment start.

2.2.2.8 Lymphocyte doubling time

Lymphocyte doubling time was calculated by the formula: $(\text{duration} * \log(2))/(\log(\text{Final counts}) - \log(\text{Initial counts}))$ where duration is the number of days between Initial counts and Final Counts and Counts are the absolute number of $CD5^+CD19^+$ tumor cells.

2.2.2.9 Collection of tissue samples and preparation of cell suspension

Withdrawal of peripheral blood from animals during the course of experiment, was drawn weekly or every second week via puncture of the submandibular vein in EDTA-coated tubes and further used for surface staining.

For collection of tissue samples at the end of experiments, mice were euthanized by CO_2 gradient and peripheral blood was drawn via cardiac puncture using a 25G syringe. Blood was collected into Eppendorf tubes (for serum preparation) or EDTA-coated tubes (for surface staining).

Spleens and inguinal lymph nodes were harvested and kept in complete mouse medium (RPMI 1640 (2mM Glu) + 10% FCS + 4 mM L-glutamine + 1% penicillin/streptomycin + 0.1% 2-mercaptoethanol) and PBS + 5% until the moment of single cell preparation. Single cell suspension were prepared by mechanical disruption of the tissues through 70µm cell strainers. In some experiments, single cell suspensions from spleens were prepared in Milteny C-tubes using a gentleMACS™ Dissociator. Erythrocytes in spleen were removed by lysis in ACK lysis buffer for 8 min, followed by two washing steps with cold PBS, and a final filter step through a 70µm cell strainers. ACK lysis was conducted for lymph nodes, if many erythrocytes were present in the lymph node cell suspension. In such case, cells were pelleted, then then resuspended in 500µl ACK lysis buffer, incubated for 1 min followed by washing steps with cold PBS. Femurs and tibia were harvested and bone marrow cells and flushed using 27G needle with 5ml PBS + 5% FCS. Traces of blood contamination were removed by 1 min treatment with 1ml of ACK lysis buffer. Cells were washed twice with cold PBS and finally suspended in FACS buffer. Cell counts were determined using Vi-CELL XR, pelleted and resuspended in appropriate concentration in FACS buffer for flow cytometric experiments or complete mouse medium for culturing purposes.

2.2.2.10 Mouse PBMC isolation from blood

For the purpose of intracellular flow cytometry staining in cells from blood, peripheral blood nuclear cells were isolated conducting a gradient separation. Room-tempered blood was mixed with the same volume of PBS and carefully layered on top of Histopaque®-1083 (2X volume). After 30 min centrifugation at RT PBMC layer was carefully removed and washed with cold PBS. ACK lysis was conducted in addition if erythrocytes were visibly remaining. In such case, PBMC pellet was then resuspended in 500µl ACK lysis buffer, incubated for 7 min followed by a washing steps with cold PBS. Cell counts were determined using Vi-CELL XR, pelleted and resuspended in appropriate concentration for flow cytometric experiments.

2.2.3 Flow cytometry

2.2.3.1 Staining of cell surface proteins

Staining of cell surface proteins was conducted using either a protocol with or without cell fixation and applied to cells retrieved from the spleen, lymph nodes and bone marrow.

Staining without fixation was performed using a homemade FACS Buffer (PBS containing 2% FCS and 0.02% sodium azide) containing the antibodies for 30 min at 4°C using previously titrated antibody dilutions. To avoid unspecific binding of antibodies to splenic myeloid cells, splenocytes ($3x10^6$) were preincubated for 15 min in FACS buffer with 2% rat serum. Cells were then washed twice with cold FACS Buffer and resuspended in 200µl of FACS buffer, which in some cases contained 0.2µg/ml DAPI (4',6Diamidin-2-phenylindol) for the purpose of live/deal discrimination. This protocol was also used for fluorescence activated cell sorting.

For surface staining with subsequent fixation, cells were stained in an antibody-PBS mix for 30 min at 4°C protected from light, washed twice with cold PBS and then incubated for 30 min at room temperature with eBioscience™ IC Fixation Buffer. Samples were washed twice with PBS, resuspended in 200µl of PBS and stored at 4°C until measurement.

Staining and fixation of cell surface proteins in whole blood was conducted using 25-50µl of peripheral blood collected in EDTA tubes to prevent coagulation. Whole blood cells were stained with an antibody-PBS mix for 30 min at 4°C protected from light. Afterwards, 2 ml of 1x eBioscience™ 1-step Fix/Lyse Solution was added to the sample and incubated for 10 min at room temperature. Samples were centrifuged and supernatants were carefully aspirated. Cells were resuspended in 150µl of 1x eBioscience™ 1-step Fix/Lyse Solution. For staining of whole blood cells where fixation was not desired 1x Biolegend RBC Lysis Buffer was used instead of 1x BD FACS™ lysing solution.

Before sample acquisition 123count™ eBeads Counting Beads (same volume as blood) were added. Absolute cells numbers in blood were calculated according to the formula: absolute count (cells/µL) = (cell count x bead volume x bead concentration)/ (bead count x cell volume).

2.2.3.2 Intracellular phospho-protein staining

For intracellular phospho-protein staining of phosphoBTK, $1.5x10^7$ splenocytes were suspended in cold PBS in a 2mL Eppendorf tube. Then cells were fixed by adding equal volume of IC Fixation Buffer was added quickly and cells were incubated for 30 min at RT. After washing twice with PBS+ 1% BSA, cells were pulse vortex to loosen the pellet and permeabilized by adding slowly 1mL methanol.

Cells were chilled on ice for 30 min, then washed and resuspended in PBS for further staining according to the protocol for lymphoid organs without fixation describes in the previous section.

2.2.3.3 Stimulation of T cells and monocytes and intracellular staining

Staining of intracellular proteins in myeloid cells and T cells from spleens was performed after incubation with respective stimuli. For T cell effector function measured by cytokines $2x10^6$ splenocytes were seeded per well of a 96-well plate and stimulated for 5 hours with 1X Cell Stimulation Cocktail (containing PMA and Ionomycin) and 1X Protein Transport Inhibitor Cocktail.
For myeloid cell stimulation $3x10^6$ splenocytes were incubated in 200µL complete mouse medium with LPS (final concentration of 1 µg/ml) at 37°C for one hour. Then 1X eBioscience™ Protein Transport Inhibitor Cocktail was added and cells were incubated for additional 5 hours.

At the end of the stimulation, cells were washed with PBS, incubated for 15 min with PBS + 2% rat serum in the case of myeloid cells, followed by another washing step. Cells were then resuspended in PBS containing 0.1% fixable viability dye and antibodies for surface stain and incubated for 30 min at 4°C protected from light. Cells were washed twice and fixed with 100µL IC Fixation Buffer for 30 min at RT. After a washing steps, cell were permeabilized and stained with antibodies against the intracellular protein or the respective isotype controls in 200µL 1X eBioscience™ Permeabilization Buffer for 30 min at RT. After washing twice with 1X eBioscience™ Permeabilization Buffer, cells were resuspended in a final volume of 200µl 1X eBioscience™ Permeabilization Buffer.
Intracellular Ki-67 staining was performed similar except that 200µL Foxp3 Fixation/Permeabilization Buffer instead of 100µL IC Fixation Buffer was used.

Data were acquired on BD LSRII, BD LSRFortessa or BD Canto flow cytometer. Same multicolor panels within one experiment were acquired at the same machine. Data analysis was performed using FlowJo V10.0.8 software. For all flow cytometric measurement, median fluorescence intensity (MFI) was recorded and normalized by subtracting the MFI of the respective fluorescence-minus-one (FMO) (containing the respective isotype control instead of the antibody, labeling the molecule of interest) control.

2.2.3.4 Fluorescence activated cell sorting

For the purpose of fluorescence activated cell sorting (FACS) isolated splenocytes were stained as described in the section before without cell fixation. For sorting of splenic monocyte subsets and

cDCs, samples were debulked from B cells prior staining using microbeads specific for mouse CD19. The magnetic cell separation procedure was carried out as described above for human CD14 section 2.2.1.1. The negative fraction (flow-through containing the unlabeled) was used for FACS sorting. Operator-free sorting of live cells was performed at the Aria II using a nozzle size of 100µm. Cells were sorted into collection buffer (PBS + 5% FCS) and all sorted populations were re-analyzed for purity. Cells were further used for extraction of RNA or simulations RNA/DNA/protein extraction using the respective Qiagen kit.

2.2.4 RNA and DNA isolation

2.2.4.1 RNA isolation

Total ribonucleic acid (RNA) was extracted using the RNeasy® Micro kit (Qiagen, Hilden, Germany) according to manufacturer's protocol. In brief, 1-10x10^5 flow-sorted cells were centrifuged and resuspended in 350µl RLT buffer + 1% β-mercaptoethanol. Complete cell lysis was attained by vigorous vortexing. Subsequently, the same volume of 70% ethanol was added to the lysate, mixed well by pipetting, transferred to an RNeasy MinElute spin column and centrifuged for 15 sec at ≥8000 x g. The flow through was discarded and the column was washed with 700µl Buffer RW1, then 500µl Buffer RPE and finally with 500µl of 80% ethanol. The column was centrifuged at full speed for 5 min with lid open to eliminate residual ethanol. Finally, RNA was eluted in 14µl of RNase-free water was stored at -80°C. RNA concentrations were determined using the NanoDrop spectrophotometer.

2.2.4.2 RNA and DNA isolation

For simultaneous isolation of total RNA and genomic DNA (and protein) for submission to RNA sequencing and whole exome sequencing of $CD5^+CD19^+$ FACS-sorted cell the AllPrep DNA/RNA/Protein Mini Kit was used according to manufacturer's protocol.

2.2.5 Array-based gene expression profiling

RNA was subjected to a quality check using a RNA Nano chip assay on an Agilent 2100 Bioanalyzer. Processing of raw data was conducted by the Genomics and Proteomics Core Facility, DKFZ. Gene expression data of myeloid cells was further analyzed using first the bioinformatics software Chipster, R, and Ingenuity Pathway analysis using the GeneChip® Mouse Gene 2.0 ST Array.

2.2.6 RNA sequencing and DNA whole exome sequencing

Total RNA and genomic DNA were isolated, subjected to RNA and DNA quality check. RNA integrity was confirmed as described above using RNA Nano chip assay on an Agilent 2100 Bioanalyzer. DNA quality was verified using the Genomic DNA ScreenTape assay at a TapeStation System, which was kindly conducted by the Sample Processing Laboratory (SLP) at DKFZ. Samples were submitted to the Genomics and Proteomics Core Facility at DKFZ. Library preparation of RNA was performed according to the Illumina TruSeq Stranded protocol on a HiSeq 2000 v4 sequencer, paired-end 125 base pairs with five samples per lane. For DNA whole exome sequencing libraries were prepared according to Agilent Low Input Exom-Seq Mouse protocol and sequenced on a HiSeq 4000 sequencer, paired-end 100 base pairs with three samples per lane.

2.2.7 Mapping and SNV calling of whole exome sequencing data

Raw sequencing reads from whole exome sequencing were mapped to mm10 reference genome. Single nucleotide variants (SNVs) were called using MuTect (SNV caller from Broad Institute) with the aligned bam files. The resulting vcf files from each treatment cohort were merged together and used to create further intersections. In order to retrieve for example resistance-specific SNVs following intersection was created: Merged Ibrutinib_late SNVs – merged Ibrutinib_early SNVs – merged Vehicle_late SNVs – merged Vehicle_early SNVs. In addition, all SNVs were subtracted from SNVs present in the parental DNA from the TCL-1 donor mouse.

2.2.8 Analysis of V(D)J rearrangement of BCR of whole exome sequencing data

Bam files were converted into fastq format and used as input for stand alone IgBLAST for identifying potential V(D)J rearrangements. The number of unique V(D)J rearrangements was then counted for each sample.

2.2.9 Gene expression profiling using differentially expressed transcripts

Raw sequencing reads from RNA sequencing were aligned to the mm10 reference genome. Read counting was performed using featureCounts. Gene expression matrix with raw read counts was used as input for DESeq2 for downstream analysis like normalization, unsupervised hierarchical clustering with 1000 most variable transcripts and identifying differentially expressed transcripts at a cut off of adjusted p-value of less than 0.05.

For gene ontology (GO) analysis DEGs with a cutoff of less than 0.05 were used. For gene set enrichment (GSE) analysis no cutoff was set. All DEGs were ranked according the adjusted *p* values before submitting to the GSEA platform.

2.2.10 Quantification of cytokines and chemokines

2.2.10.1 Preparation of mouse serum cell culture supernatant

Mouse blood was collected via cardiac puncture and allowed to clot by leaving it undisturbed at room temperature for at least 30 min. Clot was removed and serum (resulting supernatant) was obtained by two times centrifugation for 10 min at 2,000 x g at 4°C.

To obtain cell culture supernatants, cells were first centrifuged for 10 min at 300 x g at 4°C. Supernatants were transferred to a new tube and centrifuged for 15 min at x 1,000 x g at 4°C. Pelleted cells were collected for other procedures, e.g. cell viability via Annexin V/7-AAD staining and washed twice cold PBS. Serum and cell culture supernatants were immediately aliquoted and frozen at -80°C until used.

2.2.10.2 ELISA and bead-based immunoassays

Multiplexed bead-based arrays facilitating simultaneous measurement of different analytes. Human CCL2, sCD14, and IL-6 in co-culture supernatants were quantified using cytometric bead arrays according to manufacturers' protocols (BD). Murine CSF-1 was quantified within a bead panel using MILLIPLEX Mouse Cytokine/Chemokine Magnetic Bead Panel (Merck Millipore, Germany) according to manufacturers' instruction. Human CSF-1 and human TNF-α in culture supernatants were measured by enzyme-linked immunosorbent assay (ELISA) according to manufacturers' protocols (R&D Systems, Minneapolis, MN, USA).

2.2.11 Quantification of viable cells

2.2.11.1 Cell viability

Cell viability was determined by measuring the percentage of early and late apoptotic cells within a population that are able to bind the Annexin V protein and are positively stained for 7-AAD (7-Amino Actinomycin). For this purpose $1x10^6$ cells were incubated in 30µL PE Annexin V/7-AAD mix (1X Annexin V Binding Buffer containing 10% PE Annexin V and 10% 7-AAD) for 15 min at 4°C protected from light. Afterwards, 150µL 1X Annexin V Binding Buffer was added to the sample and

measured by flow cytometry gating on lymphocytes within the following 15 min. Double-negative cells were quantified as viable cells.

2.2.11.2 MTT assay for NLC quantification

NLC numbers were determined using MTT (3-(4,5-dimethylthiazol-2-yl)-2,5-diphenyltetrazolium bromide) solution as described before[201].In brief, CLL fraction (suspension cells) was removed and adherent cells were washed three times with pre-warm complete human medium. Adherent cells were then incubated with fresh medium containing 0.5mg/mL MTT for 2 hours at 37°C. The water soluble yellow MTT is reduced by mitochondrial dehydrogenase into formazan crystals by living cells. Morphology of NLCs that contain formazan was then observed by phase-contrast microscopy. Two pictures from different areas of a well, each from two technical replicates were, taken for further quantification using Image J.

2.2.11.3 Statistics

Data were analyzed using GraphPad Prism 7.02 software. Comparisons of two non-paired groups were performed using the Welch t test. It assumes that the two compared data sets are sampled from Gaussian populations, but may have different standard deviation (SD). The statistical test used for each data set is indicated in the figure legends. Replicates represent biological replicates, unless otherwise indicated in the figure legend. All graphs show means ± SD. ns = ≥ 0.05, *p < 0.01 to 0.05, **p < 0.001 to 0.01, ***p < 0.0001 to 0.001, ****p < 0.0001.

3 RESULTS

3.1 Modulating the myeloid tumor microenvironment in CLL by targeting the CSF-1 receptor

In order to target and investigate the potential role of the CSF-1R in CLL, *in vitro* experiments were performed in the initial phase. For this purpose a monoclonal antibody targeting the human CSF-1R (provided by Transgene SA., France) named TG3003 was applied in coculture setups, using either (1) human CLL-monocyte cocultures, or (2) 'NLC cocultures'.

As recapitulated in the introduction, similar to stromal cells also healthy monocytes can serve as feeder cells to promote CLL cell survival[306, 307]. This is a suitable model for investigations of monocytes in coculture with CLL cells, and at the same time for comparing the effects of the antibody with monocyte monocultures. It is also convenient in view of the challenge to isolate sufficient numbers of monocytes from CLL blood samples, since these are by definition highly enriched with leukemic cells.

In addition, the NLC coculture model represents a well-accepted autologous *in vitro* model for the CLL microenvironment[308]. In this case, unsorted CLL-PBMCs are cultured in high cell density for 8 – 14 days, and it was shown that monocytes differentiate in these cultures into supportive nurse-like cells (NLCs) which is induced by cell-cell contact with CLL cells[78]. Especially with regard to the need of an *in vitro* platform mimicking the CLL lymph node microenvironment, NLC cocultures seem a perfect solution, as lymph node biopsies from CLL patients are highly limited.

However, such *in vitro* cultures can only partially represent the *in vivo* situation and are not capable of reflecting the complex interactions between the various cells of the immune system. Therefore, the aim was to subsequently investigate effects of targeting the CSF-1/CSF-1R axis on tumor development and its TME in the Eμ-TCL-1 adoptive transfer mouse model of CLL (referred to as TCL-1 AT from here), using TG3003 antibody.

3.1.1 Targeting CSF-1R in the tumor microenvironment of CLL *in vitro*

In order to answer if the CSF-1/CSF-1R axis might be as suitable microenvironmental target for CLL treatment, first cocultures of primary human CLL cells and healthy monocytes were set up. CLL cells and monocytes were derived from PBMCs isolated from CLL patients and healthy donors by Ficoll density gradient, followed by magnetic cell sorting with anti-CD14 coated beads for monocyte enrichment. Supernatants from these cocultures were harvested at day 3, 6 and 14 and the level of CSF-1 was measured using enzyme-linked immunosorbent assay (ELISA). CSF-1 did not reach a

detectable level at day 3 (data not shown) and only in 1 out of 3 cocultures at day 6, while it was detectable in all three cocultures at day 14 (Figure 8a).

As CSF-1 was present in CLL-monocyte cocultures, the next step was to test if TG3003 treatment would impact on CSF-1R-expressing monocytes/macrophages. For this purpose, monocultures of monocytes were set up. As monocytes *in vitro* require supporting factors to survive, the monoculture was supplemented with recombinant human CSF-1 as well as another important growth factor, CSF-2, which are known to induce differentiation of monocytes to macrophages. TG3001 was added, based on pre-testing of the founder company Transgene SA, in a concentration of 1µg/mL to cocultures every second day. Cells that were treated with the control isotype antibody developed star-like shaped elongations, a typical morphology of *in vitro* differentiated macrophages, whereby the degree of elongations has been proposed to positively correlate with M2-macrophage polarization (Figure 8b)[309]. In contrast, the addition of the CSF-1R-specific antibody TG3003 to the culture prevented the formation of these elongations and favored a round cell shape, indicating a modulating effect on monocyte differentiation (Figure 8b).

Next, NLC cocultures were used to address the question if modulation of CSF-1R-expressing cells might affect the survival of CLL cells. Unsorted PBMCs from CLL patients with a high tumor load were seeded in high cell density as previously described and cultured for 14 days to induce nurse-like cell differentiation[305]. As described before, nurse-like cells differentiation started after approximately 3 to 5 days (depending on the patient donor), and as expected CLL cell survival was maintained. Application of the antibody TG3003 to the culture lead to a significant decline in the survival of CLL cells from different patients as measured by the percentage of $CD5^+CD19^+$ cells that were negative for Annexin V/7-AAD staining (Figure 8c). Higher doses of TG3003 up to 10µg/mL also did not further reduce CLL survival indicating that this dose was already sufficient to achieve the maximum effect (data not shown).

Of note, the number of NLCs in these cocultures varied between the CLL patients. In this context, it is interesting to note that indeed cocultures that displayed fewer NLC numbers in the control wells showed also a weaker anti-CSF-1R-induced disruption of CLL survival support in response to TG3003. This observation supported the hypothesis that the effect of TG3003 was mediated through CSF-1R-expressing NLCs in these cocultures. In addition, also survival of purified CLL cells (using magnetic cell sorting with anti-CD19 coated beads) in monocultures was not affected by TG3003 up to a concentration of 10µg/mL (data not shown).

To further elucidate TG3003-induced disruption of NLC-mediated survival support, different treatment regimens were conducted: TG3003 was applied (1) during the complete duration of the NLC coculture (day 1 to 14), (2) only during the first half of the NLC coculture (day 1 to 7), or (3) only

during the second half of the NLC coculture (day 8 to 14). NLC-mediated CLL cell survival was most effectively disrupted if TG3003 was present in the culture from day 1 to 14. Treatment restricted to the first week was similarly efficient in reducing survival support, whereas later treatment onset did not impact on survival support (Figure 8d).

Morphologically, NLCs appear as large and round cells and no change in their shape was observed upon TG3003 treatment. NLC cocultures treated with TG3003 displayed a decreased number of NLCs as compared to control antibody-treated cocultures (Figure 8e,f). In line with the latter observation, NLC cocultures that were treated with TG3003 during day 1 to 7 and day 1 to 14 displayed less NLC differentiation compared to control wells (data not shown). In NLC cocultures with late TG3003 treatment onset, the distribution of NLCs looked similar to the control wells. These results suggest that targeting CSF-1R signaling in monocytes with TG3003 prevented differentiation of NLCs.

Supernatants of NLC cocultures were collected and used for quantification of various secreted factors by cytometric bead array or ELISA. The cytokine CCL2, which was previously shown to be induced in monocytes by the presence of CLL cells and elevated in CLL sera, was significantly lower in TG3003-treated cultures (Figure 8g, left)[79]. Soluble CD14 (sCD14), reported to be secreted by monocytes and improving CLL survival, and IL-6 that is known to be secreted by monocytes and elevated in patient sera, were slightly decreased in the supernatants upon TG3003 treatment (not significant) (Figure 8g, middle and right)[306, 310, 311].

In contrast, CSF-1 concentrations in NLC cocultures remained stable upon TG3003 treatment (Figure 8h). This is in line with data from Transgene SA which suggested that TG3003 does not block binding and internalization of CSF-1 to the receptor. This was important for future (pre-) clinical applications, as elevated plasma CSF-1 levels, may lead to rebound effects in treated patients[312].

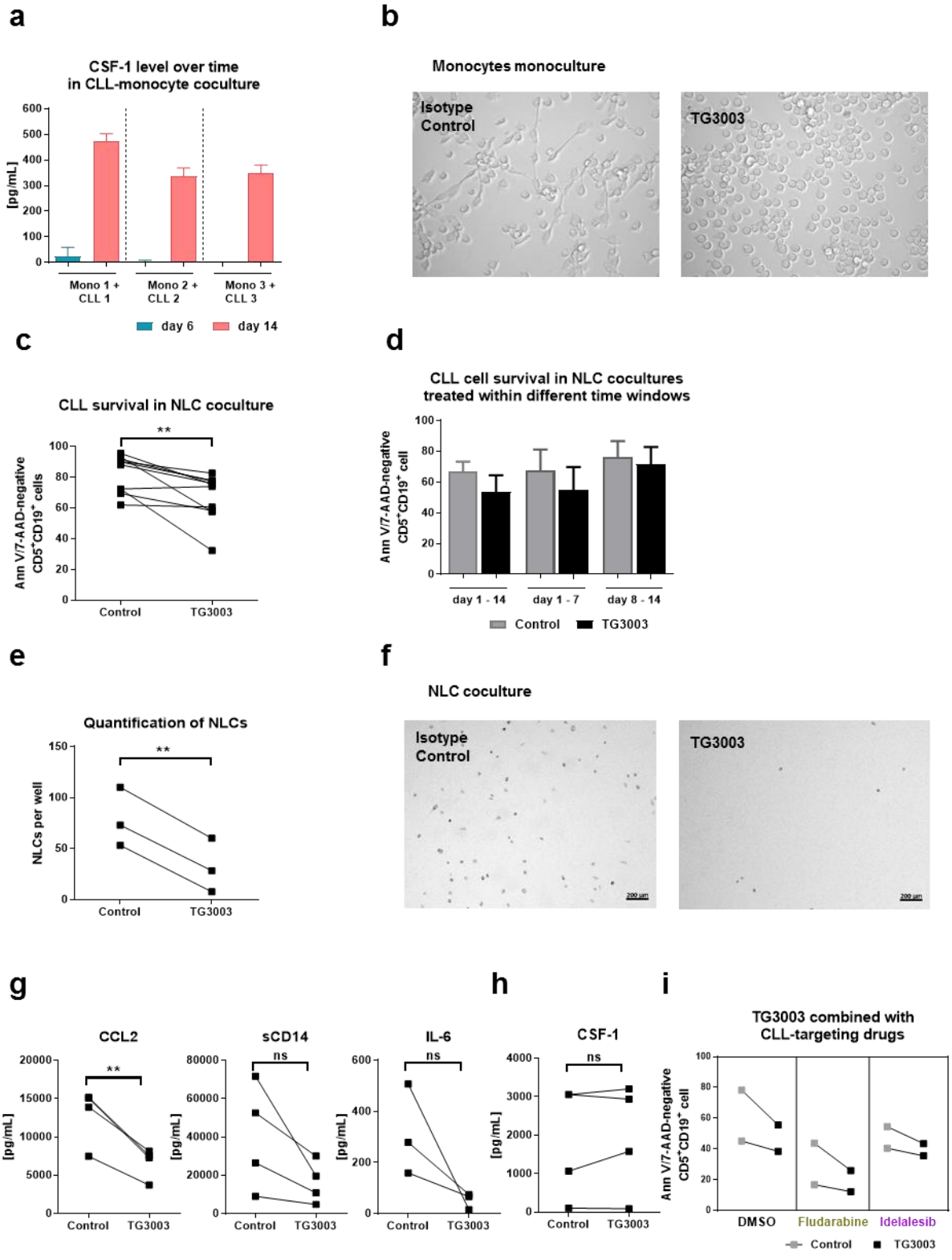

Figure 8: Anti-CSF-1R treatment impacts on NLC differentiation and thereby on CLL cell survival *in vitro*. Peripheral blood mononuclear cells (PBMCs) were isolated from CLL patient whole blood by Ficoll density gradient. To retrieve monocytes, $CD14^+$ cells were enriched using magnetic cell sorting. PBMCs from CLL patient's whole blood were used directly. **(a)** CSF-1 concentrations in the culture supernatant of CLL-monocyte cocultures ($5x10^6$ CLL cells : $2.5x10^6$ monocytes in 500µL medium/well in a 24-well plate) were assessed at day 6 and day 14 by enzyme-linked immunosorbent assay (ELISA). Each bar represents mean of three technical replicates. **(b)** Light microscopy images of monocyte monocultures ($5x10^6$ monocytes/mL)

differentiated for 5 days with recombinant human CSF-1 (20ng/mL) and CSF-2 (100ng/mL) added every second day. Monocytes were concordantly either treated with 1µg/mL isotype control (left) or anti-CSF-1R, TG3003 (right). **(c,d)** CLL PBMC were cultured in high cell density ($1.5x10^7$ cells/mL) and treated with 1µg/mL isotype control antibody or TG3003 every second day (n=10) for 14 days (c) or for the indicated time periods (day 1-14, day 1-7 or day 8-14) (n=3) (d). Viability of $CD5^+CD19^+$ CLL cells was assessed by flow cytometry using Annexin V/7-AAD staining. **(e,f)** Quantification of NLC numbers in NLC cocultures cultured for 8 days in high cell density ($1.5x10^7$ cells/mL) and treated with 1µg/mL isotype control antibody or TG3003 twice (on day 1 and day 4) (n=3) (e) and representative light microscopy image after removal of suspension cell fraction (f). NLCs were incubated in MTT solution (0.5 mg/mL) for 2 hours. Quantification was performed using ImageJ software. **(g,h)** CLL PBMCs were cultured for 14 days in a high cell density of $1.5x10^7$ cells/mL ($0.75x10^7$ CLL PBMCs in 500µL medium in a 48-well plate) and treated with 1µg/mL isotype control or TG3003 every second day. CCL2 (n=4), soluble CD14 (sCD14) (n=4), IL-6 (n=3), and CSF-1 (n=4) were measured in cell culture supernatants by cytometric bead array (g) or ELISA (h). **(i)** Annexin V/7-AAD flow cytometry assay of primary $CD5^+CD19^+$ CLL cells harvested from NLC cocultures (n=2). CLL cells were isolated and cultured for 10 days in a high cell density of $1.5x10^7$ cells/mL and treated with 1µg/mL isotype control or TG3003 every second day. In addition, Fludarabine (25µM), Idelalisib (10µM) or DMSO were added once on day 8. *P* values were determined by paired Student t-test. (Ann V/7-AAD=Annexin V/7-AAD)

Finally, anti-CSF-1R treatment in NLC cocultures was combined with the CLL-targeting drugs Fludarabine and Idelalisib. Both combination approaches lead to a stronger reduction in CLL cell survival in the cultures compared to respective monotherapies, suggesting additive or synergistic effects and therefore appearing as promising strategy for *in vivo* testing (Figure 8i). Altogether, the observed effects of targeting the CSF-1/CSF-1R axis on monocytes or NLCs in coculture with CLL cells, and especially the resulting outcome for CLL cell survival turned out to be a promising treatment option for monotherapy as well as combination therapy to be tested in a pre-clinical study.

3.1.2 Targeting CSF-1R in the tumor microenvironment of CLL *in vivo*

As CSF-1R antibody inhibited NLC formation *in vitro* and thereby reduced CLL cell survival, investigating the effect of targeting CSF-1R *in vivo* by using a CLL mouse model was the next goal. As TG3003 targets human CSF-1R, using the syngeneic TCL-1 AT model was not feasible. Hence, using a human CSF-1R knockin (KI) mouse line that expresses a chimeric CSF-1R protein comprising a human epitope within the murine CSF-1R, represented an excellent approach. This chimeric protein can be specifically targeted by TG3003 and can also bind the murine CSF-1R ligands CSF-1 and IL-34[313]. An 'almost syngeneic' transplantation of Eµ-TCL-1 tumor cells in humanized CSF-1R KI mice served as perfect approach to test TG3003 in the context of CLL, while facilitating the possibility of subsequently testing this antibody for clinical applications.

In order to prove the usability of this mouse line, a pilot study was conducted that verified tumor cell engraftment and skewing of myeloid cell populations, comparable to previous observations in adoptively transferred wildtype C57BL/6 mice (data not shown)[203].

In an independent experiment the relevance of the CSF-1/CSF-1R axis for the TCL-1 adoptive transfer (AT) model for CLL was further suggested by results of a longitudinal study with animals sacrificed at different time points (week 2, week 4, week 6, and week 8 after transplantation). Here, a slight increase of CSF-1 levels in the serum of these mice during the course of leukemia progression was observed (Appendix Figure 2a).

After that, three cohorts of CSF-1R KI mice were set up including 1) animals without tumor transplantation and without treatment ('Wildtype' = 'WT'), 2) animals injected with TCL-1 tumor and treated with the control antibody Synagis ('Control'), and 3) animals injected with tumor and treated with TG3003 ('TG3003'). Synagis, a human IgG1 monoclonal antibody against the respiratory syncytial virus, was chosen as control antibody with similarities to TG3003 but no antigen target in mice. CSF-1R KI mice were injected intravenously with a pool of TCL-1 splenocytes. The tumor cells were depleted for CD4-, CD8-, CD11c-, CD49b-, CD90.2-, Ly-6C/G (Gr-1)-, and TER119-positive cells using the EasySep™ Mouse Pan-B Cell Isolation Kit before injection, in order to achieve a high purity of $CD5^{+}CD19^{+}$ malignant B cells and avoid transfer of non-tumor cells. Treatment was started at day 1 after tumor cell injection. Synagis and TG3003 were injected intraperitoneally three times per week in a concentration of 3mg/kg, as suggested and described by Transgene SA[314]. As monocytes are rapidly repopulating cells, the last injection was conducted one day before animals were sacrificed. Mice were treated for a period of 6 weeks and tumor load was monitored in the peripheral blood every second week, in addition to signs of illness. At the endpoint of the study, all animals were sacrificed and lymphoid organs were harvested and evaluated with a special focus on the analysis of myeloid cell populations. As leukemia development was very heterogeneous in this study, animals which did not display splenomegaly at the endpoint were excluded from the analysis.

3.1.2.1 Anti-CSF-1R treatment with TG3003 impacts on myeloid cell numbers in the TCL-1 AT model

Myeloid cells were examined using a multicolor flow cytometry marker panel allowing a specific discrimination of monocytes, conventional dendritic cells (cDCs), their respective subsets and macrophages (Appendix Figure 1). Monocytes and cDC absolute cell numbers from control mice were highly elevated in the spleen compared to WT mice, whereas macrophages showed decreased numbers, all together confirming previous results on the myeloid TME in the TCL-1 AT model (Figure 9a). Treatment with TG3003 lead to a significant reduction of monocyte numbers (3.07-fold reduction) (Figure 9a, left). However, despite the antibody's strong effect on monocytes, their numbers remained significantly elevated compared to WT animals. Similarly, also cDCs were significantly reduced in numbers upon treatment (1.44-fold reduction), but also not fully normalized to WT levels (Figure 9a, middle). Interestingly, macrophages that are decreased in leukemic animals compared to WT mice seemed not further affected by the treatment in most animals (Figure 9, right).

In the bone marrow compartment, there was only a tendency (p=0.0702) towards normalization of the overall amount of CSF-1R-expressing cells, whereby the control cohort appeared to be heterogeneous (Figure 9b). CSF-1R-expressing cells in the bone marrow typically comprise monocytic and dendritic cell precursors in addition to mature monocytes. Gating on mature monocyte subsets in the bone marrow revealed a similar pattern as in the spleen, which was a partial reversal of disease-associated accumulation of monocytes upon treatment (Appendix Figure 2b). These results suggest that TG3003 systemically reduces monocyte numbers, and to some degree also cDCs.

By gating on the two main splenic monocyte subsets, distinguished by differential expression of Ly6C, a significant increase of both populations, Ly6C^{high} as well as Ly6C^{low} monocytes, was confirmed in the leukemic control group (Figure 9c,d). As expected, the Ly6C^{low} population was much stronger enriched compared to the Ly6C^{high} monocyte population (25.66-fold and 3.9-fold compared to WT mice) (Figure 9c). While TG3003 did not notably affect the Ly6C^{high} population, Ly6C^{low} monocytes displayed a significant reduction upon treatment (4.25-fold reduction). However, similar as the total monocyte population, the leukemia-induced cell numbers were only partially reduced to normal levels by TG3003.

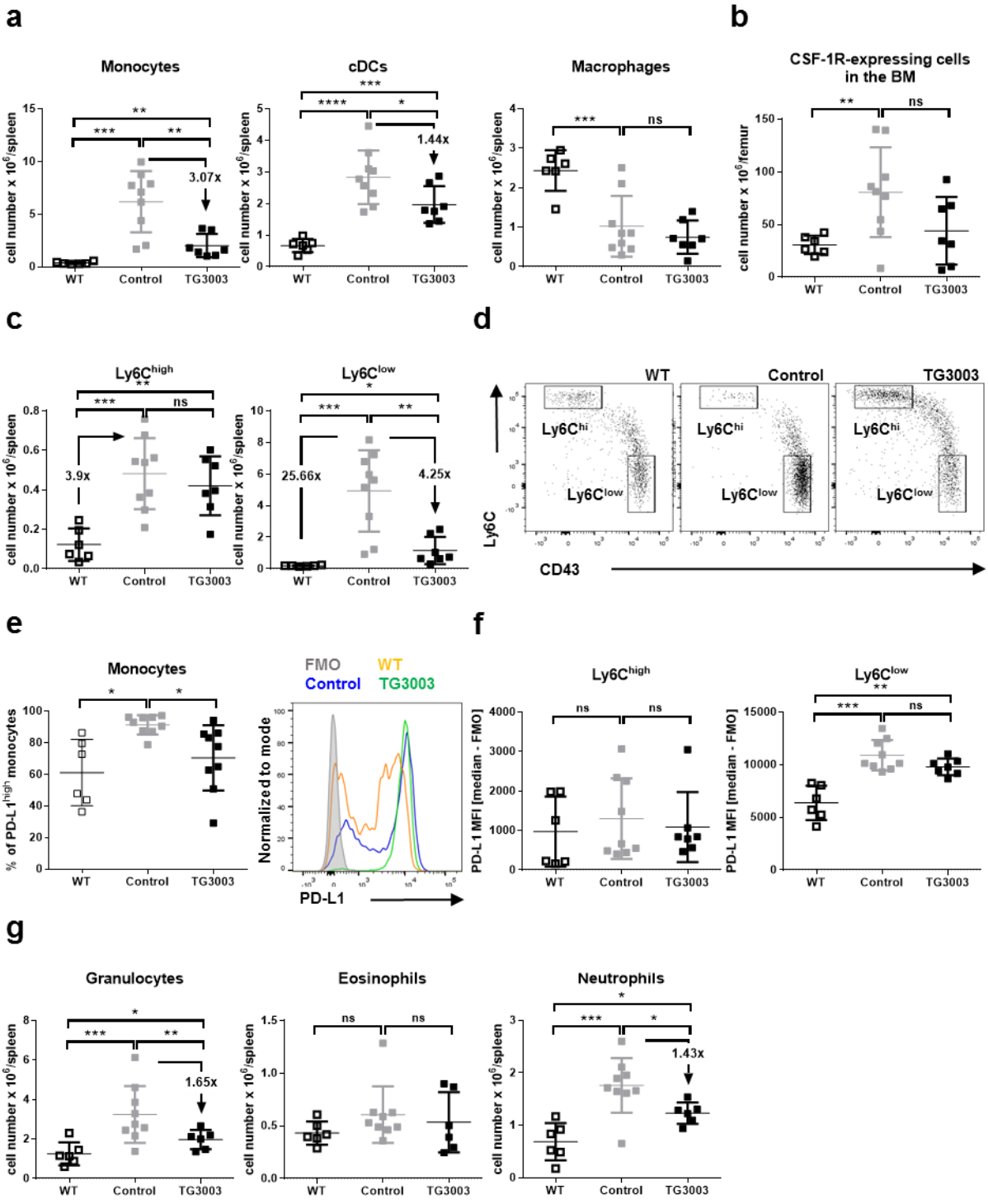

Figure 9: TG3003 treatment of CSF-1R KI mice after TCL-1 AT impacts on myeloid cell numbers.
CSF-1R KI mice were transplanted i.v. with $2x10^6$ malignant splenocytes pooled from four leukemic TCL-1 donor mice. Starting at day 1 post-transplantation, mice were injected i.p. with control antibody (Synagis) or TG3003 at 3mg/kg/week for 6 weeks. Untransplated CSF-1R KI wildtype (WT) mice (n=6) served as healthy control group. Analyses at the study endpoint were performed for animals showing >50% of $CD5^+CD19^+$ cells in the spleen and presence of clear splenomegaly (control cohort: n=9, anti-CSF-1R cohort: n=7). **(a)** Absolute numbers of monocytes (left), cDCs (middle), and macrophages (right) in the spleen as measured by flow cytometry. **(b)** Absolute numbers of CSF-1R-expressing cells in the bone marrow (BM) (one femur). **(c)** Absolute numbers and **(d)** representative flow cytometry density plots of $Ly6C^{high}$ and $Ly6C^{low}$ monocyte subsets in the spleen, after gating on monocytes. A detailed gating scheme is illustrated in Appendix Figure

1. **(e)** Percentage of PD-L1-expressing splenic monocytes (left) and representative histogram illustrating bimodal distribution of PD-L1 signal on total monocytes (right). **(f)** PD-L1 expression level on Ly6C^{high} monocytes (left) and Ly6C^{low} monocytes (right). **(g)** Absolute numbers of granulocytes (left), eosinophils (middle), and neutrophils (right) in the spleen. (splenic granulocytes: DAPI$^-$CD45$^+$CD5$^-$CD19$^-$NK.1.1$^-$CD3$^-$CD11b$^+$Ly6G$^+$; splenic eosinophils: DAPI$^-$CD45$^+$CD5$^-$CD19$^-$NK.1.1$^-$CD3$^-$CD11b$^+$Ly6G$^+$Ly6C^{hi}; splenic neutrophils: DAPI$^-$CD45$^+$CD5$^-$CD19$^-$NK.1.1$^-$CD3$^-$CD11b$^+$Ly6G$^+$Ly6C^{low}; bone marrow CSF-1R-expressing cells: DAPI$^-$ Lin$^-$ (CD19$^-$CD3$^-$Ly6G$^-$NK1.1$^-$TER119$^-$)CSF-1R$^+$.) *P* values were determined by unpaired Student t-test.

Expression of PD-L1, which controls T cell effector function as part of the PD-L1/PD-1 axis and which was shown to be capable of creating an immune suppressive TME, was measured on the different myeloid cell populations. An aberrantly high percentage of PD-L1-expressing monocytes was detected in leukemic mice in the control group, while the proportion was significantly reduced upon treatment with TG3003 (Figure 9e, left). Notably, Ly6C^{low} monocytes turned out to be the main PD-L1-expressing subpopulation with higher median fluorescence intensities (MFIs) as compared to Ly6C^{high} monocytes (Figure 9f). As TG3003 treatment neither influenced PD-L1 expression level of Ly6C^{high} nor of Ly6C^{low} monocytes (Figure 9f), this highly suggests that the observed reduction in PD-L1 percentages on total monocytes was due to a reduction in the Ly6C^{low} monocyte population as the main PD-L1-expressing subset.

In order to track effects of TG3003 on other myeloid cells in the spleen, granulocytes, and particularly eosinophils and neutrophils, were quantified. As reported before, granulocyte numbers highly increase with disease progression in the TCL1 mouse model, which seemed to be mainly attributed to neutrophils[315]. Similarly as for monocytes, targeting CSF-1R reduced the elevated neutrophil numbers, nevertheless not to a full normalization (Figure 9g).

TG3003´s mode of action was proposed to be immunomodulatory and not via blockade of CSF-1R downstream signaling. It was proposed to drive differentiation of monocytes towards a DC-phenotype *in vitro*[316]. Therefore, potential changes of DC subsets and their phenotype were investigated[316]. Along with the unchanged frequency of cDCs in the spleen, there was no detectable effect of TG3003 on the two main cDC subsets (either CD11c$^+$ CD8a$^+$ CD11b$^-$ or CD11c$^+$ CD8a$^-$ CD11b$^+$). Expression of maturation and activation markers of cDCs, such as CD86, CD54, CD83 and MHC-II remained at similar levels compared to control antibody-treated mice (data not shown).

3.1.2.2 Anti-CSF-1R treatment with TG3003 does not affect T cell numbers or T cell effector functions and does not improve disease development in the TCL-1 AT model

In addition to investigations of cell subsets in the myeloid compartment, also T cells, as crucial players of the TME were immunophenotyped with respect to typical CLL-induced changes and defects. As T cells are not the main focus of the current thesis, only a few of the results will be briefly summarized here. Firstly, quantification of T cell populations revealed that CLL-induced elevated numbers of $CD4^+$ and $CD8^+$ T cells remained high after treatment with TG3003, which is also reflected in an increased CD4/CD8 ratio, a feature that is observed in approximately 40% of CLL patients[317] (Figure 10a). Secondly, the percentages of naïve, central memory and effector T cells within $CD4^+$ and $CD8^+$ T cell populations were evaluated as previous studies have shown skewing of the T cell compartment toward effector T cells in CLL patients and in the Eμ-TCL-1 mouse model[115, 237]. While this abnormal change in T cell subset proportions was confirmed in leukemic animals, TG3003 treatment did not contribute to a normalization of the percentages of T cell subsets (data not shown). Thirdly, T cell exhaustion, arising in response to chronic antigen-mediated T cell receptor stimulation, is a hallmark of CLL and was investigated by measuring the expression of the exhaustion markers KLRG1 and LAG-3[110]. CLL-associated increase of KLRG-1 and LAG-3 expression on T cells remained at an elevated level in TG3003-treated compared to untreated animals (data not shown). And finally, the effector function of $CD4^+$ and $CD8^+$ effector T cells was investigated via intracellular FACS staining by analyzing their capacity to produce IL-2, IFN-γ, and TNF-α, upon T cell stimulation. The development of disease led to a decrease of PMA/Ionomycin-stimulated TNF-α^+ IFN-γ^- CD8 cells and an increase in the percentages of TNF-α^- IFN-γ^+ CD8 cells which was in the case of TNF-α^- IFN-γ^+ CD8 cells partially normalized (Figure 10b).

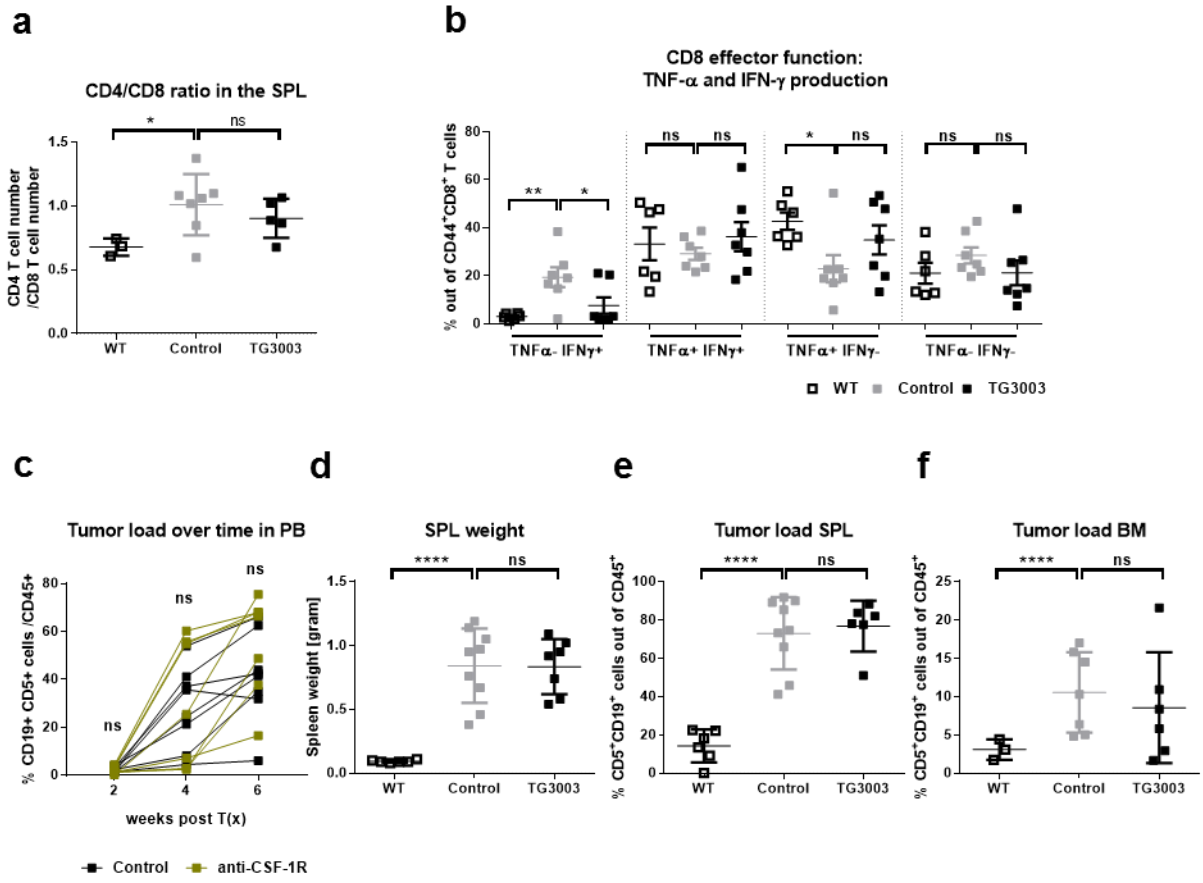

Figure 10: TG3003 treatment of CSF-1R KI mice after TCL-1 AT does not impact on T cells or disease outcome. TCL-1 AT and treatment was performed as described in Figure 9. **(a)** CD4/CD8 ratio based on absolute numbers of splenic $CD4^+$ T cells and $CD8^+$ T cells. **(b)** Percentage of TNF-α and IFN-γ producing $CD44^+CD8^+$ T cells assessed by intracellular flow cytometry following PMA/Ionomycin stimulation of isolated splenocytes for 6 hours. **(c)** Tumor load in peripheral blood (PB) over time in mice treated with control antibody (n=8) or TG3003 (n=7). **(d)** Spleen weight, and **(e)** percentage of $CD5^+CD19^+$ cells in spleen (SPL), and **(f)** bone marrow (BM) as acquired by flow cytometry are presented in the three treatment groups. (Splenic $CD4^+$ T cells: $DAPI^-CD3^+CD4^+$; splenic $CD8^+$ T cells: $DAPI^-CD3^+CD8^+$; leukemic $CD5^+CD19^+$ cells in the PB, SPL, and BM: $CD45^+CD5^+CD19^+$; PB=peripheral blood, BM=bone marrow, SPL=spleen). *P* values were determined by unpaired Student t-test.

In summary, the assessment of T cell populations did not reveal notable differences between TG3003- or control antibody-treated mice that could be attributed to an indirect effect of the observed alterations in monocyte numbers, monocyte subset composition or their decreased proportion of PD-L1, the ligand of PD-1 which is typically expressed by activated or exhausted T cells.

During the treatment period as well as at the endpoint of the study, no significant difference in tumor load in peripheral blood of TG3003-treated and control antibody-treated animals was observed (Figure 10c). Evaluation of tumor burden at the endpoint revealed no difference in spleen weight and similar percentages of malignant $CD5^+CD19^+$ cells in spleen and bone marrow (Figure 10d,e,f). Overall, despite promising initial *in vitro* results with TG3003, and considerable, partial

normalization of the monocyte compartment (in particular declined percentage of PD-L1^{high}-expressing monocytes), treatment of leukemic mice with TG3003 did not improve disease outcome in the presented study.

3.2 Monocytes and cDCs in steady state, in CLL and under the influence of Ibrutinib

To improve therapeutic targeting of myeloid cells in CLL, it is necessary to improve the understanding of how these cells develop and contribute to the pathogenesis during this disease. It is yet unclear, if myeloid cells mainly exhibit support for CLL cell survival or are rather major players in T cell suppression. Moreover, clinically applied drugs in CLL not only target the malignant cells directly, but also impact on other immune cells, including myeloid cells, and may thereby contribute both in a negative or positive way to treatment outcome. Fully understanding a drug's spectrum of activities is of special importance for the development of efficient treatment regimens. Further, even in steady state condition, the function of immune cells and their interplay with each other are not fully unraveled, adding more complexity to the understanding of the roles of these cells under disease conditions. Therefore, the goal of this study was to gain a better understanding of myeloid cells in steady state, their pathobiological role in CLL, and under the influence of Ibrutinib, a clinically potent drug that targets BTK primarily in malignant B cells, but might also have effects on immune cells in the TME. As monocytes and cDCs, two closely related myeloid cell members, accumulate during leukemia development in the TCL-1 AT model, these cells were the focus of the following studies.

3.2.1 Monocytes in steady state, in CLL and under the influence of Ibrutinib

3.2.1.1 Ly6C^{low} monocytes are altered in CLL and display an expression signature associated with activation of cellular growth and proliferation

To better characterize the CLL-induced molecular properties of Ly6C^{hi} and Ly6C^{low} monocytes, an array-based gene expression profiling (GEP) from leukemic TCL-1 AT animals, five to six weeks after adoptive transfer of 2x10^7 splenocytes (n=3) and matched healthy wildtype (=WT) control animals (n=3) was performed. Splenocytes from three WT mice were pooled per data set to retrieve sufficient RNA for the analysis. Ly6C^{hi} and Ly6C^{low} monocytes were flow sorted according to their surface markers and assessed to purity control (Appendix Table 1). Total RNA was isolated and submitted to the Genomics and Proteomics Core Facility Unit at the DKFZ for GEP using GeneChip

Mouse Gene 2.0 ST Array. Setting an adjusted *p* value of ≤ 0.05 revealed 31 genes in Ly6C^{hi} monocytes and 105 genes in Ly6C^{low} monocyte to be significantly deregulated, when comparing cells isolated from leukemic TCL-1 AT and WT mice (Figure 11a). An increased number of biological functions were found to be enriched especially in Ly6C^{low} monocytes from TCL-1 AT mice. These identified biological functions within the top five categories, were (1) *Cellular Development*, (2) *Cellular Growth and Proliferation*, (3) *Hematological System Development and Function*, (4) *Lymphoid Tissue Structure and Development*, and (5) *Tissue Morphology* (ranked by *p* value ranges) (Figure 11c). In contrast, Ly6C^{hi} monocytes displayed only a few differentially represented biological functions in TCL-1 AT and WT mice (data not shown). These were *Inflammatory Response* and *Cellular movement,* both predicted to be activated in TCL-1 AT mice. This was in line with the lower number of differentially expressed genes (DEGs) in Ly6C^{hi} compared to Ly6C^{low} monocytes, pointing to a greater influence of Ly6C^{low} monocytes in CLL.

Further, the top biological function within the top category *Cellular Growth and Proliferation* was *proliferation of mononuclear leukocytes* and comprised upregulated genes such as *Serpina3g, Il21r, Dpp4, Nfil3, Itgb3, Id3, Trem1, Jak3, C5ar1, Il1b,* and *Traf2* (Figure 11d). *Serpina3g, Il21r, Dpp4* were among the top 20 DEGs when comparing Ly6C^{low} monocytes from TCL-1 AT and WT mice (Figure 11b). This gene list serves as a basis to identify candidate genes with relevance for CLL for future investigations. In particular, genes that are significantly upregulated in Ly6C^{low} but not Ly6C^{hi} monocytes, such as *Dpp4, Nfil3, Id3, Jak3, C5ar1,* and *Traf2,* may serve as candidates for specific targeting of Ly6C^{low} monocytes.

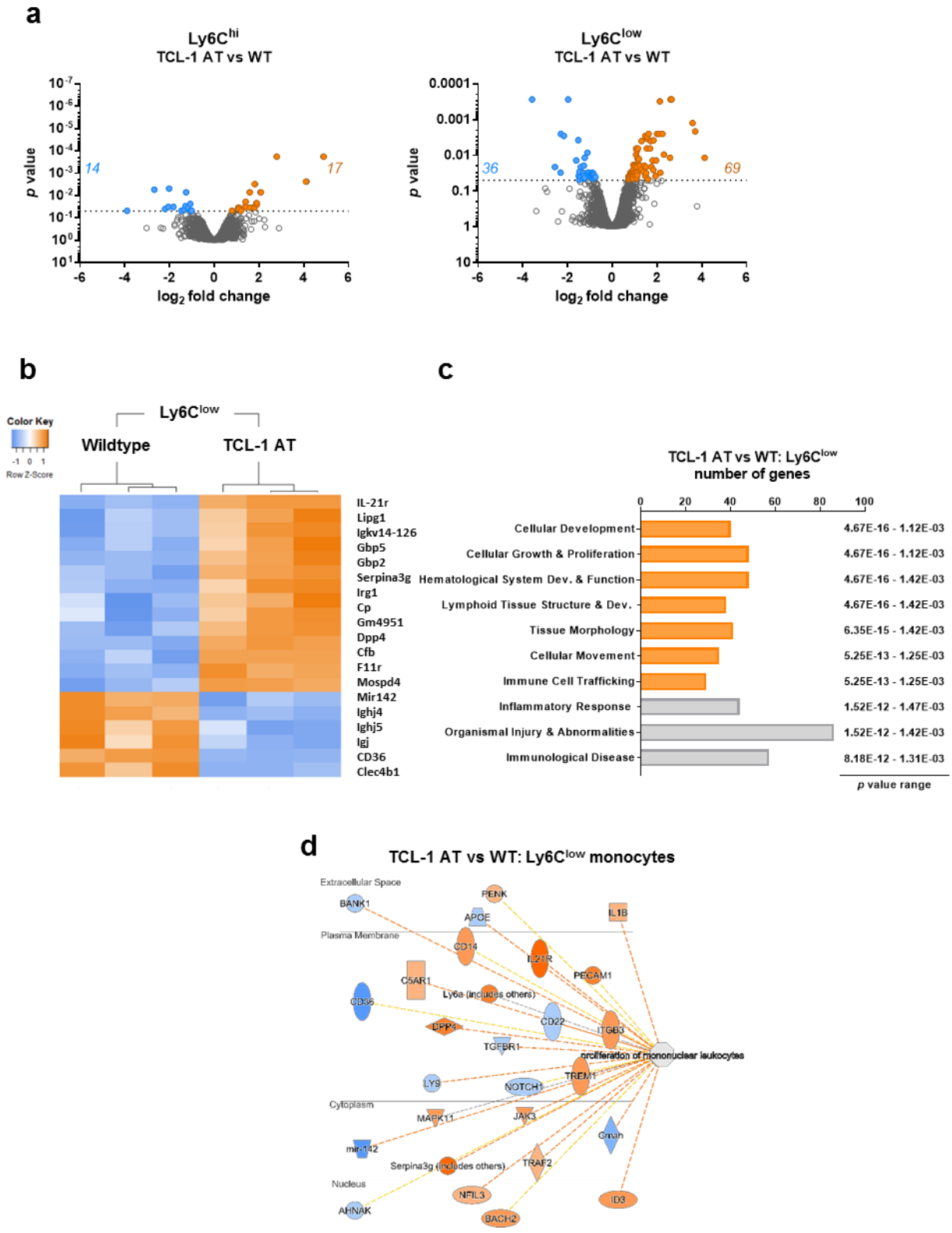

Figure 11: Differential gene expression of Ly6C^{low} monocytes in TCL-1 AT mice compared to wildtype mice is associated with activation of cellular growth and proliferation.
(a) Volcano plots showing upregulated (orange) and downregulated (blue) genes in Ly6C^{hi} (left) and Ly6C^{low} (right) monocytes from leukemic TCL-1 AT (n=3) versus WT (n=3) samples. The dotted line indicates cutoff at a *p* value of 0.05. **(b)** Heatmap of top 20 differentially expressed genes in Ly6C^{low} monocytes in TCL-1 AT (n=3) versus WT (n=3) animals **(c)** Enrichment analysis of biological functions in Ly6C^{low} monocytes (top 10 categories showed) including number of genes and *p* value ranges using IPA downstream effect analysis

(orange=category predicted to be activated, grey=category prediction unclear). **(d)** IPA network analysis of genes in Ly6C^{low} monocytes involved in the top biological function termed *proliferation of molecular leukocytes* which was predicted to be activated. A legend based on IPA tool: orange=increased measurement, blue: decreased measurement, predicted relationships=orange dashed line=leads to activation, blue dashed line=leads to inhibition, yellow dashed line=finding inconsistent with the state of the downstream molecule, gray dashed line=effect not predicted.

3.2.1.2 Ibrutinib partially reverses CLL-induced gene expression signature of Ly6C^{hi} and Ly6C^{low} monocytes

To investigate effects of Ibrutinib on Ly6C^{hi} and Ly6C^{low} monocytes, cells were flow-sorted and processed for GEP (Ibrutinib-treated: n=3) in parallel to monocytes from WT and leukemic mice, as described in the previous section. Two weeks after adoptive transfer of 2x10^7 splenocytes, animals were randomized to be treated for 2 ½ weeks with Ibrutinib added into the drinking water. Profiled samples from WT (treated with vehicle drinking water), TCL-1 AT and Ibrutinib-treated TCL-1 AT animals were confirmed to cluster according to their myeloid subpopulations (Appendix Figure 3).

Interestingly, Ly6C^{hi} and to a lesser extent Ly6C^{low} monocytes, clustered closer with samples from WT animals (Figure 12a; Appendix Figure 3). Ibrutinib treatment of TCL-1 AT mice induced differential expression of 11 genes in Ly6C^{hi} and 32 genes in Ly6C^{low} monocytes when compared to TCL-1 AT mice. These identified DEGs between TCL-1 AT and Ibrutinib-treated mice were further checked for their expression in WT samples. Notably, all of them were more similarly expressed in WT and Ibrutinib-treated samples compared to vehicle-treated mice, suggesting a normalization of their expression pattern by Ibrutinib. Further analysis of Ly6C^{high} and Ly6C^{low} monocytes using a venn diagram revealed 18 differentially expressed genes which were unique for the Ly6C^{low} subpopulation (not present in the Ly6C^{hi} DEG list) (Figure 12b,c). Out of these genes, *CD22 (SIGLEC-2), Dpp4,* and *Pecam-1* appeared to be involved in the proliferation of Ly6C^{low} monocytes suggesting that Ibrutinib might impact on the proliferative capacity of these cells (Figure 11d).

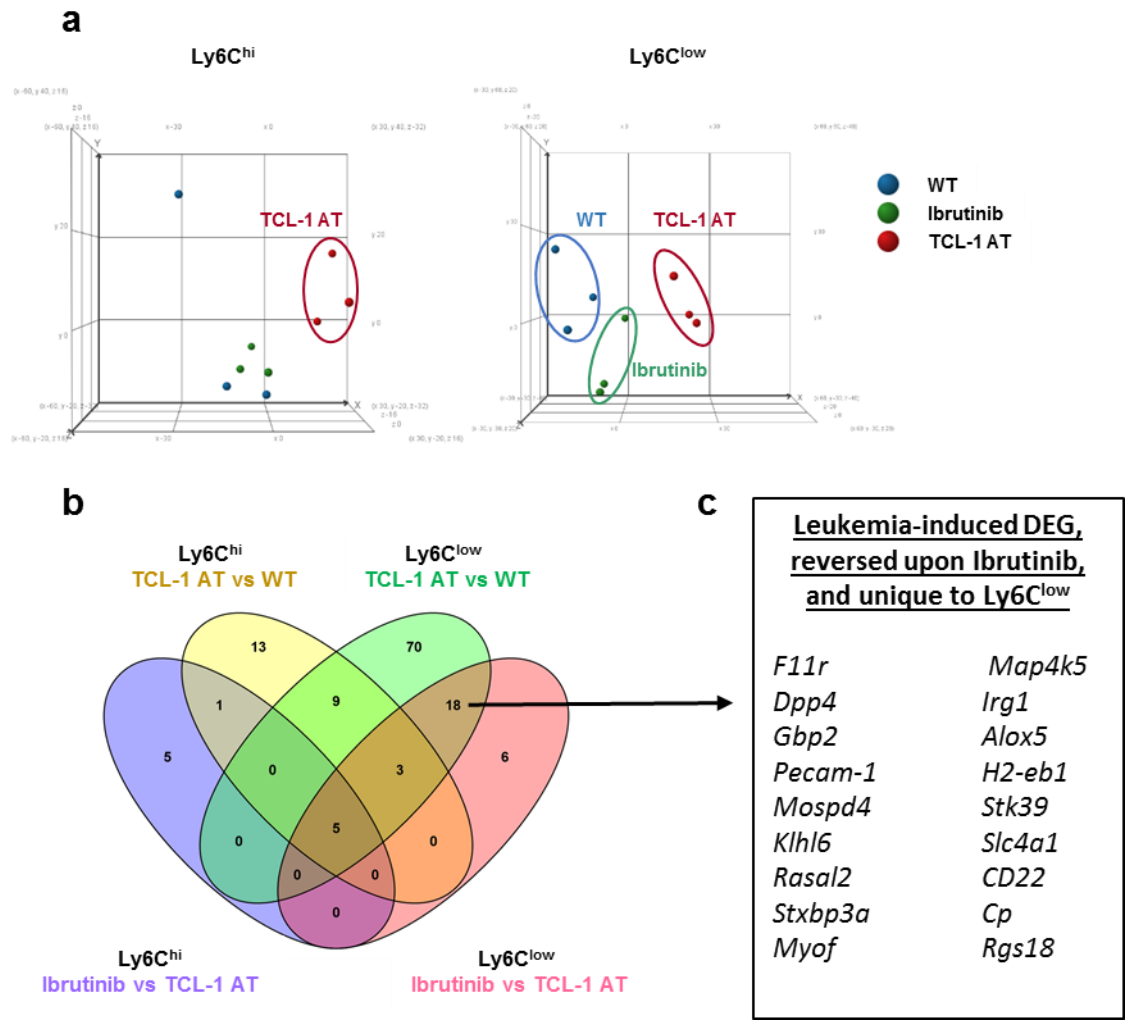

Figure 12: Ibrutinib treatment of mice normalizes leukemia-induced gene expression of Ly6C^{hi} and Ly6C^{low} monocytes.
(a) Principle component analysis (PCA) of transcriptome data of isolated splenic Ly6C^{hi} (left) and Ly6C^{low} (right) monocytes from three WT (blue), leukemic (red), and Ibrutinib-treated (green) samples each. **(b)** Venn diagram of unique and common DEGs in 'TCL-1 AT vs WT' (yellow+green) and 'Ibrutinib vs TCL-1 AT' (blue+red) in Ly6C^{hi} (yellow+blue) and Ly6C^{low} (green+red). **(c)** List of 18 DEGs in 'TCL-1 AT vs WT', expressed in the opposed direction in 'Ibrutinib vs TCL-1 AT', and only differentially deregulated in Ly6C^{low} but not Ly6C^{hi} monocytes.

In summary, these data show that Ibrutinib does affect both Ly6C^{hi} and Ly6C^{low} monocytes with a higher number of significant genes normalized in Ly6C^{low} monocytes. Samples preparations were performed at time points when there was no significant difference in tumor burden between the TCL-1 AT and Ibrutinib-treated cohort (data not shown). Therefore, the observed changes in GEP are assumed to be largely independent of secondary effects due to different amounts of CD5^{+}CD19^{+} cells.

3.2.1.3 Ibrutinib abrogates pro-survival effects of monocytes for human CLL cells *in vitro*

As gene expression profiling revealed Ibrutinib-induced changes in monocytes, it seemed likely that the drug impacts on monocyte-mediate survival of CLL cells. To address this, human CLL cells isolated from patients' blood were cocultured with Ibrutinib pre-treated human monocytes for 48 hours. This resulted in reduced survival of CLL cells compared to untreated control cultures (Figure 13a).

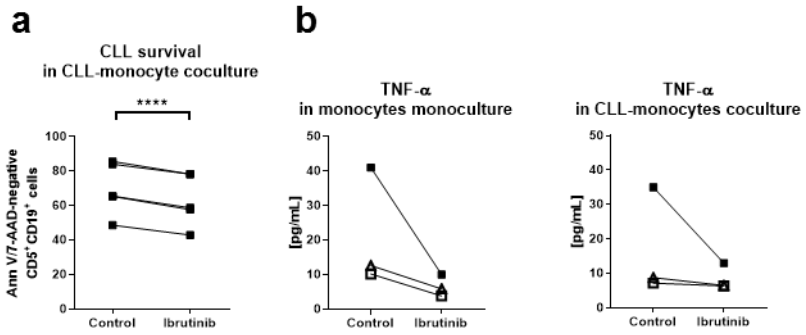

Figure 13: Ibrutinib treatment of monocytes reduced TNF-α secretion and survival support for CLL cells *in vitro*.
Monocytes were pre-treated for 1 hour with 5µM Ibrutinib, followed by washing steps to remove the drug. **(a)** Annexin V/7-AAD flow cytometry assay of primary $CD5^+CD19^+$ CLL cells harvested from CLL-monocyte cocultures (n=5) set up in a 5:1 ratio (CLL:monocytes) after 48 hours. **(b)** TNF-α level was measured by ELISA in cell culture supernatants from monocyte monocultures (n=3) and CLL-monocyte cocultures (n=3), ($2.5x10^6$ monocytes with or without $1.25x10^6$ CLL-PBMCs) with or without pre-treatment with Ibrutinib. *P* values were determined by paired Student t-test.

Quantification of TNF-α in the supernatant of these cocultures as well as in monocyte monocultures revealed decreased levels upon Ibrutinib treatment (Figure 13b), suggesting that BTK inhibition in monocytes impairs their secretion of cytokines. As monocyte-derived secreted factors, including TNF-α, are known to maintain CLL cell viability, the reduction of survival support of Ibrutinib-treated monocytes is likely partially mediated via their reduced capacity to secrete cytokines like TNF-α.

3.2.1.4 Ibrutinib inhibits phosphorylation of BTK in murine monocytes and leads to decreased cytokine levels in the TCL-1 AT mouse model

To test if the TCL-1 AT mouse model is useful to study the effect of BTK inhibition on cells of the myeloid microenvironment in CLL, phosphorylation levels of BTK were determined for different cell populations in healthy C57BL/6 WT mice treated with vehicle or Ibrutinib for 3.5 weeks. Phosphorylated BTK was detected in B cells, monocytes, granulocytes, and conventional dendritic

cells, while being significantly reduced in Ibrutinib-treated mice only in B cells and monocytes (Figure 14a).

According to literature, T cells do not express BTK but high amounts of ITK, while the other tested cell populations express BTK, but no ITK[318]. Since the only available antibody for the detection of phosphorylated BTK binds also phosphorylated ITK, a slight but not significant reduction in phosphorylated ITK in T cells by Ibrutinib was also observed (*p*=0.699) (Figure 14a).

Leukemia development in TCL-1 AT mice is associated with increased expression of several cytokines including TNF-α in monocytes (Figure 14b). As Ibrutinib treatment of mice reduced BTK activity in monocytes, we next assessed the impact of the drug on their cytokine expression levels. In line with the above described *in vitro* results, Ibrutinib treatment of mice resulted in decreased intracellular TNF-α levels compared to vehicle-treated animals (Figure 14c). Comparable results were further obtained for IL-1β (Figure 14d). Notably, gating on $Ly6C^{hi}$ and $Ly6C^{low}$ monocytes revealed that cytokines were mainly produced by the $Ly6C^{low}$ monocyte subpopulation and Ibrutinib mainly affected cytokine levels in this subpopulation (data not shown).

Intracellular TNF-α levels in cDCs were not different in WT or TCL-1 AT animals (Figure 14e) and not affected by Ibrutinib treatment (Figure 14f). However, cDCs showed lower expression of IL-1β upon Ibrutinib treatment (Figure 14g).

Of note, the percentages of TNF-α-producing monocytes from leukemic untreated and leukemic vehicle-treated animals was different in the two studies (mean of 16.53% in TCL-1 AT mice in Figure 14b versus 37.69% in vehicle-treated mice in Figure 14c). This cannot merely be explained by differences in tumor load in the two studies that might cause different levels of immune reaction by myeloid cells. The first study comparing WT and TCL-1 AT leukemic mice had a tumor load of 82.25% in the spleen. In the second study comparing Ibrutinib-treated and vehicle-treated animals, tumor load in spleen was ~85% for vehicle-treated mice and ~75% for Ibrutinib-treated mice. Also, percentages of TNF-α-producing DCs were similar in leukemic mice in both studies, although they were in general quite heterogeneous.

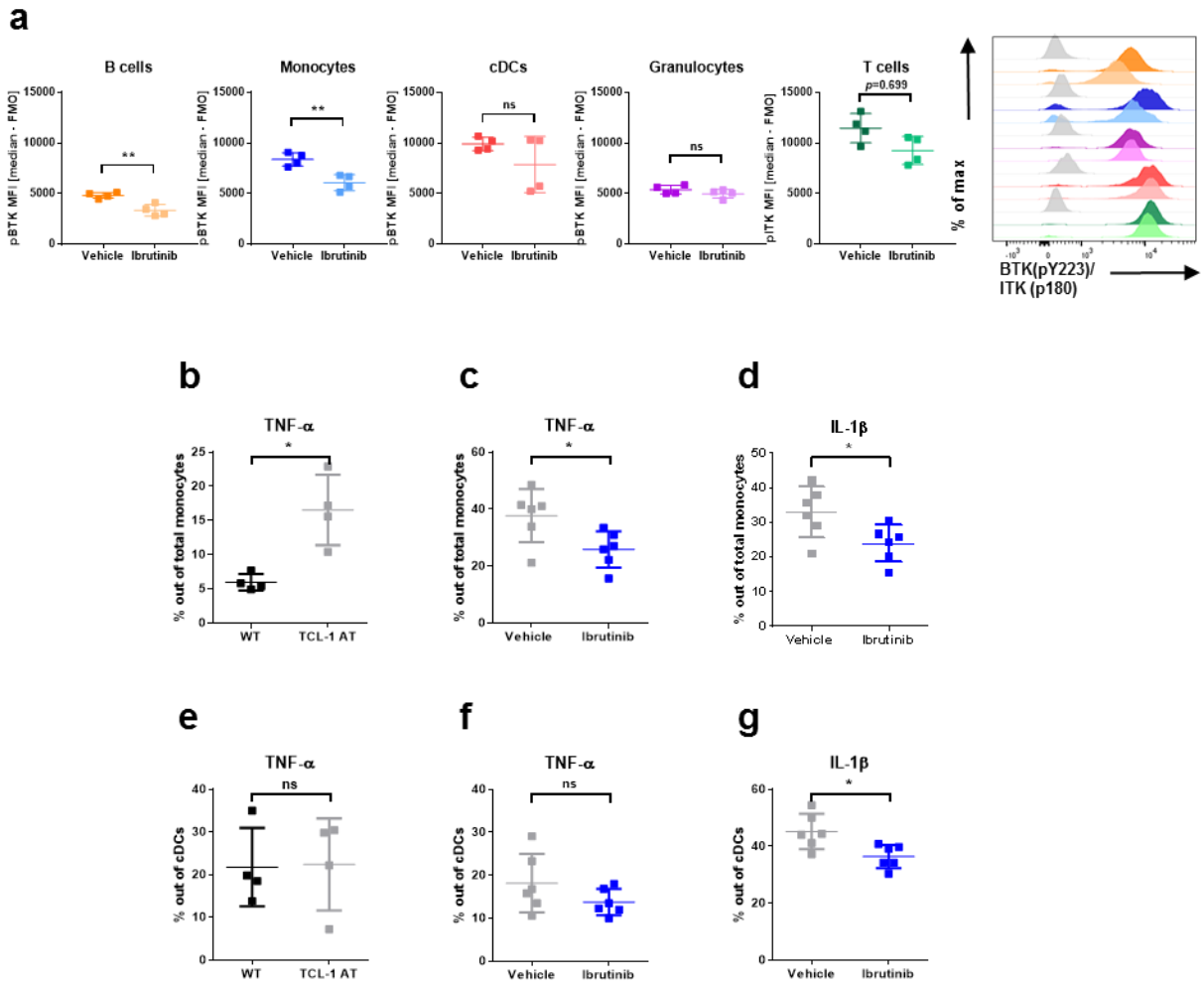

Figure 14: Ibrutinib treatment of mice reduces BTK phosphorylation and cytokine expression in monocytes. **(a)** Quantification of MFIs of phosphorylated BTK/phosphorylated ITK gated splenic B cells, monocytes, granulocytes, cDCs, and T cells from WT animals treated with vehicle (n=4) or Ibrutinib (n=4), (left); representative staggered histogram with grey histograms representing each cell population's specific FMO control. (B cells: $CD4^{-}Ly6G^{-}CD19^{+}$; monocytes: $CD19^{-}CD4^{-}CD11b^{+}Ly6G^{-}MHC\text{-}II^{low\text{-}int}CD11c^{high}CX3CR1^{hi}$; CD4+ T cells: $CD19^{-}Ly6G^{-}CD11b^{-}CD11c^{-}MHC\text{-}II^{-}CD4^{+}$; granulocytes: $CD19^{-}CD4^{-}CD11b^{+}Ly6G^{+}$; cDCs: $CD19^{-}Ly6G^{-}CD11c^{+}MHC\text{-}II^{high}$) **(b-g)** Percentage of TNF-α and IL-1β producing monocytes (b-d) and cDCs (e-g) assessed by intracellular flow cytometry after 6 hours of LPS stimulation of isolated splenocytes. Two independent experiments are shown here: **(b,e)** Comparison of healthy wildtype (WT) (n=4) and leukemic TCL-1 AT (n=4) mice; **(c,d,f,g)** Comparison of leukemic TCL-1 AT mice treated with vehicle (n=6) or Ibrutinib (n=4) for 3.5 weeks. Treatment start was at ~5% tumor load in the blood. ($Ly6C^{high}$ monocytes: Viability dye $(VD)^{-}CD19^{-}Ly6G^{-}CD11b^{+}CD11c^{low\text{-}int}MHC\text{-}II^{low}CXCR1^{+}Ly6C^{high}$; $Ly6C^{low}$ monocytes: $VD^{-}CD19^{-}Ly6G^{-}CD11b^{+}CD11c^{low\text{-}int}MHC\text{-}II^{low}CXCR1^{+}Ly6C^{low}$; cDCs: $VD^{-}CD19^{-}$ $CD11c^{high}MHC\text{-}II^{+}$) *P* values were determined by unpaired Student t-test.

In summary, these results indicate that monocytes and cDCs from TCL-1 AT mice possess a differential potential to produce cytokines and that inhibition of BTK signaling by Ibrutinib is capable of reducing cytokine expression in particular in $Ly6C^{low}$ monocytes. As these cells are the main myeloid cell population that accumulates in the TCL-1 AT model, Ibrutinib-induced changes in these cells might positively contribute to the drug's efficacy.

3.2.1.5 BTK blockade inhibits the accumulation of Ly6C^{low} monocytes in the TCL-1 AT model

To further investigate if Ibrutinib treatment in mice might impact on monocytes, cell numbers of LyC6^{hi} and Ly6C^{low} subsets were quantified in the spleen and peripheral blood. Two weeks of treatment with Ibrutinib lead to lower numbers of both monocyte subsets in peripheral blood (Figure 15a). Similarly, also splenic monocyte numbers were reduced by Ibrutinib and were at levels of WT animals (Figure 15b).

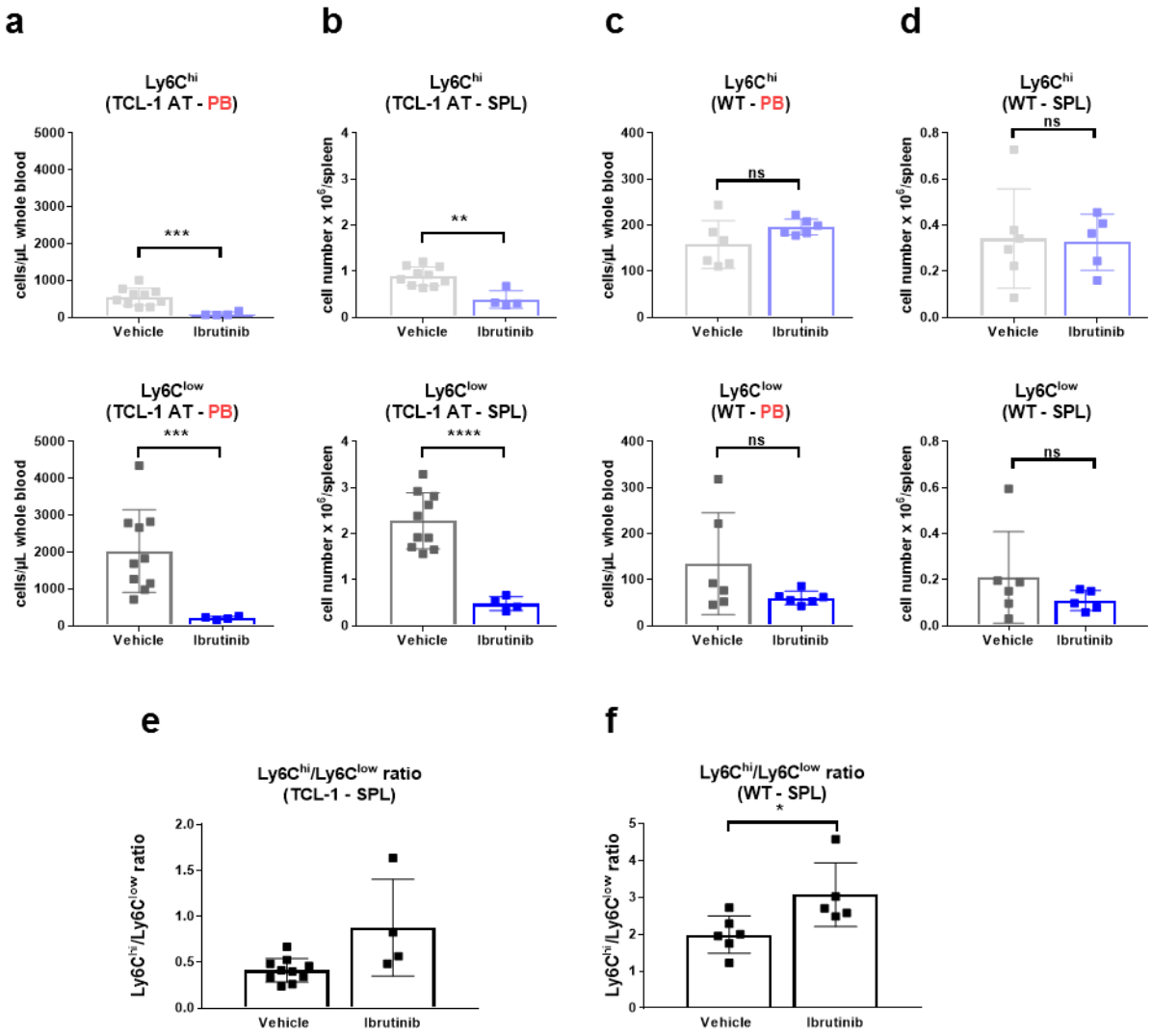

Figure 15: Ibrutinib treatment inhibits the accumulation of Ly6C^{low} monocytes in the TCL-1 AT model.
(a,b) Absolute numbers of Ly6C^{hi} monocytes (top) and Ly6C^{low} monocytes (bottom) in **(a)** peripheral blood (PB) and **(b)** spleen (SPL) from leukemic TCL-1 AT mice treated with vehicle (n=10) or Ibrutinib (n=4) for 2 weeks. **(c,d)** Absolute numbers of Ly6C^{hi} monocytes (top) and Ly6C^{low} monocytes (bottom) in **(c)** peripheral blood (PB) and **(d)** spleen (SPL) from non-leukemic wildtype (WT) mice treated with vehicle (n=6) or Ibrutinib (n=5) for 2 weeks.

Because the Ibrutinib-induced effect on cell numbers in leukemic TCL-1 AT mice was not restricted to blood monocytes but was also observed in the spleen, this excluded the possibility that subset

and cell number changes in the blood were solely due to a redistribution of cells from lymphoid organs (Figure 15a,b).

To explicitly answer the question whether the drug's effect observed at week 2 was solely due to a controlled tumor development and therefore rather an indirect effect on the microenvironment, WT mice were treated for the same period of time with Ibrutinib or vehicle control respectively. As expected, non-leukemic control animals administered with vehicle drinking water showed moderate numbers of Ly6C^{hi} and Ly6C^{low} monocytes in peripheral blood and spleen, without any of them being elevated (as indicated by the generally lower cell numbers compared to leukemic mice) (Figure 15c,d). In these wildtype animals, Ibrutinib did not lead to a reduction of the absolute number of monocyte subsets (Figure 15c,d). However, by comparing the ratios of absolute numbers of splenic Ly6C^{hi} and Ly6C^{low} monocytes for each wildtype animal, an increase of this ratio was induced by Ibrutinib, suggesting that Ibrutinib is capable of impacting directly on monocytes and their subset distribution (Figure 15e,f).

3.2.1.6 Ly6C^{hi} monocytes increase in size in the TCL-1 AT model which is normalized by Ibrutinib treatment

To further investigate monocyte subset-specific differences Ly6C^{hi} and Ly6C^{low} monocytes were checked concerning their cell size and granularity.

This revealed that Ly6C^{hi} monocytes display a higher forward and side scatter compared to Ly6C^{low} monocytes in leukemic mice (Figure 16a). This is in line with previous reports for murine monocytes[164]. However, a comparison to of each subset to the respective population in WT mice revealed an increase in size as well as granularity of Ly6C^{hi} monocytes in the TCL-1 AT model (Figure 16b). This was reversed by treatment with Ibrutinib leading to a phenotype similar to WT mice (Figure 16c). Monocytes from non-leukemic animals treated with Ibrutinib, however, did not show a difference in the forward and side scatter properties. This indicates that the observed CLL-associated size change was prevented by treatment.

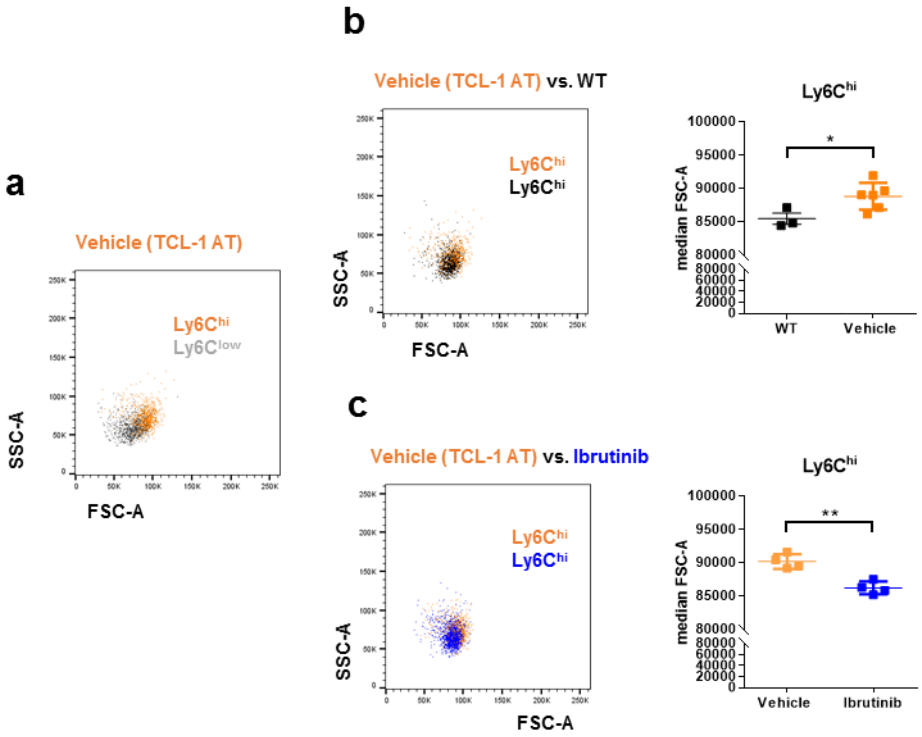

Figure 16: Ly6C^{hi} monocytes from TCL-1 AT mice exhibit an increased cell size and granularity, which is prevented by Ibrutinib.
(a) Representative overlay of flow cytometry dot plots showing forward and side scatter of Ly6C^{hi} and Ly6C^{low} monocytes from WT animals. **(b)** Overlay of flow cytometry dot plots showing forward and side scatter of Ly6C^{hi} monocytes from WT animals and TCL-1 AT animals (n=6) (left) and quantification of forward scatter intensities (right). **(c)** Overlay of flow cytometry dot plots showing forward and side scatter of Ly6C^{hi} monocytes from TCL-1 AT animals (n=4) treated for two weeks with vehicle or Ibrutinib (left) and quantification of forward scatter intensities (right). (Ly6C^{high} monocytes: Viability dye (VD)$^-$LIN$^-$(CD19$^-$CD3$^-$Ly6G$^-$NK1.1$^-$TER119$^-$)CD11b$^+$CD11c$^{low\text{-}int}$MHC-II^{low}CXCR1$^+$Ly6C^{high}; Ly6C^{low} monocytes: VD$^-$LIN$^-$CD11b$^+$CD11c$^{low\text{-}int}$MHC-II^{low}CXCR1$^+$Ly6C^{low}) *P* values were determined by unpaired Student t-test.

3.2.1.7 Ibrutinib prevents tolerogenic phenotype of Ly6Clow monocytes by preventing PD-L1 induction possibly mediated through IFN-γ

PD-L1 was reported previously to be highly upregulated on monocytes from TCL-1 mice as well as CLL patient monocytes. As shown in a previous section of this work, PD-L1 displays differential expression on Ly6C^{hi} and Ly6C^{low} monocytes and in particular, the Ly6C^{low} monocyte population represents the subpopulation expressing high PD-L1 surface levels (Figure 12e,f).

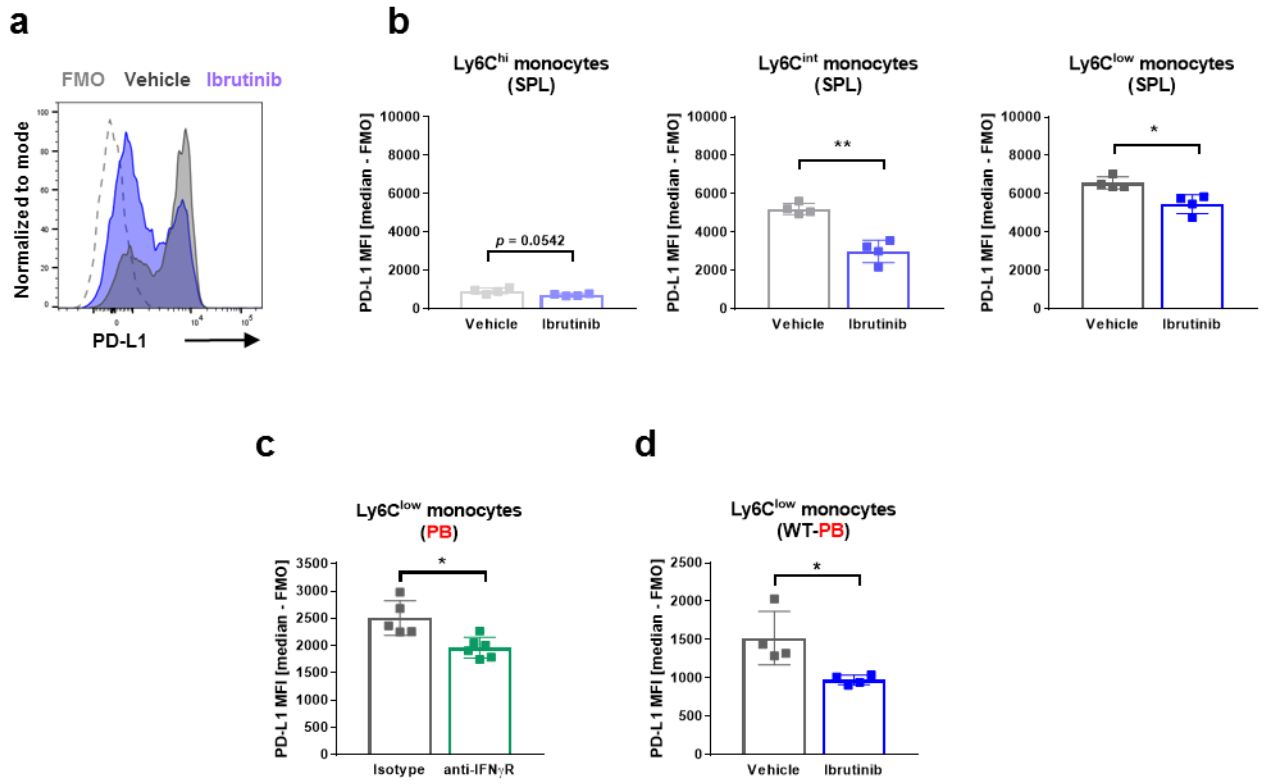

Figure 17: Ibrutinib reduces PD-L1 expression in Ly6C^{low} monocytes from TCL-1 AT and wildtype mice.
(a) Representative histogram illustrating PD-L1 expression on total splenic monocytes from mice treated with vehicle or Ibrutinib for 2 weeks. **(b)** PD-L1 expression level on Ly6C^{high} (left), Ly6C^{int} (middle) and Ly6C^{low} (right) monocytes from leukemic TCL-1 AT mice treated with vehicle (n=4) or Ibrutinib (n=4). **(c)** PD-L1 expression level on Ly6C^{low} monocytes from leukemic TCL-1 AT mice treated with anti-IFNγR (n=6) or isotype control antibody (n=5). Mice were injected i.p. with 1 mg of anti-IFNγR, or rat IgG1 isotype control antibody, followed by subsequent doses of 0.5 mg every 3 days for another 2 weeks. The present marker measurements were incorporated into a project designed by Bola Hanna. **(d)** PD-L1 expression level on Ly6C^{low} monocytes from non-leukemic wildtype mice treated with vehicle (n=4) or Ibrutinib (n=4) for two weeks. (Ly6C^{high} monocytes: Viability dye (VD)$^-$LIN$^-$(CD19$^-$CD3$^-$Ly6G$^-$NK1.1$^-$TER119$^-$)CD11b$^+$CD11c$^{low\text{-}int}$MHC-II^{low}CXCR1$^+$Ly6C^{high}; Ly6C^{low} monocytes: VD$^-$LIN$^-$CD11b$^+$CD11c$^{low\text{-}int}$MHC-II^{low}CXCR1$^+$Ly6C^{low}) *P* values were determined by unpaired Student t-test.

Splenic monocytes isolated from Ibrutinib-treated TCL-1 AT mice possessed a reduced surface level of PD-L1 on Ly6C^{low} monocytes, which was even stronger reduced on monocytes expressing intermediate levels of Ly6C (Ly6C^{int}) (Figure 17a,b). It was hypothesized that leukemia-induced T cell-derived IFN-γ could regulate PD-L1 expression, and indeed anti-IFN-γR-treated leukemic animals displayed lower levels of PD-L1 on Ly6C^{low} monocytes (Figure 17c). To exclude that reduced PD-L1 levels were merely due to the reduced tumor load achieved by anti-IFN-γR or Ibrutinib treatment, additionally, non-leukemic mice treated with Ibrutinib were analyzed. This confirmed a reduction of PD-L1 expression upon treatment also in wildtype mice (Figure 17d). These results suggest that inhibition of BTK by Ibrutinib leads to lower PD-L1 expression in monocytes which is

may still be mediated through IFN-γ, while this mechanism seems however independent of the presence specifically tumor-induced IFN-γ.

3.2.1.8 BTK inhibition normalizes CLL-associated TREM-1 overexpression on monocytes and granulocytes

As BTK is proposed to play a key role as positive regulator within the TREM-1 signaling pathway, TREM-1 expression under the influence of Ibrutinib was analyzed. In TCL-1 AT mice, TREM-1 expression was previously reported to be increased on monocytes compared to WT mice. Subset specific measurements of TREM-1 revealed that Ly6C^{low} monocytes showed higher TREM-1 levels compared to Ly6C^{hi} cells, while overall still showing a unimodal signal distribution (Figure 18a).

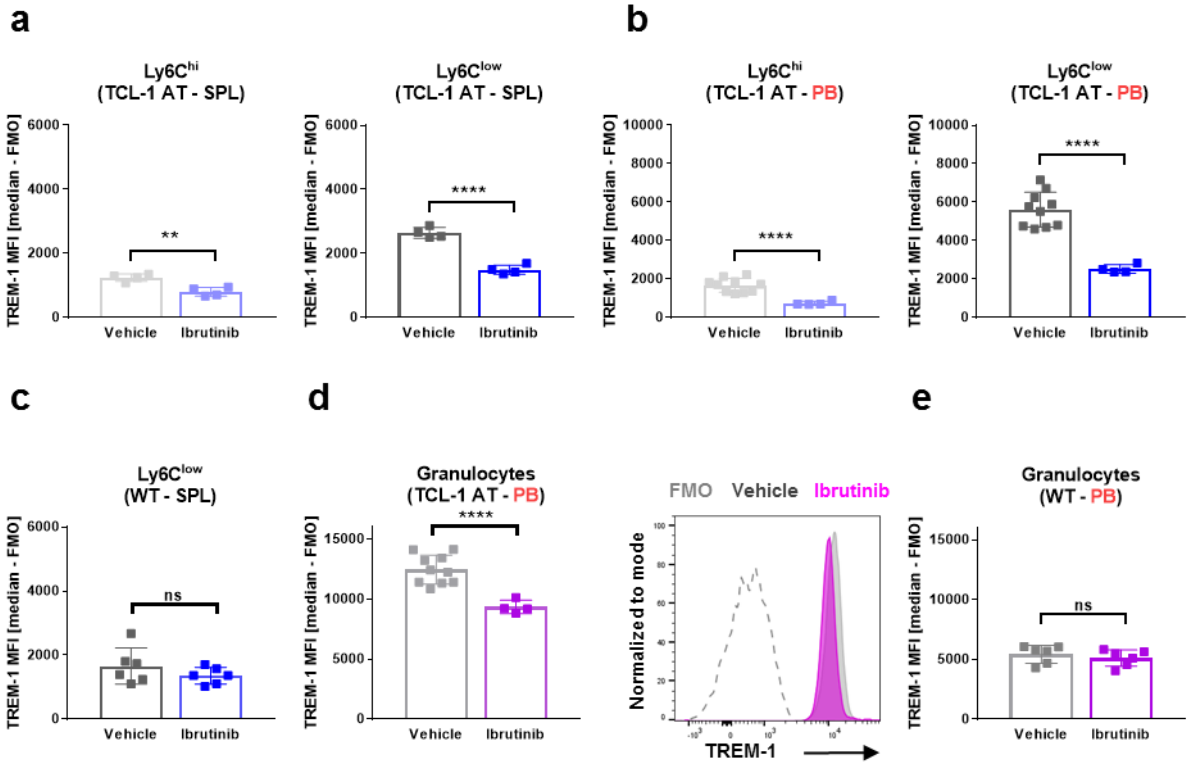

Figure 18: Ibrutinib treatment normalizes leukemia-associated TREM-1 overexpression on monocytes and granulocytes in TCL-1 AT mice.
(a) TREM-1 expression level on Ly6C^{high} (left) and Ly6C^{low} (right) monocytes from leukemic TCL-1 AT mice treated with vehicle (n=4) or Ibrutinib (n=4) for 2 weeks in the spleen (SPL). **(b)** TREM-1 expression level on Ly6C^{high} (left) and Ly6C^{low} (right) monocytes from leukemic TCL-1 AT mice treated with vehicle (n=10) or Ibrutinib (n=4) for 2 weeks in peripheral blood (PB). **(c)** TREM-1 expression level on Ly6C^{low} monocytes from non-leukemic wildtype mice treated with vehicle (n=6) or Ibrutinib (n=6) in the spleen (SPL). **(d)** TREM-1 expression level on granulocytes from leukemic TCL-1 AT mice treated with vehicle (n=10) or Ibrutinib (n=4) in peripheral blood (PB) (left) and representative histogram (right). **(e)** TREM-1 expression level on granulocytes from non-leukemic wildtype mice treated with vehicle (n=6) or Ibrutinib (n=6) in peripheral blood (PB). (Ly6C^{high} monocytes: Viability dye (VD)$^-$LIN$^-$(CD19$^-$CD3$^-$Ly6G$^-$NK1.1$^-$TER119$^-$)CD11b$^+$CD11c$^{low-int}$MHC-II^{low}CXCR1$^+$Ly6C^{high}; Ly6C^{low} monocytes: VD$^-$LIN$^-$CD11b$^+$CD11c$^{low-int}$MHC-II^{low}CXCR1$^+$Ly6C^{low}; granulocytes: VD$^-$ LIN$^-$(CD19$^-$CD3$^-$ NK1.1$^-$TER119$^-$)CD11b$^+$Ly6G$^+$) *P* values were determined by unpaired Student t-test.

TREM-1 expression on monocytes in spleen and peripheral blood was reduced after treatment of TCL-1 AT mice with Ibrutinib, with a similar strength on both monocyte subsets (Figure 18a,b). Notably, different than for PD-L1, Ibrutinib treatment of non-leukemic WT animals was not capable to reduce steady state TREM-1 expression levels (Figure 18c). Similarly, also TREM-1 induction on granulocytes was only suppressed after Ibrutinib treatment in the leukemic context but not in WT animals (Figure 18d,e).

3.2.1.9 BTK inhibition alters PECAM-1 and CD38 as part of the CLL-monocyte crosstalk

PECAM-1 and CD38 are proposed to be a ligand/receptor system orchestrating lymphocyte adhesion. In particular, they were suggested to play a role in adhesion of CLL cells to NLCs in lymph nodes of CLL patients[86].

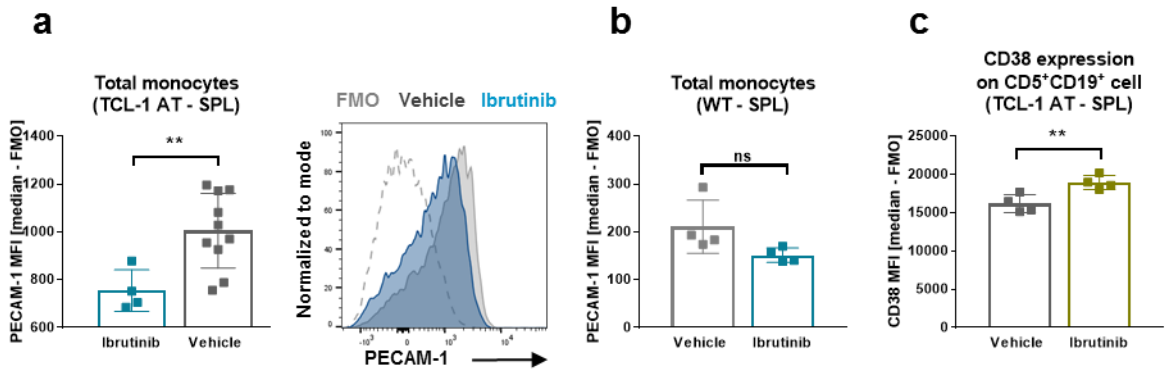

Figure 19: Ibrutinib treatment of mice alters expression of PECAM-1 and CD38 on monocytes and malignant B cells, respectively.
(a) PECAM-1 expression level (left) and representative histogram (right) of monocytes from leukemic TCL-1 AT mice treated with vehicle (n=10) or Ibrutinib (n=4) for two weeks. **(b)** PECAM-1 expression level on monocytes from non-leukemic wildtype animals (WT) treated with vehicle (n=4) or Ibrutinib (n=4) for two weeks. **(c)** CD38 expression level on $CD5^+CD19^+$ cells from leukemic TCL-1 AT mice treated with vehicle (n=4) or Ibrutinib (n=4) for two weeks. (Monocytes: Viability dye (VD)$^-$LIN$^-$($CD19^-CD3^-Ly6G^-NK1.1^-TER119^-$) $CD11b^+CD11c^{low\text{-}int}MHC\text{-}II^{low}CXCR1^+$; Leukemic $CD5^+CD19^+$ cells: VD^-CD45^+ $CD5^+CD19^+$) *P* values were determined by unpaired Student t-test.

PECAM-1 expression on total splenic monocytes from TCL-1 AT mice was elevated compared to WT mice. Ibrutinib treatment lead to significantly reduced levels compared to monocytes isolated from vehicle arm animals (Figure 19a). In addition, this Ibrutinib-induced change in PECAM-1 expression was independent of the presence of leukemic cells as it was also reduced in non-leukemic animals (Figure 19b). Within the same study, CD38, the receptor for PECAM-1, was examined on leukemic cells from the spleen. In contrast to the ligand's expression on monocytes, $CD5^+CD19^+$ leukemia cells showed an increased expression of CD38 (Figure 19c). The altered balance of the PECAM-

1/CD38 ligand/receptor system, induced by the Ibrutinib treatment, may impact on the adhesion of $CD5^+CD19^+$ to myeloid cell, thereby preventing leukemic cells from residing in their nourishing TME.

3.2.2 Conventional dendritic cells in steady state, in CLL and under the influence of Ibrutinib

3.2.2.1 cDCs from TCL-1 AT mice express a gene signature associated with developmental and functional impairment

Similar as for the monocyte subsets, also a thorough analysis of cDCs, which represent the least characterized myeloid cell population in CLL, was performed. cDCs were isolated from the same animals as used for monocyte analysis and were processed as described above (Chapter 3.2.1.1). Gene expression analysis revealed 2,279 genes in cDCs to be significantly deregulated when comparing cells isolated from leukemic TCL-1 AT and WT mice (Figure 20a). Hence, cDCs from TCL-1 AT animals, downregulated a large number of genes, while DEGs identified in $Ly6C^{hi}$ and $Ly6C^{low}$ monocytes were much lower in numbers and notably, most of them were upregulated.

Using the IPA tool, many biological functions were identified to be affected and mainly predicted to be inhibited in cDCs from TCL-1 AT mice (Figure 20b). These were among others: (1) *Hematological System development and function*, (2) *Lymphoid Structure and Development*, (3) *Cellular Growth and Maintenance*, and (4) *Cellular Development* (ranked by *p* value ranges).

Similarly, IPA revealed several dendritic cell-associated pathways to be among the top 10 canonical pathways. Among these were *Role of Macrophages, Fibroblasts and Endothelial Cell in Rheumatoid Arthritis, Phagosome Formation, Role of Pattern Recognition Receptors of Bacteria and Viruses, Protein Kinase A Signaling, NF-kB Signaling, TREM1 Signaling*, and *Phospholipase C* (Figure 20c). The majority of genes belonging to these pathways were downregulated thereby pointing to an impaired dendritic cell function in TCL-1 AT mice.

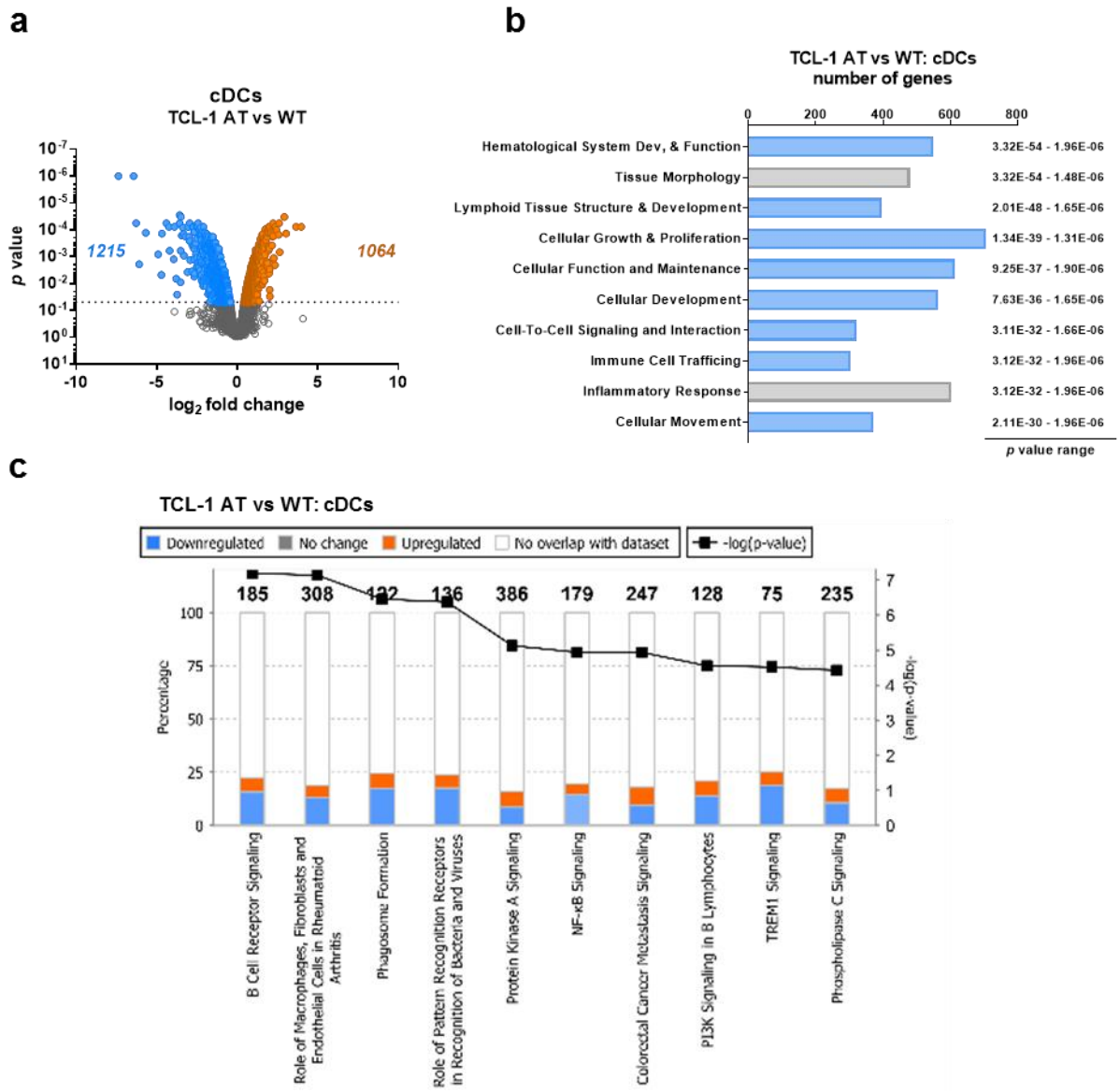

Figure 20: Gene expression profiling of cDCs from TCL-1 AT mice reveals an inhibition of pathways involved in their development and function.
(a) Volcano plots showing upregulated (orange) and downregulated (blue) genes in cDCs from leukemic TCL-1 AT (n=3) versus WT (n=3) animals. The dotted line indicates cutoff at a *p* value of 0.05. **(b)** Enrichment analysis of biological functions into categories (top 10 categories showed) using IPA downstream effect analysis, showing number of involved genes and *p* value ranges (blue=category predicted to be inhibited, grey=category prediction unclear). **(c)** Top 10 canonical pathways identified in cDCs from TCL-1 AT (n=3) versus WT (n=3) animals using IPA. See Appendix Table 1 for additional information on samples.

3.2.2.2 cDCs from TCL-1 AT mice display a CLL-associated subset composition which is normalized by Ibrutinib treatment

As previously reported, cDC numbers increase during CLL development in TCL-1 AT mice and were suggested to represent a rather immature and tolerogenic population. Therefore, it was of interest if Ibrutinib could potentially act also on this myeloid cell population in a direct or indirect manner.

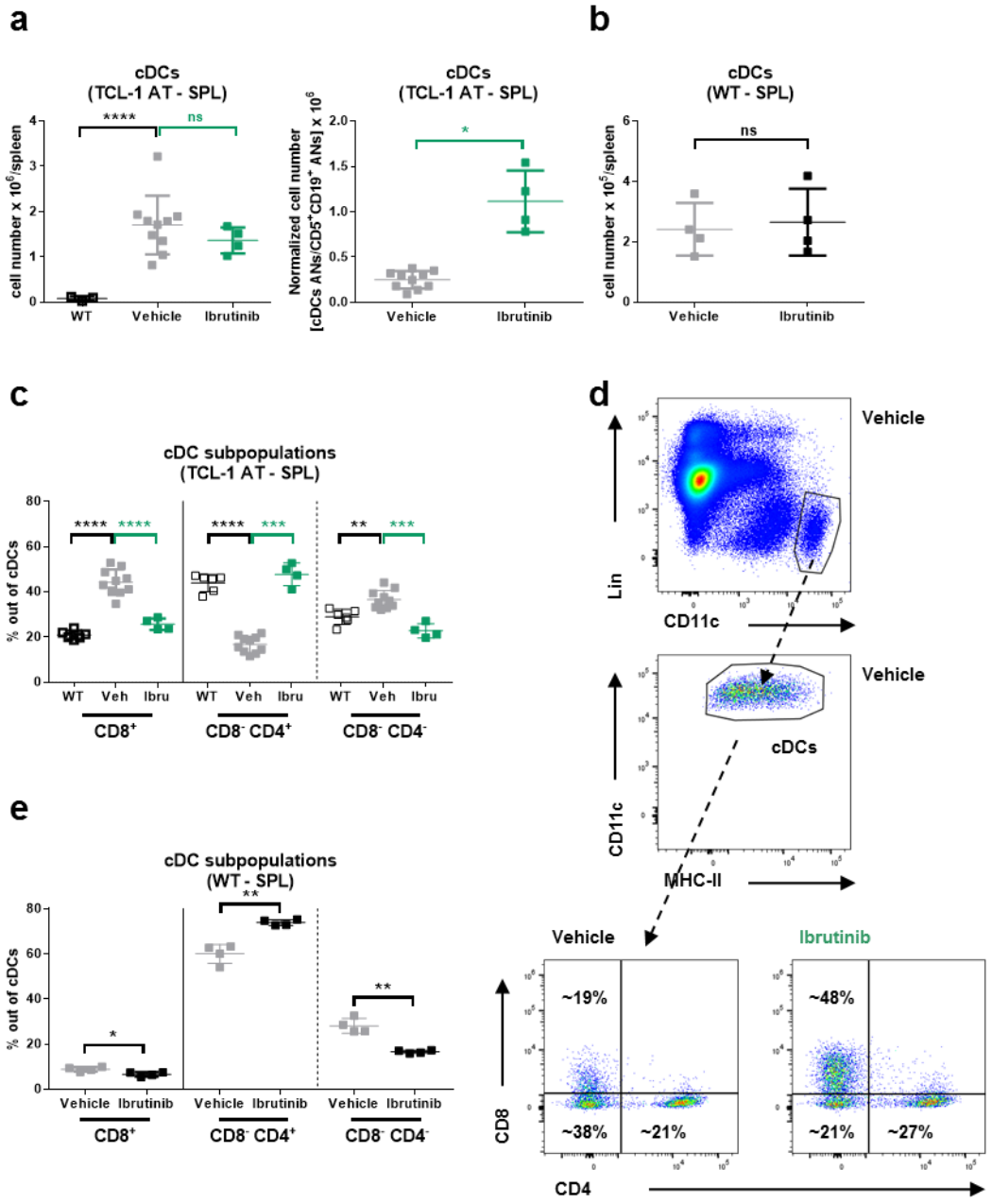

Figure 21: Ibrutinib treatment reverses the leukemia-associated alterations in cDC subset composition. **(a)** Absolute numbers (left) and tumor cell-normalized numbers (right) of cDCs in the spleen from WT (n=3) and leukemic TCL-1 AT mice treated with vehicle (n=10) or Ibrutinib (n=10) for two weeks. **(b)** Absolute numbers of cDCs in the spleen from non-leukemic WT mice treated with vehicle (n=4) or Ibrutinib (n=4) for two weeks. **(c)** Percentages of $CD8^+$ cDCs, $CD8^-CD4^+$ cDCs, and $CD8^-CD4^-$ cDCs out of total cDCs from WT mice (n=6) and TCL-1 AT mice treated with vehicle (n=10) or Ibrutinib (n=10) for two weeks, and **(d)** representative gating strategy. **(e)** Percentage of $CD8^+$ cDCs, $CD8^-CD4^+$ cDCs, and $CD8^-CD4^-$ cDCs out of total cDCs from non-leukemic WT mice treated with vehicle (n=4) or Ibrutinib (n=4) for two weeks. ($CD8^+$ cDCs: Viability dye $(VD)^-$ $LIN^-(CD19^-CD3^-Ly6G^-NK1.1^-TER119^-)CD11c^{high}MHC\text{-}II^+CD8^+$; $CD8^-CD4^+$ cDCs: $VD^-LIN^-CD11c^{high}MHC\text{-}II^+CD8^-CD4^+$; $CD8^-CD4^-$ cDCs: $VD^-LIN^-CD11c^{high}MHC\text{-}II^+CD8^-CD4^+$) *P* values were determined by unpaired Student t-test.

Different than for monocytes, Ibrutinib did not inhibit the accumulation of dendritic cells in TCL-1 AT mice compared to the vehicle-treated group (Figure 21a, left). Also in non-leukemic WT animals,

Ibrutinib treatment did not influence the number of cDCs confirming the latter results (Figure 21b). However, normalizing cDC numbers to the respective number of $CD5^+CD19^+$ CLL cells revealed that the ratio of cDCs to $CD5^+CD19^+$ cells was different in the two treatment arms (Figure 21a, right). In particular, there were more splenic cDCs in relation to $CD5^+CD19^+$ cells in the spleen when analyzing numbers two weeks after treatment, at which Ibrutinib was controlling the tumor burden in the spleen (% $CD5^+CD19^+$ cells for vehicle: 93%, for Ibrutinib: 66%).

Since cDCs are constituted of different populations, a deeper insight into their subset composition was gained. The three murine cDC populations of interest are distinguished by the following expression patterns: (i) $CD8^+$, (ii) $CD8^-CD4^+$, and (iii) $CD8^-CD4^-$. In addition to these markers, $CD8^-$ cDC subsets were confirmed to express higher levels of CD11b compared to $CD8^+$, and CD11c was also confirmed to be higher on the $CD4^+$ cDC subset as compared to the $CD4^-$ subset (Appendix Figure 4a,b). First, altered numbers (not shown) as well percentages of these three cDC subsets were assessed in TCL-1 AT vehicle-treated mice compared to WT animals. Leukemic animals displayed a significantly increased percentage of $CD8^+$ cDCs and $CD8^-CD4^-$ cDCs, and a decrease in the percentage of $CD8^-CD4^+$ cDCs on the other hand (Figure 21c,d). This suggested that $CD8^+$cDCs and $CD8^-CD4^-$ cDCs might represent the main increasing cDC populations that explain leukemia-induced accumulation of total cDCs described just before. These alterations caused a changed subset composition of cDCs compared to steady state, where $CD8^-CD4^+$ cDCs represent the most frequent subset, followed by $CD8^-CD4^-$ and finally $CD8^+$ cDCs[190]. In line with this observation, the gene expression profile of cDCs isolated from leukemic TCL-1 AT mice highly resembled $CD8^+$ DCs but not $CD4^-$ DCs among different splenic DC populations (Appendix Figure 5a,b) This confirmed, that leukemia-induced differences in DC subpopulations seem to be indeed true and not solely restricted to changes in a few marker proteins (namely CD4 and CD8 here).

Next, the impact of Ibrutinib on the proportions of cDC subsets was addressed. After two weeks of treatment, the distribution of $CD8^+$, $CD8^-CD4^+$, and $CD8^-CD4^-$ cDCs was mostly, though not fully normalized and resembled rather the distribution in WT mice (Figure 21c). Ibrutinib was able to induce a similar subpopulation skewing in a leukemia-free set-up of treated WT animals suggesting that these data present CLL-independent, Ibrutinib-mediated effects on cDCs (Figure 21e).

3.2.2.3 Ibrutinib induces a tolerogenic cDC immunophenotype in the TCL-1 AT model

Conventional dendritic cells from TCL-1 AT cells were proposed to express higher PD-L1 and lower MHC-II surface levels and display decreased percentages of double-positive $CD83^+$ $CD86^+$ cDCs[319]. Prior investigating the effect of Ibrutinib on cDCs these proposed changes between wildtype and leukemic animals were revised. Several experiments verified these changes for MHC-II and PD-L1, but could not confirm a downregulation of the costimulatory molecules CD83 and CD86 on splenic cDCs from TCL-1 AT mice compared to WT animals. Indeed, for both molecules and for ICAM-1, a dendritic cell activation marker, an increased expression was observed repeatedly in TCL-1 AT compared to wildtype mice (data not shown). Yet, it was of interest whether Ibrutinib treatment was able to result in a normalization of the activated but supposedly not fully functional cDC phenotype. Moreover, this study included a detailed analysis of the poorly characterized murine cDC subsets under treatment with Ibrutinib.

While MHC-II expression was not altered by Ibrutinib treatment (data not shown), the activation and maturation markers ICAM-1, CD86 and CD83 turned out to be significantly downregulated by the drug (Figure 22a,c,e). Interestingly, the expression levels of these molecules were differently affected in $CD8^+$, $CD8^-CD4^+$, and $CD8^-CD4^-$ cDC subsets. For instance, ICAM-1 was expressed to a lesser extent on all subsets (Figure 22b). In contrast, CD86 and CD83 were similarly downregulated on $CD8^-CD4^+$, and $CD8^-CD4^-$ cDC subsets, but not on $CD8^+$ cDCs (Figure 22d,f). However, the effect on the overall expression on total cDCs was much stronger for CD83 which can be explained by the subset shift described above (Figure 22b).

Notably, CD86 and CD83 expression on total cDCs were decreased to a similar extent upon Ibrutinib treatment of leukemia-free animals, and an unchanged low MHC-II expression was also confirmed in WT mice (data not shown). In contrast, ICAM-1 expression was not affected in that setting.
Moreover, Ibrutinib treatment lead to an increased percentage of the $PD\text{-}L1^{high}$-expressing cDC population (Figure 22g), supporting one more time that Ibrutinib may act partially counteractive on DCs by inducing an even stronger immune-suppressive surface phenotype of these cells.

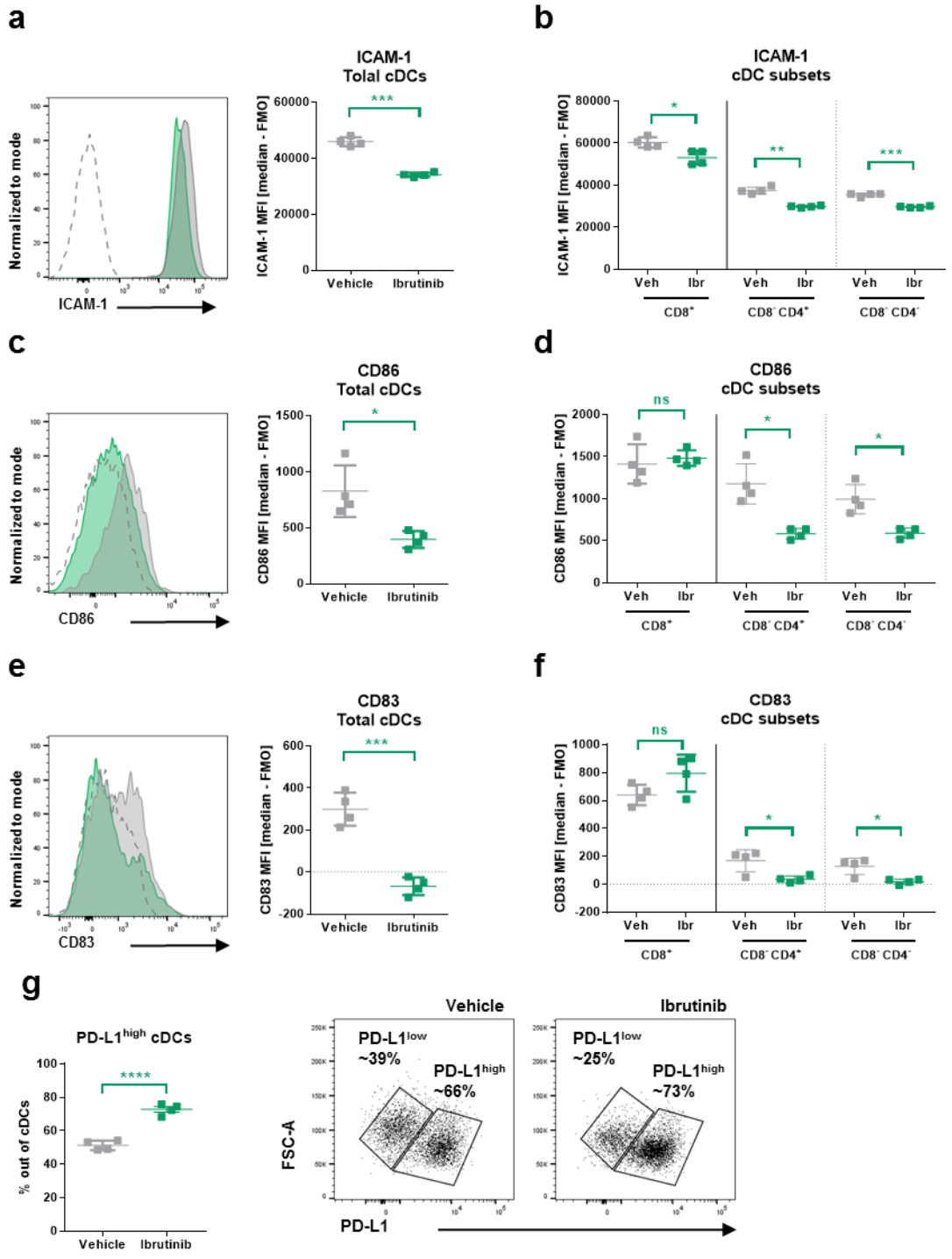

Figure 22: Ibrutinib treatment enhances a tolerogenic cDC phenotype in the TCL-1 AT model.
(a,c,e) ICAM-1 (a), CD86 (c), and CD83 (e) expression level on total splenic cDCs from mice treated with vehicle (n=4) or Ibrutinib (n=4) for two weeks. Representative flow cytometry histograms (left) and quantification of data (right). **(b,d,f)** Quantification of ICAM-1 (b), CD86 (d), and CD83 (f) expression on $CD8^+$, $CD8^-CD4^+$, and $CD8^-CD4^-$ cDC subpopulations from mice treated with vehicle (n=4) or Ibrutinib (n=4) for two weeks. **(g)** Percentage of PD-$L1^{high}$-expressing cDCs (left) and representative density plots from mice treated with vehicle (n=10) or Ibrutinib (n=10) (right) for two weeks. (cDCs: Viability dye (VD)$^-$LIN$^-$(CD19$^-$CD3$^-$Ly6G$^-$NK1.1$^-$TER119$^-$)CD11c^{high}MHC-II$^+$; $CD8^+$ cDCs: VD$^-$LIN$^-$CD11c^{high}MHC-II$^+$CD8$^+$; $CD8^-CD4^+$ cDCs: VD$^-$LIN$^-$CD11c^{high}MHC-II$^+$CD8$^-$CD4$^+$; $CD8^-CD4^-$ cDCs: VD$^-$LIN$^-$CD11c^{high}MHC-II$^+$CD8$^-$CD4$^+$) *P* values were determined by unpaired Student t-test.

In addition, IL-12β, a pro-inflammatory cytokine, which is associated with $CD8^+$ cDCs, showed a decreased level in intracellular flow cytometry staining of total cDCs from TCL-1 AT compared to WT mice that was not further changed upon Ibrutinib treatment (Appendix Figure 4c,d)[188, 189]. This again suggested, that despite an enrichment of the $CD8^+$ cDCs subpopulation their capability for cytokine production with respect to their functionality might be impaired in leukemic versus healthy animals.

3.2.2.4 Inhibition of IL-10RA receptor signaling partially reverses tolerogenic phenotype of cDCs in TCL-1 AT mice

The effect of Ibrutinib on cDC activation, maturation, and tolerogenic markers seemed not favorable towards a restoration of the implied functional impairment of cDCs and even further supported the suggested dysfunctionality of these cells. This raised the question of how cDCs may possibly be targeted in order to regain their full capacity for antigen presentation and activation.
In order to determine possible target molecules, a closer look on predicted upstream regulators, identified based on the gene expression results of their downstream targets, was performed using IPA. This type of analysis enables the identification of signaling axes and molecules of interest independent of their expression levels that may or may not be altered.
IL-10 receptor A (IL-10RA) turned out to be among the top five predicted regulators and at the same time is known to be an important player in dendritic cell maturation and activation (Figure 23a)[320].

To evaluate the relevance of IL-10RA, TCL-1 AT mice were injected i.p. with an antibody directed against anti-IL-10RA or a respective isotype control antibody. After 2 weeks of treatment, isolated splenic cDCs from anti-IL-10RA-treated mice showed significantly increased levels of MHC-II. ICAM-1, CD86 and CD83 expression were slightly but not significantly increased, while generally rather low for CD86 and CD83 (Figure 23b) and unchanged for PD-L1 (data not shown). These results suggest an involvement of the IL-10/IL-10 receptor axis in the activity of splenic dendritic cells in leukemic TCL-1 AT mice.

a

Upstream Regulator	Predicted Activation State	Activation z-score	p-value of overlap
TP53		-0,066	4,56E-17
IFNG		0,791	9,72E-16
CSF2	Activated	4,092	2,01E-15
IL10RA	Inhibited	-2,619	1,01E-13
IL4		1,167	8,41E-13

b

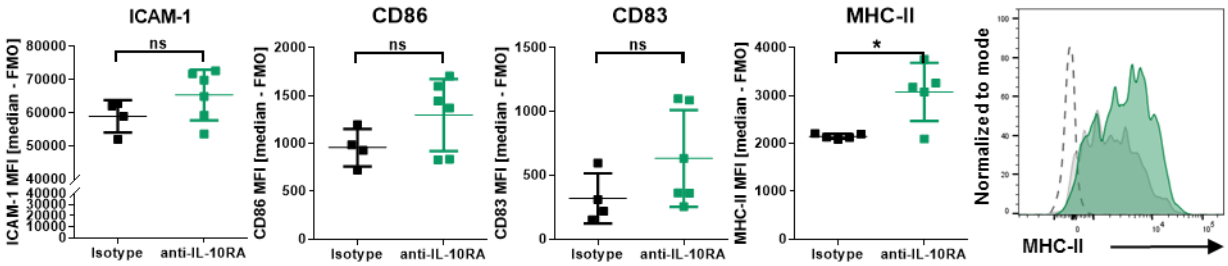

Figure 23: Inhibition of IL-10RA receptor signaling partially reverses tolerogenic phenotype of cDCs in TCL-1 AT mice.
(a) Top five predicted upstream regulators in cDCs from leukemic compared to WT mice identified in the GEP data using IPA. **(b)** CD83, CD54, CD86, and MHC-II expression levels on splenic cDCs cells from TCL-1 AT mice treated with anti-IL-10RA (n=6/5) or isotype antibody (n=4/5), measured by flow cytometry. Leukemic mice were injected i.p. with 1 mg of anti-IL-10RA, or rat IgG1 isotype control antibody, followed by subsequent doses of 0.5 mg every 3 days for another 2 weeks. The present marker measurements were incorporated into a project designed by Bola Hanna. (cDCs: Viability dye (VD)$^-$LIN$^-$(CD19$^-$CD3$^-$Ly6G$^-$NK1.1$^-$TER119$^-$)CD11c^{high}MHC-II$^+$) *P* values were determined by the unpaired Student t-test.

In addition, TCL-1 AT mice were treated with an antibody blocking IFNγ receptor (anti-IFNγR), another predicted upstream regulator identified in the cDC gene expression data (Figure 23a). The absence of IFNγ-mediated signaling lead to a very small and insignificant decrease in activation and maturation marker levels compared to isotype control (data not shown).

However, both treatments resulted in unfavorable disease outcome as the tumor load was increased in animals receiving one or the other antibody (data not shown). Thus, the observed changes in expression levels of CD83, CD54 and CD86 which were of opposing directions in the two groups (anti-IL-10RA or anti-IFNγR), were unlikely caused by changes in tumor burden but were presumably a direct consequence of the impaired access to Il-10. Thus, immunomodulation of the IL-10 receptor-mediated signaling might partially contribute to the reversal of the observed CLL-induced cDC phenotype.

3.3 Treatment of TCL-1 AT mice with Ibrutinib results in tumor cell-intrinsic resistance to the drug

While investigating effects of Ibrutinib on the myeloid TME in TCL-1 AT mice, a time-restricted response to treatment and tumor cell-intrinsic acquired resistance to Ibrutinib was observed. In the first 4-6 weeks of Ibrutinib treatment, the expected favorable outcome on disease development in TCL-1 AT mice was obtained. As control of leukemia development was not long-lasting, resistance development in Ibrutinib-treated mice was assumed. To validate and further investigate this observation, the initial goal was to confirm this observation by adoptive transfer of a different tumor sample into C57BL/6 mice. A comparative characterization of such generated Ibrutinib sensitive and resistant tumors was obtained by whole exome and transcriptome analyses. In addition, the growth kinetics of re-transplanted tumors that had undergone previous Ibrutinib or vehicle treatment was monitored.

3.3.1 Loss of treatment response to Ibrutinib

To confirm loss of treatment efficacy of Ibrutinib over time, animals were adoptively transferred with $1.3x10^7$ splenocytes originating from a leukemic TCL-1 AT mouse (tumor: 1J4) by i.p. injection, and randomization into two groups was conducted, once the leukemia was established with a mean tumor load of at least 50% in peripheral blood (week 2 post-transplantation) (Appendix Figure 6a). Mice were then treated either with 25 mg/kg/day Ibrutinib (Ibr arm) or vehicle (Veh arm). Ibrutinib initially controlled disease progression leading to lower absolute numbers of malignant $CD5^+CD19^+$ cells compared to vehicle-treated mice (Figure 24a). Mice were sacrificed at three different time points: (1) An early time point where animals from the Ibrutinib arm were considered to be still sensitive to Ibrutinib (week 1 post treatment); (2) two later time points where animals had reached a high tumor load of at least 100,000 leukemic cells/µL blood which occurred first in the vehicle arm (week 3) and later in the Ibrutinib arm (week 6). At all three endpoints, leukemic cells from spleens were harvested, sorted by flow cytometry and frozen for later processing (Appendix Table 2).

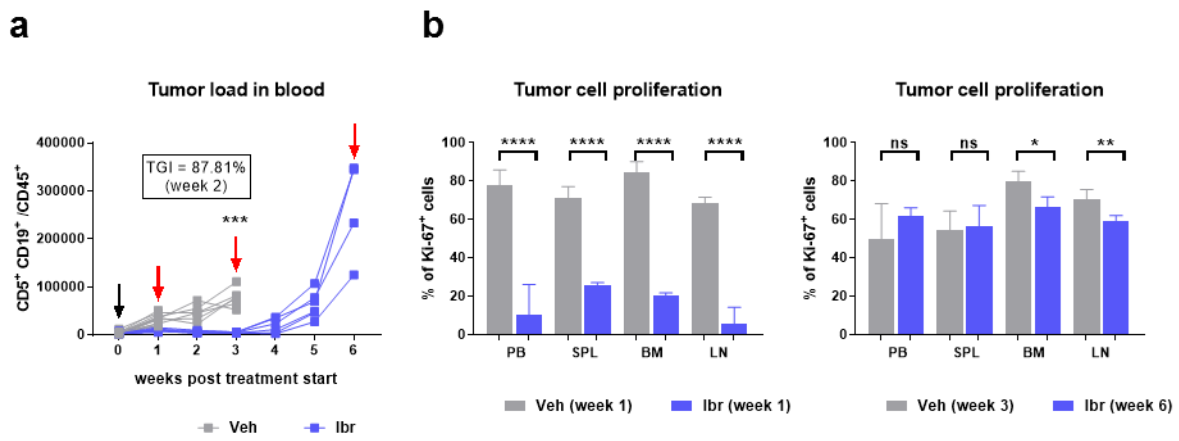

Figure 24: Loss of treatment response to Ibrutinib in the TCL-1 AT model.
(a) Absolute numbers of $CD5^+CD19^+$ cells in the peripheral blood from mice adoptively transferred with malignant splenocytes isolated from spleens of leukemic TCL-1 mice. Mice were randomized 2 weeks post-transplantation (=week 0) and treatment was started (black arrow) with vehicle (n=14, grey) or Ibrutinib (n=12, blue). Animals were sacrificed at different endpoints (red arrows). **(b)** Percentages of Ki-67-positive cells out of $CD5^+CD19^+$ cells in peripheral blood (PB), spleen (SPL), bone marrow (BM), and inguinal lymph nodes (LN) from mice adoptively transferred with tumor 1J4 and treated with vehicle (n=6) or Ibrutinib (n=6) for one week (left), or three weeks for vehicle (n=6) and six weeks for Ibrutinib (n=3) (right). TGI=Tumor growth inhibition. (Leukemic $CD5^+CD19^+$ cells: $CD45^+CD5^+CD19^+$) *P* values were determined by unpaired Student t-test.

Comparison of percentages of Ki-67-expressing $CD5^+CD19^+$ cells from different organs after one week of treatment revealed significantly lower percentages of proliferating cells in animals treated with Ibrutinib (Figure 24b,left). Comparison of percentages of Ki-67-expressing $CD5^+CD19^+$ cells from vehicle-treated animals at week three and Ibrutinib-treated animals at week six indicated that this difference was less prominent in the bone marrow and lymph nodes and disappeared in blood and spleen at these later time points (Figure 24b,right). In accordance with the latter observation also differences in spleen weight and tumor load in lymphoid organs, initially controlled by Ibrutinib treatment, became less distinct over time (Appendix Figure 6a-d). Hence, these data support the hypothesis of acquired resistance to Ibrutinib in this model.

3.3.1.1 Re-transplantation of resistant tumors

In order to monitor the responsiveness and growth kinetics of re-transplanted tumors that had undergone previous Ibrutinib or vehicle treatment, two tumors from a first round of treatment of each arm (vehicle=Veh and Ibrutinib=Ibr) with similar tumor load and cell viability were chosen. The second round of transplantation, randomization, and treatment with Ibrutinib (Veh_Ibr and Ibr_Ibr) or vehicle (Veh_Veh and Ibr_Veh) was conducted in the same manner as described in the section before (number of cells, route of administration etc) (Figure 25a).

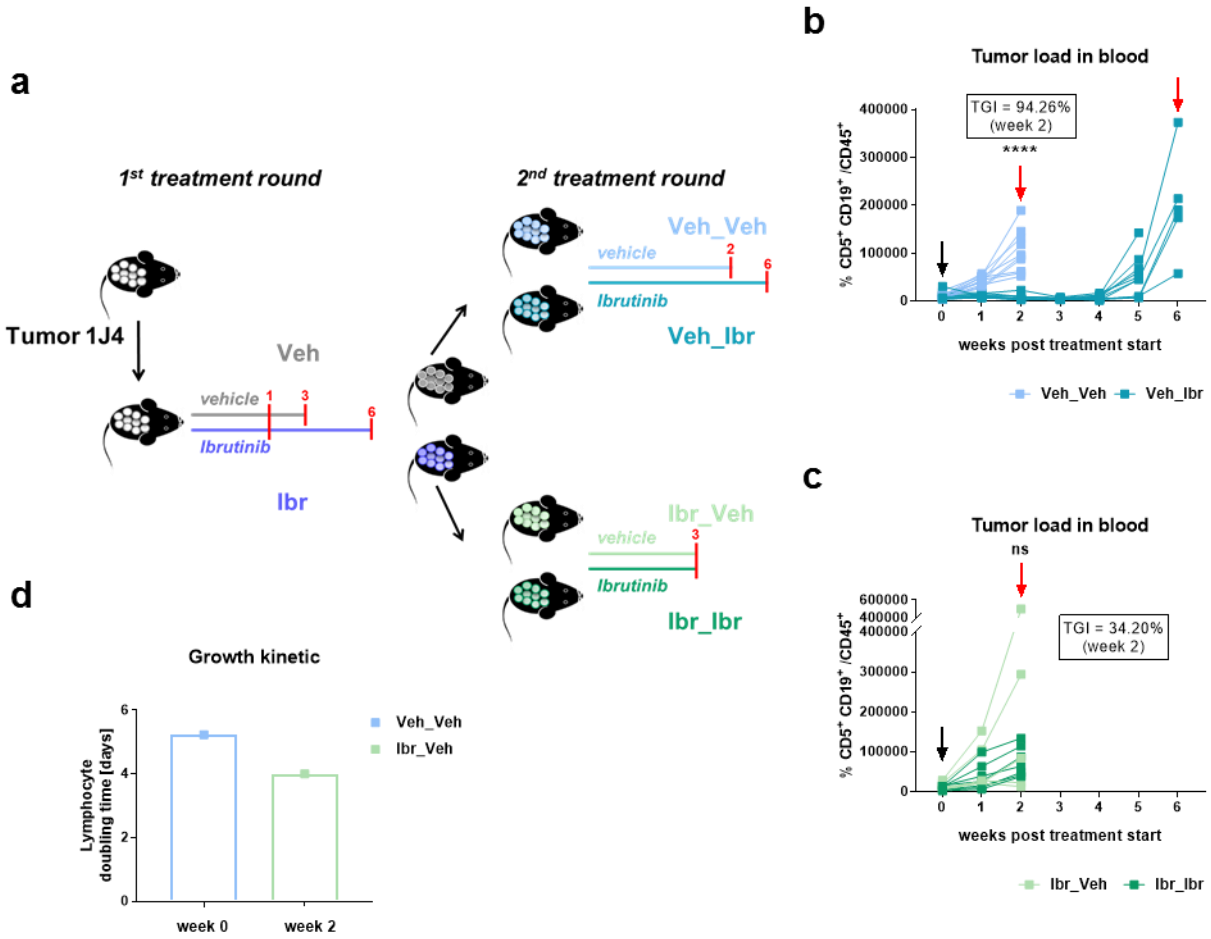

Figure 25: Re-transplantation of Ibrutinib-treated tumor cells provides evidence for cell-intrinsic resistance. **(a)** Experimental setup of serial adoptive transfer of TCL-1 tumors and treatment of mice (Veh=vehicle, Ibr=Ibrutinib). Study endpoints are depicted as red lines. **(b,c)** Absolute numbers of $CD5^+CD19^+$ cells in peripheral blood of mice during vehicle (Veh) or Ibrutinib (Ibr) treatment. Mice were randomized for treatment at week 0 (black arrow) and sacrificed at different time points (red arrows). Group sizes were: Veh_Veh: n=10, Veh_Ibr: n=10, Ibr_Veh: n=7, Ibr_Ibr: n=6. (Leukemic $CD5^+CD19^+$ cells: $CD45^+CD5^+CD19^+$) **(d)** Average growth kinetics of re-transplanted tumors within 2nd treatment round just before start of vehicle treatment and at week 2 post-treatment start. TGI=Tumor growth inhibition. (Leukemic $CD5^+CD19^+$ cells: $CD45^+CD5^+CD19^+$) *P* values were determined by unpaired Student t-test.

The re-transplanted tumor previously treated with vehicle engrafted similarly as the parental tumor and treatment was started at 2 weeks post tumor injection. In contrast, animals transplanted with a tumor that was previously treated with Ibrutinib displayed a delayed onset of disease establishment and randomization/treatment start was conducted one week later which was 3 weeks post tumor transplantation (not shown here).

Animals re-transplanted with vehicle tumors initially responded to Ibrutinib (Veh-Ibr arm), while also these animals displayed a loss of response from week 4 post treatment start on (Figure 25b). Within the Ibr-Veh arm, two animals rapidly developed leukemia with high absolute numbers of $CD5^+CD19^+$ cells. For the remaining mice of this group, leukemia development was not considerably different than for animals treated for the second round with Ibrutinib (Ibr-Ibr arm) (Figure 25c).

Hence, there was no treatment response to Ibrutinib with tumor cells that had previously been treated with Ibrutinib. Calculation of growth kinetics of re-transplanted tumors revealed shorter doubling times for Ibrutinib-pretreated tumors compared to vehicle-pretreated tumors at week 2 post transplantation start (Figure 25d). Taken together, these data clearly show that Ibrutinib treatment of TCL-1 AT mice results in the development of resistance to the drug that is intrinsic to the tumor cells.

3.3.2 Phenotypical changes in Ibrutinib-resistant CLL cells

Interestingly, four weeks post-treatment start the majority of Ibrutinib-treated animals displayed two sub-populations of $CD5^{+}CD19^{+}$ cells in peripheral blood, that could be distinguished by high and intermediate expression of CD19 ($CD19^{hi}$ and $CD19^{int}$ cells) (Figure 26a). When analyzing these populations over time, the percentage of the $CD19^{int}$ sub-population increased and after six weeks of treatment became the dominant cell population. $CD19^{int}$ and $CD19^{hi}$ subpopulation were observed in 6 out of 11 animals in the Ibr arm and 8 out of 10 animals in the Veh_Ibr arm. For this study, we were not able to determine whether this is an event occurring solely within the Ibrutinib-treated cohort, since at the time point of evident sub-population appearance all vehicle-treated animals were already sacrificed due to high tumor load. However, an accumulation of $CD19^{int}$ leukemic cells that was restricted to Ibrutinib-treated mice was confirmed in an independently performed treatment study in which animals from the vehicle arm survived longer (data not shown here).

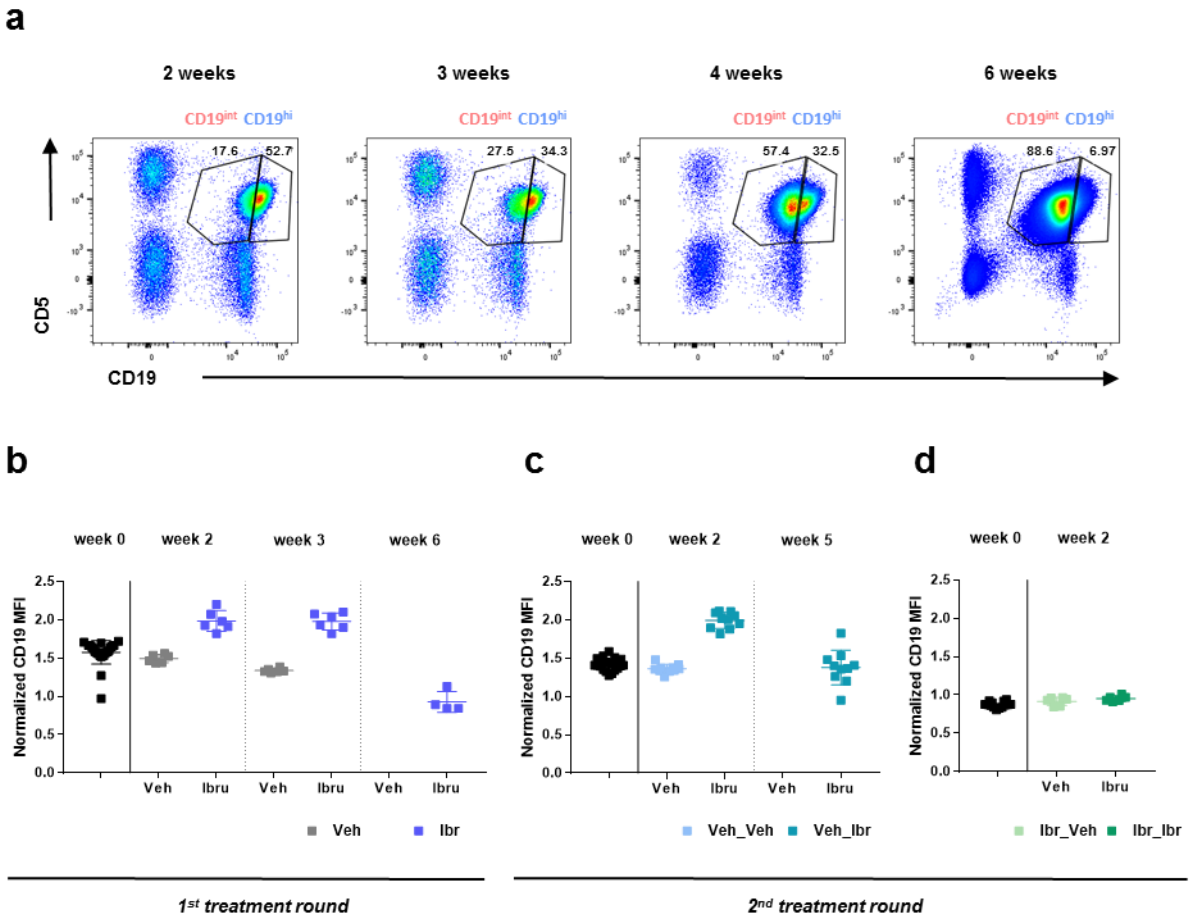

Figure 26: Ibrutinib-resistant TCL-1 tumor cells develop a CD19^{int} sub-population.
(a) Representative flow cytometry dot plots showing the percentages of CD5^{+}CD19^{int} and CD5^{+}CD19^{hi} cells in peripheral blood of mice from 1st treatment round at week 2, 3, 4, and 6 after treatment start. **(b-d)** CD19 MFI values of leukemic CD19^{+}CD5^{+} cells were normalized to respective values of CD19^{+}CD5^{-} normal B cells (median CD19 MFI on CD19^{+}CD5^{+} cells / median CD19 MFI on CD19^{+}CD5^{-} cells) in blood of mice **(b)** from 1st treatment round, **(c)** from 2nd treatment round with previous vehicle treatment, or **(d)** from 2nd treatment round with previous Ibrutinib treatment. (Leukemic CD5^{+}CD19^{+} cells: CD45^{+}CD5^{+}CD19^{+}) *P* values were determined by unpaired Student t-test.

Interestingly, tumors from animals that were treated with Ibrutinib in the first round, did not display such development of sub-populations based on CD19 expression, neither in the vehicle nor in the Ibrutinib arm of the second treatment round (data not shown). To quantify these observations, CD19 expression levels on tumor cells were normalized to CD19 levels on normal B cells which was calculated as ratio of CD19 MFI from CD5^{+}CD19^{+} cells vs CD19 MFI of CD5^{-}CD19^{+} cells. This showed that Ibrutinib treatment at week 2 and 3 induced an increase in CD19 expression in leukemic cells which was lost after 5 to 6 weeks of treatment, presumably when cells acquired resistance to the drug (Figure 26 b,c). Of note, treatment with vehicle did not alter the expression of CD19 on leukemic cells. Tumor cells from mice that had been previously treated with Ibrutinib and did not respond to the drug during the second round of treatment showed no increase in CD19 levels, but rather displayed relatively low CD19 expression during the whole experiment (Figure 26d). These

results indicate that Ibrutinib induces an increase in CD19 expression only in sensitive tumor cells, whereas Ibrutinib resistant tumors show generally lower levels of CD19 expression. Further, tumor cells that were used for re-transplantation of the second treatment round possessed low CD19 expression levels also in the spleen, reflecting the CD19 expression levels at week 0 in Figure 26c) and d) (Appendix Figure 6e).

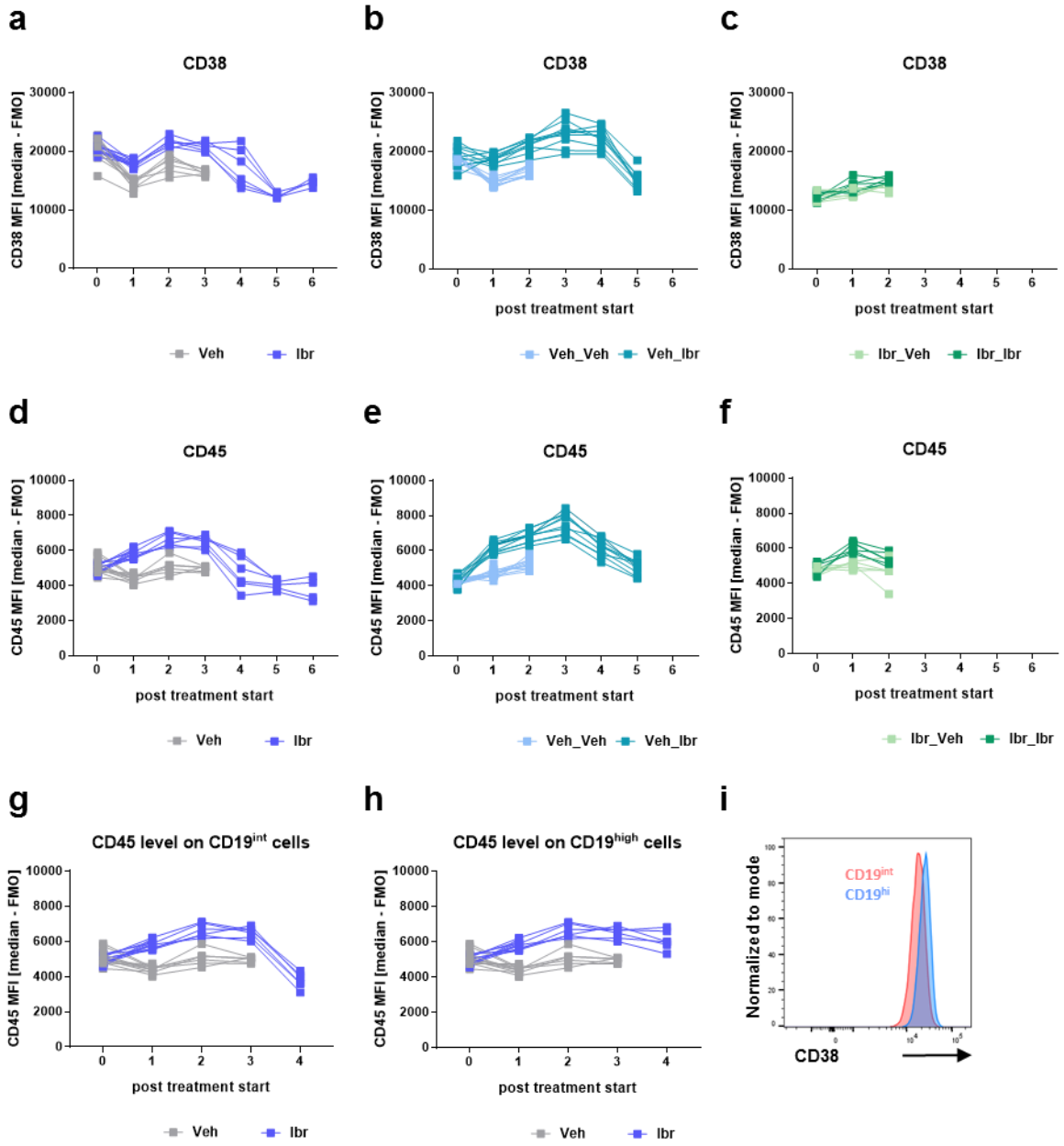

Figure 27: Ibrutinib-resistant TCL-1 leukemia cells show phenotypical changes.
(a-c) CD38 expression level on $CD5^+CD19^+$ cells in blood from mice of the 1st and 2nd treatment round was analyzed by flow cytometry over time. **(d-f)** CD45 expression level on $CD5^+CD19^+$ cells in blood from mice of the 1st and 2nd treatment round was analyzed by flow cytometry over time. **(g,h)** Cell subset-specific quantification of CD45 expression levels on $CD5^+CD19^{int}$ and $CD5^+CD19^{hi}$ cells in blood from mice of the 1st treatment round. **(i)** Representative histogram of CD38 expression on $CD5^+CD19^{int}$ and $CD5^+CD19^{hi}$ cells in peripheral blood from mice of the 1st treatment round at week 4. (Leukemic $CD5^+CD19^+$ cells: $CD45^+CD5^+CD19^+$)

As part of the weekly tumor load measurements in peripheral blood, cells were stained for CD38, a marker associated with enhanced aggressiveness in CLL patients. In addition, also the expression level of CD45 was quantified over time. Compared to the vehicle control, Ibrutinib induced a higher expression of CD45 and CD38 on malignant cells only in sensitive tumors (Ibr and Veh_Ibr) (Figure 27a,b,d,e). For resistant tumors (Ibr_Ibr), this induction of expression was absent for CD38 and only modest for CD45 at week 1 (Figure 27 c,f). Interestingly, the higher expression levels of CD45 and CD38 started to decline again at the time point when the two malignant cell sub-populations defined by their differential CD19 expression appeared (week 4), suggesting again that this change phenotypical change is associated with Ibrutinib-resistant leukemia cells. Cell subset-specific quantification of CD45 and CD38 expression levels revealed a drop in expression upon resistance development only in $CD19^{int}$ cells, while $CD19^{high}$ cells retained rather stable expression levels (Figure 27g-i).

Summarized, these findings show that Ibrutinib resistance in the TCL-1 AT model is associated with phenotypical changes in the malignant cells, which include decreased CD19, CD45 and CD38 expression levels, all of which are known to be involved in the BCR pathway.

3.3.3 Analysis of WES data of Ibrutinib resistant tumors

In order to characterize mechanisms of Ibrutinib resistance, whole exome sequencing was performed from samples collected before and after treatment with vehicle or Ibrutinib at different time points (Figure 25 a). It is known that CLL patients, treated with Ibrutinib display a greater degree of clonal selection[301, 321]. Thus, the aim was to investigate whether such clonal selection would also arise in TCL-1 AT mice, treated with Ibrutinib. In order to determine the clonal architecture of the murine tumors, V(D)J rearrangement of the BCR were determined from WES data by IgBLAST.

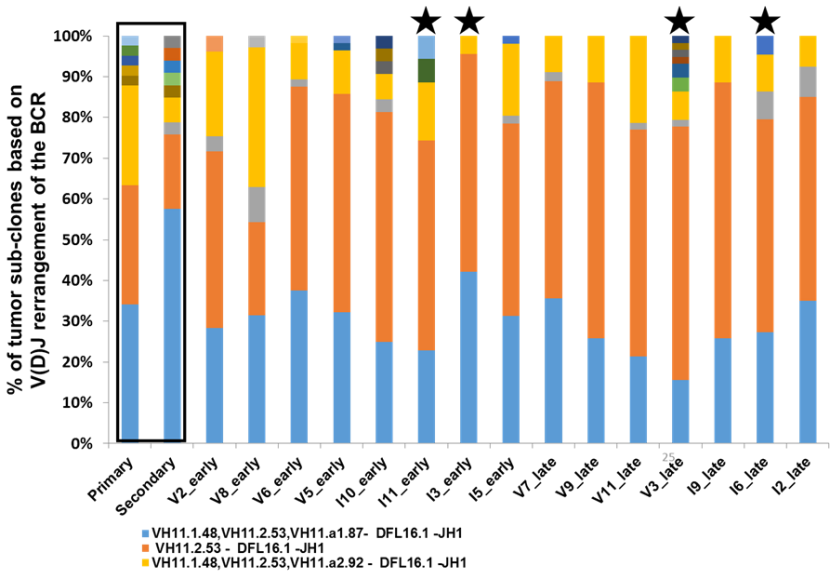

Figure 28: Clonal architecture based on V(D)J rearrangements of the BCR.
Identification of tumor subclones from WES of primary and secondary CLL mouse tumors based on V(D)J rearrangements of the BCR using IgBLAST. Each color represents a unique V(D)J BCR rearrangement. The three major V(D)J rearrangements are depicted in the legend. Primary = original tumor from primary Eμ-TCL-1 donor mouse. Secondary = primary tumor was injected into C57BL/6 mice and expanded for the purpose of this study. Stars indicate samples with highly elevated numbers of mutations that will be explained in the following. Data analysis was performed by Yashna Paul.

The first observation of this analysis was that the primary tumor from the parental donor TCL-1 mouse was oligoclonal with regard to its V(D)J region and consisted of two to three major clones (Figure 28, left box). This was not expected as CLL patients usually harbor one major B cell clone. Additionally, the contribution of the predominant BCR clones only marginally changed upon serial transplantation and the major BCR clones remained the same. This was also the case for vehicle-treated as well as Ibrutinib-treated animals early and late during treatment (Figure 28).

In contrast to the unchanged architecture of the V(D)J rearranged BCR clones, four samples were identified displaying a high number of somatic mutations with very low allele frequency (Figure 28, marked with stars, Appendix Figure 7 a,b). These elevated numbers of mutations appeared in resistant (Ibr_late) and sensitive (Ibr_early and Veh_late) samples and therefore are unlikely to be directly linked to the resistance mechanism. Notably, these somatic variants were distributed across the whole genome without an apparent pattern (not shown). In addition, there was no increase of the proportion of somatic sequence variations annotated at dbSNP (The Single Nucleotide Polymorphism database), which would have implied a contamination with germline DNA of the recipient mice in these samples (Appendix Figure 7 b).

								Allele Frequencies	
Gene Name	**Chr.**	**Pos.**	**Ref.**	**Alt.**	**Effect**	**Gene Region**	**dbSNP status**	**I9_late**	**I2_late**
Grb14	2	65022658	G	T	n.a.	5'UTR	n.a.		0.039
Ets1	9	32728680	G	T	stopgain	exonic	n.a.	0.013	
Sos1	17	80434006	A	G	Nonsyn_SNV	exonic	n.a.		0.016
Sos1	17	80455053	C	A	Nonsyn_SNV	exonic	n.a.	0.012	
Vav1	17	57311789	C	T	Nonsyn_SNV	exonic	n.a.		0.042
Nfatc1	18	80663367	C	A	Nonsyn_SNV	exonic	n.a.	0.022	

Table 1: Single nucleotide variations in BCR pathway genes.
Identification of potential mutations in BCR pathway-related genes, present in samples from two Ibrutinib-resistant mice, but no other sample. (BCR = B cell receptor, Chr. = chromosome, Pos. = position, Ref. = reference, Alt. = alteration, Nonsyn = nonsynonymus, SNV = single nucleotide variation, n.a. = not available). Major data analysis was performed by Yashna Paul.

Next, the aim was to determine if Ibrutinib resistance in the TCL-1 AT model had evolved due to point mutations in Btk, Plcγ2 or other genes of the BCR signaling pathway. Mutations present in the DNA of resistant animals but not Ibrutinib-sensitive and vehicle group animals were studied. For this analysis, samples with high numbers of low frequency mutations labeled with stars in Figure 28 (including one Ibrutinib-resistant case), were removed from the analysis in order to exclude false positive passenger mutations. Mutations were filtered for nonsynonymus single nucleotide variations (SNVs) in exonic or 5'UTR regions and subsequently compared to a list of 86 genes involved in the BCR pathway including B cell commitment, cytoskeletal rearrangement, protein biosynthesis and transcription (exported from Ingenuity knowledge base). Grb14, Ets1, Sos1, Vav1, and Nfatc1 were identified to match these criteria while only Sos1 appeared in both animals (Table 1).

In summary, no single recurrent mutation that would likely contribute to drug resistance was identified, as all mutated genes displayed very low allele frequencies <15% (e.g. 1.3% and 1.6% for Sos1).

3.3.4 Gene expression profiling of Ibrutinib-resistant Eμ-TCL1 tumors

As no mutations in Btk and Plcγ2 and only one recurrent low allele frequency mutation in Sos1 (so far not found in patients) were identified in Ibrutinib-resistant tumors, it was hypothesized that changes in the gene expression signature could account for the rather rapid resistance

development in this mouse model. Transcriptome data of the same treated tumor samples described in the WES study, were first used for unsupervised hierarchical clustering analysis (Figure 29 a).

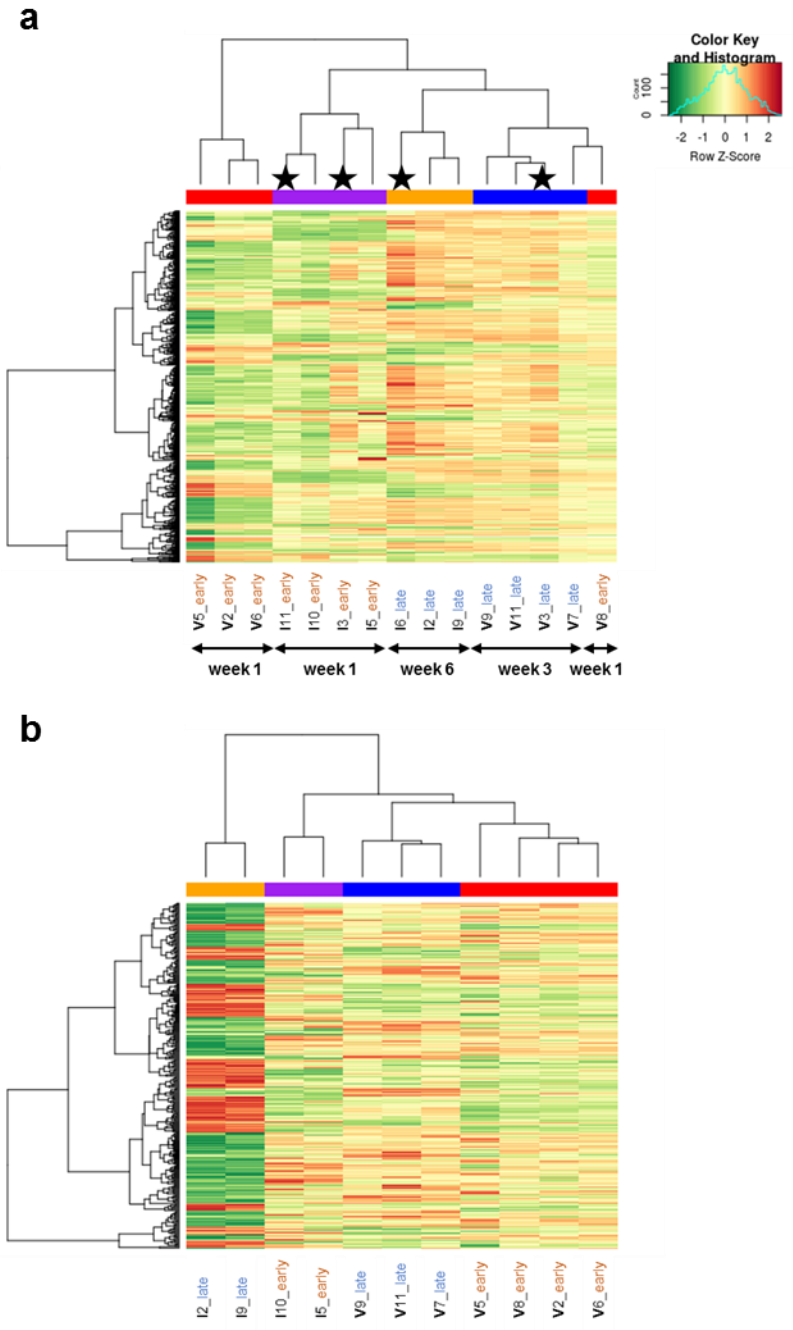

Figure 29: Unsupervised and supervised hierarchical clustering of RNA sequencing transcripts.
(a) Unsupervised hierarchical clustering of the 1000 most variable transcripts across all samples. Stars indicate samples with highly elevated number of low allele frequency mutations. **(b)** Supervised clustering of DEGs between Ibrutinib resistant and sensitive samples, which is *Ibr_late Vs Ibr_early + Ve_late + Veh_early*. Samples with highly elevated number of low allele frequency mutations were excluded from the analysis. Data analysis was performed by Yashna Paul.

Besides one sample (V8_early), all samples clustered according to their treatment group. The analysis revealed, that the drug's effect was not the only deciding factor for clustering the samples (vehicle samples vs Ibrutinib-treated samples), but the disease period seemed to play an important role as well. The order of sample clustering can be summarized from right to left with increasing distance as followed: *week 3 vehicle – week 6 Ibrutinib (resistant) – week 1 Ibrutinib – week 1 vehicle* (sample V8_early excluded).

Ibrutinib late and Vehicle late clustered the closest, presumably because of the many shared characteristics of the full blown tumor disease at this point. The second closest group with respect to the Ibrutinib_late samples is the Ibrutinib_early group, hinting towards a shared expression signature caused by the treatment. And finally, Ibrutinib_early samples displayed the largest distance with the vehicle_early group, likely due to the difference in efficacy of Ibrutinib and its beneficial impact on the tumor cells, controlling the disease at this time point.

Next, two differentially expressed gene (DEG) lists were created: (1) DEGs differential between *Ibr_late VS Ve_late* to identify transcripts highly expressed in non-responsive versus responsive tumors, and (2) *Ibr_late VS Ibr_early + Ve_late + Veh_early* in order to filter for more specific DEGs in the resistant samples only.

Besides one gene, these two lists were identical regarding their transcript content (341/342 DEGs), while however, the second DEG list showed lower *p* values for some genes. Thus, the subsequent gene ontology (GO) and gene set enrichment (GSE) analysis were performed with the latter DEG list.

Several biological complexes including *fatty acid synthase complex*, *BcL-2 family complex*, and *NF-kB complex* were identified among others, involving Pim2 and Igf1-r all well-known genes in the context of cancer (Figure 30).

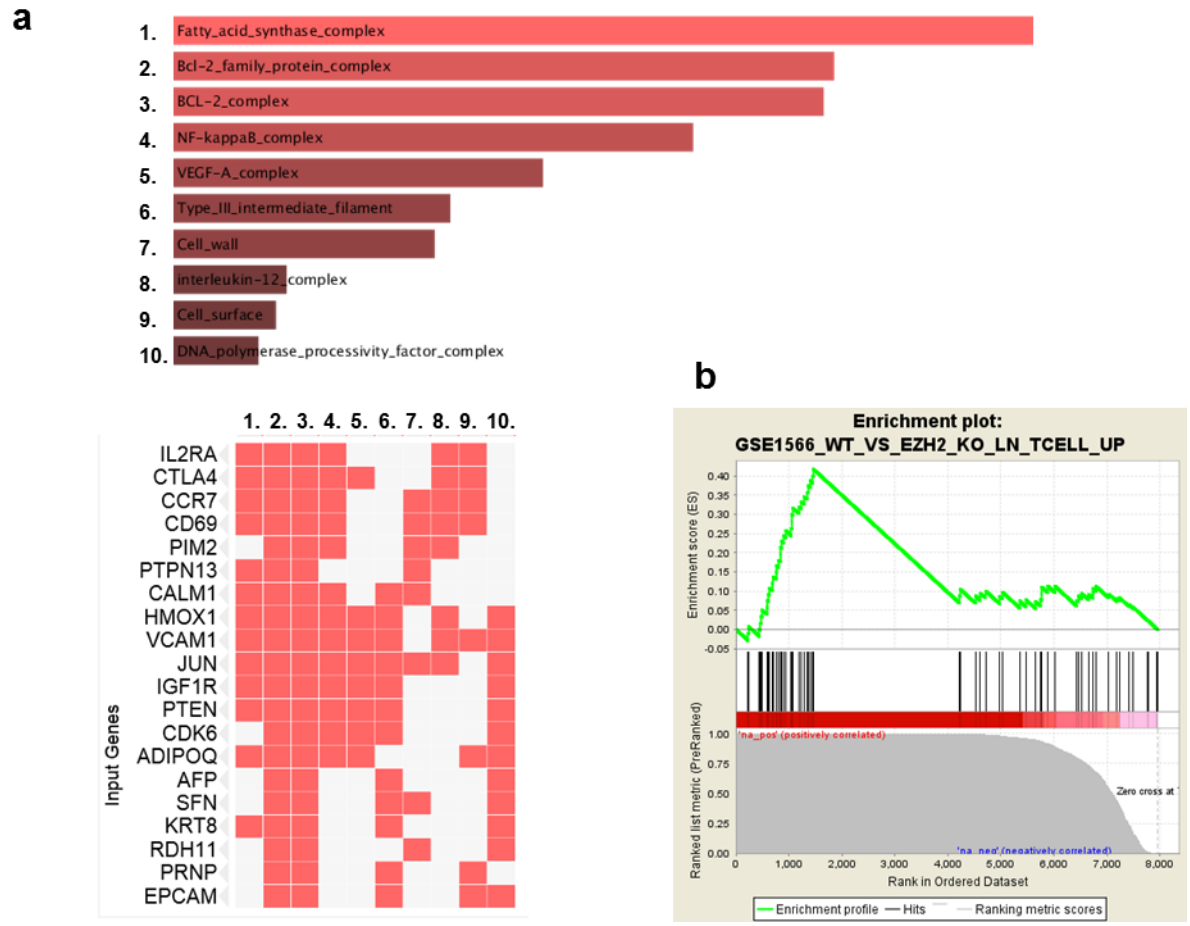

Figure 30: Gene ontology and gene set enrichment analysis of Ibrutinib resistance-specific transcripts. DEGs between *Ibrutinib_late VS Ibr_early + Ve_late + Veh_early* were applied to downstream analyses. **(a)** Gene ontology (GO) analysis of 203 upregulated DEGs was performed using Jensen COMPARTMENTS via the Ma'ayan lab web-tool EnrichR (see methods). **(b)** Gene set enrichment (GSE) analysis of pre-ranked DEGs, applied to mouse gene sets, showing the most significant enriched gene set with a NES (normalized enrichment score) of 2.64.

Further, performing of gene set enrichment analysis *p* value pre-ranked list of resistance-specific DEGs revealed the gene set GSE1566_*WT_VS_EZH2_KO_LN_TCELL_UP* to be most strongly enriched in resistant tumor cells. EZH2 (Enhancer of zeste homolog 2) participates in histone methylation and therefore might point towards an altered epigenetic state acquired by Ibrutinib-resistant tumor cells[322].

In summary, the transcriptional profiling analysis resulted in the identification of several upregulated genes and enriched gene sets, which require further testing and validation by other methods. Downstream analyses will then focus on characterizing the role of these genes and pathways in Ibrutinib resistance, and the identification of potential target molecules to improve treatment approaches for patients that relapse under Ibrutinib treatment.

4 DISCUSSION

4.1 Modulating the myeloid tumor microenvironment in CLL by targeting the CSF-1 receptor

Targeting the CSF-1R using a monoclonal antibody, named TG3003, changed monocyte/macrophage morphology in monocultures, reduced NLC numbers in NLC cocultures that mimic the lymph node microenvironment, slightly reduced the expression of factors with functional relevance in the CLL TME, and finally disrupted NLC-mediated survival support for CLL cells. These promising *in vitro* results served as the basis to move forward in testing TG3003 in a preclinical model of CLL using the TCL-1 AT in humanized CSF-1R KI mice.

In recent years, targeting CSF-1R has been the focus of many preclinical cancer studies. Meanwhile, it has been shown by several groups that targeting CSF-1R signaling in mouse tumor models can have various effects on disease outcome. Most of these studies are focusing on solid tumors where TAMs were initially described and high TAM densities were linked to poor prognosis, as in breast and ovarian cancer[323]. But also in CLL, a higher number of $CD163^+/CD68^+$ myeloid cells in lymph nodes of CLL patients correlates with shorter overall survival[324].

In many solid tumors with involvement of CSF-1R-expressing TAMs, CSF-1 was reported to be elevated in the patients' blood sera[325, 326, 327]. Quantification of CSF-1 in sera from CLL patients compared to healthy donors revealed slightly elevated CSF-1 levels (Dr. Angela Schulz, DKFZ Heidelberg, unpublished). Similarly, CSF-1 quantification in sera from TCL-1 AT mice compared to healthy wildtype mice revealed a modest but not significant increase of this factor with disease progression. The absence of a significantly upregulated CSF-1 in human and mouse sera could possibly point to a high consumption of this protein by the elevated monocyte number of in CLL patients and the TCL-1 AT model. Apart from blood, CSF-1 could be locally produced in lymphatic tissues. For example, CSF-1 secretion might be induced in the lymph nodes where it mediates the transition of monocytes towards tumor-promoting phenotypes, as suggested by results of this study showing secretion of CSF-1 in CLL-monocyte cocultures after 14 days. Similarly as proposed for solid tumors, also in CLL the malignant cells might be the source of CSF-1 in these cocultures[328]. Assessing CSF-1 levels in monocyte monocultures is not simple as the addition of CSF-1 itself is required for the maintenance of monocyte survival. Moreover, myeloid cells can produce CSF-1 themselves and thereby create a feedback loop[329]. However, at least in the TCL-1 AT model, an altered CSF-1 production by monocytes themselves was not observed by GEP data presented in the

second section of this thesis. Neither CSF-1, nor CSF-1R were different in their gene expression levels in monocytes from TCL-1 AT mice compared to healthy wildtype mice (Appendix Table 3).

The CSF-1/CSF-1R axis is essential for the generation of cells from the myeloid lineage as depicted in the introduction. Hence, the postulation was that targeting this axis would interfere with one or more of the proposed mechanisms CSF-1R is known to be involved in: (1) myeloid cell differentiation, (2) monocytic commitment, and (3) survival, proliferation and chemotaxis of macrophages[141].

The proposed mode of action of TG3003 was not via complete blockade of the CSF-1R pathway, but rather allowing binding of CSF-1 and partial signaling which would result in reprogramming of monocytes or TAMs, and their differential skewing towards DCs[316]. However, even though CSF-1 levels did not increase upon treatment of NLC cocultures with TG3003 *in vitro* (supporting that CSF-1 was used up by the cells), this antibody seemed to act in a different manner than proposed. Rather than having a reeducating effect on the myeloid microenvironment with consequences on adaptive immunity, TG3003 prevented the accumulation of NLCs *in vitro,* as well as monocytes and cDCs *in vivo*. In addition, the expression of surface molecules required for adhesion, co-stimulation of T cells, and antigen presentation remained at critically low levels in cDCs in leukemic mice after treatment with TG3003. In line with the observation that cDCs retain their leukemia-associated phenotype, adaptive immunity with respect to T cells was also not altered. Hence, this study suggests that TG3003 inhibits survival, proliferation, and/or differentiation of monocytes, rather than reprogramming of tumor-supporting myeloid cells.

As TG3003 was able to reduce monocyte numbers in blood, spleen as well as CSF-1R-expressing cells in the bone marrow, its effect appears to be of systemic nature rather than limited to a specific microenvironment. This was of advantage for preclinical testing, as myeloid cells in the TCL-1 AT model accumulate in blood, spleen and bone marrow as well. However, in the TCL-1 AT model, TG3003 affected myeloid cell populations with different intensities. In the spleen, TG3003 mainly reduced Ly6C^{low} absolute numbers but showed only a modest trend towards fewer Ly6C^{hi} monocytes. Similarly, Lenzo and colleagues have shown previously that mice treated with a neutralizing anti-CSF-1R antibody (AFS98) under steady state conditions had significantly lower levels of the Ly6C^{low} monocyte population, while the authors did not note a compensatory increase in the number of Ly6C^{hi} monocytes[330]. Moreover, in steady state Ly6C^{low} monocytes express higher surface levels of CSF-1R than Ly6C^{hi} monocytes, as confirmed by the GEP data analysis comparing the two wildtype subsets (Appendix Table 3). This differential expression of CSF-1R on monocyte subsets was confirmed for bone marrow and blood by published data[318]. Hence, it appears plausible

that TG3003 may act on the transition of Ly6C^{hi} monocytes to the Ly6C^{low} subpopulation. Moreover, the impact of TG3003 on cDC numbers might reflect the dependency of their generation on monocytic precursor cells.

Notably, TG3003 did not actively kill monocytes *in vitro,* and when added at later time points to NLC cocultures (when these had already differentiated), it also did not impact on their numbers, underscoring myeloid cell differentiation as one main mechanism targeted by this antibody. Interestingly, macrophage numbers which were decreased in the TCL-1 AT model, were not further changed by the antibody supporting that TG3003 impacts mainly on the differentiation of macrophages and DCs from monocytes, and not on their survival. Pyonteck and colleagues observed regression of tumors in a glioma model due to depletion of tissue-resident microglia using the brain-penetrant CSF-1R inhibitor BLZ945[331]. In contrast, newly recruited macrophages were specifically protected from CSF-1R-induced death in this study. The fact that different myeloid cell populations can be selectively targeted by different antibodies/inhibitors is of relevance as it is not yet clear whether NLCs in CLL patients are blood monocyte-derived (as mimicked in the NLC coculture model) or rather differentiate from tissue-resident macrophages.

Recent attempts have addressed the importance of monocytes and macrophages in CLL mouse models. In a study by Hanna *et al*., myeloid cells were targeted using a genetic knockout mouse of CCR2 for the adoptive transfer of TCL-1 splenocytes in order to prevent chemotaxis and recruitment of monocytes in CLL[203]. This study revealed significantly lower percentages and numbers of monocytes in the spleen of leukemic mice. However, even though there was a slight tendency towards decreased tumor cell numbers in CCR2−/− mice compared with WT controls, the impact on tumor development was not significant. Of note, even though, the CCL2/CCR2 axis is generally considered specific for recruitment of monocytes also other cell types have been reported to express CCR2. For example, it was reported that in BALB/c mice approximately 2-10% of CD8$^+$ T cells and 5-15% of CD4$^+$ T cells are positive for CCR2[332]. Also in humans, CCR2 has been described to be expressed on T cells and memory cell differentiation was associated with an increase in chemokine responsiveness[333].

Hanna *et al*. showed that depletion of myeloid cells using Clodronate liposomes as an early intervention resulted in remarkable reduction of disease progression in the TCL-1 AT model[203]. Liposomes are efficiently taken up by phagocytic cells and thereby Clodronate is delivered to the cells causing their death[334]. TCL-1 AT mice treated with Clodronate liposomes showed extremely low numbers of Ly6C^{hi} and Ly6C^{low} monocytes and also a significant decrease in cDC numbers. In contrast to the obtained results with TG3003, the remaining cDCs showed a normalized phenotype,

as exemplified by higher MHC-II and lower PD-L1 expression following Clodronate treatment[203]. Moreover, this treatment resulted in a normalized T cell subset composition with an increased percentage of naïve $CD4^+$ and $CD8^+$ T cells and a lower percentage of memory/effector T cells in spleen, peripheral blood, and peritoneal cavity. Most importantly, Clodronate liposome treatment delayed leukemia development in TCL-1 AT mice. As an explanation, it was proposed that myeloid cell depletion by this treatment affected T-cell subset composition via altering their trafficking and migration. This was supported by results showing reduced secretion of inflammatory cytokines and chemoattractants for T cells, such as TNF-α, CXCL9, and CXCL16, in Clodronate-treated mice.

Even though this study served as a proof of principle for the importance of myeloid cells in CLL progression, there are considerations that need to be taken into account. In fact, phagocytic cells do not only comprise monocytes, macrophages, and dendritic cells, but also mast cells and neutrophils, and as already described in the introduction, neutrophils have been clearly shown to be involved in CLL development as well[315, 335]. Furthermore, even B cells were reported to be capable of phagocytosis[336]. Hence, treatment of mice with Clodronate liposomes might not exclusively target myeloid cells, but its success might be in part due to effects on other bystander cells.

In contrast to this cell killing-approach, TG3003 treatment was intended as an elegant and specific approach to modulate myeloid cells and suppress their tumor-promoting activities.

In a more recent publication, Galletti *et al*. comprehensively investigated different TAM depletion strategies including Clodronate liposomes and monoclonal antibodies against CSF-1R in various CLL transplantation mouse models[217]. Firstly, the authors conducted a similar approach as Hanna *et al*. using Clodronate liposomes in TCL-1 AT mice, but with late intervention onset (day 16 post-transplantation). This resulted in reduced percentages of tumor cells in peripheral blood, spleen, and to a stronger extent in the peritoneal cavity, the site of Clodronate injection. While percentages of $CD11b^+F4/80^+$ monocytes and macrophages in the spleen and peritoneal cavity were significantly lower, Clodronate had no effect on effector and central memory $CD8^+$ T cells and no effect on regulatory T cells when applied at this late time point of the disease. This is in contrast to the study of Hanna *et al*., however consistent with the results on T cells in the TG3003 study.

Furthermore, Galletti *et al*. investigated the effect of a human monoclonal antibody (RG7155) in a xenograft transplantation model using the human MEC1 CLL cell line transplanted into RAG2-/- mice that are deficient for mature B and T cells. Two i.v. administrations of the anti-CSF-1R antibody RG1755 significantly lowered the cell number of $CD11b^+F4/80^+$ myeloid cells in the spleen but had no impact on the number of human leukemic cells in the same organ. On the other hand, RG7155

had only a modest, non-significant impact on $CD11b^+F4/80^+$ cells in the bone marrow while significantly lowering the tumor load in this but no other organ.

Further, the group tested an anti-mouse CSF-1R antibody (2G2) in the TCL-1 AT model. In this study, the numbers of $CD44^+CD62L^{low/neg}$ effector memory, as well as $CD44^+CD62L^+$ central memory $CD8^+$ T cells in the spleen were increased by 2G2 treatment. Moreover, the number of $CD44^+$IFN-γ-producing cells in the spleen was also elevated. These observations differ from the here presented results obtained with TG3003, which did neither impact on $CD4^+$ and $CD8^+$ T cell numbers, nor their effector function with respect to TNF-α and IFN-γ production. Effects of 2G2 treatment on tumor development in the TCL1 AT model were not presented in this study.

Overall, it remains unclear whether targeting CSF-1R with RG7155 or 2G2 impacts on CLL development in mice, as no other lymphoid organ besides the bone marrow showed reduced tumor load with RG7155 antibody[217]. This raises the question which factors are responsible for limiting treatment success with anti-CSF-1R antibodies. Several reasons are conceivable, such as (1) compensatory recruitment of other immune cells or replenishment by higher de novo monocyte production, (2) resistance development, (3) variability in CSF-1R-dependency, or (4) insufficient depletion of myeloid cells by the antibodies.

One possible compensatory mechanism could be via increased recruitment of neutrophils[337]. During inflammation, it is the neutrophils that facilitate the recruitment of monocytes to tissue sites[338]. It is possible, that killing of monocytes promotes inflammatory cytokine secretion which in turn leads to recruitment of neutrophils. Interestingly, Galletti and colleagues measured higher percentages of neutrophils in the blood upon RG7155 treatment, but lower percentages upon Clodronate-mediated depletion[217]. In the here presented study, TG3003 partially normalized CLL-associated, elevated granulocyte/neutrophil numbers in the spleen, leading to the conclusion that neutrophils are not recruited due to the decrease in monocyte numbers. As all precursor cells of the myeloid lineage express CSF-1R, it appears plausible that granulocytes/neutrophils as members of the myeloid cell lineage might be directly affected by TG3003 as well.

Acquired resistance in response to monotherapy targeting CSF-1R has indeed lately been observed and addressed. In a preclinical glioblastoma model, treatment with BLZ945, a small molecule kinase inhibitor for CSF-1R, resulted in a 50% relapse rate after initial responses[339]. TAMs were not depleted in this model but shifted in their phenotype towards M1 macrophages. These cells were shown to produce IGF-1 which triggers an IGF-1R-driven hyperactivation of PI3K in cancer cells,

which was at least partially accounting for the observed resistance. This was further proven as a combination of inhibitors targeting CSF-1R and IGF-1R or PI3K resulted in prolonged survival of mice[339]. Besides this acquired resistance, there are also earlier reports of inherent resistance in mice, where despite effective macrophage depletion using PLX3397, tumor growth in an orthotopic PyMT mammary tumor transplantation model was not changed in monotherapy[340].

Incomplete depletion of myeloid cell populations and therefore insufficient changes in the immune profile might represent the main reason for the lack of efficacy in the study with TG3003. Even so TG3003 significantly decreased monocyte numbers, these were still clearly more abundant in treated mice compared to wildtypes. Hence, one explanation could be that these remaining monocytes are sufficient to promote leukemia, as for example suggested by their secretion of T cell chemoattractants, further underscoring their impact on tumor progression. As the studies by Hanna *et al*. and Galletti *et al*. did not include control cohorts of untreated animals, the efficiencies of monocyte depletion in those studies remain unclear[203, 217]. However, there are several examples of solid tumor models, where upon targeting of CSF-1R, the macrophage number was somewhat reduced but not completely. For example, Patawardhan *et al*. reported a decrease of macrophages in tissue samples in peripheral nerve sheath tumors in response to the CSF-1R inhibitor PLX3397 treatment, but no complete depletion[341]. A similar observation of remaining TAMs was also made by Quail and colleagues in glioblastoma multiforme tumors that were resistant to BLZ945[339]. Hence, it remains unclear whether in these studies a more efficient depletion of TAMs would promote a positive disease outcome, and whether also TG3003 would show a favorable outcome when used in higher doses.

In order to proof that specific and efficient ablation of CSF-1R-expressing cells as a late intervention (after onset of the disease) would be favorable with regard to leukemia progression, the plan was to use MM^{DRT} mice (provided by Dr. Markus Feuerer). This mouse strain is generated by crossing two mouse lines[342]. The first mouse strain carries a human diphtheria toxin receptor (DTR)-mCherry fusion protein under the Csf1r promotor with a floxed stop sequence arranged upstream of it ($Csf1r^{LSL\text{-}DTR}$ mice). The second strain carries the gene sequence for a Cre recombinase under the promotor for the gene coding for lysozyme protein ($Lysm^{Cre}$ mice). In crossed animals, mice can be depleted from myeloid phagocytic cells that express lysozyme and CSF-1R when treated with diphtheria toxin[342]. A pilot study with adoptively transferred TCL-1 splenocytes into these MM^{DTR} mice and subsequent repeated diphtheria toxin injections lead to initial ablation of monocytes in peripheral blood. However rebound effects with increased myelopoiesis were observed, and no

effect on tumor load in the blood was evident (data not shown). Therefore, this approach was not further followed.

Conclusions and Outlook

The here presented *in vivo* approach of targeting CSF-1R signaling with TG3003 as an early intervention in the TCL-1 AT CLL mouse model revealed partial normalization of myeloid cell populations, no improvement in terms of disease development, and considerable room for improvement of this interesting treatment strategy. As depicted above, one aim could be a more efficient targeting of myeloid cells, for example through higher dosing of TG3003, or the use of other more efficient antibodies or inhibitors for CSF-1R. Moreover, even though CSF-1R targeting was apparently ineffective alone, it could potentially improve response to other therapies. Indeed, several studies have reported enhanced treatment efficacy when CSF-1R inhibitors were used in combination with other drugs, even in cases where CSF-1R inhibition alone was ineffective.

4.2 Monocytes and cDCs in steady state, in CLL and under the influence of Ibrutinib

The enrichment of Ly6C^{low} monocytes in CLL patients' blood as well as in different lymphoid organs of the Eμ-TCL-1 mouse model of CLL was described previously[202, 203]. Before investigating how Ibrutinib might influence monocytes and their subset distribution, it was important to understand gene expression changes that are induced by the leukemia itself. There are very few investigations on the specific contribution of the two main monocyte subpopulations to CLL pathobiology, and these are mostly based on *in vitro* studies. The gene expression analysis presented in this thesis revealed that Ly6C^{low} monocytes are not only enriched in leukemic mice but also considerably altered in their gene expression signature. Transcriptional differences in Ly6C^{low} monocytes of wildtype and leukemic mice were associated with activation of cellular growth and proliferation.

Potential target genes in Ly6C^{low} monocytes identified by GEP

The acquired GEP data set provides a number of possible CLL-specific target genes in monocytes that might be useful to interfere with the 'activation of cellular growth and proliferation' program of this subset of cells. Implicated genes included CD14 and PECAM-1, which have been previously reported to support the crosstalk between CLL cells and their myeloid microenvironment as summarized in the introduction[80, 343]. Other promising candidate genes are currently investigated within the group, mainly in the context of understanding the oncogenic role of monocytes and

granulocytes. Several novel candidates, so far unrecognized in the context of myeloid cells in CLL, were identified, such as IL-21r (top upregulated gene), Dpp4, Irg1, and F11r. The potential of a few of these candidates as drug candidates for CLL will be discussed in the following paragraph.

IL-21, the ligand for the upregulated IL-21r, was previously reported to enhance FcRγ-mediated phagocytosis of human monocytes and SYK was identified as a novel molecular target of IL-21-mediated singaling[344]. Moreover, IL-21 was reported to maintain the expression of the Fc receptor CD16 on monocytes via the production of IL-10 by human naïve $CD4^+$ T cells[345]. Interestingly, bone marrow $CD14^+$ cells from patients with multiple myeloma significantly upregulated IL-21R that is involved in osteoclast formation[346]. However, in order to assess whether IL-21 or IL-21R are suitable for therapeutic purposes, their role for normal B or CLL cells have to be considered as well: A study by De Totero and colleagues suggested that IL-21 promotes apoptosis in CLL cells[347]. This finding was underscored by a publication from Browning *et al*., in which the authors proposed that IL-21 mediates cytotoxicity of CLL cells as part of the mechanism of Lenalidomide's clinical activity in CLL[348]. In contrast to these findings, Pascutti *et al*. suggested that IL-21, produced by activated follicular helper T cells, contributes to the induction of proliferation in CLL cells in the nourishing niche in lymph nodes[349]. Taken together, the IL-21/IL-21R axis as a potential target for monocytes will require further investigations on both, monocytes and CLL cells and careful evaluation of possible counteractive treatment effects on disease development.

Dipeptidyl peptidase IV (DPP-4; or CD26) is an exopeptidase that among others cleaves chemoattractant MCP-2 upon binding and thereby is able to modulate chemotaxis[350, 351]. Indeed in a mouse model of atherosclerosis, a disease in which chronic inflammation is a key process in the pathogenesis, treatment with the high-affinity DPP-4 inhibitor Alogliptin reduced adipose tissue macrophages and plaque macrophages[352, 353]. In the same study, DPP-4 inhibition prevented monocyte migration and actin polymerization in *in vitro* assays via a Rac-dependent mechanism. Moreover, DPP-4 inhibition prevented *in vivo* migration of labeled monocytes to the aorta in response to exogenous TNF-α and DPP-4[352]. The DPP-4 inhibitor Sitagliptin was further shown to attenuate atherosclerosis by promoting M2 macrophage polarization[354]. Several DPP-4 inhibitors are currently in clinical trials (Alogliptin, Sitagliptin, and Linagliptin) and may be of interest to target monocytes in CLL.

Another highly interesting candidate, upregulated in $Ly6C^{low}$ monocytes is the junction adhesion molecule F11r (or JAM-A; CD321). F11r can serve as a ligand for the integrin LFA1, involved in leukocyte transendothelial migration[355]. However, the specific biological function of F11r in monocytes has not been assessed so far, even though there has been a report describing its

involvement in disease-related monocytes. In this study, Pong *et al*. identified F11r among the transcripts that were differentially expressed between brainstem microglia and bone marrow monocytes in non-neoplastic brain. High-grade murine gliomas contained F11r+ microglia and macrophages and F11r expression correlated with glioblastoma malignancy grade and survival of mice[356]. Interestingly, also monocytes isolated from HIV-infected individuals were identified to express increased surface F11r compared to cells from individuals without HIV[357]. The authors found, that F11r was critical for the extravasation of $CD14^{+}CD16^{+}$ monocytes, demonstrated by their decreased migration across the blood brain barrier when treated with blocking antibody against F11r[357]. Notably, recently Boissard *et al*. performed gene expression (meta-)analysis of NLCs, *in vitro* derived from PBMCs of CLL patients, and compared these with monocytes from healthy individuals. F11r was among a list of 27 genes that were associated with functional ontology criteria, such as 'cell binding function' and 'cell membrane expression', on which they, however, did not comment further[358]. Future studies will be required to evaluate whether F11r-expressing monocytes in the context of CLL represent a unique subset of monocytes that produces specific chemokines and cytokines critical for CLL leukemogenesis and progression, and therefore might serve as a novel therapeutic target to limit seeding of $Ly6C^{low}$ monocytes to leukemic niches.

Previous reports have suggested, that myeloid cells in CLL may possess a suppressive phenotype. For example, Jitschin *et al*. reported the presence of suppressive $CD14^{+}HLA\text{-}DR^{low}$ MDSCs in CLL patients, expressing high IDO levels and T cell suppressive capability[204]. However, besides a more activated and motile ('Cellular movement', 'Immune cell trafficking') phenotype, major pathways that would suggest a suppressive MDSC phenotype in CLL-associated monocytes could not be confirmed. Genes typically associated with suppressive myeloid cell phenotype and function, such as IDO and Arg1, were manually checked for their presence among the DEG and not found to be changed. Also, genes that would suggest a metabolic impairment of monocytes were not altered in their expression level. However, as most of these candidates are enzymes, they might rather affect their activity. Therefore, a potential role of metabolic alterations in CLL monocytes cannot be excluded by this study.

Ibrutinib's effect on monocytes

One major goal of this study was to investigate, which CLL-associated changes in monocytes might be reversed by Ibrutinib treatment, or contrary might be further promoted which is of major interest to develop rational combination therapies. The higher transcriptional similarity of $Ly6C^{hi}$ and $Ly6C^{low}$ monocytes from leukemic animals treated with Ibrutinib and their respective wildtype counterparts suggested that Ibrutinib reverses CLL-induced gene expression changes. A special

focus was given to the question whether transcriptional changes observed in Ibrutinib-treated mice were positively or negatively associated with the number of leukemic $CD5^+CD19^+$ cells, which are the main target of Ibrutinib. For example, inhibition of BTK by Ibrutinib was found to significantly reduce surface TREM-1 levels on both monocyte subsets as well as granulocytes in different organs. In a recent publication, Ibrutinib was demonstrated to inhibit TREM-1-mediated activation of neutrophils by inhibiting oxidative burst and shedding of CD62L *in vitro* and *in vivo*[359]. These data fit to the proposal that BTK is a positive regulator of the TREM-1 signaling pathway[287, 288]. However, the lack of the effect on TREM-1 in treated healthy mice suggests at least a partial dependency of its expression levels on the tumor load, rather than on a BTK-dependent regulation of TREM-1 in this model. Moreover, it is not clear whether there exists a native feedback loop that would result in a downregulation of TREM-1 by Ibrutinib in monocytes.

PD-L1, in contrast, was an example for a direct effect of Ibrutinib on its expression level, irrespective of the involvement of tumor cells and/or tumor-induced IFNγ. This indicates that BTK in myeloid cells might be directly linked to the initiation of their immune suppressive properties via regulation of PD-L1 expression. However, it cannot be excluded that non-tumor microenvironmental components in healthy animals may mediate Ibrutinib's inhibiting potential on PD-L1 in monocytes. The complexity of the immune system further requires simplifying (*in vitro*) experiments in order to answer how exactly Ibrutinib acts on these different pathways.

In summary, this study shows that Ibrutinib positively impacts on a number of molecules and signaling axes that promote leukemia development by being involved in immune suppression, inflammation, and CLL-myeloid cell crosstalk (PD-L1, TREM-1, PECAM-1/CD38 axis). This may contribute to the clinical efficacy of Ibrutinib on tumor development via the monocytic microenvironment of CLL.

Conventional dendritic cells and their role in CLL

Little is known about dendritic cells in the myeloid CLL microenvironment, despite the fact that these immune cells are considered to be indispensable for antigen presentation to T cells and recruitment of effector T cells[360]. Orsini and colleagues provided first evidence for an abnormal phenotype of dendritic cells in the context of CLL[361]. The isolation of DC precursors from peripheral blood of CLL patients revealed a lack of expression of the maturation antigen CD83 and the costimulatory molecule CD80, while CD86 was even slightly increased. The authors showed that this phenotype could be also induced in normal DC precursors ($CD3^-$, $CD16^-$, $CD11b^-$, $CD4^+$) when cocultured with CLL cells. They furthermore suggested some functional impairment with respect to

T cell activation. However, the main pitfall of this *in vitro* study was the low purity of DC precursors ranging from 32–87% when isolated from healthy donors and 27–64% from CLL patients.

To obtain highly pure cDC fractions for comprehensive gene expression profiling, cells were isolated by flow cytometry from TCL-1 AT and wildtype mice. cDCs from TCL-1 AT mice displayed a high number of downregulated genes, which was mirrored in a number of inhibited biological functions and various downregulated signaling pathways in the leukemic state. The data clearly revealed that cDCs from TCL-1 AT mice display a tremendous change in the expression pattern of genes that are important for detection and phagocytosis of foreign particles. In support of that, pathways including 'Role of Pattern Recognition Receptors of Bacteria and Viruses and Phagosome Formations' were downregulated as suggested by the gene expression signature analysis. Hence, the GEP suggested that CLL induces impairment of antigen loading in MHC-II molecules and of cytokine-mediated stimulation of T cell responses in cDCs. Moreover, additional features, such as inhibited NF-κB signaling and TREM-1 signaling, also illustrate the far-reaching 'downstream' signaling consequences. NF-κB signaling in DCs is well-known to be essential for DC differentiation, antigen presentation, and MHC-II regulation [362, 363]. Notably, TREM-1 signaling has been previously reported to enhance TLR and NOD-like receptor (as part of PRRs) signaling and be important for host defense[364, 365, 366, 367]. It is worth to mention that TREM-1 itself was not differentially expressed in cDCs from WT or leukemic mice, neither detected by GEP nor by flow cytometry. Instead, TREM-3, an activating receptor of the same family, was downregulated in cDCs. Murine TREM-3 was proposed to have a similar function as TREM-1 and to arise from Trem-1 gene duplication[368].

Changes of the subset composition of the DC compartment may also differentially regulate cell-mediated immunity. Hence, the increased percentage of $CD8^+$ cDCs indicates a Th1 immune response, comprising the production of IL-12 and IFNγ, characteristics assigned to this DC subset[190]. In a publication from Ruffel *et al.*, the authors clearly demonstrated that for example $CD8^+$ T cell-dependent responses to chemotherapy are blocked by macrophage-derived IL-10 that suppressed IL-12 expression in dendritic cells[369]. However, IL-12 expression in cDCs was reduced in leukemic mice compared to WT mice, further suggesting that these cells might not be able to induce appropriate immune responses. Unpublished group-internal mouse and human data on T cells propose a Th1 response in CLL. At this point, it is not yet clear whether DCs contribute to such a Th1 response or not.

cDCs in the TCL-1 AT model under Ibrutinib treatment

To address the question which effects Ibrutinib might have on the impaired phenotype of cDCs in CLL, functionally relevant markers were investigated in TCL-1 AT mice upon treatment with Ibrutinib. One observation made, was the changed cDC subset composition that was independent of the presence of leukemic cells. One might assume that the changed cell composition in the spleen might create an altered microenvironmental milieu that is more beneficial as less CLL-derived stimuli are present. In contrast to this assumption, ICAM-1, CD86, and CD83 were even further decreased by Ibrutinib treatment and also an increased percentage of the PD-L1-expressing proportion of cDCs was quantified. Hence, Ibrutinib seems to aggravate the impaired phenotype of cDCs.

In a recent *in vitro* study, Natarajan *et al*. suggested that Ibrutinib promotes maturation and activation of dendritic cells[370]. The authors observed an enhanced development and maturation of bone marrow-derived DCs, among others exemplified by an increased percentage of the $CD11c^+$ population, which in turn displayed higher MFI expression levels for MHC-II and CD80 (a maturation marker expressed on DCs but also B cells). Furthermore, LPS-induced cytokine secretion was higher in Ibrutinib-treated DCs for IL-10 and IFN-β (measured by ELISA in culture supernatants). On the other hand, IL-12 was significantly reduced and TNF-α showed a slight tendency towards a reduction, which is similar to the results presented here. These data initially seem, at least in part contradictory and even more with respect to their final conclusion that Ibrutinib promotes maturation and activation of dendritic cells. However, there are a few points to be considered with respect to technical aspects as well as the author's general perspective. Like in many *in vitro* studies, the study technically suffered from impure cDC populations as the authors cultured PBMCs with CSF-2 which is known to induce DC differentiation, and considered all $CD11c^+$ cells as DCs, which were > 60 %. These impure $CD11c^+$ cells may include other cells such as for example B cells that also express CD11c. Hence, the exact source of the secreted cytokines in response to LPS stimulation in the presence of Ibrutinib is debatable. Further, this published study focused on *in vitro* effects of Ibrutinib on the development of healthy bone marrow-derived DCs, and not on CLL-associated DCs that show an impaired phenotype and are treated *in vivo* with Ibrutinib, which might be the reason for the observed differences. The results presented in this thesis much closer reflect the situation of DC development in a mouse model of CLL.

Potential treatment approaches to restore CLL-associated impaired phenotype of cDCs

The goal of this study was to identify targetable molecules that are suitable for therapy approaches to restore the CLL-associated cDC phenotype. Among others, the IL-10RA was predicted as an

upstream regulator that was inhibited in cDCs sorted from leukemic TCL-1 AT mice compared to cDCS from wildtype mice. This was surprising as the IL-10/IL-10RA axis is considered to mediate suppression of DCs leading to inhibited maturation and a tolerogenic phenotype[320, 371]. For example, IL-10 pretreatment inhibited the LPS-induced up-regulation of CD40 and CD86 on DC which was suggested to be mediated through suppression of the PI3K/Akt pathway and of IκB kinase activity/NFκb inhibition[372]. A neutralizing anti-IL-10 antibody induced spontaneous maturation in DCs *in vitro* and enhanced immune responses *in vivo*[373]. Therefore, it was of interest whether inhibition of IL-10R signaling would have a similar effect in leukemic animals. Indeed, even though the gene expression profiling revealed an inhibited IL-10RA pathway, its blockade showed a partial reversal of the tolerogenic cDC phenotype. However, despite an 'improved' cDC phenotype, disease progression in these animals even worsened. It remains difficult to evaluate which might be the reasons for the negative impact on the tumor burden. This will likely be focus for future studies.

Conclusions and Outlook

In summary, this study shows that Ibrutinib treatment impacts transcriptionally and functionally on cDCs and monocytes. On the one hand, Ibrutinib induces a partial reversal of many CLL-associated alterations in $Ly6C^{hi}$ and $Ly6C^{low}$ monocytes and therefore normalizes the transcriptome of monocytes. On the other hand, it further enhances and worsens the immature tolerogenic phenotype of cDCs. Notably, Ibrutinib treatment was reported to significantly downregulate multiple gene signatures in $CD19^{+}$ cells from CLL patients, including genes that are involved in cytokine signaling and cell adhesion, and therefore most likely impacts on the interaction of malignant cells with their microenvironment[374]. Altogether, these results show that the general high efficacy of Ibrutinib in CLL patients arises from complex activities of the drug on the tumor and its microenvironment. Combination therapies with improved efficacies might include drugs that promote the function of DCs, or DC-mediated vaccination approaches. The latter is based on *ex vivo* generation of functionally potent dendritic cells that have been manipulated to be able to take up and present tumor antigen *in vivo* and thereby to elicit potent anti-tumor immunity[375, 376]. This approach has been proven to be feasible, and promising results in CLL were obtained within the last years[375, 376].

4.3 CLL tumor-microenvironment-independent and cell-intrinsic resistance to Ibrutinib

Major findings

In line with the growing number of Ibrutinib-treated patients who relapse with resistance and fulminant disease progression, treatment of TLC-L1 AT mice with Ibrutinib did not result in long-lasting response, but was rather characterized by a loss of efficacy which was accompanied by an induced proliferation of leukemic cells. Furthermore, re-transplantation of tumor cells from animals previously treated with Ibrutinib showed lack of treatment response to Ibrutinib, confirming that these cells indeed had acquired resistance to Ibrutinib. The appearance of a leukemic sub-population with weaker expression of CD19, CD38 and CD45 along with treatment, exclusively in mice that received Ibrutinib further suggested a resistance-specific phenotype of $CD5^{+}CD19^{+}$ CLL cells under the selection pressure of Ibrutinib.

Relevance of phenotypic differences between sensitive and resistant tumors

One clear difference between retransplanted tumors that previously received vehicle or Ibrutinib was their different potential to engraft in recipient mice. The capacity to engraft and to then achieve a substantial and detectable tumor load in the blood, the defined criterion to start treatment, was decreased in tumors of Ibrutinib-pretreated animals and therefore delayed treatment start for one week. One explanation for this is that BTK activity might be required for leukemia cell engraftment. Freshly transplanted tumor cells most likely still show inhibition of BTK signaling, as Ibrutinib irreversibly binds to the kinase. Over time this inhibition is lost due to turnover of BTK, and cells that regained BTK activity might then engraft with a time delay. Another explanation could be that Ibrutinib treatment had induced robust molecular changes downstream of BTK leading to impaired engraftment. This might also affect only some of the leukemic cells, and as the remaining cells which still possess the capacity to engraft are less in numbers, it requires longer until they expand sufficiently to become detectable. It is difficult to clearly state if this trait is cell-intrinsic and belongs to the resistant phenotype of the cells, or if continuous Ibrutinib treatment and permanent BTK blockade is responsible for the delay in engraftment. One hint, that the resistant tumor cells had stably acquired changes, was the observed decreased expression of CD19 at the end of the first treatment round which stayed similarly low in the second treatment round.

CD19 serves as a costimulatory molecule for amplifying BCR signaling[377]. B cells from mice deficient for CD19 display hyporesponsiveness to BCR-mediated signals and generate modest immune

responses[378]. Notably, a physical and functional association between CD19 and BTK has been investigated[379]. In particular, the interaction of CD19 and BTK was not required for initial BTK phosphorylation, but CD19 expression was necessary to maintain the phosphorylation of BTK[379]. Moreover, CD19-induced Ca^{2+} influx, in turn, depends on BTK[379]. In CLL patients, CD19 expression levels are lower compared to healthy donors[380, 381]. In a study by Herishanu *et al*., the authors investigated the intratumoral diversity of CLL cells in response to IgM stimulation and CD19 engagement, and could classify CD19-responsive and CD19-nonresponsive cells[382]. The authors showed that the responsive subpopulation expressed higher levels of surface CD19, and of c-*myc* mRNA. In this study, responsiveness (and CD19 expression) positively correlated with disease progression[382].

In addition to CD19, also the surface molecules CD38 and CD45 are involved in the BCR signaling. CD45 is a receptor-like tyrosine phosphatase and pan-leukocyte marker[383]. It dephosphorylates inhibitory tyrosine kinases of the Src family, such as Lyn, and by this positively regulates antigen receptor signaling in B cells[383]. In CD45-/- B cells, BCR ligation failed to activate Pi3k, NF-κb, Erk1, or Erk2 kinases[384].

CD38 was described to have diverse functional properties. As elucidated before, CD38 functions as an adhesion molecule binding CD31 for example on NLCs[343]. In addition, CD38 serves as a bifunctional extracellular enzyme, catalyzing the transformation of NAD^+ into cyclic ADP-ribose (cADPR), and cADPR into ADPR[385]. cADPR induces mobilization of internal calcium and promotes proliferative responses in activated B cells[385]. Moreover, CD38 is dependent on the expression of the BCR complex and involved in augmenting BCR responses resulting in IL-2 production[385]. Overall, the decreased expression of these BCR-associated surface molecules on Ibrutinib-resistant leukemia cells points towards a potentially weakened BCR signaling which raises the question which compensatory mechanism might cause the enhanced proliferation and survival of Ibrutinib resistant cells [384].

Ibrutinib resistance in CLL patients versus the TCL-1 AT model

The progression rate of CLL patients on Ibrutinib treatment constitutes about 18 percent[298]. Ten out of 15 patients develop resistance due to somatically acquired mutations in genes encoding BTK and its downstream target PLCγ2. The remaining patients experience heterogeneous transformation to more aggressive lymphoma, mainly DLBCL and Hodgkin Lymphoma. Loss of treatment response to Ibrutinib in the TCL-1 AT mouse model has been repeatedly observed in different studies conducted over the course of this thesis and the penetrance of resistance was 100 percent. This illustrates that the TCL-1 AT model reflects in this respect only a subgroup of CLL patients. Besides the many commonalities between CLL in humans and the TCL-1 AT model, there

are striking differences between the two which are of interest for the current subject. While in patients, CLL represents an accumulation of mainly non-cycling B cells, leukemia cells in Eμ-TCL-1 mice have higher proportions of proliferating cells, but also more apoptotic cells compared to non-leukemic lymphocytes[234]. In the here presented study, a high rate of proliferation was detected not only in resistant tumors but also in the vehicle-treated (sensitive) tumors. Moreover, tumor cells in all analyzed lymphoid organs, including peripheral blood, were positive for Ki-67, while in human patients, the proliferative cell pool is located in the pseudo follicles in the lymph nodes and makes up 0.1-1% of the entire CLL clone per day. The outcome of the high rate of leukemia cell proliferation in TCL-1 AT mice might be an enhanced acquisition of genetic mutations that contribute to disease evolution and resistance development.

Richter's transformation, as a potential event conferring Ibrutinib resistance

Ahn *et al*. comprehensively studied 15 CLL patient cases with progression on Ibrutinib treatment[298]. Mutations in BTK and PLCγ2 were mostly found in patients with CLL progression after more than 18 months of treatment, but not associated with the early, mostly aggressive transformations. Four out of 15 cases with early transformation were considered as Richter's transformation. Hence, it was hypothesized that resistance development against Ibrutinib in the TCL-1 AT model might represent or be similar to patients developing Richter's transformation. There are several points that argue for, but more observations against this hypothesis: Commonly used but not reliable clinical features for the prediction of Richter's transformation in patients are a short lymphocyte doubling time, and a high percentage of bone marrow involvement, which are also given in the Ibrutinib-resistant TCL-1 AT mice[19]. An increased size of tumor cells is another feature of most Richter transformation cases, which was not observed based on the FSC/SSC characteristics of the murine leukemic cells acquired by flow cytometry (data not shown)[386]. Elevated ß-2 microglobulin and LDH levels are commonly valued as signs of Richter's transformation but were not measured in the present study[19]. One clinical feature more clearly associated with Richter's transformation is the involvement of lymph nodes in patients which was not observed in the presented animal study[19]. But as also mouse models for more aggressive B-cell lymphoma, like DLBCL, show mostly tumor growth in the spleen and not in the lymph nodes, the site of disease in patients, it remains unclear whether mice are in general good models to study lymphoma development in lymph nodes. Further, there exist several biological characteristics that are associated with a higher risk of Richter's transformation for CLL patients, such as ZAP70, CD49d, and CD38 overexpression, while at least CD38 oppositely was downregulated in Ibrutinib-resistant $CD5^+CD19^+$ cells in mice[19]. Two molecular drivers suggested to be involved in Richter's transformation are TP53 and CDKN2A. Acquired loss of function mutations in TP53 lead to c-Myc activation which drives aggressive tumor

cell growth. Other genetic characteristic, associated with high-risk Richter's transformation are mutations leading to Richter's transformation are trisomy 12 and Notch mutations [19].
The WES data discussed in the following section will also help to identify such Richter transformation-associated genetic events.

Whole exome sequencing of resistant and sensitive tumors

DNA whole exome sequencing was the method of choice to retrieve a broad and deep view of the genetic mutational landscape in Ibrutinib-resistant TCL-1 AT tumor cells. Analyzing the typical candidate regions for mutations observed in Ibrutinib resistant patients (exon 15 of BTK, and exons 19, 20, and 24 of PLCγ2) by targeted sequencing would have underestimated the clonal complexity of the tumor[298]. Landau *et al*. have reported that patients who received therapy exhibited a greater degree of clonal evolution and that this increased tumor heterogeneity was linked to a poor clinical outcome[387]. Hence, DNA exome sequencing does not only allow for a broad insight into genomic aberrations acquired by the tumor cells, but - based on sequences of immunoglobulin genes - it also permits an estimation of the subclonal structure of the tumor and of the abundance of specific mutations in a given tumor. The above-described finding of the outgrowth of a therapy-driven $CD19^{int}$ leukemic population suggests that a subpopulation of the tumor might have been positively selected by the therapy. Whether this population was present prior to treatment and had an inherited selection advantage or rather developed *de novo* due to acquired mutations is one of the central questions in order to explain the resistance mechanism.
The finding of several expanded B cell clones in the primary and secondary TCL-1 model suggests additional clonal processes and implies the existence of 'several tumors' within one patient. Indeed, there are a few reports on the existence of several immunoglobulin clones in CLL patients. For example, Nakamine and colleagues suggested, that even a different immunoglobulin isotype might not necessarily represent a unique tumor clone by demonstrating a common cytogenetic abnormality (trisomy 12) in both the CLL and DLBCL cells in a patient with Richter's transformation displaying different immunoglobulin isotypes. The authors proposed that these two tumors originated from a single progenitor cell that contained the same genomic abnormality[388].
Indeed, a similar scenario could be possible in the TCL-1 model. The development of leukemia in the primary Eμ-TCL-1 model, which serves as the donor for the adoptive transfer experiments, is based on the transgenic overexpression of the human TCL-1 gene, confined to mature and immature B-cells[220]. Therefore, additional transforming events driving tumorigenesis may happen before V(D)J rearrangement takes place in B cell follicles, resulting in polyclonal V(D)J rearranged BCRs in this model. Hence, this represents an additional difference between the TCL-1 model and the majority of CLL patients.

However, the absence of a selection process for a BCR clone after Ibrutinib treatment remains somewhat puzzling. One explanation could be, that such an Ibrutinib-selected clone would be "hidden" as a minor fraction within a BCR clone and therefor is not obvious. Another possibility could be, that the majority of tumor cells become non-responsive to the treatment and an inherent resistance capacity is attributed to all tumor cells from the TCL-1 model. Such an inherent resistance ability could or example lead to a changed epigenetic program or a metabolic switch resulting in non-responsive cells.

Transcriptional changes as drivers of Ibrutinib resistance

As only low frequency nucleotide variations in BCR pathway genes were detected, they were excluded as cause for the loss of response to Ibrutinib. Therefore, it was hypothesized that the rapid *de novo* resistance development in TCL-1 AT mice after a few weeks of treatment could be in part due to phenotypic adaptations, including compensatory signaling, changes in the kinome, and/or other adaptive responses. Hence, RNA sequencing was chosen in addition to DNA exome sequencing to elucidate a potential compensatory signaling in Ibrutinib resistant leukemia cells.

The gene set enrichment analysis suggested a gene set that was identified in wildtype versus Ezh2 KO T cells, to be enriched in Ibrutinib resistant tumor cells. Ezh2 is part of a methyltransferase complex that has been linked to actin polymerization in different cell types, including polymerization-dependent antigen receptor signaling in T cells[389]. In the context of B cells, EZH2 was suggested to be involved in germinal center formation, immunoglobulin heavy chain rearrangement and DLBCL development[390, 391, 392, 393]. The here presented data show that Ezh2 itself was not deregulated in Ibrutinib resistant tumors. The respective gene set contained interesting molecules that are known to be required for B cell differentiation (Ebf1), progression from G1 to S phase of the cell cycle (Cdc25a), and molecules previously identified to be deregulated in CLL (Ccdc61, Adam10, and Atpif1)[394, 395, 396]. At the time being, the relevance of this gene set and its individual genes further need to be tested and validated.

Performing GO analysis with DEG from in the resistant samples compared to all other groups, revealed several interesting transcripts, including the receptor tyrosine kinase Pim2. A role for PIM2 in the context of CLL was suggested, as it is overexpressed in poor prognosis CLL patients[397]. Interestingly, another PIM kinase family member, PIM1, has been recently linked to an Ibrutinib-resistant ABC DLBCL subtype, where a point mutation was suggested to stabilize PIM1 and result in an enhanced NF-κB signaling[398].

Another upregulated gene in resistant tumor cells was Igf1-r. Notably, recently high IGF1-R expression was linked to worse prognosis in CLL patients that are resistant to a PI3K-δ inhibitor [399]. In a serial adoptive transfer mouse model of CLL, transplanting the TCL1-192 cell line into immunocompromised CB17.SCID mice, overexpression of IGF1-R was identified as a result to the treatment-induced selection pressure resulting from continuous PI3K-δ inhibitor treatment[400].

Conclusions and Outlook

In brief, the results of this study are currently at a stage where validation of the identified differentially expressed molecules and pathways has to follow. Subsequent studies will focus on the characterization of mechanisms that are potentially involved in resistance development to Ibrutinib in the TCL-1 AT model. Treatment regimens, co-targeting these phenotypic adaptations in the resistant cells may induce broader, deeper, and more durable responses in CLL patients. This is of high relevance as successful therapies for relapsed, refractory, and treatment resistant cases are still lacking and an urgent clinical need in CLL. The observed resistance to Ibrutinib in the TCL-1 AT model for CLL may help to investigate and to target therapy-induced cancer evolution, that is a branched evolutionary process and the reason why many treatments ultimately fail.

APPENDIX

Sample name	Treatment condition	Cell population	Sort panel	Sort Purity	RIN
H1_A	Wildtype/Vehicle	Ly6C^{hi} monocytes	DAPI^{-}Lin^{-} (CD19^{-} CD3^{-}NK.1.1^{-} TER119^{-}) CD11b^{+}CD11c$^{low-int}$MHCII^{-} F4/80^{int}Ly6C^{hi}	n.a.	5.7
H2_A	Wildtype/Vehicle			n.a.	7.20
H3_A	Wildtype/Vehicle			n.a.	7.9
V1_A	Leukemic/Vehicle			93.3	5.2
V2_A	Leukemic/Vehicle			92.1	7.1
V4_A	Leukemic/Vehicle			81.4	5.3
I1_A	Ibrutinib			98	7.9
I3_A	Ibrutinib			84.6	6.00
I4_A	Ibrutinib			93	6.80
H1_B	Wildtype/Vehicle	Ly6C^{low} monocytes	DAPI^{-}Lin^{-} CD11b^{+}CD11c$^{low-int}$MHCII^{-} F4/80^{int}Ly6C^{low}	n.a.	7.6
H2_B	Wildtype/Vehicle			n.a.	7.4
H3_B	Wildtype/Vehicle			n.a.	8.1
V1_B	Leukemic/Vehicle			95.7	6
V2_B	Leukemic/Vehicle			96.8	6.6
V4_B	Leukemic/Vehicle			93.3	6,7
I1_B	Ibrutinib			97.7	7.6
I3_B	Ibrutinib			93.3	7.1
I4_B	Ibrutinib			90.1	8.3
H1_C	Wildtype/Vehicle	conventional DCs	DAPI-Lin-CD11c^{high}MHCII^{+}	n.a.	7.70
H2_C	Wildtype/Vehicle			n.a.	7.70
H3_C	Wildtype/Vehicle			n.a.	8.30
V1_C	Ibrutinib			97.4	6.90
V2_C	Ibrutinib			98	7.30
V4_C	Ibrutinib			93.4	6.7
I1_C	Leukemic/Vehicle			93.5	8.60
I3_C	Leukemic/Vehicle			92.1	7.00
I4_C	Leukemic/Vehicle			97.7	7.60

Appendix Table 1: Information on samples of cDCs, Ly6C^{hi}, and Ly6C^{low} monocytes used for gene expression profiling.
Sample name, treatment condition, sorted cell population, sort panel, sort purity, and RIN (RNA integrity number) after RNA isolation are provided. Wildtype animals were treated with vehicle drinking water as well, for better comparison to vehicle control-treated and Ibrutinib-treated animals.

Sample name	Treatment condition	Sort Purity	RIN	DIN
V2_er	week 1 post treatment start with vehicle	99.1	9.9	9.1
V5_er		99.4	9.7	9.3
V6_er		98.7	9.8	9.2
V8_er		98.9	9.8	8.7
I3_er	week 1 post treatment start with Ibrutinib	96.9	9.4	9.1
I5_er		98.4	10.0	7.9
I10_er		97.3	9.6	8.7
I11_er		97.7	9.5	9.1
V3_la	week 3 post treatment start with vehicle	98.6	9.8	9.1
V7_la		98.3	10.0	9
V9_la		98.8	9.9	8.9
V11_la		98.9	9.4	9.2
I2_la	week 6 post treatment start with Ibrutinib	99	9.4	8.7
I6_la		98.3	9.6	9.5
I9_la		99	9.7	9.2

Appendix Table 2: RNA and DNA sequencing of Ibrutinib sensitive and resistant tumor cells.
Leukemic $CD5^+CD19^+$ were sorted by flow cytometry ($DAPI^-CD45^+CD5^+CD19^+$) from freshly isolated splenocytes. Sort purities were assessed before flash freezing cell pellets in appropriate amounts of RLT buffer. RNA and DNA were isolated and submitted for mRNA (library preparation: 'total RNA', 125 base paired-end; 5 samples/lane on HiSeq2000) and DNA Exome (library preparation: 'low input exome-seq mouse', 100 base paired-end; 3 samples/lane in Hiseq4000) sequencing to the DKFZ Genomics and Proteomics Core Facility Unit.

	$Ly6C^{hi}$		**$Ly6C^{low}$**		**cDCs**	
	WT	**TCL-1 AT**	**WT**	**TCL-1 AT**	**WT**	**TCL-1 AT**
CSF-1	6.1	6	6.2	5.9	6	5.5
CSF-1R	11.8	11.8	12.2	12.2	9.4	8.1

Appendix Table 3: Detailed GEP data of selected molecules of cDCs, $Ly6C^{hi}$, and $Ly6C^{low}$ monocytes used for gene expression profiling.
Normalized array signal intensity of CSF-1 and CSF-1R, averaged from each three samples per condition from GEP of myeloid cells.

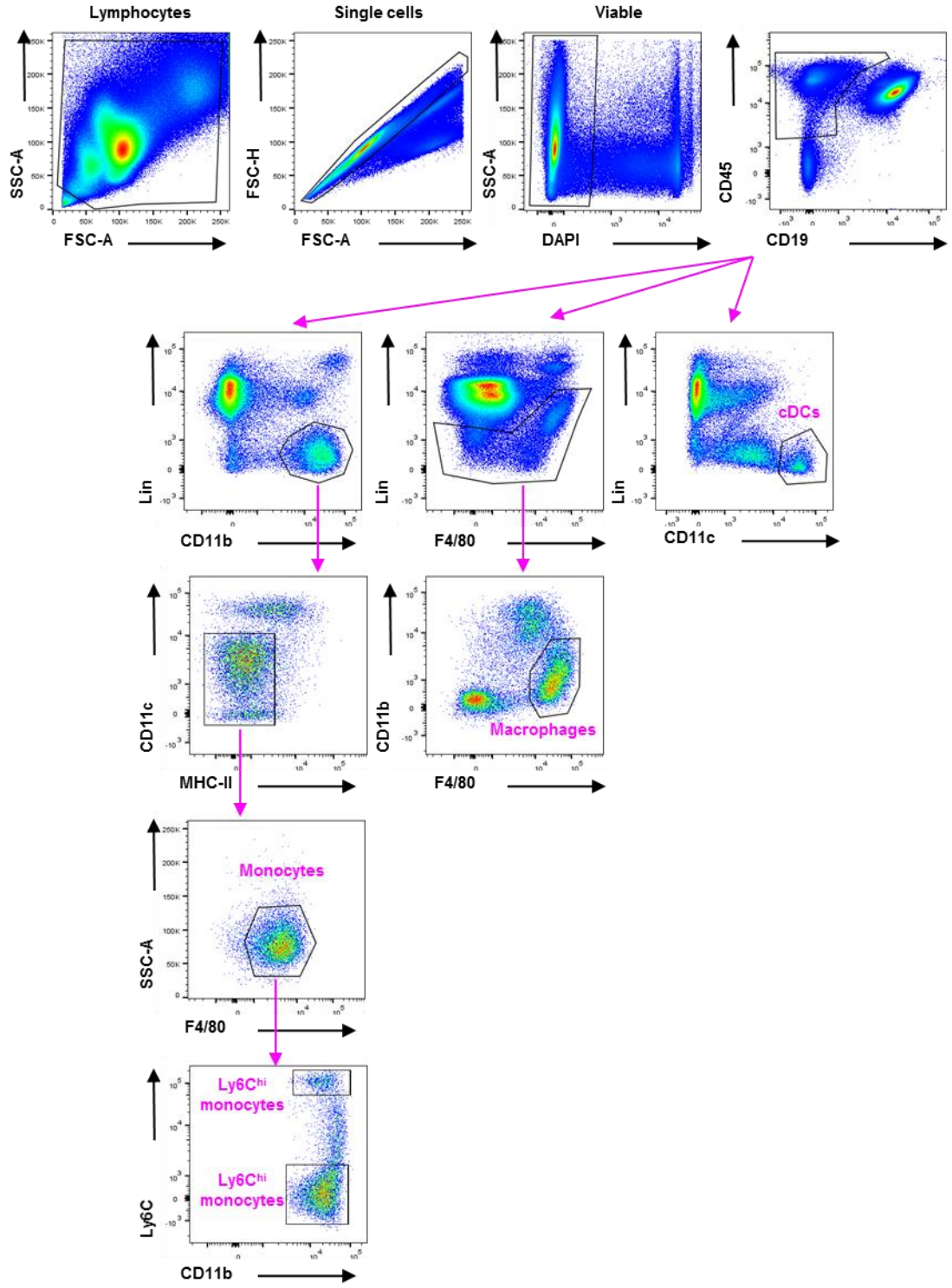

Appendix Figure 1: Gating scheme, exemplified for splenic Ly6C^{hi} and Ly6C^{low} monocytes, macrophages, and cDCs.

After exclusion of duplets viable cells were gated as follows: monocytes: DAPI$^-$CD45$^+$CD19$^-$Lin$^-$(CD3$^-$Ly6G$^-$NK1.1$^-$TER119$^-$)CD11b$^+$CD11c$^{low\text{-}int}$MHC-II^{low}F4/80^{int}; Ly6C^{high} monocytes: DAPI$^-$CD45$^+$CD19$^-$Lin$^-$CD11b$^+$CD11c$^{low\text{-}int}$MHC-II^{low}F4/80^{int}Ly6C^{high}; Ly6C^{low} monocytes: DAPI$^-$CD45$^+$CD19$^-$Lin$^-$CD11b$^+$CD11c$^{low\text{-}int}$MHC-II^{low}F4/80^{int}Ly6C^{low}. Either CD11b (as here) or CD43 (as in Figure 9d) was used for final gating on Ly6C^{high} and Ly6C^{low} monocytes); macrophages: DAPI$^-$CD45$^+$CD19$^-$Lin$^-$CD11b^{low}F4/80^{high}; cDCs: DAPI$^-$CD45$^+$CD19$^-$Lin$^-$CD11c^{high}.

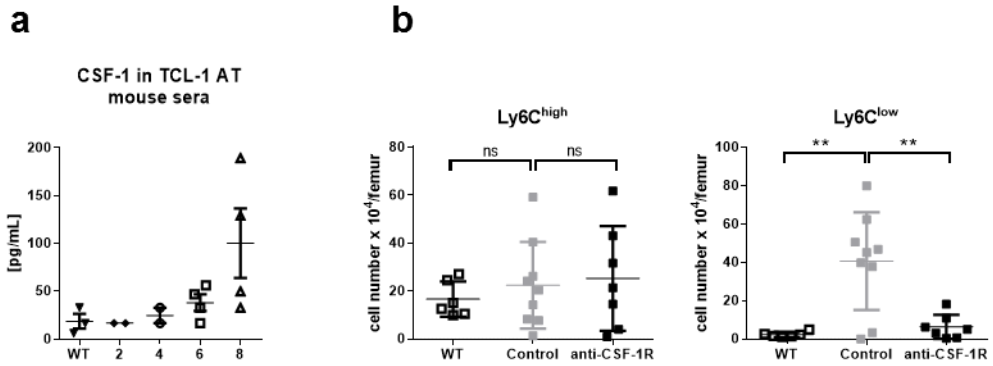

Appendix Figure 2: CSF-1 level in TCL-1 AT mice over time and monocyte subsets in BM of CSF-1 KI AT mice
(a) CSF-1 was measured in sera from mice adoptively transferred i.v. with $1.8x10^6$ leukemic splenocytes and sacrificed at week 2 (n=2), week 4 (n=2), week 6 (n=4), and week 8 (n=4) post transplantation and untransplated WT mice (n=4) at week 8 by Luminex bead array. **(b)** Absolute numbers of Ly6C^{high} monocytes (left) and Ly6C^{low} monocytes (right) gated from CSF-1R-expressing cells in the bone marrow (BM) as measured by flow cytometry. CSF-1R KI mice were adoptively transferred i.v. with $2x10^6$ splenocytes, pooled from four leukemic donor mice. Mice were treated with control antibody (Synagis) or TG3003 at 3mg/kg/week via i.p. injections starting at day 1 post-transplantation. Untransplated CSF-1R KI wildtype (WT) mice (n=6) served as healthy control group. Analyses were performed for animals that showed >50% of CD5$^+$CD19$^+$ cells in the spleen and clear signs of splenomegaly (control cohort: n=9, anti-CSF-1R cohort: n=7). (BM Ly6C^{high} monocytes: DAPI$^-$Lin$^-$CSF-1R$^+$Ly6C$^+$; BM Ly6C^{low} monocytes: DAPI$^-$Lin$^-$CSF-1R$^+$Ly6C$^-$) *P* values were determined by unpaired Student t-test.

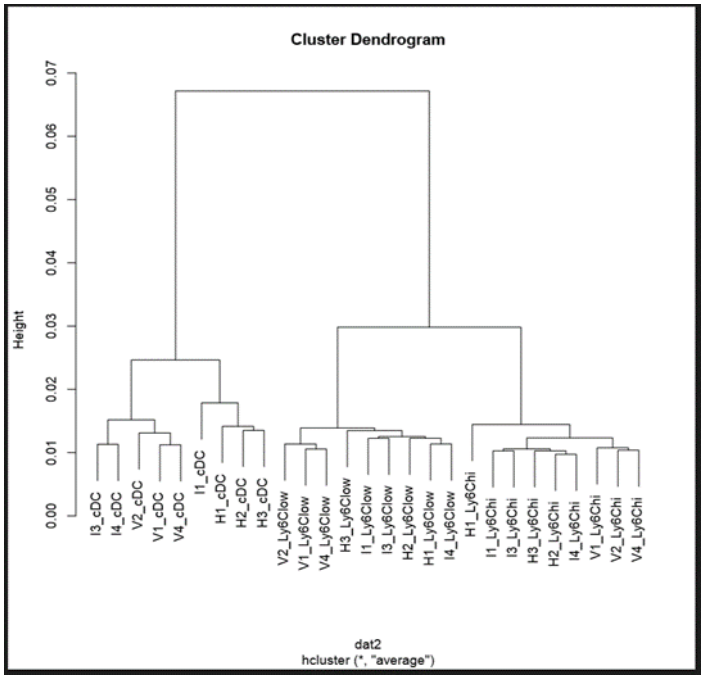

Appendix Figure 3: Cluster dendrogram of gene expression profiled Ly6C^{hi} and Ly6C^{low} monocytes and cDCs.
Cluster dendrogram of profiled WT, TCL-1 AT and Ibrutinib-treated samples showing that cDCs (left), Ly6C^{hi} (middle) and Ly6C^{low} monocytes (right) cluster independently. Within all three cell populations, samples from TCL-1 AT mice (V=vehicle) cluster closely together. Samples from WT animals (H=healthy;WT) and Ibrutinib-treated leukemic mice (I=Ibrutinib) cluster together.

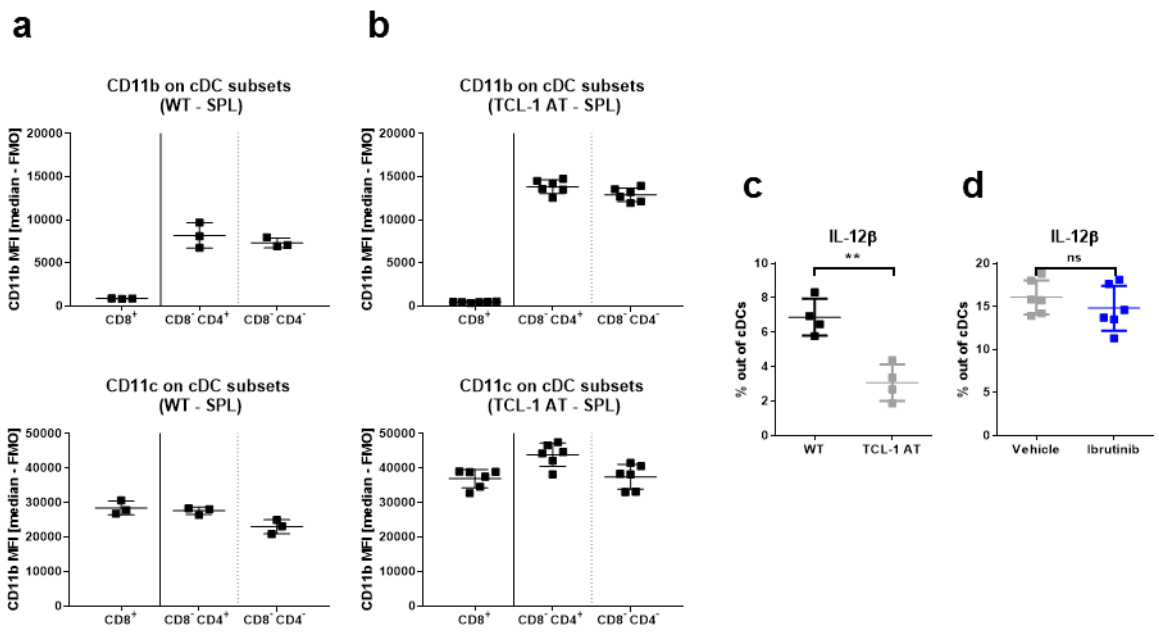

Appendix Figure 4: cDC subset composition in TCL-1 AT and WT mice and IL-12β production by cDCs. **(a,b)** CD11b (top) and CD11c (bottom) expression on $CD8^+$ cDCs, $CD8^-CD4^+$ cDCs, and $CD8^-CD4^-$ cDCs out of total cDCs from non-leukemic WT mice (n=3) (a) and TCL-1 AT mice (n=6) (right). ($CD8^+$ cDCs: Viability dye $(VD)^-LIN^-(CD19^-CD3^-Ly6G^-NK1.1^-TER119^-)CD11c^{high}MHC^-II^+CD8^+$; $CD8^-CD4^+$ cDCs: VD-LIN-$CD11c^{high}$MHC-$II^+CD8^-CD4^+$; CD8-CD4- cDCs: VD-LIN-$CD11c^{high}$MHC-II+CD8-CD4+; cDCs: VD^-CD19^- $CD11c^{high}MHC\text{-}II^+$) **(c,d)** Percentage of IL-12β producing cDCs assessed by intracellular flow cytometry after 6 hours of LPS stimulation of isolated splenocytes. Two independent experiments are shown here: **(c)** Comparison of healthy wildtype (WT) (n=4) and leukemic TCL-1 AT (n=4) mice; **(d)** Comparison of leukemic TCL-1 AT mice treated with vehicle (n=6) or Ibrutinib (n=4) for 3.5 weeks. Treatment start was at ~5% tumor load in the blood. (cDCs: Viability dye $(VD)^-$ $CD19^-$ $CD11c^{high}MHC\text{-}II^+$) *P* values were determined by unpaired Student t-test.

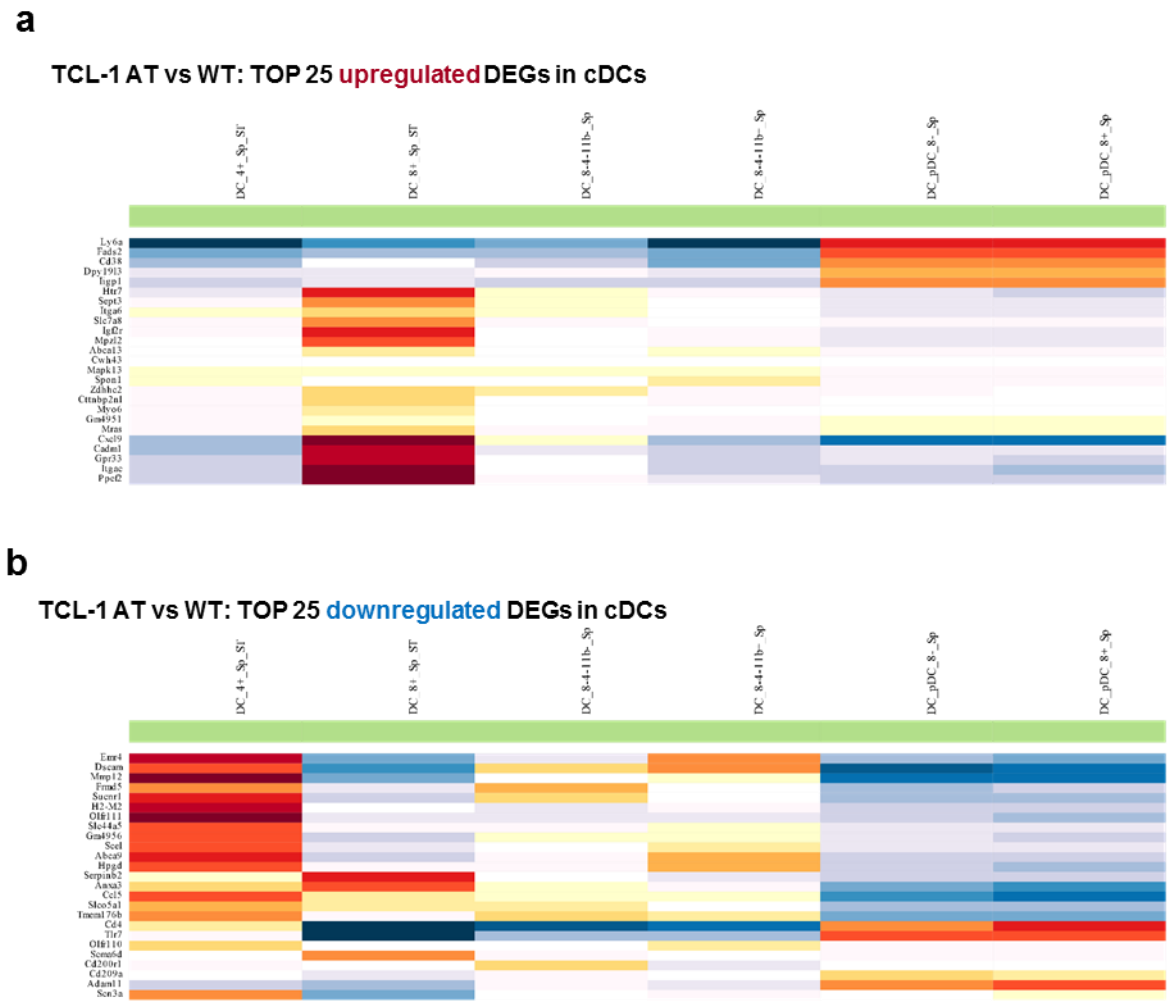

Appendix Figure 5: Heatmap of top DEGs from TCL-1 AT vs WT mice in comparison to publically available datasets.

Heatmap of 25 upregulated and 25 downregulated genes (TCL-1 AT (n=3) versus WT (n=3)) in comparison to six available splenic dendritic cell gene expression signatures (Immgen data base, v1 datasets)[318] which include: $CD4^+$ DCs, $CD8^+$ DCs, $CD8^-CD4^-CD11b^-$, $CD8^-CD4^-CD11b^+$, $CD8^-$ pDCs, and $CD8^+$ pDCs. **(a)** Top 25 upregulated DEGs show greatest overlap with expression of respective genes in splenic $CD8^+$ DCs ('DC 8+_ST'). **(b)** Top 25 downregulated DEGs show least overlap with expression of respective genes in splenic $CD4^+$ DCs ('DC 4+_ST'). (DEG=differentially expressed genes)

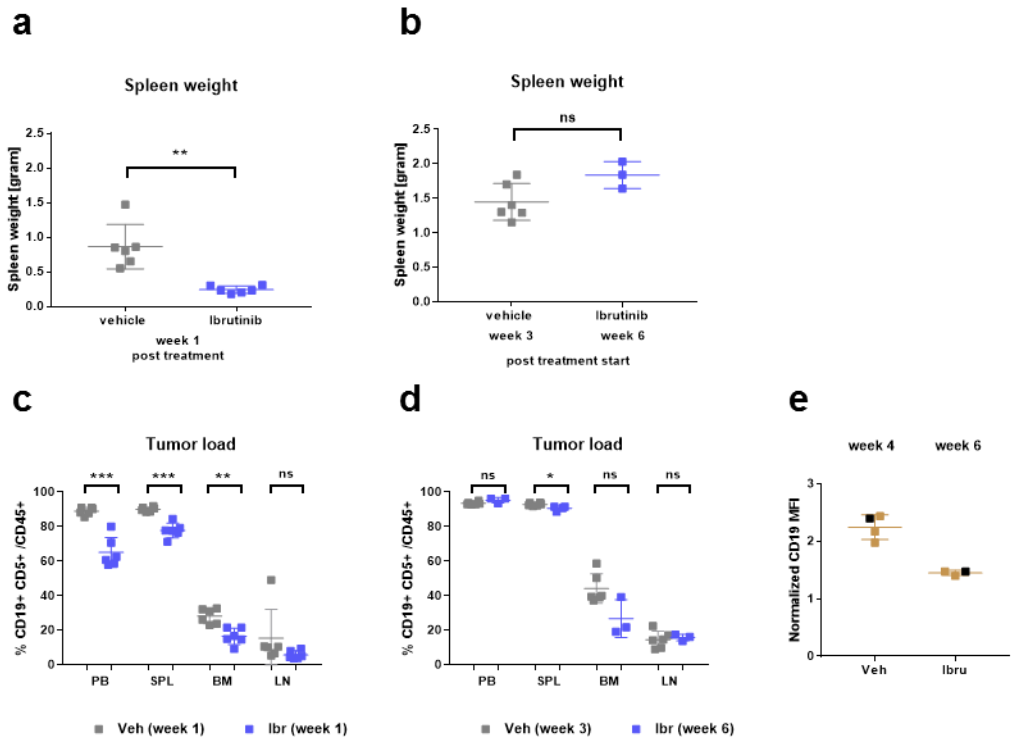

Appendix Figure 6: Spleen weight and tumor load in lymphoid organs in Ibrutinib- and vehicle-treated mice. **(a-d)** Spleen weight (a,b) and percentages of $CD5^+CD19^+$ cells in peripheral blood (PB), spleen (SPL), bone marrow (BM), and inguinal lymph nodes (LN) (c,d) of mice, adoptively transferred with clone 1J4 splenocytes and treated with vehicle (n=6) or Ibrutinib (n=6) for one week (left), and vehicle for three weeks (n=6) or Ibrutinib for six weeks (n=3) (left). **(e)** CD19 MFI values of leukemic $CD19^+CD5^+$ cells were normalized to respective values of $CD19^+CD5^-$ normal B cells (median CD19 MFI on $CD19^+CD5^+$ cells / median CD19 MFI on $CD19^+$CD5- cells) in spleen of mice transplanted with tumors and treated with vehicle or Ibrutinib. Animals were sacrificed at week 4 and week 6 post treatment start to achieve comparable tumor loads for re-injection. Black data points represent values from those tumor samples that were re-injected for the purpose of 2nd treatment round. *P* values were determined by unpaired Student t-test.

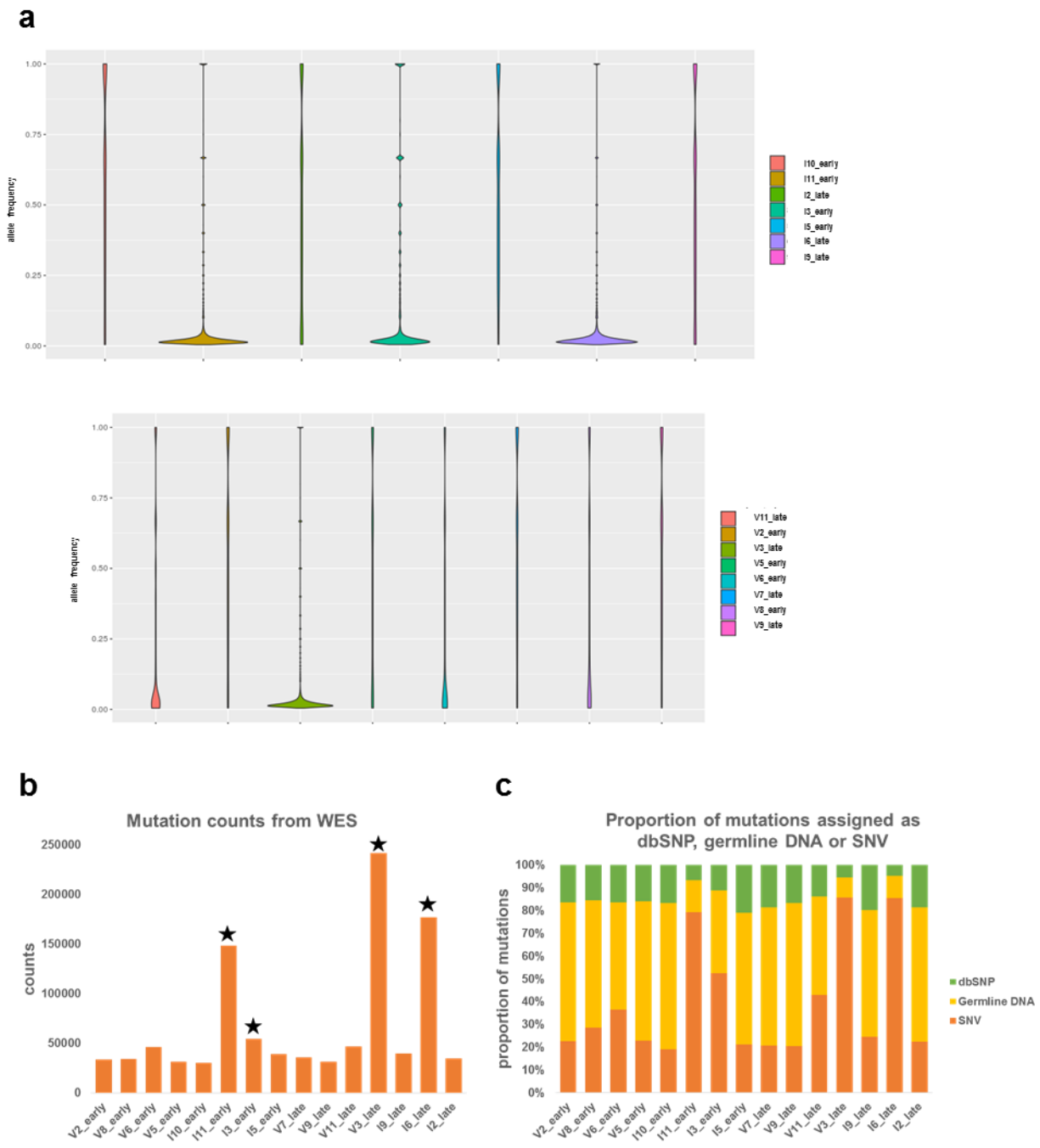

Appendix Figure 7: Characterization of mutational variants from WES.
(a) Mutation allele frequencies **(b)** counts and **(c)** proportions of SNVs, germline DNA, and dbSNPs of Ibrutinib-resistant and sensitive samples. Data analysis was performed by Yashna Paul.

LITERATURE

1. Hanahan, D. & Weinberg, R.A. Hallmarks of cancer: the next generation. *Cell* 144, 646-674 (2011).

2. Mittal, D., Gubin, M.M., Schreiber, R.D. & Smyth, M.J. New insights into cancer immunoediting and its three component phases--elimination, equilibrium and escape. *Curr Opin Immunol* 27, 16-25 (2014).

3. Buckley, C.D., Gilroy, D.W., Serhan, C.N., Stockinger, B. & Tak, P.P. The resolution of inflammation. *Nature reviews. Immunology* 13, 59-66 (2013).

4. Crusz, S.M. & Balkwill, F.R. Inflammation and cancer: advances and new agents. *Nat Rev Clin Oncol* 12, 584-596 (2015).

5. Kuper, H., Adami, H.O. & Trichopoulos, D. Infections as a major preventable cause of human cancer. *Journal of internal medicine* 248, 171-183 (2000).

6. Niwa, T. *et al.* Inflammatory processes triggered by Helicobacter pylori infection cause aberrant DNA methylation in gastric epithelial cells. *Cancer research* 70, 1430-1440 (2010).

7. Venerito, M., Vasapolli, R., Rokkas, T., Delchier, J.C. & Malfertheiner, P. Helicobacter pylori, gastric cancer and other gastrointestinal malignancies. *Helicobacter* 22 Suppl 1 (2017).

8. Guerra, C. *et al.* Chronic pancreatitis is essential for induction of pancreatic ductal adenocarcinoma by K-Ras oncogenes in adult mice. *Cancer cell* 11, 291-302 (2007).

9. Dunn, G.P., Bruce, A.T., Ikeda, H., Old, L.J. & Schreiber, R.D. Cancer immunoediting: from immunosurveillance to tumor escape. *Nature immunology* 3, 991-998 (2002).

10. Dunn, G.P., Old, L.J. & Schreiber, R.D. The three Es of cancer immunoediting. *Annu Rev Immunol* 22, 329-360 (2004).

11. Rozovski, U., Keating, M.J. & Estrov, Z. Targeting inflammatory pathways in chronic lymphocytic leukemia. *Crit Rev Oncol Hematol* 88, 655-666 (2013).

12. (NIH), N.C.I. Cancer Stat Facts: Chronic Lymphocytic Leukemia (CLL). *https://seer.cancer.gov/statfacts/html/clyl.html* (2017).

13. Ahmed, S., Siddiqui, A.K., Rossoff, L., Sison, C.P. & Rai, K.R. Pulmonary complications in chronic lymphocytic leukemia. *Cancer* 98, 1912-1917 (2003).

14. Hallek, M. Chronic lymphocytic leukemia: 2017 update on diagnosis, risk stratification, and treatment. *Am J Hematol* 92, 946-965 (2017).

15. Hallek, M. *et al.* Guidelines for the diagnosis and treatment of chronic lymphocytic leukemia: a report from the International Workshop on Chronic Lymphocytic Leukemia updating the National Cancer Institute-Working Group 1996 guidelines. *Blood* 111, 5446-5456 (2008).

16. Kenneth Murphy, C.W. Janeway's Immunobiology *Taylor & Francis Group* 9, 904 (2016).

17. Kipps, T.J. *et al.* Chronic lymphocytic leukaemia. *Nat Rev Dis Primers* 3, 17008 (2017).

18. Rawstron, A.C. *et al.* Monoclonal B-cell lymphocytosis and chronic lymphocytic leukemia. *The New England journal of medicine* 359, 575-583 (2008).

19. Parikh, S.A., Kay, N.E. & Shanafelt, T.D. How we treat Richter syndrome. *Blood* 123, 1647-1657 (2014).

20. Rai, K.R. *et al.* Clinical staging of chronic lymphocytic leukemia. *Blood* 46, 219-234 (1975).

21. Binet, J.L. *et al.* A new prognostic classification of chronic lymphocytic leukemia derived from a multivariate survival analysis. *Cancer* 48, 198-206 (1981).

22. Zengin, N. *et al.* Comparison of Rai and Binet Classifications in Chronic Lymphocytic Leukemia. *Hematology* 2, 125-129 (1997).

23. Kikushige, Y. *et al.* Self-renewing hematopoietic stem cell is the primary target in pathogenesis of human chronic lymphocytic leukemia. *Cancer cell* 20, 246-259 (2011).

24. Damm, F. *et al.* Acquired initiating mutations in early hematopoietic cells of CLL patients. *Cancer discovery* 4, 1088-1101 (2014).

25. Caligaris-Cappio, F. B-chronic lymphocytic leukemia: a malignancy of anti-self B cells. *Blood* 87, 2615-2620 (1996).

26. Caligaris-Cappio, F., Gobbi, M., Bofill, M. & Janossy, G. Infrequent normal B lymphocytes express features of B-chronic lymphocytic leukemia. *The Journal of experimental medicine* 155, 623-628 (1982).

27. Dorshkind, K. & Montecino-Rodriguez, E. Fetal B-cell lymphopoiesis and the emergence of B-1-cell potential. *Nature reviews. Immunology* 7, 213-219 (2007).

28. Hamblin, T.J., Davis, Z., Gardiner, A., Oscier, D.G. & Stevenson, F.K. Unmutated Ig V(H) genes are associated with a more aggressive form of chronic lymphocytic leukemia. *Blood* 94, 1848-1854 (1999).

29. Seifert, M. *et al.* Cellular origin and pathophysiology of chronic lymphocytic leukemia. *The Journal of experimental medicine* 209, 2183-2198 (2012).

30. Seifert, M., Scholtysik, R. & Küppers, R. Origin and pathogenesis of B cell lymphomas. *Methods in molecular biology (Clifton, N.J.)* 971, 1-25 (2013).

31. Chu, C.C. *et al.* Many chronic lymphocytic leukemia antibodies recognize apoptotic cells with exposed nonmuscle myosin heavy chain IIA: implications for patient outcome and cell of origin. *Blood* 115, 3907-3915 (2010).

32. Agathangelidis, A. *et al.* Stereotyped B-cell receptors in one-third of chronic lymphocytic leukemia: a molecular classification with implications for targeted therapies. *Blood* 119, 4467-4475 (2012).

33. Hayakawa, K. *et al.* Early generated B1 B cells with restricted BCRs become chronic lymphocytic leukemia with continued c-Myc and low Bmf expression. *The Journal of experimental medicine* 213, 3007-3024 (2016).

34. Nilsson, J.A. & Cleveland, J.L. Myc pathways provoking cell suicide and cancer. *Oncogene* 22, 9007-9021 (2003).

35. Pinon, J.D., Labi, V., Egle, A. & Villunger, A. Bim and Bmf in tissue homeostasis and malignant disease. *Oncogene* 27 Suppl 1, S41-52 (2008).

36. Oakes, C.C. *et al.* DNA methylation dynamics during B cell maturation underlie a continuum of disease phenotypes in chronic lymphocytic leukemia. *Nat Genet* 48, 253-264 (2016).

37. Fabbri, G. & Dalla-Favera, R. The molecular pathogenesis of chronic lymphocytic leukaemia. *Nature reviews. Cancer* 16, 145-162 (2016).

38. Dohner, H. *et al.* Genomic aberrations and survival in chronic lymphocytic leukemia. *The New England journal of medicine* 343, 1910-1916 (2000).

39. Klein, U. *et al.* The DLEU2/miR-15a/16-1 cluster controls B cell proliferation and its deletion leads to chronic lymphocytic leukemia. *Cancer cell* 17, 28-40 (2010).

40. Cimmino, A. *et al.* miR-15 and miR-16 induce apoptosis by targeting BCL2. *Proc Natl Acad Sci U S A.* 102, 13944-13949 (2005).

41. Dohner, H. *et al.* p53 gene deletion predicts for poor survival and non-response to therapy with purine analogs in chronic B-cell leukemias. *Blood* 85, 1580-1589 (1995).

42. Stankovic, T. *et al.* Inactivation of ataxia telangiectasia mutated gene in B-cell chronic lymphocytic leukaemia. *Lancet* 353, 26-29 (1999).

43. Schaffner, C., Stilgenbauer, S., Rappold, G.A., Dohner, H. & Lichter, P. Somatic ATM mutations indicate a pathogenic role of ATM in B-cell chronic lymphocytic leukemia. *Blood* 94, 748-753 (1999).

44. Skowronska, A. *et al.* Biallelic ATM inactivation significantly reduces survival in patients treated on the United Kingdom Leukemia Research Fund Chronic Lymphocytic Leukemia 4 trial. *J Clin Oncol* 30, 4524-4532 (2012).

45. Parker, H. & Strefford, J.C. The mutational signature of chronic lymphocytic leukemia. *Biochem J* 473, 3725-3740 (2016).

46. Schuh, A. *et al.* Monitoring chronic lymphocytic leukemia progression by whole genome sequencing reveals heterogeneous clonal evolution patterns. *Blood* 120, 4191-4196 (2012).

47. Landau, D.A. *et al.* Mutations driving CLL and their evolution in progression and relapse. *Nature* 526, 525-530 (2015).

48. Kulis, M. *et al.* Epigenomic analysis detects widespread gene-body DNA hypomethylation in chronic lymphocytic leukemia. *Nat Genet* 44, 1236-1242 (2012).

49. Cahill, N. *et al.* 450K-array analysis of chronic lymphocytic leukemia cells reveals global DNA methylation to be relatively stable over time and similar in resting and proliferative compartments. *Leukemia* 27, 150-158 (2013).

50. Landau, D.A. *et al.* Locally disordered methylation forms the basis of intratumor methylome variation in chronic lymphocytic leukemia. *Cancer cell* 26, 813-825 (2014).

51. Oakes, C.C. *et al.* Evolution of DNA methylation is linked to genetic aberrations in chronic lymphocytic leukemia. *Cancer discovery* 4, 348-361 (2014).

52. Young, R.M. & Staudt, L.M. Targeting pathological B cell receptor signalling in lymphoid malignancies. *Nat Rev Drug Discov* 12, 229-243 (2013).

53. Reth, M. Antigen receptor tail clue. *Nature* 338, 383-384 (1989).

54. Saijo, K. *et al.* Essential role of Src-family protein tyrosine kinases in NF-kappaB activation during B cell development. *Nature immunology* 4, 274-279 (2003).

55. Rowley, R.B., Burkhardt, A.L., Chao, H.G., Matsueda, G.R. & Bolen, J.B. Syk protein-tyrosine kinase is regulated by tyrosine-phosphorylated Ig alpha/Ig beta immunoreceptor tyrosine activation motif binding and autophosphorylation. *J Biol Chem* 270, 11590-11594 (1995).

56. Oellerich, T. *et al.* The B-cell antigen receptor signals through a preformed transducer module of SLP65 and CIN85. *Embo j* 30, 3620-3634 (2011).

57. Shinohara, H. *et al.* PKC beta regulates BCR-mediated IKK activation by facilitating the interaction between TAK1 and CARMA1. *The Journal of experimental medicine* 202, 1423-1431 (2005).

58. Hendriks, R.W., Yuvaraj, S. & Kil, L.P. Targeting Bruton's tyrosine kinase in B cell malignancies. *Nature reviews. Cancer* 14, 219-232 (2014).

59. Deane, J.A. & Fruman, D.A. Phosphoinositide 3-kinase: diverse roles in immune cell activation. *Annu Rev Immunol* 22, 563-598 (2004).

60. Dal Porto, J.M. *et al.* B cell antigen receptor signaling 101. *Molecular immunology* 41, 599-613 (2004).

61. Fais, F. *et al.* Chronic lymphocytic leukemia B cells express restricted sets of mutated and unmutated antigen receptors. *J Clin Invest* 102, 1515-1525 (1998).

62. Herishanu, Y. The lymph node microenvironment promotes B-cell receptor signaling, NF-kB activation, and tumor proliferation in chronic lymphocytic leukemia. *Blood* 117 (2011).

63. Mockridge, C.I. *et al.* Reversible anergy of sIgM-mediated signaling in the two subsets of CLL defined by VH-gene mutational status. *Blood* 109, 4424-4431 (2007).

64. Minden, M.D.-v. *et al.* Chronic lymphocytic leukaemia is driven by antigen-independent cell-autonomous signalling. *Nature* 489, 309-312 (2012).

65. Yarkoni, Y., Getahun, A. & Cambier, J.C. Molecular underpinning of B-cell anergy. *Immunol Rev* 237, 249-263 (2010).

66. O'Neill, S.K. *et al.* Monophosphorylation of CD79a and CD79b ITAM motifs initiates a SHIP-1 phosphatase-mediated inhibitory signaling cascade required for B cell anergy. *Immunity* 35, 746-756 (2011).

67. Getahun, A., Beavers, N.A., Larson, S.R., Shlomchik, M.J. & Cambier, J.C. Continuous inhibitory signaling by both SHP-1 and SHIP-1 pathways is required to maintain unresponsiveness of anergic B cells. *The Journal of experimental medicine* 213, 751-769 (2016).

68. Packham, G. *et al.* The outcome of B-cell receptor signaling in chronic lymphocytic leukemia: proliferation or anergy. *Haematologica* 99, 1138-1148 (2014).

69. Cambier, J.C., Gauld, S.B., Merrell, K.T. & Vilen, B.J. B-cell anergy: from transgenic models to naturally occurring anergic B cells? *Nature Reviews Immunology* 7, 633-643 (2007).

70. Rosenwald, A. *et al.* Relation of gene expression phenotype to immunoglobulin mutation genotype in B cell chronic lymphocytic leukemia. *The Journal of experimental medicine* 194, 1639-1647 (2001).

71. Chen, L. *et al.* Expression of ZAP-70 is associated with increased B-cell receptor signaling in chronic lymphocytic leukemia. *Blood* 100, 4609-4614 (2002).

72. Herman, S.E. *et al.* Bruton tyrosine kinase represents a promising therapeutic target for treatment of chronic lymphocytic leukemia and is effectively targeted by PCI-32765. *Blood* 117, 6287-6296 (2011).

73. Park, H. *et al.* Regulation of Btk function by a major autophosphorylation site within the SH3 domain. *Immunity* 4, 515-525 (1996).

74. Rawlings, D.J. *et al.* Activation of BTK by a phosphorylation mechanism initiated by SRC family kinases. *Science* 271, 822-825 (1996).

75. Kim, Y.J., Sekiya, F., Poulin, B., Bae, Y.S. & Rhee, S.G. Mechanism of B-cell receptor-induced phosphorylation and activation of phospholipase C-gamma2. *Molecular and cellular biology* 24, 9986-9999 (2004).

76. Bajpai, U.D., Zhang, K., Teutsch, M., Sen, R. & Wortis, H.H. Bruton's tyrosine kinase links the B cell receptor to nuclear factor kappaB activation. *The Journal of experimental medicine* 191, 1735-1744 (2000).

77. Petro, J.B., Rahman, S.M., Ballard, D.W. & Khan, W.N. Bruton's tyrosine kinase is required for activation of IkappaB kinase and nuclear factor kappaB in response to B cell receptor engagement. *The Journal of experimental medicine* 191, 1745-1754 (2000).

78. Burger, J.A. *et al.* Blood-derived nurse-like cells protect chronic lymphocytic leukemia B cells from spontaneous apoptosis through stromal cell–derived factor-1. *Blood* 96, 2655-2663 (2000).

79. Schulz, A. *et al.* Inflammatory cytokines and signaling pathways are associated with survival of primary chronic lymphocytic leukemia cells in vitro: a dominant role of CCL2. *Haematologica* 96, 408-416 (2011).

80. Seiffert, M. *et al.* Soluble CD14 is a novel monocyte-derived survival factor for chronic lymphocytic leukemia cells, which is induced by CLL cells in vitro and present at abnormally high levels in vivo. *Blood* 116, 4223-4230 (2010).

81. Kurtova, A.V. *et al.* Diverse marrow stromal cells protect CLL cells from spontaneous and drug-induced apoptosis: development of a reliable and reproducible system to assess stromal cell adhesion-mediated drug resistance. *Blood* 114, 4441-4450 (2009).

82. Panayiotidis, P., Jones, D., Ganeshaguru, K., Foroni, L. & Hoffbrand, A.V. Human bone marrow stromal cells prevent apoptosis and support the survival of chronic lymphocytic leukaemia cells in vitro. *British Journal of Haematology* 92, 97-103 (1996).

83. Schmid, C. & Isaacson, P.G. Proliferation centres in B-cell malignant lymphoma, lymphocytic (B-CLL): an immunophenotypic study. *Histopathology* 24, 445-451 (1994).

84. Lampert, I.A., Wotherspoon, A., Van Noorden, S. & Hasserjian, R.P. High expression of CD23 in the proliferation centers of chronic lymphocytic leukemia in lymph nodes and spleen. *Hum Pathol* 30, 648-654 (1999).

85. Wolowiec, D. *et al.* Bone marrow angiogenesis and proliferation in B-cell chronic lymphocytic leukemia. *Analytical and quantitative cytology and histology* 26, 263-270 (2004).

86. Deaglio, S. *et al.* CD38 and ZAP-70 are functionally linked and mark CLL cells with high migratory potential. *Blood* 110, 4012-4021 (2007).

87. Stamatopoulos, B. *et al.* Gene expression profiling reveals differences in microenvironment interaction between patients with chronic lymphocytic leukemia expressing high versus low ZAP70 mRNA. *Haematologica* 94, 790-799 (2009).

88. Burger, J.A., Ghia, P., Rosenwald, A. & Caligaris-Cappio, F. *The microenvironment in mature B-cell malignancies: a target for new treatment strategies*, vol. 114, 2009.

89. Ten Hacken, E. & Burger, J.A. Microenvironment interactions and B-cell receptor signaling in Chronic Lymphocytic Leukemia: Implications for disease pathogenesis and treatment. *Biochimica et biophysica acta* 1863, 401-413 (2016).

90. Burger, J.A. Nurture versus nature: the microenvironment in chronic lymphocytic leukemia. *Hematology Am Soc Hematol Educ Program* 2011, 96-103 (2011).

91. Haderk, F. *et al.* Tumor-derived exosomes modulate PD-L1 expression in monocytes. *Sci Immunol* 2 (2017).

92. Mohle, R., Failenschmid, C., Bautz, F. & Kanz, L. Overexpression of the chemokine receptor CXCR4 in B cell chronic lymphocytic leukemia is associated with increased functional response to stromal cell-derived factor-1 (SDF-1). *Leukemia* 13, 1954-1959 (1999).

93. Burger, J.A., Burger, M. & Kipps, T.J. Chronic Lymphocytic Leukemia B Cells Express Functional CXCR4 Chemokine Receptors That Mediate Spontaneous Migration Beneath Bone Marrow Stromal Cells. *Blood* 94, 3658-3667 (1999).

94. Burger, J.A., Zvaifler, N.J., Tsukada, N., Firestein, G.S. & Kipps, T.J. Fibroblast-like synoviocytes support B-cell pseudoemperipolesis via a stromal cell-derived factor-1- and CD106 (VCAM-1)-dependent mechanism. *J Clin Invest* 107, 305-315 (2001).

95. Zhang, W. *et al.* Stromal control of cystine metabolism promotes cancer cell survival in chronic lymphocytic leukaemia. *Nature cell biology* 14, 276-286 (2012).

96. Paggetti, J. *et al.* Exosomes released by chronic lymphocytic leukemia cells induce the transition of stromal cells into cancer-associated fibroblasts. *Blood* 126, 1106-1117 (2015).

97. Maffei, R. *et al.* Physical contact with endothelial cells through beta1- and beta2- integrins rescues chronic lymphocytic leukemia cells from spontaneous and drug-induced apoptosis and induces a peculiar gene expression profile in leukemic cells. *Haematologica* 97, 952-960 (2012).

98. Maffei, R. *et al.* Endothelin-1 promotes survival and chemoresistance in chronic lymphocytic leukemia B cells through ETA receptor. *PloS one* 9, e98818 (2014).

99. Heinig, K. *et al.* Access to follicular dendritic cells is a pivotal step in murine chronic lymphocytic leukemia B-cell activation and proliferation. *Cancer discovery* 4, 1448-1465 (2014).

100. Chilosi M *et al.* Immunohistochemical demonstration of follicular dendritic cells in bone marrow involvement of B-cell chronic lymphocytic leukemia. *Cancer* 56, 328-332 (1985).

101. Pedersen, I.M. *et al.* Protection of CLL B cells by a follicular dendritic cell line is dependent on induction of Mcl-1. *Blood* 100, 1795-1801 (2002).

102. Kern, C. *et al.* Involvement of BAFF and APRIL in the resistance to apoptosis of B-CLL through an autocrine pathway. *Blood* 103, 679-688 (2004).

103. Endo, T. *et al.* BAFF and APRIL support chronic lymphocytic leukemia B-cell survival through activation of the canonical NF-kappaB pathway. *Blood* 109, 703-710 (2007).

104. Nishio, M. *et al.* Nurselike cells express BAFF and APRIL, which can promote survival of chronic lymphocytic leukemia cells via a paracrine pathway distinct from that of SDF-1{alpha} 10.1182/blood-2004-03-0889. *Blood* 106, 1012-1020 (2005).

105. Cols, M. *et al.* Stromal endothelial cells establish a bidirectional crosstalk with chronic lymphocytic leukemia cells through the TNF-related factors BAFF, APRIL, and CD40L. *J. Immunol.* 188, 6071-6083 (2012).

106. Kitada, S., Zapata, J.M., Andreeff, M. & Reed, J.C. Bryostatin and CD40-ligand enhance apoptosis resistance and induce expression of cell survival genes in B-cell chronic lymphocytic leukaemia. *British journal of haematology* 106, 995-1004 (1999).

107. Os, A. *et al.* Chronic lymphocytic leukemia cells are activated and proliferate in response to specific T helper cells. *Cell reports* 4, 566-577 (2013).

108. Ghia, P. *et al.* Chronic lymphocytic leukemia B cells are endowed with the capacity to attract CD4+, CD40L+ T cells by producing CCL22. *European journal of immunology* 32, 1403-1413 (2002).

109. Scielzo, C. *et al.* The functional in vitro response to CD40 ligation reflects a different clinical outcome in patients with chronic lymphocytic leukemia. *Leukemia* 25, 1760-1767 (2011).

110. McClanahan, F. *et al. Mechanisms of PD-L1/PD-1 mediated CD8 T-cell dysfunction in the context of aging-related immune defects in the Eμ-TCL1 CLL mouse model*, 2015.

111. Riches, J.C. & Gribben, J.G. Understanding the Immunodeficiency in Chronic Lymphocytic Leukemia: Potential Clinical Implications. *Hematology/Oncology Clinics of North America* 27, 207-235 (2013).

112. Brusa, D. *et al.* The PD-1/PD-L1 axis contributes to T-cell dysfunction in chronic lymphocytic leukemia. *Haematologica* 98, 953-963 (2013).

113. Ramsay, A.G. *et al.* Chronic lymphocytic leukemia T cells show impaired immunological synapse formation that can be reversed with an immunomodulating drug. *J. Clin. Invest.* 118, 2427-2437 (2008).

114. Ramsay, A.G., Clear, A.J., Fatah, R. & Gribben, J.G. *Multiple inhibitory ligands induce impaired T-cell immunologic synapse function in chronic lymphocytic leukemia that can be blocked with lenalidomide: establishing a reversible immune evasion mechanism in human cancer*, vol. 120, 2012.

115. Riches, J.C. *et al.* T cells from CLL patients exhibit features of T-cell exhaustion but retain capacity for cytokine production. *Blood* 121, 1612-1621 (2013).

116. Reiners, K.S. *et al.* Soluble ligands for NK cell receptors promote evasion of chronic lymphocytic leukemia cells from NK cell anti-tumor activity. *Blood* 121, 3658-3665 (2013).

117. Veuillen, C. *et al.* Primary B-CLL resistance to NK cell cytotoxicity can be overcome in vitro and in vivo by priming NK cells and monoclonal antibody therapy. *Journal of clinical immunology* 32, 632-646 (2012).

118. Huergo-Zapico, L. *et al.* Expansion of NK cells and reduction of NKG2D expression in chronic lymphocytic leukemia. Correlation with progressive disease. *PloS one* 9, e108326 (2014).

119. Reiners, K.S. *et al.* Soluble ligands for NK cell receptors promote evasion of chronic lymphocytic leukemia cells from NK cell anti-tumor activity. *Blood* 121, 3658-3665 (2013).

120. Akashi, K., Traver, D., Miyamoto, T. & Weissman, I.L. A clonogenic common myeloid progenitor that gives rise to all myeloid lineages. *Nature* 404, 193-197 (2000).

121. Spangrude, G.J., Heimfeld, S. & Weissman, I.L. Purification and characterization of mouse hematopoietic stem cells. *Science* 241, 58-62 (1988).

122. Kondo, M., Weissman, I.L. & Akashi, K. Identification of clonogenic common lymphoid progenitors in mouse bone marrow. *Cell* 91, 661-672 (1997).

123. Seita, J. & Weissman, I.L. Hematopoietic stem cell: self-renewal versus differentiation. *Wiley interdisciplinary reviews. Systems biology and medicine* 2, 640-653 (2010).

124. Morrison, S.J. & Weissman, I.L. The long-term repopulating subset of hematopoietic stem cells is deterministic and isolatable by phenotype. *Immunity* 1, 661-673 (1994).

125. Auffray, C. *et al.* CX3CR1+ CD115+ CD135+ common macrophage/DC precursors and the role of CX3CR1 in their response to inflammation. *The Journal of experimental medicine* 206, 595-606 (2009).

126. Theoleyre, S. *et al.* The molecular triad OPG/RANK/RANKL: involvement in the orchestration of pathophysiological bone remodeling. *Cytokine & growth factor reviews* 15, 457-475 (2004).

127. Wiktor-Jedrzejczak, W. *et al.* Total absence of colony-stimulating factor 1 in the macrophage-deficient osteopetrotic (op/op) mouse. *Proceedings of the National Academy of Sciences of the United States of America* 87, 4828-4832 (1990).

128. Ginhoux, F. & Jung, S. Monocytes and macrophages: developmental pathways and tissue homeostasis. *Nature reviews. Immunology* 14, 392-404 (2014).

129. Geissmann, F. *et al.* Blood monocytes: distinct subsets, how they relate to dendritic cells, and their possible roles in the regulation of T-cell responses. *Immunol Cell Biol* 86, 398-408 (2008).

130. Varol, C. *et al.* Monocytes give rise to mucosal, but not splenic, conventional dendritic cells. *The Journal of experimental medicine* 204, 171-180 (2007).

131. Onai, N. *et al.* Identification of clonogenic common Flt3+M-CSFR+ plasmacytoid and conventional dendritic cell progenitors in mouse bone marrow. *Nature immunology* 8, 1207-1216 (2007).

132. Geissmann, F. *et al.* Development of monocytes, macrophages, and dendritic cells. *Science* 327, 656-661 (2010).

133. Stanley, E.R., Chen, D.M. & Lin, H.S. Induction of macrophage production and proliferation by a purified colony stimulating factor. *Nature* 274, 168-170 (1978).

134. Guilbert, L.J. & Stanley, E.R. Specific interaction of murine colony-stimulating factor with mononuclear phagocytic cells. *J Cell Biol* 85, 153-159 (1980).

135. Yeung, Y.G., Jubinsky, P.T., Sengupta, A., Yeung, D.C. & Stanley, E.R. Purification of the colony-stimulating factor 1 receptor and demonstration of its tyrosine kinase activity. *Proceedings of the National Academy of Sciences of the United States of America* 84, 1268-1271 (1987).

136. Sarrazin, S. *et al.* MafB restricts M-CSF-dependent myeloid commitment divisions of hematopoietic stem cells. *Cell* 138, 300-313 (2009).

137. Mossadegh-Keller, N. *et al.* M-CSF instructs myeloid lineage fate in single haematopoietic stem cells. *Nature* 497, 239-243 (2013).

138. Byrne, P.V., Guilbert, L.J. & Stanley, E.R. Distribution of cells bearing receptors for a colony-stimulating factor (CSF-1) in murine tissues. *J Cell Biol* 91, 848-853 (1981).

139. MacDonald, K.P. *et al.* The colony-stimulating factor 1 receptor is expressed on dendritic cells during differentiation and regulates their expansion. *Journal of immunology* 175, 1399-1405 (2005).

140. Nandi, S. *et al.* The CSF-1 receptor ligands IL-34 and CSF-1 exhibit distinct developmental brain expression patterns and regulate neural progenitor cell maintenance and maturation. *Developmental biology* 367, 100-113 (2012).

141. Stanley, E.R. & Chitu, V. CSF-1 receptor signaling in myeloid cells. *Cold Spring Harb Perspect Biol* 6 (2014).

142. Rieger, M.A., Hoppe, P.S., Smejkal, B.M., Eitelhuber, A.C. & Schroeder, T. Hematopoietic cytokines can instruct lineage choice. *Science* 325, 217-218 (2009).

143. Gobert Gosse, S., Bourgin, C., Liu, W.Q., Garbay, C. & Mouchiroud, G. M-CSF stimulated differentiation requires persistent MEK activity and MAPK phosphorylation independent of Grb2-Sos association and phosphatidylinositol 3-kinase activity. *Cellular signalling* 17, 1352-1362 (2005).

144. Kelley, T.W. *et al.* Macrophage colony-stimulating factor promotes cell survival through Akt/protein kinase B. *J Biol Chem* 274, 26393-26398 (1999).

145. Murray, J.T., Craggs, G., Wilson, L. & Kellie, S. Mechanism of phosphatidylinositol 3-kinase-dependent increases in BAC1.2F5 macrophage-like cell density in response to M-CSF: phosphatidylinositol 3-kinase inhibitors increase the rate of apoptosis rather than inhibit DNA synthesis. *Inflammation research : official journal of the European Histamine Research Society ... [et al.]* 49, 610-618 (2000).

146. Golden, L.H. & Insogna, K.L. The expanding role of PI3-kinase in bone. *Bone* 34, 3-12 (2004).

147. Chang, M. *et al.* Phosphatidylinostitol-3 kinase and phospholipase C enhance CSF-1-dependent macrophage survival by controlling glucose uptake. *Cellular signalling* 21, 1361-1369 (2009).

148. Munugalavadla, V., Borneo, J., Ingram, D.A. & Kapur, R. p85alpha subunit of class IA PI-3 kinase is crucial for macrophage growth and migration. *Blood* 106, 103-109 (2005).

149. Yu, W. *et al.* Macrophage proliferation is regulated through CSF-1 receptor tyrosines 544, 559, and 807. *J Biol Chem* 287, 13694-13704 (2012).

150. Robb, L. Cytokine receptors and hematopoietic differentiation. *Oncogene* 26, 6715-6723 (2007).

151. Kaushansky, K. Lineage-specific hematopoietic growth factors. *The New England journal of medicine* 354, 2034-2045 (2006).

152. Pollard, J.W. Trophic macrophages in development and disease. *Nature reviews. Immunology* 9, 259-270 (2009).

153. Hettinger, J. *et al.* Origin of monocytes and macrophages in a committed progenitor. *Nature immunology* 14, 821-830 (2013).

154. Hopkinson-Woolley, J., Hughes, D., Gordon, S. & Martin, P. Macrophage recruitment during limb development and wound healing in the embryonic and foetal mouse. *J Cell Sci* 107 (Pt 5), 1159-1167 (1994).

155. Jakubzick, C. *et al.* Minimal differentiation of classical monocytes as they survey steady-state tissues and transport antigen to lymph nodes. *Immunity* 39, 599-610 (2013).

156. Serbina, N.V. & Pamer, E.G. Monocyte emigration from bone marrow during bacterial infection requires signals mediated by chemokine receptor CCR2. *Nature immunology* 7, 311-317 (2006).

157. Jakubzick, C.V., Randolph, G.J. & Henson, P.M. Monocyte differentiation and antigen-presenting functions. *Nature reviews. Immunology* 17, 349-362 (2017).

158. Ingersoll, M.A. *et al.* Comparison of gene expression profiles between human and mouse monocyte subsets. *Blood* 115, e10-19 (2010).

159. Randolph, G.J., Beaulieu, S., Lebecque, S., Steinman, R.M. & Muller, W.A. Differentiation of monocytes into dendritic cells in a model of transendothelial trafficking. *Science* 282, 480-483 (1998).

160. Yona, S. *et al.* Fate mapping reveals origins and dynamics of monocytes and tissue macrophages under homeostasis. *Immunity* 38, 79-91 (2013).

161. Thomas, G.D. *et al.* Deleting an Nr4a1 Super-Enhancer Subdomain Ablates Ly6Clow Monocytes while Preserving Macrophage Gene Function. *Immunity* 45, 975-987 (2016).

162. Hanna, R.N. *et al.* The transcription factor NR4A1 (Nur77) controls bone marrow differentiation and the survival of Ly6C- monocytes. *Nature immunology* 12, 778-785 (2011).

163. Landsman, L. *et al.* CX3CR1 is required for monocyte homeostasis and atherogenesis by promoting cell survival. *Blood* 113, 963-972 (2009).

164. Gamrekelashvili, J. *et al.* Regulation of monocyte cell fate by blood vessels mediated by Notch signalling. *Nature Communications* 7 (2016).

165. Liu, K. *et al.* Origin of dendritic cells in peripheral lymphoid organs of mice. *Nature immunology* 8, 578-583 (2007).

166. Serbina, N.V., Salazar-Mather, T.P., Biron, C.A., Kuziel, W.A. & Pamer, E.G. TNF/iNOS-producing dendritic cells mediate innate immune defense against bacterial infection. *Immunity* 19, 59-70 (2003).

167. Robben, P.M., LaRegina, M., Kuziel, W.A. & Sibley, L.D. Recruitment of Gr-1+ monocytes is essential for control of acute toxoplasmosis. *The Journal of experimental medicine* 201, 1761-1769 (2005).

168. Zhu, B. *et al.* Plasticity of Ly-6C(hi) myeloid cells in T cell regulation. *Journal of immunology* 187, 2418-2432 (2011).

169. Slaney, C.Y., Toker, A., La Flamme, A., Backstrom, B.T. & Harper, J.L. Naive blood monocytes suppress T-cell function. A possible mechanism for protection from autoimmunity. *Immunol Cell Biol* 89, 7-13 (2011).

170. Augier, S. *et al.* Inflammatory blood monocytes contribute to tumor development and represent a privileged target to improve host immunosurveillance. *Journal of immunology* 185, 7165-7173 (2010).

171. Gabrilovich, D.I., Ostrand-Rosenberg, S. & Bronte, V. Coordinated regulation of myeloid cells by tumours. *Nature reviews. Immunology* 12, 253-268 (2012).

172. Biswas, S.K. & Mantovani, A. Macrophage plasticity and interaction with lymphocyte subsets: cancer as a paradigm. *Nature immunology* 11, 889-896 (2010).

173. Murray, P.J. *et al.* Macrophage activation and polarization: nomenclature and experimental guidelines. *Immunity* 41, 14-20 (2014).

174. Gordon, S. & Martinez, F.O. Alternative activation of macrophages: mechanism and functions. *Immunity* 32, 593-604 (2010).

175. Stein, M., Keshav, S., Harris, N. & Gordon, S. Interleukin 4 potently enhances murine macrophage mannose receptor activity: a marker of alternative immunologic macrophage activation. *The Journal of experimental medicine* 176, 287-292 (1992).

176. Asselin-Paturel, C. & Trinchieri, G. Production of type I interferons: plasmacytoid dendritic cells and beyond. *The Journal of experimental medicine* 202, 461-465 (2005).

177. Kadowaki, N. *et al.* Subsets of human dendritic cell precursors express different toll-like receptors and respond to different microbial antigens. *The Journal of experimental medicine* 194, 863-869 (2001).

178. Sapoznikov, A. *et al.* Organ-dependent in vivo priming of naive CD4+, but not CD8+, T cells by plasmacytoid dendritic cells. *The Journal of experimental medicine* 204, 1923-1933 (2007).

179. Irla, M. *et al.* MHC class II-restricted antigen presentation by plasmacytoid dendritic cells inhibits T cell-mediated autoimmunity. *The Journal of experimental medicine* 207, 1891-1905 (2010).

180. Kuwajima, S. *et al.* Interleukin 15-dependent crosstalk between conventional and plasmacytoid dendritic cells is essential for CpG-induced immune activation. *Nature immunology* 7, 740-746 (2006).

181. Mildner, A. & Jung, S. Development and function of dendritic cell subsets. *Immunity* 40, 642-656 (2014).

182. Fairn, G.D. & Grinstein, S. How nascent phagosomes mature to become phagolysosomes. *Trends in immunology* 33, 397-405 (2012).

183. Kagan, J.C. & Iwasaki, A. Phagosome as the organelle linking innate and adaptive immunity. *Traffic* 13, 1053-1061 (2012).

184. Guermonprez, P., Valladeau, J., Zitvogel, L., Thery, C. & Amigorena, S. Antigen presentation and T cell stimulation by dendritic cells. *Annu Rev Immunol* 20, 621-667 (2002).

185. Belz, G.T., Carbone, F.R. & Heath, W.R. Cross-presentation of antigens by dendritic cells. *Critical reviews in immunology* 22, 439-448 (2002).

186. Vremec, D., Pooley, J., Hochrein, H., Wu, L. & Shortman, K. CD4 and CD8 expression by dendritic cell subtypes in mouse thymus and spleen. *Journal of immunology* 164, 2978-2986 (2000).

187. Robbins, S.H. *et al.* Novel insights into the relationships between dendritic cell subsets in human and mouse revealed by genome-wide expression profiling. *Genome Biol* 9, R17 (2008).

188. Pulendran, B. *et al.* Distinct dendritic cell subsets differentially regulate the class of immune response in vivo. *Proceedings of the National Academy of Sciences of the United States of America* 96, 1036-1041 (1999).

189. Maldonado-Lopez, R. *et al.* CD8alpha+ and CD8alpha- subclasses of dendritic cells direct the development of distinct T helper cells in vivo. *The Journal of experimental medicine* 189, 587-592 (1999).

190. Shortman, K. & Heath, W.R. The CD8+ dendritic cell subset. *Immunol Rev* 234, 18-31 (2010).

191. Shortman, K. Burnet oration: dendritic cells: multiple subtypes, multiple origins, multiple functions. *Immunol Cell Biol* 78, 161-165 (2000).

192. Tsukada, N. Distinctive features of "nurselike" cells that differentiate in the context of chronic lymphocytic leukemia. *Blood* 99, 1030-1037 (2002).

193. Ysebaert, L. & Fournie, J.J. Genomic and phenotypic characterization of nurse-like cells that promote drug resistance in chronic lymphocytic leukemia. *Leukemia & lymphoma* 52, 1404-1406 (2011).

194. Boissard, F., Fournie, J.J., Laurent, C., Poupot, M. & Ysebaert, L. Nurse like cells: chronic lymphocytic leukemia associated macrophages. *Leukemia & lymphoma* 56, 1570-1572 (2015).

195. Filip, A.A. *et al.* Circulating microenvironment of CLL: are nurse-like cells related to tumor-associated macrophages? *Blood cells, molecules & diseases* 50, 263-270 (2013).

196. Burger, J.A. *et al.* High-level expression of the T-cell chemokines CCL3 and CCL4 by chronic lymphocytic leukemia B cells in nurselike cell cocultures and after BCR stimulation. *Blood* 113, 3050-3058 (2009).

197. Burkle, A. *et al.* Overexpression of the CXCR5 chemokine receptor, and its ligand, CXCL13 in B-cell chronic lymphocytic leukemia. *Blood* 110, 3316-3325 (2007).

198. Deaglio, S. *et al.* CD38 and CD100 lead a network of surface receptors relaying positive signals for B-CLL growth and survival. *Blood* 105, 3042-3050 (2005).

199. Binder, M. *et al.* Stereotypical chronic lymphocytic leukemia B-cell receptors recognize survival promoting antigens on stromal cells. *PloS one* 5, e15992 (2010).

200. Audrito, V. *et al.* Extracellular nicotinamide phosphoribosyltransferase (NAMPT) promotes M2 macrophage polarization in chronic lymphocytic leukemia. *Blood* 125, 111-123 (2015).

201. Jia, L. *et al.* Extracellular HMGB1 promotes differentiation of nurse-like cells in chronic lymphocytic leukemia. *Blood* 123, 1709-1719 (2014).

202. Maffei, R. *et al.* The monocytic population in chronic lymphocytic leukemia shows altered composition and deregulation of genes involved in phagocytosis and inflammation. *Haematologica* 98, 1115-1123 (2013).

203. Hanna, B.S. *et al.* Depletion of CLL-associated patrolling monocytes and macrophages controls disease development and repairs immune dysfunction in vivo. *Leukemia* 30, 570-579 (2016).

204. Jitschin, R. CLL-cells induce IDOhi CD141HLA-DRlo myeloid-derived suppressor cells that inhibit T-cell responses and promote TRegs. *Blood* 124 (2014).

205. Gabrilovich, D.I. *et al.* The terminology issue for myeloid-derived suppressor cells. *Cancer research* 67, 425; author reply 426 (2007).

206. Hanks, B.A. Immune evasion pathways and the design of dendritic cell-based cancer vaccines. *Discovery medicine* 21, 135-142 (2016).

207. Burger, J.A. & Gribben, J.G. The microenvironment in chronic lymphocytic leukemia (CLL) and other B cell malignancies: insight into disease biology and new targeted therapies. *Seminars in cancer biology* 24, 71-81 (2014).

208. Boimel, P.J. *et al.* Contribution of CXCL12 secretion to invasion of breast cancer cells. *Breast Cancer Res* 14, R23 (2012).

209. Qian, B.Z. *et al.* CCL2 recruits inflammatory monocytes to facilitate breast-tumour metastasis. *Nature* 475, 222-225 (2011).

210. Hagemann, T. *et al.* "Re-educating" tumor-associated macrophages by targeting NF-κB. *The Journal of experimental medicine* 205, 1261-1268 (2008).

211. Yaddanapudi, K. *et al.* Control of Tumor-Associated Macrophage Alternative Activation by Macrophage Migration Inhibitory Factor. *The Journal of Immunology* 190, 2984-2993 (2013).

212. Beatty, G.L. *et al.* CD40 agonists alter tumor stroma and show efficacy against pancreatic carcinoma in mice and humans. *Science* 331, 1612-1616 (2011).

213. Vonderheide, R.H. Prospect of targeting the CD40 pathway for cancer therapy. *Clinical cancer research : an official journal of the American Association for Cancer Research* 13, 1083-1088 (2007).

214. Welford, A.F. *et al.* TIE2-expressing macrophages limit the therapeutic efficacy of the vascular-disrupting agent combretastatin A4 phosphate in mice. *J Clin Invest* 121, 1969-1973 (2011).

215. SP, D.A. *et al.* Alliance A091103 a phase II study of the angiopoietin 1 and 2 peptibody trebananib for the treatment of angiosarcoma. *Cancer Chemother Pharmacol* 75, 629-638 (2015).

216. Strachan, D.C. *et al.* CSF1R inhibition delays cervical and mammary tumor growth in murine models by attenuating the turnover of tumor-associated macrophages and enhancing infiltration by CD8 T cells. *Oncoimmunology* 2, e26968 (2013).

217. Galletti, G. *et al.* Targeting Macrophages Sensitizes Chronic Lymphocytic Leukemia to Apoptosis and Inhibits Disease Progression. *Cell reports* (2016).

218. Lia, M. *et al.* Functional dissection of the chromosome 13q14 tumor-suppressor locus using transgenic mouse lines. *Blood* 119, 2981-2990 (2012).

219. Zapata, J.M., Krajewska, M., Morse, H.C., 3rd, Choi, Y. & Reed, J.C. TNF receptor-associated factor (TRAF) domain and Bcl-2 cooperate to induce small B cell lymphoma/chronic lymphocytic

leukemia in transgenic mice. *Proceedings of the National Academy of Sciences of the United States of America* 101, 16600-16605 (2004).

220. Bichi, R. *et al.* Human chronic lymphocytic leukemia modeled in mouse by targeted TCL1 expression. *Proceedings of the National Academy of Sciences of the United States of America* 99, 6955-6960 (2002).

221. Herling, M. *et al.* TCL1 shows a regulated expression pattern in chronic lymphocytic leukemia that correlates with molecular subtypes and proliferative state. *Leukemia* 20, 280-285 (2006).

222. Virgilio, L. *et al.* Identification of the TCL1 gene involved in T-cell malignancies. *Proceedings of the National Academy of Sciences of the United States of America* 91, 12530-12534 (1994).

223. Pekarsky, Y. *et al.* Tcl1 expression in chronic lymphocytic leukemia is regulated by miR-29 and miR-181. *Cancer research* 66, 11590-11593 (2006).

224. Herling, M. *et al.* High TCL1 levels are a marker of B-cell receptor pathway responsiveness and adverse outcome in chronic lymphocytic leukemia. *Blood* 114, 4675-4686 (2009).

225. Yan, X.J. *et al.* B cell receptors in TCL1 transgenic mice resemble those of aggressive, treatment-resistant human chronic lymphocytic leukemia. *Proceedings of the National Academy of Sciences of the United States of America* 103, 11713-11718 (2006).

226. Chen, S.S. *et al.* Autoantigen can promote progression to a more aggressive TCL1 leukemia by selecting variants with enhanced B-cell receptor signaling. *Proceedings of the National Academy of Sciences of the United States of America* 110, E1500-1507 (2013).

227. Iacovelli, S. *et al.* Two types of BCR interactions are positively selected during leukemia development in the Emu-TCL1 transgenic mouse model of CLL. *Blood* 125, 1578-1588 (2015).

228. Pekarsky, Y. *et al.* Tcl1 enhances Akt kinase activity and mediates its nuclear translocation. *Proceedings of the National Academy of Sciences of the United States of America* 97, 3028-3033 (2000).

229. Laine, J., Kunstle, G., Obata, T., Sha, M. & Noguchi, M. The protooncogene TCL1 is an Akt kinase coactivator. *Mol Cell* 6, 395-407 (2000).

230. Pekarsky, Y. *et al.* Tcl1 functions as a transcriptional regulator and is directly involved in the pathogenesis of CLL. *Proceedings of the National Academy of Sciences of the United States of America* 105, 19643-19648 (2008).

231. Simonetti, G., Bertilaccio, M.T., Ghia, P. & Klein, U. Mouse models in the study of chronic lymphocytic leukemia pathogenesis and therapy. *Blood* 124, 1010-1019 (2014).

232. Bresin, A. *et al.* TCL1 transgenic mouse model as a tool for the study of therapeutic targets and microenvironment in human B-cell chronic lymphocytic leukemia. *Cell Death Dis* 7, e2071 (2016).

233. Simonetti, G., Bertilaccio, M.T.S., Ghia, P. & Klein, U. Mouse models in the study of chronic lymphocytic leukemia pathogenesis and therapy. *Blood* 124, 1010-1019 (2014).

234. Enzler, T. *et al.* Chronic lymphocytic leukemia of Emu-TCL1 transgenic mice undergoes rapid cell turnover that can be offset by extrinsic CD257 to accelerate disease progression. *Blood* 114, 4469-4476 (2009).

235. Lascano, V. *et al.* Chronic lymphocytic leukemia disease progression is accelerated by APRIL-TACI interaction in the TCL1 transgenic mouse model. *Blood* 122, 3960-3963 (2013).

236. Reinart, N. *et al. Delayed development of chronic lymphocytic leukemia in the absence of macrophage migration inhibitory factor*, vol. 121, 2013.

237. Hofbauer, J.P. *et al.* Development of CLL in the TCL1 transgenic mouse model is associated with severe skewing of the T-cell compartment homologous to human CLL. *Leukemia* 25, 1452-1458 (2011).

238. Gorgun, G. *et al.* Eμ-TCL1 mice represent a model for immunotherapeutic reversal of chronic lymphocytic leukemia-induced T-cell dysfunction. *PNAS* 106, 6250-6255 (2009).

239. Liu, T.M. *et al.* OSU-T315: a novel targeted therapeutic that antagonizes AKT membrane localization and activation of chronic lymphocytic leukemia cells. *Blood* 125, 284-295 (2015).

240. Hertlein, E. *et al.* 17-DMAG targets the nuclear factor-kappaB family of proteins to induce apoptosis in chronic lymphocytic leukemia: clinical implications of HSP90 inhibition. *Blood* 116, 45-53 (2010).

241. Jamroziak, K., Pula, B. & Walewski, J. Current Treatment of Chronic Lymphocytic Leukemia. *Curr Treat Options Oncol* 18, 5 (2017).

242. Hallek, M. *et al.* Addition of rituximab to fludarabine and cyclophosphamide in patients with chronic lymphocytic leukaemia: a randomised, open-label, phase 3 trial. *Lancet* 376, 1164-1174 (2010).

243. Fischer, K. *et al.* Long-term remissions after FCR chemoimmunotherapy in previously untreated patients with CLL: updated results of the CLL8 trial. *Blood* 127, 208-215 (2016).

244. Eichhorst, B. *et al.* First-line chemoimmunotherapy with bendamustine and rituximab versus fludarabine, cyclophosphamide, and rituximab in patients with advanced chronic lymphocytic leukaemia (CLL10): an international, open-label, randomised, phase 3, non-inferiority trial. *Lancet Oncol* 17, 928-942 (2016).

245. Wierda, W.G. *et al.* Ofatumumab as single-agent CD20 immunotherapy in fludarabine-refractory chronic lymphocytic leukemia. *J Clin Oncol* 28, 1749-1755 (2010).

246. Owen, C.J. & Stewart, D.A. Obinutuzumab for the treatment of patients with previously untreated chronic lymphocytic leukemia: overview and perspective. *Ther Adv Hematol* 6, 161-170 (2015).

247. Maffei, R. *et al.* Lenalidomide in chronic lymphocytic leukemia: the present and future in the era of tyrosine kinase inhibitors. *Crit Rev Oncol Hematol* 97, 291-302 (2016).

248. Ito, T. *et al.* Identification of a primary target of thalidomide teratogenicity. *Science* 327, 1345-1350 (2010).

249. Fecteau, J.F. *et al.* Lenalidomide inhibits the proliferation of CLL cells via a cereblon/p21WAF1/Cip1-dependent mechanism independent of functional p53. *Blood* 124, 1637-1644 (2014).

250. Sher, T. *et al.* Efficacy of lenalidomide in patients with chronic lymphocytic leukemia with high-risk cytogenetics. *Leukemia & lymphoma* 51, 85-88 (2010).

251. Strati, P. *et al.* Lenalidomide induces long-lasting responses in elderly patients with chronic lymphocytic leukemia. *Blood* 122, 734-737 (2013).

252. Badoux, X.C. *et al.* Phase II study of lenalidomide and rituximab as salvage therapy for patients with relapsed or refractory chronic lymphocytic leukemia. *J Clin Oncol* 31, 584-591 (2013).

253. Byrd, J.C. *et al.* Ibrutinib versus ofatumumab in previously treated chronic lymphoid leukemia. *The New England journal of medicine* 371, 213-223 (2014).

254. Furman, R.R. *et al.* Idelalisib and rituximab in relapsed chronic lymphocytic leukemia. *The New England journal of medicine* 370, 997-1007 (2014).

255. Roberts, A.W. *et al.* Targeting BCL2 with Venetoclax in Relapsed Chronic Lymphocytic Leukemia. *The New England journal of medicine* 374, 311-322 (2016).

256. Robertson, L.E., Plunkett, W., McConnell, K., Keating, M.J. & McDonnell, T.J. Bcl-2 expression in chronic lymphocytic leukemia and its correlation with the induction of apoptosis and clinical outcome. *Leukemia* 10, 456-459 (1996).

257. Oltersdorf, T. *et al.* An inhibitor of Bcl-2 family proteins induces regression of solid tumours. *Nature* 435, 677-681 (2005).

258. van Delft, M.F. *et al.* The BH3 mimetic ABT-737 targets selective Bcl-2 proteins and efficiently induces apoptosis via Bak/Bax if Mcl-1 is neutralized. *Cancer cell* 10, 389-399 (2006).

259. Souers, A.J. *et al.* ABT-199, a potent and selective BCL-2 inhibitor, achieves antitumor activity while sparing platelets. *Nature medicine* 19, 202-208 (2013).

260. Byrd, J.C. *et al.* Acalabrutinib (ACP-196) in Relapsed Chronic Lymphocytic Leukemia. *The New England journal of medicine* 374, 323-332 (2016).

261. Walter, H.S. *et al.* A phase 1 clinical trial of the selective BTK inhibitor ONO/GS-4059 in relapsed and refractory mature B-cell malignancies. *Blood* 127, 411-419 (2016).

262. O'Brien, S. *et al.* Duvelisib (IPI-145), a PI3K-δ,γ Inhibitor, Is Clinically Active in Patients with Relapsed/Refractory Chronic Lymphocytic Leukemia. *Blood* 124, 3334-3334 (2014).

263. O'Connor, O.A. *et al.* TGR-1202, a Novel Once Daily PI3K-Delta Inhibitor, Demonstrates Clinical Activity with a Favorable Safety Profile in Patients with CLL and B-Cell Lymphoma. *Blood* 126, 4154-4154 (2015).

264. Sawas, A. *et al.* A phase 1/2 trial of ublituximab, a novel anti-CD20 monoclonal antibody, in patients with B-cell non-Hodgkin lymphoma or chronic lymphocytic leukaemia previously exposed to rituximab. *British journal of haematology* 177, 243-253 (2017).

265. Porter, D.L., Levine, B.L., Kalos, M., Bagg, A. & June, C.H. Chimeric antigen receptor-modified T cells in chronic lymphoid leukemia. *The New England journal of medicine* 365, 725-733 (2011).

266. Turtle, C.J. *et al.* Durable Molecular Remissions in Chronic Lymphocytic Leukemia Treated With CD19-Specific Chimeric Antigen Receptor-Modified T Cells After Failure of Ibrutinib. *J Clin Oncol* 35, 3010-3020 (2017).

267. Milone, M.C. *et al.* Chimeric receptors containing CD137 signal transduction domains mediate enhanced survival of T cells and increased antileukemic efficacy in vivo. *Molecular therapy : the journal of the American Society of Gene Therapy* 17, 1453-1464 (2009).

268. Porter, D.L. *et al.* Chimeric antigen receptor T cells persist and induce sustained remissions in relapsed refractory chronic lymphocytic leukemia. *Science translational medicine* 7, 303ra139 (2015).

269. Davila, M.L. & Brentjens, R. Chimeric antigen receptor therapy for chronic lymphocytic leukemia: what are the challenges? *Hematol Oncol Clin North Am* 27, 341-353 (2013).

270. Byrd, J.C. *et al.* Targeting BTK with ibrutinib in relapsed chronic lymphocytic leukemia. *The New England journal of medicine* 369, 32-42 (2013).

271. Wang , M.L. *et al.* Targeting BTK with Ibrutinib in Relapsed or Refractory Mantle-Cell Lymphoma. *New England Journal of Medicine* 369, 507-516 (2013).

272. Honigberg, L.A. *et al.* The Bruton tyrosine kinase inhibitor PCI-32765 blocks B-cell activation and is efficacious in models of autoimmune disease and B-cell malignancy. *Proceedings of the National Academy of Sciences of the United States of America* 107, 13075-13080 (2010).

273. Vetrie, D. *et al.* The gene involved in X-linked agammaglobulinaemia is a member of the src family of protein-tyrosine kinases. *Nature* 361, 226-233 (1993).

274. Tsukada, S. *et al.* Deficient expression of a B cell cytoplasmic tyrosine kinase in human X-linked agammaglobulinemia. *Cell* 72, 279-290 (1993).

275. Hendriks, R.W., Bredius, R.G., Pike-Overzet, K. & Staal, F.J. Biology and novel treatment options for XLA, the most common monogenetic immunodeficiency in man. *Expert opinion on therapeutic targets* 15, 1003-1021 (2011).

276. Aoki, Y., Isselbacher, K.J. & Pillai, S. Bruton tyrosine kinase is tyrosine phosphorylated and activated in pre-B lymphocytes and receptor-ligated B cells. *Proceedings of the National Academy of Sciences of the United States of America* 91, 10606-10609 (1994).

277. Saouaf, S.J. *et al.* Temporal differences in the activation of three classes of non-transmembrane protein tyrosine kinases following B-cell antigen receptor surface engagement. *Proceedings of the National Academy of Sciences of the United States of America* 91, 9524-9528 (1994).

278. Kil, L.P. *et al.* Btk levels set the threshold for B-cell activation and negative selection of autoreactive B cells in mice. *Blood* 119, 3744-3756 (2012).

279. Kil, L.P. *et al.* Bruton's tyrosine kinase mediated signaling enhances leukemogenesis in a mouse model for chronic lymphocytic leukemia. *American journal of blood research* 3, 71-83 (2013).

280. Sakuma, C., Sato, M., Takenouchi, T. & Kitani, H. Specific binding of the WASP N-terminal domain to Btk is critical for TLR2 signaling in macrophages. *Molecular immunology* 63, 328-336 (2015).

281. de Rooij, M.F. *et al.* The clinically active BTK inhibitor PCI-32765 targets B-cell receptor- and chemokine-controlled adhesion and migration in chronic lymphocytic leukemia. *Blood* 119, 2590-2594 (2012).

282. Ponader, S. *et al.* The Bruton tyrosine kinase inhibitor PCI-32765 thwarts chronic lymphocytic leukemia cell survival and tissue homing in vitro and in vivo. *Blood* 119, 1182-1189 (2012).

283. de Weers, M. *et al.* The Bruton's tyrosine kinase gene is expressed throughout B cell differentiation, from early precursor B cell stages preceding immunoglobulin gene rearrangement up to mature B cell stages. *European journal of immunology* 23, 3109-3114 (1993).

284. Smith, C.I. *et al.* Expression of Bruton's agammaglobulinemia tyrosine kinase gene, BTK, is selectively down-regulated in T lymphocytes and plasma cells. *The Journal of Immunology* 152, 557-565 (1994).

285. Byrne, J.C. *et al.* Bruton's tyrosine kinase is required for apoptotic cell uptake via regulating the phosphorylation and localization of calreticulin. *Journal of immunology* 190, 5207-5215 (2013).

286. Ni Gabhann, J. *et al.* Btk regulates macrophage polarization in response to lipopolysaccharide. *PloS one* 9, e85834 (2014).

287. Ormsby, T. *et al.* Btk is a positive regulator in the TREM-1/DAP12 signaling pathway. *Blood* 118, 936-945 (2011).

288. Schenk, M., Bouchon, A., Seibold, F. & Mueller, C. TREM-1--expressing intestinal macrophages crucially amplify chronic inflammation in experimental colitis and inflammatory bowel diseases. *J Clin Invest* 117, 3097-3106 (2007).

289. Ren, L. *et al.* Analysis of the Effects of the Bruton's tyrosine kinase (Btk) Inhibitor Ibrutinib on Monocyte Fcgamma Receptor (FcgammaR) Function. *J Biol Chem* 291, 3043-3052 (2016).

290. Zaitseva, L. *et al.* Ibrutinib inhibits SDF1/CXCR4 mediated migration in AML. *Oncotarget* (2014).

291. Rushworth, S.A., Murray, M.Y., Zaitseva, L., Bowles, K.M. & MacEwan, D.J. Identification of Bruton's tyrosine kinase as a therapeutic target in acute myeloid leukemia. *Blood* 123 (2014).

292. Dubovsky, J.A. *et al.* Ibrutinib is an irreversible molecular inhibitor of ITK driving a Th1-selective pressure in T lymphocytes. *Blood* 122, 2539-2549 (2013).

293. Fraietta, J.A. *et al.* Ibrutinib enhances chimeric antigen receptor T-cell engraftment and efficacy in leukemia. *Blood* 127, 1117-1127 (2016).

294. Long, M. *et al.* Ibrutinib treatment improves T cell number and function in CLL patients. *J Clin Invest* 127, 3052-3064 (2017).

295. Podhorecka, M. *et al.* Changes in T-cell subpopulations and cytokine network during early period of ibrutinib therapy in chronic lymphocytic leukemia patients: the significant decrease in T regulatory cells number. *Oncotarget* 8, 34661-34669 (2017).

296. Yin, Q. *et al.* Ibrutinib Therapy Increases T Cell Repertoire Diversity in Patients with Chronic Lymphocytic Leukemia. *Journal of immunology* 198, 1740-1747 (2017).

297. Woyach, J.A. *et al.* Resistance mechanisms for the Bruton's tyrosine kinase inhibitor ibrutinib. *The New England journal of medicine* 370, 2286-2294 (2014).

298. Ahn, I.E. *et al.* Clonal evolution leading to ibrutinib resistance in chronic lymphocytic leukemia. *Blood* 129, 1469-1479 (2017).

299. Albitar, A. *et al.* Using high-sensitivity sequencing for the detection of mutations in BTK and PLCgamma2 genes in cellular and cell-free DNA and correlation with progression in patients treated with BTK inhibitors. *Oncotarget* 8, 17936-17944 (2017).

300. Woyach, J.A. How I manage ibrutinib-refractory chronic lymphocytic leukemia. *Blood* 129, 1270-1274 (2017).

301. Burger, J.A. *et al.* Clonal evolution in patients with chronic lymphocytic leukaemia developing resistance to BTK inhibition. *Nat Commun* 7, 11589 (2016).

302. Reiff, S.D. *et al.* Evaluation of the novel Bruton's tyrosine kinase (BTK) inhibitor GDC-0853 in chronic lymphocytic leukemia (CLL) with wild type or C481S mutated BTK. *Journal of Clinical Oncology* 34, 7530-7530 (2016).

303. Jones, J.A. *et al.* Venetoclax activity in CLL patients who have relapsed after or are refractory to ibrutinib or idelalisib. *Journal of Clinical Oncology* 34, 7519-7519 (2016).

304. Deng, J. *et al.* Bruton's tyrosine kinase inhibition increases BCL-2 dependence and enhances sensitivity to venetoclax in chronic lymphocytic leukemia. *Leukemia* (2017).

305. Burger, J.A. *et al.* Blood-derived nurse-like cells protect chronic lymphocytic leukemia B cells from spontaneous apoptosis through stromal cell-derived factor-1. *Blood* 96, 2655-2663 (2000).

306. Seiffert, M. *et al.* Soluble CD14 is a novel monocyte-derived survival factor for chronic lymphocytic leukemia cells, which is induced by CLL cells in vitro and present at abnormally high levels in vivo. *Blood* 116, 4223-4230 (2010).

307. Lagneaux, L., Delforge, A., Bron, D., De Bruyn, C. & Stryckmans, P. Chronic lymphocytic leukemic B cells but not normal B cells are rescued from apoptosis by contact with normal bone marrow stromal cells. *Blood* 91, 2387-2396 (1998).

308. Filip, A.A., Cisel, B. & Wasik-Szczepanek, E. Guilty bystanders: nurse-like cells as a model of microenvironmental support for leukemic lymphocytes. *Clin Exp Med* 15, 73-83 (2015).

309. McWhorter, F.Y., Wang, T., Nguyen, P., Chung, T. & Liu, W.F. Modulation of macrophage phenotype by cell shape. *Proceedings of the National Academy of Sciences of the United States of America* 110, 17253-17258 (2013).

310. Xie, J. & Yi, Q. Beta2-microglobulin as a potential initiator of inflammatory responses. *Trends in immunology* 24, 228-229; author reply 229-230 (2003).

311. Yan, X.J. *et al.* Identification of outcome-correlated cytokine clusters in chronic lymphocytic leukemia. *Blood* 118, 5201-5210 (2011).

312. Hume, D.A. & MacDonald, K.P. Therapeutic applications of macrophage colony-stimulating factor-1 (CSF-1) and antagonists of CSF-1 receptor (CSF-1R) signaling. *Blood* 119, 1810-1820 (2012).

313. Grellier, B. *et al.* 3D modeling and characterization of the human CD115 monoclonal antibody H27K15 epitope and design of a chimeric CD115 target. *mAbs* 6, 533-546 (2014).

314. S.A.), H.H.T. TG3003, an immunomodulatory anti-CD115 mAb targeting M2-macrophage polarization in the tumor microenvironment *AACR Annual Meeting, Philadelphia, PA, USA, 18-22 April 2015, Abst. 288* (2015).

315. Gatjen, M. *et al.* Splenic marginal zone granulocytes acquire an accentuated neutrophil B cell-helper phenotype in chronic lymphocytic leukemia. *Cancer research* (2016).

316. Haegel, H. *et al.* A unique anti-CD115 monoclonal antibody which inhibits osteolysis and skews human monocyte differentiation from M2-polarized macrophages toward dendritic cells. *mAbs* 5, 736-747 (2013).

317. Gonzalez-Rodriguez, A.P. *et al.* Prognostic significance of CD8 and CD4 T cells in chronic lymphocytic leukemia. *Leukemia & lymphoma* 51, 1829-1836 (2010).

318. http://www.immgen.org/databrowser/index.html.

319. Hanna, B. Characterizing and targeting the tumor microenvironment in chronic lymphocytic leukemia. Dissertation, Ruperto-Carola University of Heidelberg, 2016, Heidelberg, 2016.

320. De Smedt, T. *et al.* Effect of interleukin-10 on dendritic cell maturation and function. *European journal of immunology* 27, 1229-1235 (1997).

321. Landau, D.A. *et al.* Evolution and impact of subclonal mutations in chronic lymphocytic leukemia. *Cell* 152, 714-726 (2013).

322. Vire, E. *et al.* The Polycomb group protein EZH2 directly controls DNA methylation. *Nature* 439, 871-874 (2006).

323. Zhang, Q.W. *et al.* Prognostic significance of tumor-associated macrophages in solid tumor: a meta-analysis of the literature. *PloS one* 7, e50946 (2012).

324. Boissard, F. *et al.* Nurse-like cells impact on disease progression in chronic lymphocytic leukemia. *Blood Cancer Journal* 6, e381 (2016).

325. Scholl, S.M. *et al.* Circulating levels of the macrophage colony stimulating factor CSF-1 in primary and metastatic breast cancer patients. A pilot study. *Breast Cancer Res Treat* 39, 275-283 (1996).

326. Gadducci, A. *et al.* Serum macrophage colony-stimulating factor (M-CSF) levels in patients with epithelial ovarian cancer. *Gynecol Oncol* 70, 111-114 (1998).

327. Aharinejad, S. *et al.* Elevated CSF1 serum concentration predicts poor overall survival in women with early breast cancer. *Endocr Relat Cancer* 20, 777-783 (2013).

328. Lidor, Y.J. *et al.* Constitutive production of macrophage colony-stimulating factor and interleukin-6 by human ovarian surface epithelial cells. *Experimental cell research* 207, 332-339 (1993).

329. Wu, J., Zhu, J.Q. & Zhu, D.X. The regulatory effects of macrophages on colony stimulating factor-1 (CSF-1) production. *The International journal of biochemistry* 22, 513-517 (1990).

330. Lenzo, J.C. *et al.* Control of macrophage lineage populations by CSF-1 receptor and GM-CSF in homeostasis and inflammation. *Immunol Cell Biol* 90, 429-440 (2012).

331. Pyonteck, S.M. *et al.* CSF-1R inhibition alters macrophage polarization and blocks glioma progression. *Nature medicine* 19, 1264-1272 (2013).

332. Mack, M. *et al.* Expression and characterization of the chemokine receptors CCR2 and CCR5 in mice. *Journal of immunology* 166, 4697-4704 (2001).

333. Zhang, H.H. *et al.* CCR2 identifies a stable population of human effector memory CD4+ T cells equipped for rapid recall response. *Journal of immunology* 185, 6646-6663 (2010).

334. http://www.clodronateliposomes.org/ashwindigital.asp?docname=mechanism.

335. Silva, M.T. & Correia-Neves, M. Neutrophils and macrophages: the main partners of phagocyte cell systems. *Frontiers in immunology* 3, 174 (2012).

336. Zhu, Q. *et al.* Human B cells have an active phagocytic capability and undergo immune activation upon phagocytosis of Mycobacterium tuberculosis. *Immunobiology* 221, 558-567 (2016).

337. Pahler, J.C. *et al.* Plasticity in tumor-promoting inflammation: impairment of macrophage recruitment evokes a compensatory neutrophil response. *Neoplasia* 10, 329-340 (2008).

338. Kolaczkowska, E. & Kubes, P. Neutrophil recruitment and function in health and inflammation. *Nature reviews. Immunology* 13, 159-175 (2013).

339. Quail, D.F. *et al.* The tumor microenvironment underlies acquired resistance to CSF-1R inhibition in gliomas. *Science* 352, aad3018 (2016).

340. DeNardo, D.G. *et al.* Leukocyte complexity predicts breast cancer survival and functionally regulates response to chemotherapy. *Cancer discovery* 1, 54-67 (2011).

341. Patwardhan, P.P. *et al.* Sustained inhibition of receptor tyrosine kinases and macrophage depletion by PLX3397 and rapamycin as a potential new approach for the treatment of MPNSTs. *Clinical cancer research : an official journal of the American Association for Cancer Research* 20, 3146-3158 (2014).

342. Schreiber, H.A. *et al.* Intestinal monocytes and macrophages are required for T cell polarization in response to Citrobacter rodentium. *The Journal of experimental medicine* 210, 2025-2039 (2013).

343. Deaglio, S. *et al.* CD38/CD31 interactions activate genetic pathways leading to proliferation and migration in chronic lymphocytic leukemia cells. *Molecular medicine (Cambridge, Mass.)* 16, 87-91 (2010).

344. Vallières, F. & Girard, D. IL-21 Enhances Phagocytosis in Mononuclear Phagocyte Cells: Identification of Spleen Tyrosine Kinase as a Novel Molecular Target of IL-21. *The Journal of Immunology* 190, 2904-2912 (2013).

345. Liu, Y. *et al.* Interleukin-21 maintains the expression of CD16 on monocytes via the production of IL-10 by human naive CD4+ T cells. *Cellular immunology* 267, 102-108 (2011).

346. Bolzoni, M. *et al.* IL21R expressing CD14+CD16+ monocytes expand in multiple myeloma patients leading to increased osteoclasts. *Haematologica* 102, 773-784 (2017).

347. de Totero, D. *et al.* The opposite effects of IL-15 and IL-21 on CLL B cells correlate with differential activation of the JAK/STAT and ERK1/2 pathways. *Blood* 111, 517-524 (2008).

348. Browning, R.L. *et al.* Lenalidomide Induces Interleukin-21 Production by T Cells and Enhances IL21-Mediated Cytotoxicity in Chronic Lymphocytic Leukemia B Cells. *Cancer immunology research* 4, 698-707 (2016).

349. Pascutti, M.F. *et al.* IL-21 and CD40L signals from autologous T cells can induce antigen-independent proliferation of CLL cells. *Blood* 122, 3010-3019 (2013).

350. Van Coillie, E. *et al.* Functional comparison of two human monocyte chemotactic protein-2 isoforms, role of the amino-terminal pyroglutamic acid and processing by CD26/dipeptidyl peptidase IV. *Biochemistry* 37, 12672-12680 (1998).

351. Iwata, S. *et al.* CD26/dipeptidyl peptidase IV differentially regulates the chemotaxis of T cells and monocytes toward RANTES: possible mechanism for the switch from innate to acquired immune response. *Int Immunol* 11, 417-426 (1999).

352. Shah, Z. *et al.* Long-term dipeptidyl-peptidase 4 inhibition reduces atherosclerosis and inflammation via effects on monocyte recruitment and chemotaxis. *Circulation* 124, 2338-2349 (2011).

353. Duan, L., Rao, X., Xia, C., Rajagopalan, S. & Zhong, J. The regulatory role of DPP4 in atherosclerotic disease. *Cardiovascular diabetology* 16, 76 (2017).

354. Brenner, C. *et al.* DPP-4 inhibition ameliorates atherosclerosis by priming monocytes into M2 macrophages. *International journal of cardiology* 199, 163-169 (2015).

355. Ostermann, G., Weber, K.S., Zernecke, A., Schroder, A. & Weber, C. JAM-1 is a ligand of the beta(2) integrin LFA-1 involved in transendothelial migration of leukocytes. *Nature immunology* 3, 151-158 (2002).

356. Pong, W.W. *et al.* F11R is a novel monocyte prognostic biomarker for malignant glioma. *PloS one* 8, e77571 (2013).

357. Williams, D.W., Anastos, K., Morgello, S. & Berman, J.W. JAM-A and ALCAM are therapeutic targets to inhibit diapedesis across the BBB of CD14+CD16+ monocytes in HIV-infected individuals. *Journal of leukocyte biology* 97, 401-412 (2015).

358. Boissard, F. *et al.* Nurse-like cells promote CLL survival through LFA-3/CD2 interactions. *Oncotarget* 8, 52225-52236 (2017).

359. Stadler, N. *et al.* The Bruton tyrosine kinase inhibitor ibrutinib abrogates triggering receptor on myeloid cells 1 mediated neutrophil activation. *Haematologica* (2017).

360. Bousso, P. T-cell activation by dendritic cells in the lymph node: lessons from the movies. *Nature reviews. Immunology* 8, 675-684 (2008).

361. Orsini, E., Guarini, A., Chiaretti, S., Mauro, F.R. & Foa, R. The circulating dendritic cell compartment in patients with chronic lymphocytic leukemia is severely defective and unable to stimulate an effective T-cell response. *Cancer research* 63, 4497-4506 (2003).

362. Baltathakis, I., Alcantara, O. & Boldt, D.H. Expression of different NF-kappaB pathway genes in dendritic cells (DCs) or macrophages assessed by gene expression profiling. *Journal of cellular biochemistry* 83, 281-290 (2001).

363. Yoshimura, S., Bondeson, J., Foxwell, B.M., Brennan, F.M. & Feldmann, M. Effective antigen presentation by dendritic cells is NF-kappaB dependent: coordinate regulation of MHC, co-stimulatory molecules and cytokines. *Int Immunol* 13, 675-683 (2001).

364. Bouchon, A., Dietrich, J. & Colonna, M. Cutting Edge: Inflammatory Responses Can Be Triggered by TREM-1, a Novel Receptor Expressed on Neutrophils and Monocytes. *Journal of immunology* 164, 4991-4995 (2000).

365. Bouchon, A., Facchetti, F., Weigand, M.A. & Colonna, M. TREM-1 amplifies inflammation and is a crucial mediator of septic shock. *Nature* 410, 1103-1107 (2001).

366. Netea, M.G. *et al.* Triggering receptor expressed on myeloid cells-1 (TREM-1) amplifies the signals induced by the NACHT-LRR (NLR) pattern recognition receptors. *Journal of leukocyte biology* 80, 1454-1461 (2006).

367. Hommes, T.J. *et al.* Role of triggering receptor expressed on myeloid cells-1/3 in Klebsiella-derived pneumosepsis. *American journal of respiratory cell and molecular biology* 53, 647-655 (2015).

368. Chung, D.H., Seaman, W.E. & Daws, M.R. Characterization of TREM-3, an activating receptor on mouse macrophages: definition of a family of single Ig domain receptors on mouse chromosome 17. *European journal of immunology* 32, 59-66 (2002).

369. Ruffell, B. *et al.* Macrophage IL-10 blocks CD8+ T cell-dependent responses to chemotherapy by suppressing IL-12 expression in intratumoral dendritic cells. *Cancer cell* 26, 623-637 (2014).

370. Natarajan, G. *et al.* A Tec kinase BTK inhibitor ibrutinib promotes maturation and activation of dendritic cells. *Oncoimmunology* 5, e1151592 (2016).

371. Boks, M.A. *et al.* IL-10-generated tolerogenic dendritic cells are optimal for functional regulatory T cell induction--a comparative study of human clinical-applicable DC. *Clin Immunol* 142, 332-342 (2012).

372. Bhattacharyya, S. *et al.* Immunoregulation of dendritic cells by IL-10 is mediated through suppression of the PI3K/Akt pathway and of IkappaB kinase activity. *Blood* 104, 1100-1109 (2004).

373. Corinti, S., Albanesi, C., la Sala, A., Pastore, S. & Girolomoni, G. Regulatory activity of autocrine IL-10 on dendritic cell functions. *Journal of immunology* 166, 4312-4318 (2001).

374. Herman, S.E.M. *et al.* Dynamic Alterations in Gene Expression in Ibrutinib Treated CLL Reveal Profound Impact on Multiple Signaling Pathways. *Blood* 128, 189-189 (2016).

375. Palucka, K. & Banchereau, J. Cancer immunotherapy via dendritic cells. *Nature reviews. Cancer* 12, 265-277 (2012).

376. Weinstock, M., Rosenblatt, J. & Avigan, D. Dendritic Cell Therapies for Hematologic Malignancies. *Molecular therapy. Methods & clinical development* 5, 66-75 (2017).

377. Tedder, T.F., Inaoki, M. & Sato, S. The CD19-CD21 complex regulates signal transduction thresholds governing humoral immunity and autoimmunity. *Immunity* 6, 107-118 (1997).

378. Sato, S., Steeber, D.A., Jansen, P.J. & Tedder, T.F. CD19 expression levels regulate B lymphocyte development: human CD19 restores normal function in mice lacking endogenous CD19. *Journal of immunology* 158, 4662-4669 (1997).

379. Fujimoto, M. *et al.* Complementary roles for CD19 and Bruton's tyrosine kinase in B lymphocyte signal transduction. *Journal of immunology* 168, 5465-5476 (2002).

380. Ginaldi, L. *et al.* Levels of expression of CD19 and CD20 in chronic B cell leukaemias. *Journal of clinical pathology* 51, 364-369 (1998).

381. Yang, W. *et al.* Diminished expression of CD19 in B-cell lymphomas. *Cytometry B Clin Cytom* 63, 28-35 (2005).

382. Herishanu, Y. *et al.* Divergence in CD19-mediated signaling unfolds intraclonal diversity in chronic lymphocytic leukemia, which correlates with disease progression. *Journal of immunology* 190, 784-793 (2013).

383. Zikherman, J., Doan, K., Parameswaran, R., Raschke, W. & Weiss, A. Quantitative differences in CD45 expression unmask functions for CD45 in B-cell development, tolerance, and survival. *Proceedings of the National Academy of Sciences of the United States of America* 109, E3-12 (2012).

384. Huntington, N.D. *et al.* CD45 links the B cell receptor with cell survival and is required for the persistence of germinal centers. *Nature immunology* 7, 190-198 (2006).

385. Lund, F.E., Yu, N., Kim, K.M., Reth, M. & Howard, M.C. Signaling through CD38 augments B cell antigen receptor (BCR) responses and is dependent on BCR expression. *Journal of immunology* 157, 1455-1467 (1996).

386. Woroniecka, R. *et al.* Cytogenetic and flow cytometry evaluation of Richter syndrome reveals MYC, CDKN2A, IGH alterations with loss of CD52, CD62L and increase of CD71 antigen expression as the most frequent recurrent abnormalities. *Am J Clin Pathol* 143, 25-35 (2015).

387. Landau, D. *et al.* Evolution and Impact of Subclonal Mutations in Chronic Lymphocytic Leukemia. *Cell* 152, 714-726 (2013).

388. Nakamine, H. *et al.* Richter's syndrome with different immunoglobulin light chain types. Molecular and cytogenetic features indicate a common clonal origin. *Am J Clin Pathol* 97, 656-663 (1992).

389. Su, I.H. *et al.* Polycomb group protein ezh2 controls actin polymerization and cell signaling. *Cell* 121, 425-436 (2005).

390. Su, I.H. *et al.* Ezh2 controls B cell development through histone H3 methylation and Igh rearrangement. *Nature immunology* 4, 124-131 (2003).

391. Beguelin, W. *et al.* EZH2 is required for germinal center formation and somatic EZH2 mutations promote lymphoid transformation. *Cancer cell* 23, 677-692 (2013).

392. Peker, D. *et al.* EZH2 Upregulation Is Associated with Unfavorable Prognosis in Diffuse Large B-Cell Lymphoma through Potential RUNX3 Downregulation. *Blood* 128, 5301-5301 (2016).

393. Teater, M.R. *et al.* EZH2 and BCL6 Cooperate To Create The Germinal Center B-Cell Phenotype and Induce Lymphomas Through Formation and Repression Of Bivalent Chromatin Domains. *Blood* 122, 1-1 (2013).

394. Vilagos, B. *et al.* Essential role of EBF1 in the generation and function of distinct mature B cell types. *The Journal of experimental medicine* 209, 775-792 (2012).

395. Sur, S. & Agrawal, D.K. Phosphatases and kinases regulating CDC25 activity in the cell cycle: clinical implications of CDC25 overexpression and potential treatment strategies. *Molecular and cellular biochemistry* 416, 33-46 (2016).

396. Scores, T.C.T.P.E.E. Chronic lymphocytic leukemia cell Gene Set. http://amp.pharm.mssm.edu/Harmonizome/gene_set/chronic+lymphocytic+leukemia+cell/TISSUES+Curated+Tissue+Protein+Expression+Evidence+Scores.

397. Huttmann, A. *et al.* Gene expression signatures separate B-cell chronic lymphocytic leukaemia prognostic subgroups defined by ZAP-70 and CD38 expression status. *Leukemia* 20, 1774-1782 (2006).

398. Kuo, H.P. *et al.* The role of PIM1 in the ibrutinib-resistant ABC subtype of diffuse large B-cell lymphoma. *American journal of cancer research* 6, 2489-2501 (2016).

399. Annika Scheffold, B.M.C.J., Johannes Bloehdorn, Eugen Tausch, Jasmin Bahlo, Sandra Robrecht, Kirsten Fischer, Michael Hallek, Hartmut Döhner, Daniel Mertens, and Stephan Stilgenbauer. High IGF1R Expression Is Associated with Worse Prognosis in CLL and Impacts Response to PI3K-δ Inhibitor Treatment *ASH Abstract, Oral presentation, 59th Annual Meeting & Expostion* (2017, December).

400. Scheffold, A. *et al.* In Vivo modeling of Resistance to PI3Kδ Inhibitor Treatment Using EμTCL1-Tg Tumor Transfer Model. *Blood* 128, 190-190 (2016).

PUBLICATIONS

B.S. Hanna, F. McClanahan, H. Yazdanparast, N. Zaborsky, V. Kalter, P. M. Rossner, A. Benner, C. Durr, A. Egle, J. G. Gribben, P. Lichter, and M. Seiffert, 'Depletion of Cll Associated Patrolling Monocytes and Macrophages Controls Disease Development and Repairs Immune Dysfunction in Vivo', Leukemia (2015).

K. Hardt, S.B. Heick, B. Betz, T. Goecke, H. Yazdanparast, R. Küppers, K. Servan, V. Steinke, N. Rahner, M. Morak, E. Holinski-Feder, C. Engel, G. Möslein, HK. Schackert, M. von Knebel Doeberitz, C. Pox, P. Propping and the German HNPCC consortium, J.H. Hegemann, and B. Royer-Pokora, 'Missense variants in hMLH1 identified in patients from the German HNPCC consortium and functional studies', Familial Cancer (2011)

ACKNOWLEDGMENTS

First of all, I would like to thank Prof. Dr. Peter Lichter for giving me the opportunity to conduct my PhD thesis in his division. I am thankful for his highly valuable scientific input and mentoring throughout my PhD. I also want to thank him for his kind personality and his great effort to create a warm and open atmosphere that was transferred to the entire division.

I am most grateful to my supervisor Dr. Martina Seiffert for giving me excellent and essential scientific input during the last four years. I really want to thank Tina for giving me the opportunity for independent work, while at the same time being supportive regarding any request. Her incessantly positive and motivating nature and her understanding personality made me always feel comfortable under her supervision.

I also want to express my thanks to Dr. Marc Zapatka for his important scientific contribution on the Ibrutinib resistance project. In addition, I want to thank Yashna Paul for performing the analyses on the whole exome and RNA sequencing data.

I would like to thank Prof. Dr. Stephan Stilgenbauer, Prof. Dr. Thorsten Zenz, Dr. Dimitar Efremov, Dr. Annika Scheffold, and Sebastian Scheinost for fruitful collaborative exchange.

Moreover, I am grateful to my TAC members Prof. Dr. Viktor Umansky, Prof. Dr. Alwin Krämer, Dr. Markus Feuerer, and Prof. Dr. Michael Boutros for their time and their scientific contributions during my TAC meetings.
I especially want to thank Prof. Dr. Viktor Umansky, Prof. Dr. Rüdiger Hell and Dr. Christiane Opitz for their willingness to participate in my thesis committee.

I would like to thank the Flow Cytometry Core Facility at DKFZ and in particular Dr. Steffen Schmitt for providing an excellent service and being understanding for the unpredictability of experiments and the need for short notice flow sort appointments.

I further would like to thank Dr. Matthias Schick and Dr. Oliver Heil for their support, helping me with the analyses of the myeloid gene expression data.

I would like to thank Franziska Haderk for answering all questions that a new PhD student can have, for sharing the one or the other buffy coat and entertaining moment with me at night.

I want to thank Bola Hanna for always sharing his scientific knowledge, asking critical questions and being inspiring.

Many thanks go to all former and temporary members and guests of the CLL subgroup for fruitful scientific discussions as well as amusing moments: Lavinia Arseni, Laura LLao Cid, Yasmin Demerdash, Claudia Dürr, Ann-Christin Gaupel, Ramy Girgis, Eriong Lee, Alaa Madi, Sybille Ohl, Selcen Öztürk and Lena Schulze-Edinghausen. In addition, I would like to thank Michael Persicke and Christine Wolf.

Especially I would like to thank Ralph Schulz for helping me conducting experiments and being a reliable colleague. I don't want to miss thanking Neus Carabaza Gimenez and her great contribution to experiments during these busy days. I also want to thank Philipp Rößner and Norman Mack for helping with mouse work experiments.

A special thank also goes to Verena Kalter, whose technical assistance was a cornerstone in all lab-related regards and who became a highly valued and essential colleague in the past four years.

I would also like to thank all former 'PhD pool' members, especially Christin Schmitt, Niclas Kneisel, Emma Philipps, and Marc Zuckermann, as this time was incredibly fun and made me find friends who made the time of my PhD even more enjoyable.

I further would like to thank Frauke Devens, Petra Schröter, and Achim Stephan for their constant readiness to take over last-minute orders.

I want to thank Michael Hain for providing fast IT support at any time of the day.

And I would like to thank all members of B06x for creating a nice work atmosphere. I really enjoyed working surrounded by such a positive environment.

I would like to thank my friend and partner, Marc Christian Thier, for being supportive, gentle and understanding, especially during the last months.

Am aller meisten möchte ich mich aber bei meiner Familie bedanken, vor allem bei meiner Mutter Arefeh Rahimi und meinem Vater Nasser Yazdanparast. Ihr Vertrauen und ihre Zuversicht haben mir die letzten Jahre Rückhalt gegeben und waren die größte Motivation für mich. Diese Arbeit ist auch ein Dank an sie.